Development and Characterization of a Novel Mouse Model of Single and Repetitive Mild Traumatic Brain Injury

Thesis

DEVELOPMENT AND CHARACTERIZATION OF A NOVEL MOUSE MODEL OF SINGLE AND REPETITIVE MILD TRAUMATIC BRAIN INJURY

Benoit Christian Mouzon M.Sc.

Thesis presented for the degree of Doctor of Philosophy
July 2013

Graduate Program in Neuroscience

The Roskamp Institute
2040 Whitfield Ave
34243 Sarasota, FL

The Open University
Milton Keynes
MK76 AA, UK

Date of Submission : 12 July 2013
Date of Award: 7 October 2013

Declaration

I hereby declare that the work presented in this thesis is my own, except where stated. This work has not been submitted for any other degree or professional qualification.

Benoit Mouzon

Acknowledgments

I would like to express my immense gratitude to my supervisors Dr. Fiona Crawford and Dr. Corbin Bachmeier for their advice, guidance and endless assistance though the course of my studies. I would also like to thank Dr. William Stewart from University of Glasgow who served as my Ph.D. co-supervisor and hosted me at the Glasgow Southern General Hospital to share his histological/pathological expertise and many invaluable discussions. I am grateful to Janice Stewart also from the Glasgow Southern General Hospital for her help with the preparation of fixed sections.

My deepest thanks goes to Dr. Gogce Crynen for assistance with the analytical statistics, Dr. Scott Ferguson, Helena Chaytow and Austin Ferro for the behavioral studies, and Dr. Joseph-Olobumni Ojo with neuropathological studies. The work reported in this thesis would have not been possible without the staff of the vivarium, respectively Sheree Cade and John Adams. I would also like to thank Dr. Michael Stewart my external supervisors for his guidance through the program.

Many thanks go out to Dr. Peter Davies and Christopher Acker from the Feinstein Institute for Medical Research for their discussions and technical assistance by performing various tau assays.

Not to forget all of my co-authors. You have all been tremendously hard-working colleagues and this work could not have been completed without your contributions.

Warm appreciation goes out to my wonderful wife Ann, for her years of love, and never-ending support, and for filling my life with joy, laughter and love. In perspective, I would like to thank my parents from who my achievements are in large part a result of the values they instilled in me.

To conclude, I would like to thank the Roskamp Foundation for financially supporting my studies.

Abstract

Mild traumatic brain injury (mTBI) or concussion is the most common form of TBI, and although a single concussion rarely results in long-term neurological dysfunction, repeated mild traumatic brain injury (r-mTBI) is a recognized risk factor for later development of neurodegenerative disease. However, the mechanisms contributing to neurodegeneration following TBI remain obscure. Animal models provide a means to examine the factors and mechanisms involved in TBI in experiments that cannot be conducted using human participants.

The purpose of this thesis was to develop and fully characterize a reproducible, non-invasive mTBI model that will facilitate the study of repetitive brain injury. In the present study, male wild type mice received a midline concussive blow via an electromagnetic impactor, tuned to produce an injury without fracturing the skull. The injured mice were used to examine the chronic neurobehavioral, neuropathological and biochemical outcomes following single and r-mTBI up to 18 months following injury. Importantly, our findings recapitulate many aspects of human long term TBI sequelae, in particular persistent neuroinflammation, white matter injury, and axonal pathology in the corpus callosum. Our results provide the first evidence that, whilst a single concussion produces transient neurobehavioral changes and pathology which remains static in the period following injury, r-mTBI produces behavioral and pathological changes which continue to evolve many months post injury.

There have been a number of clinical studies implicating tau in TBI pathology. As such, we investigated the relationship between tau pathologies after trauma in a transgenic mouse model expressing all 6 isoforms of human tau protein on a null murine background (hTau). Our results revealed that that single and r-mTBI induced a modest cortical increase in the soluble fraction of three different p-tau epitopes at 24 h post last injury. Moreover, this increase was not associated with worse behavioral performance when compared to wild type animals. Therefore, tau hyperphosphorylation appears to have a contributory, but not primary, role in the acute phase post-injury. Additional prospective studies in both humans and animal models are required to characterize the contribution of tau to TBI sequelae.

The experimental data presented here suggest that inflammation and axonal injury (as seen in both wild-type and hTau models) appear to play a role in the events following single or repetitive mTBI and strongly correlates with the behavioral changes post-injury. The relationship between a history of mTBI and neuroinflammation are likely to be complex and warrant further work to elucidate their association with neurodegenerative disease. This work represents the development of a novel model, and the demonstration of its relevance to human TBI. This model can now be used for further exploration of TBI-related effects and for evaluation of potential therapeutic and diagnostic approaches, as is discussed throughout the thesis.

Table of contents

Chapter 1

Chapter 2

Chapter 3

Chapter 4

Chapter 5

List of Tables

List of Figures

List of abbreviations

ABC	Avidin-Biotin Complex
AD	Alzheimer's Disease
AGD	Agyrophillic Grain Disease
ALS	Amyotrophic Lateral Sclerosis
ANOVA	Analysis Of Variance
APOE	Apolipoprotein E
APP	Amyloid Precursor Protein
Aβ	Amyloid Beta
BCA	bicinchonic acid
BDNF	brain-derived neurotrophic factor
BINT	Blast Induced Neurotrauma
BM	Barnes Maze
BS	Brain Stem
CA1	Cornu Ammonis Region 1
CA3	Cornu Ammonis Region 3
CC	Corpus Callosum
CCI	Controlled cortical Impact
CDC	Centers for Disease Control
CDK5	Cyclin-Dependent Kinases 5
cDNA	complementary Deoxyribonucleic Acid
CHI	Closed Head Injury
CNS	Central Nervous System
CTE	Chronic Traumatic Encephalopathy
CV	Cresyl Violet
DAB	3,3'-diaminobenzidine
DG	Dentate Gyrus
DP	Dementia Pugilistica
DS	Dendritic Segment
ec	entorhinal cortex
EDTA	Ethylenediaminetetra acetic acid
EGFP	Enhanced Green Fluorescent Protein
ELISA	Enzyme-Linked Immuno-Sorbent Assay
EM	Electromagnetic
ERK2	Extracellular-Signal-Regulated Kinase 2
FA	Fractional Anisotropy
FPI	Fluid Percussion Injury
FTLD-tau	Frontotemporal Lobar Degeneration With Tau Inclusions

GCS	Glasgow Coma Scale
GFAP	Glial Fibrillary Acidic Protein
GSK3-β	Glycogen Synthase Kinase 3
H&E	Haemotoxylin and Eosin
HRP	Horseradish Peroxidase
hTau	Human Tau
Iba-1	Ionized Calcium-Binding Adapter Molecule-1
ICP	Intracranial Pressure
KO	Knockout
LFB	Luxol Fast Blue
MAP	Microtubule-Associated Protein
MAPT	Microtubule-Associated Protein Tau
MOM	Mouse On Mouse
M-PER	Mammalian Protein Extraction Reagent
MRI	Magnetic Resonance Imaging
mRNA	messenger Ribonucleic Acid
MS	Membranous Segment
MT	Microtubule
mTBI	mild Traumatic Brain Injury
MTBs	Microtubule Binding Repeat
MWM	Morris Water Maze
nbM	nucleus basalis of Meynert
NFTs	Neurofibrillary tangles
PBS	Phosphate Buffered Saline
PCS	Post Concussive Syndrome
PET	Positron Emission Tomography
PHF	Paired Helical Filaments
PSP	Progressive Supranuclear Palsy
p-tau	Phospho Tau
PTSD	Post Traumatic Stress Disorder
r-mTBI	repetitive mild Traumatic Brain Injury
RPM	Revolution Per Minute
SAS	Statistical Analysis System
SEM	Standard Error of the Mean
s-mTBI	single mild Traumatic Brain Injury
SS	Somatic Segment
TBI	Traumatic Brain Injury
TDP-43	TAR DNA binding protein 43
TUNEL	Deoxynucleotidyl Transferase dUTP Nick End Labeling
WT	Wild Type

Chapter 1

1. General introduction:

Traumatic Brain Injury (TBI) is defined by the Centers for Disease Control and Prevention (CDC) as an external force (arising from blunt or penetrating trauma or from acceleration/deceleration forces) that significantly disrupts brain function. Changes in brain function can include any of the following: a period of loss or alteration in consciousness (e.g., confusion, disorientation); loss of memory (amnesia) of events immediately before or after the injury; neurological deficits (e.g., weakness, loss of balance, change in vision); or intracranial lesions. The presence and duration of these features are used to define the severity of the injury that has occurred and are now recognized to persist or emerge weeks, months or even years after the event.

Over the past decade, the scientific literature on TBI and mild trauma has increased considerably. For example, using the search engine PubMed (National Library of Medicine) for the term "traumatic brain injury" there were 27,566 articles published-between the years of 2003-2012, compared to 14,123 for the years 1993-2002. During this time, a number of models, theories and hypotheses regarding the injury mechanisms and consequences have been presented in the TBI field. Despite major advances in this field of medicine, TBI and mild traumatic brain injury (mTBI), also referred as concussion, are puzzling neurological disorders and one of the least understood injuries facing the scientific community. The need for multidisciplinary research on mTBI is evident from the emerging understanding of the complexity of TBI pathogenesis. As such, scientists have to collaborate with many different research fields, such as traumatology, neurosurgery, internal medicine, neurology, psychiatry

and/or psychology in order to obtain as complete a picture as possible of TBI sequelae, and hopefully identify paths toward treatment.

1.1. Traumatic brain injury in humans:

Sports related concussions have attracted public and political attention in recent years in part because of increased media attention regarding the adverse health consequences (neurodegenerative diseases, behavioral problems) and suicides in high profile individuals that has then drawn attention to the frequency and outcome of mTBI that professional athletes sustain[1-8]. The clinical significance for further research on mTBI stems from the fact that the main cause of death in athletes is from blows to the brain [9]. Concussion symptoms may appear mild, but these effects can lead to significant, life-long impairment affecting an individual's ability to function physically, cognitively, and psychologically. Therefore, athletes who prematurely return to play are highly susceptible to future trauma and often experience more severe brain injuries with subsequent concussions. Athletes with a history of an mTBI who return to competition upon symptom resolution are still at risk for the cumulative effects of concussion as measured by increased symptomatology or slowed recovery on neuropsychological tests[10-14].

1.2. Classification of traumatic brain injury:

Traumatic brain injury classifications can be clinical, mechanistic, or pathological. Pathological classifications separate diffuse from focal injury with histological assessments or through brain imaging techniques (computed tomography (CT) and diffusion tensor imaging

(DTI)). Mechanical classifications describe the type of impact: penetrating, blast, impact, inertia loading. Clinically there are four main types of brain injury: mild (no loss of consciousness and a lack of skull fractures), moderate (loss of consciousness of a few minutes or presence of skull fractures), severe (coma with or without skull fractures) and penetrating TBI in which the dura mater, the outer layer of the meninges, is penetrated. About 75% of all TBI's are classified as mild with the remaining 25% described as moderate or The Glasgow Coma Scale (GCS) is the most commonly used system to asses TBI severity[15] (Table 1.1). The scale was published in 1974 by Graham Teasdale and Bryan J. Jennett, Professors of Neurosurgery at the University of Glasgow's Institute of Neurological Sciences at the Southern General Hospital. Determining the severity of injury consists of grading the patient's level of consciousness. The grade is based on verbal, motor, and eye-opening reactions to stimuli. The patient score can fluctuate between 3 (indicating deep unconsciousness (e.g. coma) and 15 (fully conscious). severe. Several techniques are used to determine severity and classification of the injury.

Eye opening (E)	Spontaneous	4
	To speech	3
	To pain	2
	Nil	1
Best motor response (M)	Obeys	6
	Localizes	5
	Withdrawn	4
	Abnormal flexion	3
	Extensor response	2
	Nil	1
Verbal response (V)	Oriented	5
	Confused conversation	4
	Inappropriate words	3
	Incomprehensible sounds	2
	Nil	1
Coma score (E + M + V)=3–15		

Table.1.1: Glasgow Coma Scale.

1.3. Concussions:

Concussion or mTBI (from the Latin concutere ("to shake violently") or concussus ("action of striking together")) is a form of TBI incurred through head impact or change of acceleration, or both, accompanied by some alteration or limited loss of consciousness with no gross pathology. Concussions are also the mildest and most common form of traumatic brain injury. Although the incidences of these injuries are high, concussions have been called a "silent epidemic" because the symptoms are so subtle that the majority of people who have experienced a concussion do not seek medical attention[16,17]. As a result, the consequences of concussions have long being underestimated. Time to recovery varies depending on the severity of the

injury but most people recover within days and weeks after the original injury while a small fraction experience post concussive syndrome[18,19] (PCS).

The consequences of multiple concussion/repetitive-mTBI were first described by an English pathologist, Harrison S. Martland who in 1928 noted chronic motor and neuropsychiatric symptoms in former boxers[20]. A decade later, further case reports indicated that repetitive mTBI (r-mTBI) might result in an early form of TBI-induced dementia termed "dementia pugilistica"[21] (DP). Up until 2002 when Dr. Bennet Omalu first described chronic traumatic encephalopathy (CTE) in former American football players, DP/CTE was recognized as a peculiar condition confined to boxers[22]. With the appreciation that the pathology was not restricted to boxing, or pugilism, the term CTE was introduced to better reflect the wide range of mTBI exposure situations. Recent media attention sparking considerable public awareness with stories of the consequences of r-mTBI in high profile athletes (particularly in the United States) as well as the incidence of mTBI in the military, has prompted the scientific community to focus on the consequences of mild injury (especially repeated mTBI).

1.3.1. Symptoms and pathology:

Signs and symptoms of concussion can be ascribed to multiple taxa, both physiological and neurological. Headache is the most common while others, such as nausea, difficulty balancing, dizziness, insomnia, fatigue, memory loss, depression, anxiety, irritability, impulsivity, poor concentration and personality changes, may be consequent to cerebral damage, endocrine or autonomic nervous system dysfunction[23-25]. In addition, visual and auditory symptoms include seeing bright lights, light sensitivity, blurred vision, double vision,

and tinnitus[23,24]. Unlike moderate or severe head injury, the neurological disturbance associated with a concussion often occurs without identifiable brain damage. There is no obvious pathology, and regular imaging techniques such as CT and magnetic resonance imaging (MRI) used in cases of moderate and severe head injury reveal no signs of structural changes. Moreover, as concussion is not associated with acute mortality, it is difficult to obtain post mortem tissue for pathological analysis.

Due to these limitations, researchers have developed new techniques to improve the diagnosis of concussions. Among these, DTI is a magnetic resonance imaging technique that measures the directional diffusion of water in neural tracts, which is often abnormal after mTBI. For example, a decrease in fractional anisotropy (FA) in the corpus callosum correlates with axonal degradation and discontinuities with excess water between tracts or in perivascular spaces[26,27]. However, the relationship between these injuries and behavioral changes remains variable across individuals and is poorly understood. The inflammatory response following the concussion could also be assessed in vivo using the positron emission tomography (PET) ligand [11C](R)PK11195 (PK)[28]. This last study suggests that at chronic time points, microglial activation correlates with the degree of cognitive impairment, and thus warrants further longitudinal studies as a potential biomarker to assess the severity of the injury and the potential outcome. However, the abnormality may also be associated with other preexisting conditions such as psychiatric illness, neurodegenerative disease, history of injuries, and alcohol/drug abuse.

1.3.2. Repeated concussion:

The acute and chronic biomechanics and pathophysiology of concussion are still not well understood and can lead to significant sequelae from either single or multiple concussions[29]. The combination of post concussive symptoms and a second impact may be cumulative and thus it is important to know when professional athletes may return to play. Indeed, previous reports and studies have shown that professional athletes exposed to concussion rates exceeding that occurring in the general population may develop ongoing impairment and later degenerative condition such as CTE[30-32]. This problem is also of great interest to victims of car crashes or physical abuse in the civilian population, and to combat veterans as many military personnel sustain more than one combat concussive injury during their service[33,34]. Pathological studies of postmortem brain tissue taken from both former athletes and veterans who had sustained repeated concussions displayed CTE symptoms with evidence of white matter injury, neuroinflammation, brain atrophy, and amyloid and tau deposition[4,8,35,36]. Animal studies have demonstrated that the duration of the disturbed cellular and physiological metabolism after the first injury reflects the time-course of vulnerability to future mTBI making the brain vulnerable to further injuries[37,38]. In mice, repeated mTBI results in progressive white matter injury, axonal injury, chronic inflammation and behavioral dysfunction[29,39-41]. Repetitive but not single mTBI (s-mTBI) in a transgenic mouse model of Alzheimer's disease (Tg2576) was attributed to acceleration of brain amyloid beta accumulation and oxidative stress which support the hypothesis that r-mTBI could work synergistically to promote the onset of neurological disease[42]. A relevant laboratory model is thus needed to explore the pathogenesis and mechanisms of human mTBI. To this end, my doctorate research has involved the development and characterization of a novel experimental model of mild TBI to facilitate

identification of the mechanisms underlying the neurological and behavioral dysfunctions resulting from single concussion and repeated concussions.

1.3.3. Tau pathology and repetitive mTBI:

The tau protein is an intracellular, microtubule-associated protein (MAP) that is highly enriched in axons[43]. The major function of tau is to bind to tubulin, the main component of microtubules (MTs), which results in the stabilization of MT polymers and the cell structure. However, a growing body of evidence suggests that tau could be a multifunctional protein interacting with signaling networks, and as a regulator of the intracellular trafficking of organelles and molecules involved at the pre and postsynaptic level[44,45]. Tau has also a pathogenic role in neurodegenerative disorders exhibiting extensive accumulation of neurofibrillary tangles (NFTs), neuropil threads, and glial tangles in conditions collectively termed tauopathies[46,47]. These include Alzheimer's disease (AD); frontotemporal lobar degeneration with tau inclusions (FTLD-tau) such as Pick's disease, progressive supranuclear palsy (PSP); agyrophillic grain disease (AGD); amyotrophic lateral sclerosis (ALS); some forms of Parkinson's disease and CTE[3,48-51]. In CTE, the modified tau protein (phosphorylated, truncated, hyperphosphorylated, aggregated, polymerized) accumulates and aggregates in the human brain[52]. These structures are aggregates of filamentous polymers called paired helical filaments (PHF), where the main component is tau in its phosphorylated form[43,47]. Many of these pathogenic forms of tau resemble some of the pathologic changes seen with AD, including abundant widespread tau deposits. The relationship between mTBI and tau pathologies remains unclear, but has received considerable focus owing to the increased interest in CTE,

highlighted above, and the apparently critical involvement of tau in CTE pathology. The role and functions of tau after mTBI will be addressed and discussed in further detail in chapter 4.

1.4. Animal models of head trauma:

Although there is substantial similarity between the brains of humans and other mammals, it is important to realize that no single laboratory animal model can fully reproduce the clinical mechanisms encountered by the human brain following injury. Of the species available to use, mice and rats allow efficient analyses of the pathological and behavioral consequences associated with TBI. The most notable differences between rodent and human models is the craniospinal angle, white to grey matter ratio, and brain geometry[53-55]. That said, the development of an animal model that replicates certain pathological components or phases of clinical trauma is essential to understanding the mechanisms involved in human brain injury and to developing appropriate treatment strategies. Over the past decades, investigators have attempted to establish and characterize clinically relevant laboratory models of human TBI. Although large animal models such as swine and non-human primates have been used successfully to investigate specific aspects of TBI [56-62], many investigators have accepted rodent models as the most suitable and ethical choice to study brain trauma. Their relatively small size and cost allows repetitive measurements for a wide range of physiological and behavioral measurements, and also enables the consequences of TBI to potentially be readily examined over the lifespan of the animal. Another benefit of rodent models is the ability to examine the consequences of TBI in a very controlled situation, before attempting translation to the human setting, with animals receiving a specific, homogenous, replicable injury with age, sex, and

genetic background all controlled. Furthermore, mice are the most common specie for the use of transgenic technology and thus scientists can use a wide panel of rodent strains that have been genetically modified by either inserting new genetic information/mutation or simply knocking out the activity of a gene. The use of genetically engineered animals offers the advantage of investigating of the effects of specific gene modulation that may influence response to TBI (such as Apolipoprotein E (APOE)) that would not be easily feasible in higher animal models such as in primates.

Accordingly, numerous rodent models have been developed that mimic different aspects of the complex spectrum of human TBI. Of these, the most commonly used are the weight-drop, fluid percussion injury (FPI), and the controlled cortical impact model (CCI) (see 1.3.2 below). The following sections will summarize the different animal models that were available when I started this project and how researchers modified them to study mTBI.

1.4.1. Mild TBI models:

Several models of TBI have been adapted to mimic the clinical consequences of r-mTBI[40,63,64]. While the definition of mTBI in human is straight forward as previously described (section 1.2.), the criteria for evaluating mTBI in animals models remain to be harmonized. Indeed, the current literature may be confusing as many researchers use the term mTBI to define the milder version of their experimental model. In fact, these injuries are simply a milder version of a severe TBI and consequently do not reflects the clinical characteristic of human mTBI. Series of criteria can be established according to human mTBI definition and translated into animals models. For example, measurable outcomes such as mild cognitive deficits,

impaired motor coordination, loss of consciousness (right reflex for animals), and white matter injury with DTI can be evaluated in both animals and humans. It is vital to choose experimental model that replicate certain pathological components of mild clinical trauma. For our study, these requirements were as follow: 1) a short period of post traumatic apnea less than 30 sec, 2) a short period of righting reflex less than 6 min, 3) no skull fractures, 4) no major hemorrhage, 5) mild cognitive deficits and 6) axonal injury associated with neuroinflammation. The absence of skull fracture and hemorrhage are a characteristic of human mTBI and can be easily assessed in rodent to differentiate mild to moderate TBI. The righting reflex, a mesencephalic reflex is recognized an animal analog to loss of consciousness and is now accepted as a good indicator similar to the loss of consciousness in human. In our laboratory, a right reflex suppression less than 6 min was considered as mild injury while any right reflex superior to 6 min were considered as moderate TBI. Using a FPI or CCI which require longer duration of anesthesia, righting reflex suppression less than 15 min is considered as a mTBI, 15-20 min as moderate and superior of 20 min as severe.

1.4.2. Weight-drop:

Well known in the TBI field, the weight drop injury model uses gravitational forces to produce either a focal [65-67] or diffuse injury [68]. The impact can be delivered either on the exposed skull [69], or directly on the dura [70] of the anesthetized animal (Fig.1.1). In Feeney's weight drop, the impact is delivered to the intact dura, which cause a severe focal injury similar to CCI. The original Mammarou's weight drop model is classified as a moderate to severe TBI and results with high mortality rate, widespread damages of neurons, axons, dendrites, and

extensive axonal injury in the corpus callosum and the long tracts of the brain stem[66]. Because diffuse axonal injury is often observed in the clinical situation, this makes the weight-drop injury model an appropriate tool in studying neuronal and axonal changes in TBI. Since then, Marmarou's model has been modified to allow repeated head impact in lightly anesthetized mice and to produce different grade of diffuse brain injury with varying weights and drop heights[68]. This method has been recently used by Kane et al[71] and Mannix et all[72] to study repeated mTBI, a form of CHI commonly occurring in contact sports, physical abuse and among the military population. In Kane's model, repeated mTBI caused short term behavioral impairments, mild astrocytic reactivity and increased phospho-tau without microglial activation[71]. More importantly, Mannix et al suggests that the cognitive effects of r-mTBI are cumulative and reports persistent cognitive deficits associated with increased astrocytosis but not tau phosphorylation or amyloid beta or plaques[72]. A drawback of this model is the high variability of the injury severity and a high mortality rate due to apnea and skull fractures.

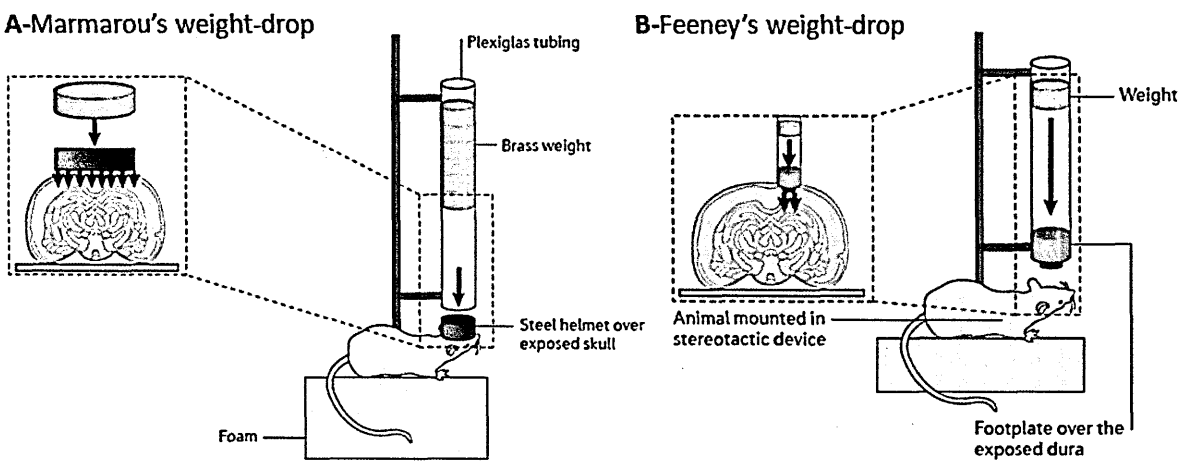

Figure.1.1: Features of weight drop apparatus. (A) In the Marmarou model, the device uses a brass weight to induce closed head injury (CHI). A metal disk is placed over the skull to prevent bone fracture. The In Feeney's model (B), a free weight is released directly onto the exposed dura. Reprinted by

permission from Macmillan Publishers Ltd: Nature Reviews, Xiongl, Ye., et al. "Animal models of traumatic brain injury." 14(2): 128-142, copyright 2013.

1.4.3. Fluid percussion injury:

Fluid percussion injury is another widely used model to study TBI, especially in the rat. The FPI model induces brain injury by rapidly injecting fluid volumes onto the intact dural surface of the brain through a craniectomy[56,57,62,73-76] (Fig.1.2). With graded levels of injury severity achieved by adjusting the force of the fluid pressure pulse, FPI can produce different severity of brain injury (mild, moderate and severe). In general, this type of injury has been used to replicate moderate to severe clinical TBI and produces a combination of focal cortical contusion and diffuse subcortical injury regardless of the injury location[77], centrally around the midline [78], or laterally to the sagittal suture[79]. Recently, mild lateral FPI have been adapted from its more severe setting by decreasing the pressure of the fluid applied to the brain to better reflect a clinically relevant mTBI. A single mild lateral FPI in rats and mice induced transient behavioral and neuropathological changes[80-82], whereas 3 or 5 mild lateral FPI caused cortical neuronal loss and cumulative behavioral deficits[83] . The main weakness of this model is that it requires long anesthesia to trepan and inflict the injury and not representative in terms of mechanism of injury to human mTBI. The inflicted injury is also variable between laboratories due to the fact that some investigators will induce the trauma either centrally or laterally. In addition, this model also does not allow the investigator to perform behavioral analyses immediately post injury due to the side effects of the long anesthesia while performing the surgery.

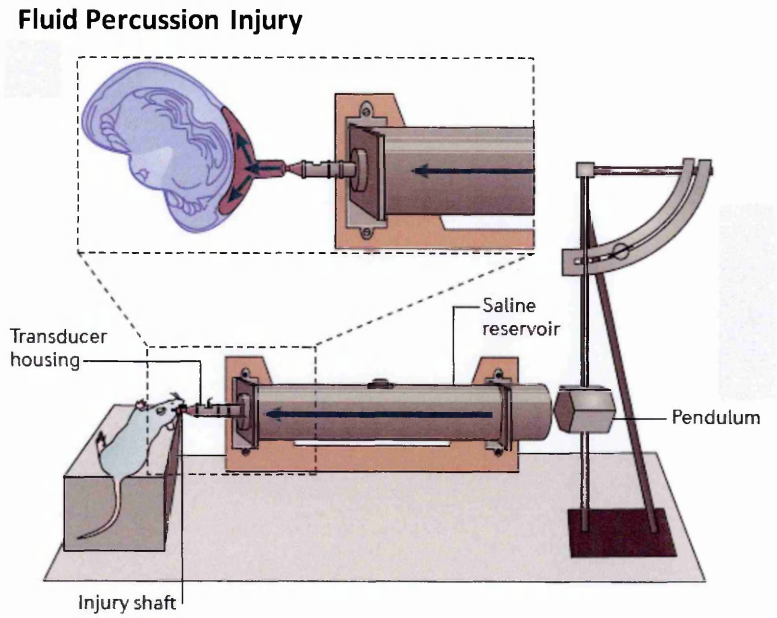

Figure.1.2: Features of a fluid percussion injury apparatus. The fluid percussion injury device uses rapid injection of a fluid pulse into the epidural space. Reprinted by permission from Macmillan Publishers Ltd: Nature Reviews, Xiongl, Ye., et al. "Animal models of traumatic brain injury." 14(2): 128-142, copyright 2013.

1.4.4. Controlled cortical impact:

The controlled cortical impact model introduced in the late 1980's [84] utilizes a pneumatic pistol to deform the exposed dura and provide a controlled impact and quantifiable biomechanical parameters (Fig.1.3). The advantage of this model is that it uses a graded and reproducible brain injury through a predefined dural compression depth and dwell time. Similar to the FPI, this model was developed to study moderate to severe TBI, but can be adjusted by varying the amount of brain deformation and the velocity of the impactor. In rodents, CCI always results in a focal brain injury with cortical contusion, hemorrhage and BBB disruption [85]. The delayed progression of brain damage is accompanied by neuronal cell death, inflammatory events, microglial activation, astrogliosis, axonal damage and cognitive deficits[55,86-88]. The

mildest form of CCI uses a velocity of 2.8m/sec and 0.2 mm brain impact depth. With a single mTBI this model caused a mild extend of cell death accompanied by extensive dendrite degeneration and synapse reduction in the cortex[89]. Similar to the FPI model, the major drawback of this injury is that it requires long anesthesia and a craniectomy that may compensate for intracranial pressure (ICP) increase.

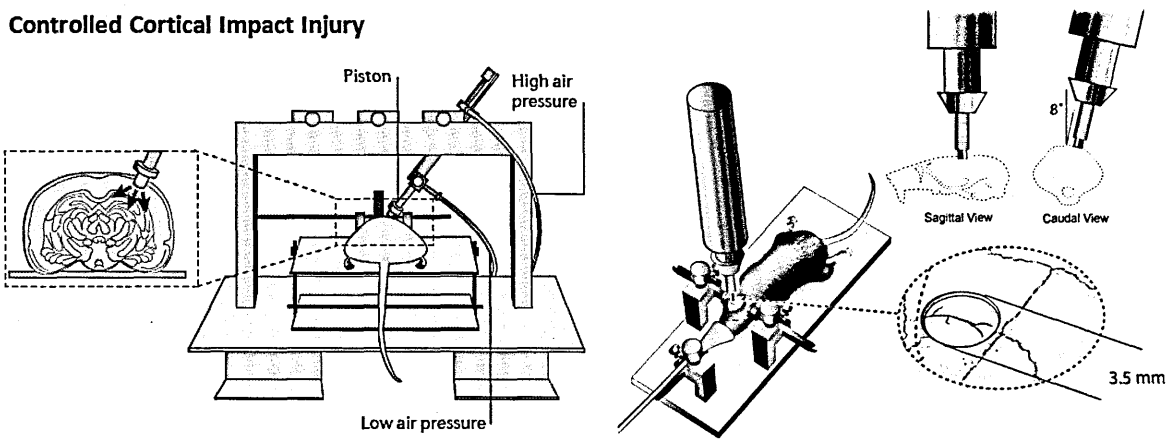

Figure.1.3: Drawing of the mouse controlled cortical impact injury apparatus showing the impactor and part of its mounting system, the craniectomy location, and the orientation of the impactor tip to ensure perpendicularity to the exposed dura and to the surface of the brain. The model uses an air or electromagnetic driven piston to penetrate the brain at a known distance and velocity. Reprinted by permission from Macmillan Publishers Ltd: Nature Reviews, Xiongl, Ye., et al. "Animal models of traumatic brain injury." 14(2): 128-142, copyright 2013 and from Journal of Neuroscience Methods, 160(2): 187-196, Onyszchuk, G., B. Al-Hafez, et al, A mouse model of sensorimotor controlled cortical impact: Characterization using longitudinal magnetic resonance imaging, behavioral assessments and histology, Pages No., 187-196, Copyright 2007, with permission from Elsevier.

Overall, CCI and FPI were widely used and are well characterized model but are also the least useful as they do not replicate the mechanisms of mTBI in human due to the extensive surgical preparation. For that reason, a closed version of the CCI model was also developed allowing a direct blow to the skull without surgical intervention and minimizing the confounding effects of prolonged anesthesia on TBI outcome. Closed-head injury is not only a type of mTBI

in which the skull and dura mater remain intact but also allows multiple mTBI on the same animal[90,91].

The closed version of the CCI model in mice and the weight drop model are more analogy in terms of mechanism of injury and are also amenable multiple injury. In terms of reproducibility, the CCI apparatus incorporates an electromagnetic (EM) coil-based delivery device, which delivers consistent strike velocities while, at the same time, reducing rebound hits that can occur with other brain injury methods (e.g. the weight drop model).

1.4.5. Blast injury:

Due to the emergence of blast induced neurotrauma (BINT) and its particular relevance to the military, a considerable number of animal models have been proposed to be suitable for blast research. Open field exposure [as compared to confined space] to blast provides data for effects of blast that may be most relevant to human military situations but require large amounts of explosives and the experiments are hard to replicate[92,93]. Thus, blast tube models are more commonly used to study the effect of the blast wave on small animals (Fig.1.4). As it is the case with other mTBI models, there are considerable variations within the available BINT models and a disagreement about what is meant by mild blast injury. For example, Elder et al reported a significant increase in post-traumatic stress disorder (PTSD) symptoms in absence of histopathological changes or mortality rate[94]. In contrast, Kochanek's mild BINT model produced 25% mortality rate from apnea and histopathological changes[95]. In a more recent model of repetitive mild BINT, Gama Sosa and colleagues[96] reports intreventricular

hemorrhages with tears at 24h post injury. Other models of BINT showed prolonged behavioral and motor abnormalities, increase tau phosphorylation, axonal injury, chronic neuroinflammation and neurodegeneration with or without macroscopic tissue damage[35,96,97]. The consequences of BINT remain to be standardized across each laboratory model. Because this type of injury is specific to the military population and misrepresent the majority of mTBI, we decided to not pursue our studies with this model.

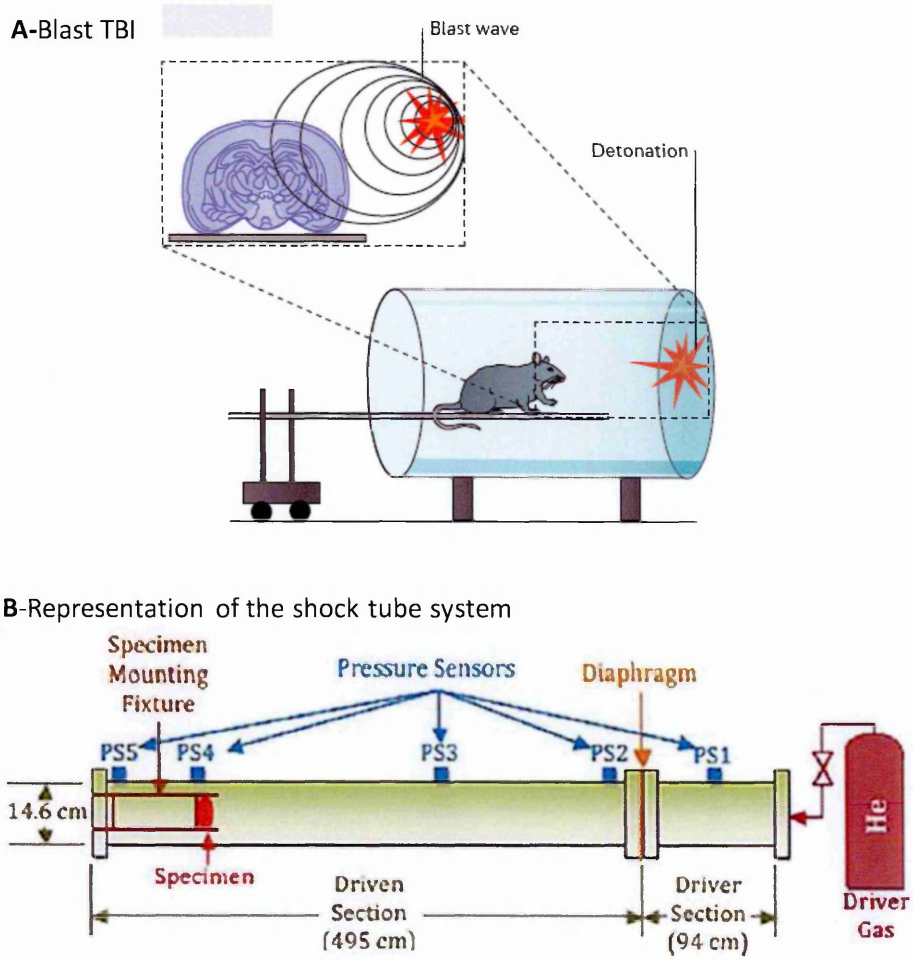

Figure.1.4: (A) Drawing of a blast tube apparatus. Blast brain injury can be caused by the primary injury related to the blast. Reprinted by permission from Macmillan Publishers Ltd: Nature Reviews, Xiongl, Ye., et al. "Animal models of traumatic brain injury." 14(2): 128-142, copyright 2013. (B) Schematic representation of the shock tube system. The system allows direct measurement of the various shock

loading characteristics, including static pressure, total pressure, and overpressure impulse. The driver section is pressurized with helium gas until the pressure differential between the driver and driven sections exceeds the material failure threshold of the diaphragm. The threshold to initiate the rupture can be changed by selecting various combinations of Kapton and polyethylene sheets. Reprinted from Neurobiology of Disease, 41(2): 538-51, Cernak, I., A.C. Merkle, et al, The pathobiology of blast injuries and blast-induced neurotrauma as identified using a new experimental model of injury in mice, Pages No., 538-51, Copyright 2011, with permission from Elsevier.

1.5. Hypothesis:

The models of head injury described above establish and imitate certain aspects of the biomechanics and pathobiology of human TBI. They have enabled an understanding of the primary damage occurring at the time of injury and identification of complex mechanisms of secondary injury. The primary damage mainly includes anatomical lesions such as contusion, laceration, or hemorrhage with secondary injury including swelling and edema. However, these models are not best suited to model mTBI which is estimated to account for 80-95% of all human cases of TBI [98] and they do not easily allow analysis of repetitive injury. To this end, my project aimed to develop a clinically relevant laboratory model of closed head concussion, and to characterize the neurobehavioral and neuropathological consequences of both single mTBI and r-mTBI over time. Specifically, I propose to test the following hypotheses in the following chapters:

1. Chapter 2: After a single mTBI, a state of transient brain vulnerability exists during which the occurrence of repetitive concussion lead to greater behavioral dysfunction and pathological abnormalities. Such study is achievable by the development of an animal model CHI model is more representative of mild TBI/concussive conditions (e.g. minimally invasive, short

period of right reflex, no skull fracture or hemorrhage) and is amenable to the study of more than two repeated concussions.

2. Chapter 3: i) r-mTBI is associated with long term deficits in cognitive and increased inflammation and axonal degeneration, ii) the effect of a single mTBI is transient iii) r-mTBI increases tau hyper-phosphorylation at 12 months post mTBI.
3. Chapter 4: r-mTBI is associated with increased of amyloid-β (Aβ) deposition and tau accumulation with worse behavioral performance. In order to address this question, our hTau transgenic mouse model was used.

1.6. Synopsis:

In tandem with the development of a reproducible, clinically relevant laboratory model of mTBI, these studies were designed to expand on previous literature by describing the progression of symptoms following both single and r-mTBI. Behavioral assays were conducted in parallel with histopathological analyses to understand the potential association between neurobehavioral deficits and its associated pathology at acute and chronic time points following the injury (ies). In the following chapter (Chapter 2), the development of the model and the acute effects of single and r-mTBI were investigated to determine the neurobehavioral and neuropathological changes associated with the injury, and thereby further assess the validity of our model. Chapter 3 focuses on the chronic structural and functional changes after mTBI. The chronic neurobehavioral outcomes were evaluated at 6, 12 and 18 months post-injury/anesthesia using the Barnes maze. At 6 and 12 months post-mTBI the evolution of the same neuropathological changes observed at early time points was reassessed. Given the increasing interest in the role of tau in mTBI (as outlined above) we then used our validated model of mTBI in mice genetically modified to express the different human forms of tau (the human tau (hTau) transgenic mouse), to facilitate investigation of the role of tau in human TBI (Chapter 4). Chapter 5 summarizes the current studies that were aimed at characterizing and identifying the long term neuropathological and neurobehavioral consequences of single and r-mTBI and also discuss ongoing research and future directions.

1.7. References:

1 Omalu, B. I., Fitzsimmons, R. P., Hammers, J. & Bailes, J. Chronic traumatic encephalopathy in a professional American wrestler. *Journal of forensic nursing* **6**, 130-136, doi:10.1111/j.1939-3938.2010.01078.x (2010).

2 Omalu, B. I., Hamilton, R. L., Kamboh, M. I., DeKosky, S. T. & Bailes, J. Chronic traumatic encephalopathy (CTE) in a National Football League Player: Case report and emerging medicolegal practice questions. *Journal of forensic nursing* **6**, 40-46, doi:10.1111/j.1939-3938.2009.01064.x (2010).

3 Omalu, B. *et al.* Emerging histomorphologic phenotypes of chronic traumatic encephalopathy in American athletes. *Neurosurgery* **69**, 173-183; discussion 183, doi:10.1227/NEU.0b013e318212bc7b (2011).

4 McKee, A. C. *et al.* The spectrum of disease in chronic traumatic encephalopathy. *Brain : a journal of neurology*, doi:10.1093/brain/aws307 (2012).

5 Broglio, S. P. *et al.* Cumulative head impact burden in high school football. *Journal of neurotrauma* **28**, 2069-2078, doi:10.1089/neu.2011.1825 (2011).

6 Broglio, S. P., Surma, T. & Ashton-Miller, J. A. High school and collegiate football athlete concussions: a biomechanical review. *Annals of biomedical engineering* **40**, 37-46, doi:10.1007/s10439-011-0396-0 (2012).

7 Gavett, B. E., Stern, R. A., Cantu, R. C., Nowinski, C. J. & McKee, A. C. Mild traumatic brain injury: a risk factor for neurodegeneration. *Alzheimer's research & therapy* **2**, 18, doi:10.1186/alzrt42 (2010).

8 Gavett, B. E., Stern, R. A. & McKee, A. C. Chronic traumatic encephalopathy: a potential late effect of sport-related concussive and subconcussive head trauma. *Clinics in sports medicine* **30**, 179-188, xi, doi:10.1016/j.csm.2010.09.007 (2011).

9 Mueller, F. O. & Cantu, R. C. Catastrophic injuries and fatalities in high school and college sports, fall 1982-spring 1988. *Medicine and science in sports and exercise* **22**, 737-741 (1990).

10 Cantu, R. C. Head and spine injuries in youth sports. *Clinics in sports medicine* **14**, 517-532 (1995).

11 Cantu, R. C. Athletic head injury. *Current sports medicine reports* **2**, 117-119 (2003).

12 Kushner, D. Mild traumatic brain injury: toward understanding manifestations and treatment. *Archives of internal medicine* **158**, 1617-1624 (1998).

13 Kushner, D. S. Concussion in sports: minimizing the risk for complications. *American family physician* **64**, 1007-1014 (2001).

14 Iverson, G. L., Gaetz, M., Lovell, M. R. & Collins, M. W. Cumulative effects of concussion in amateur athletes. *Brain injury : [BI]* **18**, 433-443, doi:10.1080/02699050310001617352 (2004).

15 Teasdale, G. & Jennett, B. Assessment of coma and impaired consciousness. A practical scale. *Lancet* **2**, 81-84 (1974).

16 Goldstein, M. Traumatic brain injury: a silent epidemic. *Annals of neurology* **27**, 327, doi:10.1002/ana.410270315 (1990).

17 Langlois, J. A., Marr, A., Mitchko, J. & Johnson, R. L. Tracking the silent epidemic and educating the public: CDC's traumatic brain injury-associated activities under the TBI Act of 1996 and the Children's Health Act of 2000. *The Journal of head trauma rehabilitation* **20**, 196-204 (2005).

18 King, N. S. & Kirwilliam, S. Permanent post-concussion symptoms after mild head injury. *Brain injury : [BI]* **25**, 462-470, doi:10.3109/02699052.2011.558042 (2011).

19 Maroon, J. C., Lepere, D. B., Blaylock, R. L. & Bost, J. W. Postconcussion syndrome: a review of pathophysiology and potential nonpharmacological approaches to treatment. *The Physician and sportsmedicine* **40**, 73-87, doi:10.3810/psm.2012.11.1990 (2012).

20 Martland, H. Punch Drunk. *J.Am.Med.Assoc* **91**, 1103-1107 (1928).

21 Millspaugh, J. Dementia pugillistica. *U.S. Nav. Med. Bull.* **35**, 357-362 (1937).

22 Omalu, B. I. *et al.* Chronic traumatic encephalopathy in a national football league player: part II. *Neurosurgery* **59**, 1086-1092; discussion 1092-1083, doi:10.1227/01.NEU.0000245601.69451.27 (2006).

23 Blennow, K., Hardy, J. & Zetterberg, H. The neuropathology and neurobiology of traumatic brain injury. *Neuron* **76**, 886-899, doi:10.1016/j.neuron.2012.11.021 (2012).

24 Mott, T. F., McConnon, M. L. & Rieger, B. P. Subacute to chronic mild traumatic brain injury. *American family physician* **86**, 1045-1051 (2012).

25 Lucas, S. Headache management in concussion and mild traumatic brain injury. *PM & R : the journal of injury, function, and rehabilitation* **3**, S406-412, doi:10.1016/j.pmrj.2011.07.016 (2011).

26 Jang, S. H. Diffusion tensor imaging studies on corticospinal tract injury following traumatic brain injury: a review. *NeuroRehabilitation* **29**, 339-345, doi:10.3233/NRE-2011-0710 (2011).

27 Sharp, D. J. & Ham, T. E. Investigating white matter injury after mild traumatic brain injury. *Current opinion in neurology* **24**, 558-563, doi:10.1097/WCO.0b013e32834cd523 (2011).

28 Ramlackhansingh, A. F. *et al.* Inflammation after trauma: microglial activation and traumatic brain injury. *Annals of neurology* **70**, 374-383, doi:10.1002/ana.22455 (2011).

29 Mouzon, B. *et al.* Repetitive mild traumatic brain injury in a mouse model produces learning and memory deficits accompanied by histological changes. *Journal of neurotrauma* **29**, 2761-2773, doi:10.1089/neu.2012.2498 (2012).

30 Guskiewicz, K. M. *et al.* Association between recurrent concussion and late-life cognitive impairment in retired professional football players. *Neurosurgery* **57**, 719-726; discussion 719-726 (2005).

31 Guskiewicz, K. M. *et al.* Cumulative effects associated with recurrent concussion in collegiate football players: the NCAA Concussion Study. *JAMA : the journal of the American Medical Association* **290**, 2549-2555, doi:10.1001/jama.290.19.2549 (2003).

32 McCrory, P. Sports concussion and the risk of chronic neurological impairment. *Clinical journal of sport medicine : official journal of the Canadian Academy of Sport Medicine* **21**, 6-12, doi:10.1097/JSM.0b013e318204db50 (2011).

33 Elder, G. A. & Cristian, A. Blast-related mild traumatic brain injury: mechanisms of injury and impact on clinical care. *The Mount Sinai journal of medicine, New York* **76**, 111-118, doi:10.1002/msj.20098 (2009).

34 Galarneau, M. R., Woodruff, S. I., Dye, J. L., Mohrle, C. R. & Wade, A. L. Traumatic brain injury during Operation Iraqi Freedom: findings from the United States Navy-Marine Corps Combat Trauma Registry. *Journal of neurosurgery* **108**, 950-957, doi:10.3171/JNS/2008/108/5/0950 (2008).

35 Goldstein, L. E. *et al.* Chronic traumatic encephalopathy in blast-exposed military veterans and a blast neurotrauma mouse model. *Science translational medicine* **4**, 134ra160, doi:10.1126/scitranslmed.3003716 (2012).

36 Omalu, B. *et al.* Chronic traumatic encephalopathy in an Iraqi war veteran with posttraumatic stress disorder who committed suicide. *Neurosurgical focus* **31**, E3, doi:10.3171/2011.9.FOCUS11178 (2011).

37 Prins, M. L., Alexander, D., Giza, C. C. & Hovda, D. A. Repeated mild traumatic brain injury: mechanisms of cerebral vulnerability. *Journal of neurotrauma* **30**, 30-38, doi:10.1089/neu.2012.2399 (2013).

38 Longhi, L. *et al.* Temporal window of vulnerability to repetitive experimental concussive brain injury. *Neurosurgery* **56**, 364-374; discussion 364-374 (2005).

39 Creeley, C. E., Wozniak, D. F., Bayly, P. V., Olney, J. W. & Lewis, L. M. Multiple episodes of mild traumatic brain injury result in impaired cognitive performance in mice. *Academic emergency medicine : official journal of the Society for Academic Emergency Medicine* **11**, 809-819 (2004).

40 DeFord, S. M. *et al.* Repeated mild brain injuries result in cognitive impairment in B6C3F1 mice. *Journal of neurotrauma* **19**, 427-438, doi:10.1089/08977150252932389 (2002).

41 Shitaka, Y. *et al.* Repetitive closed-skull traumatic brain injury in mice causes persistent multifocal axonal injury and microglial reactivity. *Journal of neuropathology and experimental neurology* **70**, 551-567, doi:10.1097/NEN.0b013e31821f891f (2011).

42 Uryu, K. *et al.* Repetitive mild brain trauma accelerates Abeta deposition, lipid peroxidation, and cognitive impairment in a transgenic mouse model of Alzheimer amyloidosis. *The Journal of neuroscience : the official journal of the Society for Neuroscience* **22**, 446-454 (2002).

43 Avila, J., Lucas, J. J., Perez, M. & Hernandez, F. Role of tau protein in both physiological and pathological conditions. *Physiological reviews* **84**, 361-384, doi:10.1152/physrev.00024.2003 (2004).

44 Morris, M., Maeda, S., Vossel, K. & Mucke, L. The many faces of tau. *Neuron* **70**, 410-426, doi:10.1016/j.neuron.2011.04.009 (2011).

45 Spillantini, M. G. & Goedert, M. Tau pathology and neurodegeneration. *Lancet neurology* **12**, 609-622, doi:10.1016/S1474-4422(13)70090-5 (2013).

46 Koo, E. H. *et al.* Precursor of amyloid protein in Alzheimer disease undergoes fast anterograde axonal transport. *Proceedings of the National Academy of Sciences of the United States of America* **87**, 1561-1565 (1990).

47 Mazanetz, M. P. & Fischer, P. M. Untangling tau hyperphosphorylation in drug design for neurodegenerative diseases. *Nature reviews. Drug discovery* **6**, 464-479, doi:10.1038/nrd2111 (2007).

48 Santpere, G. & Ferrer, I. Delineation of early changes in cases with progressive supranuclear palsy-like pathology. Astrocytes in striatum are primary targets of tau phosphorylation and GFAP oxidation. *Brain pathology* **19**, 177-187, doi:10.1111/j.1750-3639.2008.00173.x (2009).

49 Rajput, A. *et al.* Parkinsonism, Lrrk2 G2019S, and tau neuropathology. *Neurology* **67**, 1506-1508, doi:10.1212/01.wnl.0000240220.33950.0c (2006).

50 Dickson, D. W., Kouri, N., Murray, M. E. & Josephs, K. A. Neuropathology of frontotemporal lobar degeneration-tau (FTLD-tau). *Journal of molecular neuroscience : MN* **45**, 384-389, doi:10.1007/s12031-011-9589-0 (2011).

51 Pollock, N. J., Mirra, S. S., Binder, L. I., Hansen, L. A. & Wood, J. G. Filamentous aggregates in Pick's disease, progressive supranuclear palsy, and Alzheimer's disease share antigenic determinants with microtubule-associated protein, tau. *Lancet* **2**, 1211 (1986).

52 McKee, A. C. *et al.* Chronic traumatic encephalopathy in athletes: progressive tauopathy after repetitive head injury. *Journal of neuropathology and experimental neurology* **68**, 709-735, doi:10.1097/NEN.0b013e3181a9d503 (2009).

53 Cernak, I. Animal models of head trauma. *NeuroRx : the journal of the American Society for Experimental NeuroTherapeutics* **2**, 410-422, doi:10.1602/neurorx.2.3.410 (2005).

54 Laurer, H. L. & McIntosh, T. K. Experimental models of brain trauma. *Current opinion in neurology* **12**, 715-721 (1999).

55 Morales, D. M. *et al.* Experimental models of traumatic brain injury: do we really need to build a better mousetrap? *Neuroscience* **136**, 971-989, doi:10.1016/j.neuroscience.2005.08.030 (2005).

56 Sullivan, H. G. *et al.* Fluid-percussion model of mechanical brain injury in the cat. *Journal of neurosurgery* **45**, 521-534 (1976).

57 Millen, J. E., Glauser, F. L. & Fairman, R. P. A comparison of physiological responses to percussive brain trauma in dogs and sheep. *Journal of neurosurgery* **62**, 587-591, doi:10.3171/jns.1985.62.4.0587 (1985).

58 Browne, K. D., Chen, X. H., Meaney, D. F. & Smith, D. H. Mild traumatic brain injury and diffuse axonal injury in swine. *Journal of neurotrauma* **28**, 1747-1755, doi:10.1089/neu.2011.1913 (2011).

59 Gennarelli, T. A. *et al.* Diffuse axonal injury and traumatic coma in the primate. *Annals of neurology* **12**, 564-574, doi:10.1002/ana.410120611 (1982).

60 Raghupathi, R. & Margulies, S. S. Traumatic axonal injury after closed head injury in the neonatal pig. *Journal of neurotrauma* **19**, 843-853, doi:10.1089/08977150260190438 (2002).

61 Raghupathi, R., Mehr, M. F., Helfaer, M. A. & Margulies, S. S. Traumatic axonal injury is exacerbated following repetitive closed head injury in the neonatal pig. *Journal of neurotrauma* **21**, 307-316, doi:10.1089/089771504322972095 (2004).

62 Zauner, A. *et al.* Cerebral metabolism after fluid-percussion injury and hypoxia in a feline model. *Journal of neurosurgery* **97**, 643-649, doi:10.3171/jns.2002.97.3.0643 (2002).

63 Weber, J. T. Experimental models of repetitive brain injuries. *Progress in brain research* **161**, 253-261, doi:10.1016/S0079-6123(06)61018-2 (2007).

64 Wang, Y. *et al.* Tightly coupled repetitive blast-induced traumatic brain injury: development and characterization in mice. *Journal of neurotrauma* **28**, 2171-2183, doi:10.1089/neu.2011.1990 (2011).

65 Flierl, M. A. *et al.* Mouse closed head injury model induced by a weight-drop device. *Nature protocols* **4**, 1328-1337, doi:10.1038/nprot.2009.148 (2009).

66 Foda, M. A. & Marmarou, A. A new model of diffuse brain injury in rats. Part II: Morphological characterization. *Journal of neurosurgery* **80**, 301-313, doi:10.3171/jns.1994.80.2.0301 (1994).

67 Shohami, E., Shapira, Y. & Cotev, S. Experimental closed head injury in rats: prostaglandin production in a noninjured zone. *Neurosurgery* **22**, 859-863 (1988).

68 Marmarou, A. *et al.* A new model of diffuse brain injury in rats. Part I: Pathophysiology and biomechanics. *Journal of neurosurgery* **80**, 291-300, doi:10.3171/jns.1994.80.2.0291 (1994).

69 Chen, Y., Constantini, S., Trembovler, V., Weinstock, M. & Shohami, E. An experimental model of closed head injury in mice: pathophysiology, histopathology, and cognitive deficits. *Journal of neurotrauma* **13**, 557-568 (1996).

70 Dail, W. G., Feeney, D. M., Murray, H. M., Linn, R. T. & Boyeson, M. G. Responses to cortical injury: II. Widespread depression of the activity of an enzyme in cortex remote from a focal injury. *Brain research* **211**, 79-89 (1981).

71 Kane, M. J. *et al.* A mouse model of human repetitive mild traumatic brain injury. *Journal of neuroscience methods* **203**, 41-49, doi:10.1016/j.jneumeth.2011.09.003 (2012).

72 Mannix R, M. W., Mandeville J, Grant PE, et al. Clinical Correlates in an Experimental Model of Repetitive Mild Brain Injury. *Annals of neurology*, doi:doi: 10.1002/ana.23858 (2013).

73 Carbonell, W. S. & Grady, M. S. Regional and temporal characterization of neuronal, glial, and axonal response after traumatic brain injury in the mouse. *Acta neuropathologica* **98**, 396-406 (1999).

74 Dixon, C. E., Lighthall, J. W. & Anderson, T. E. Physiologic, histopathologic, and cineradiographic characterization of a new fluid-percussion model of experimental brain injury in the rat. *Journal of neurotrauma* **5**, 91-104 (1988).

75 Perri, B. R. *et al.* Metabolic quantification of lesion volume following experimental traumatic brain injury in the rat. *Journal of neurotrauma* **14**, 15-22 (1997).

76 Pfenninger, E. G., Reith, A., Breitig, D., Grunert, A. & Ahnefeld, F. W. Early changes of intracranial pressure, perfusion pressure, and blood flow after acute head injury. Part 1: An experimental

study of the underlying pathophysiology. *Journal of neurosurgery* **70**, 774-779, doi:10.3171/jns.1989.70.5.0774 (1989).

77 Thompson, H. J. *et al.* Lateral fluid percussion brain injury: a 15-year review and evaluation. *Journal of neurotrauma* **22**, 42-75, doi:10.1089/neu.2005.22.42 (2005).

78 McIntosh, T. K., Noble, L., Andrews, B. & Faden, A. I. Traumatic brain injury in the rat: characterization of a midline fluid-percussion model. *Central nervous system trauma : journal of the American Paralysis Association* **4**, 119-134 (1987).

79 McIntosh, T. K. *et al.* Traumatic brain injury in the rat: characterization of a lateral fluid-percussion model. *Neuroscience* **28**, 233-244 (1989).

80 Shultz, S. R., MacFabe, D. F., Foley, K. A., Taylor, R. & Cain, D. P. Sub-concussive brain injury in the Long-Evans rat induces acute neuroinflammation in the absence of behavioral impairments. *Behavioural brain research* **229**, 145-152, doi:10.1016/j.bbr.2011.12.015 (2012).

81 Spain, A. *et al.* Mild fluid percussion injury in mice produces evolving selective axonal pathology and cognitive deficits relevant to human brain injury. *Journal of neurotrauma* **27**, 1429-1438, doi:10.1089/neu.2010.1288 (2010).

82 Alder, J., Fujioka, W., Lifshitz, J., Crockett, D. P. & Thakker-Varia, S. Lateral fluid percussion: model of traumatic brain injury in mice. *Journal of visualized experiments : JoVE*, doi:10.3791/3063 (2011).

83 Shultz, S. R. *et al.* Repeated mild lateral fluid percussion brain injury in the rat causes cumulative long-term behavioral impairments, neuroinflammation, and cortical loss in an animal model of repeated concussion. *Journal of neurotrauma* **29**, 281-294, doi:10.1089/neu.2011.2123 (2012).

84 Lighthall, J. W. Controlled cortical impact: a new experimental brain injury model. *Journal of neurotrauma* **5**, 1-15 (1988).

85 Dhillon, H. S., Donaldson, D., Dempsey, R. J. & Prasad, M. R. Regional levels of free fatty acids and Evans blue extravasation after experimental brain injury. *Journal of neurotrauma* **11**, 405-415 (1994).

86 Chen, S. F., Hsu, C. W., Huang, W. H. & Wang, J. Y. Post-injury baicalein improves histological and functional outcomes and reduces inflammatory cytokines after experimental traumatic brain injury. *British journal of pharmacology* **155**, 1279-1296, doi:10.1038/bjp.2008.345 (2008).

87 Koshinaga, M. *et al.* Rapid and widespread microglial activation induced by traumatic brain injury in rat brain slices. *Journal of neurotrauma* **17**, 185-192 (2000).

88 Smith, D. H. *et al.* A model of parasagittal controlled cortical impact in the mouse: cognitive and histopathologic effects. *Journal of neurotrauma* **12**, 169-178 (1995).

89 Gao, X. & Chen, J. Mild traumatic brain injury results in extensive neuronal degeneration in the cerebral cortex. *Journal of neuropathology and experimental neurology* **70**, 183-191, doi:10.1097/NEN.0b013e31820c6878 (2011).

90 Hylin, M. J. *et al.* Repeated mild closed head injury impairs short-term visuospatial memory and complex learning. *Journal of neurotrauma*, doi:10.1089/neu.2012.2717 (2013).

91 Laurer, H. L. *et al.* Mild head injury increasing the brain's vulnerability to a second concussive impact. *Journal of neurosurgery* **95**, 859-870, doi:10.3171/jns.2001.95.5.0859 (2001).

92 Rubovitch, V. *et al.* A mouse model of blast-induced mild traumatic brain injury. *Experimental neurology* **232**, 280-289, doi:10.1016/j.expneurol.2011.09.018 (2011).

93 Lu, J. *et al.* Effect of blast exposure on the brain structure and cognition in Macaca fascicularis. *Journal of neurotrauma* **29**, 1434-1454, doi:10.1089/neu.2010.1591 (2012).

94 Elder, G. A. *et al.* Blast exposure induces post-traumatic stress disorder-related traits in a rat model of mild traumatic brain injury. *Journal of neurotrauma* **29**, 2564-2575, doi:10.1089/neu.2012.2510 (2012).

95 Kochanek, P. M. *et al.* Screening of biochemical and molecular mechanisms of secondary injury and repair in the brain after experimental blast-induced traumatic brain injury in rats. *Journal of neurotrauma* **30**, 920-937, doi:10.1089/neu.2013.2862 (2013).

96 Sosa, M. A. *et al.* Blast overpressure induces shear-related injuries in the brain of rats exposed to a mild traumatic brain injury. *Acta Neuropathologica Communications* **1**, 51 (2013).

97 Koliatsos, V. E. *et al.* A mouse model of blast injury to brain: initial pathological, neuropathological, and behavioral characterization. *Journal of neuropathology and experimental neurology* **70**, 399-416, doi:10.1097/NEN.0b013e3182189f06 (2011).

98 Signoretti, S., Vagnozzi, R., Tavazzi, B. & Lazzarino, G. Biochemical and neurochemical sequelae following mild traumatic brain injury: summary of experimental data and clinical implications. *Neurosurgical focus* **29**, E1, doi:10.3171/2010.9.FOCUS10183 (2010).

Chapter 2

2. Development, optimization and characterization of a novel mouse model of concussive brain injury:

2.1. Introduction:

There is growing recognition that for both repetitive and single moderate to severe injuries, the adverse effects of traumatic brain injury (TBI) may continue for many years after the original event, with trauma representing the strongest environmental risk factor for developing neurodegenerative disorders, including Alzheimer's disease (AD)[1-4]. Studying mild brain injury (mTBI) in humans is challenging, as it is restricted to cognitive assessment and brain imaging to evaluate such injuries, thus there is a dire need in the field of TBI research for better animal models in order to elucidate the pathobiology that follows post single and repetitive mTBI (s-mTBI and r-mTBI). Although the full complexity of human brain injury cannot be completely addressed in laboratory models, they offer the ability to investigate molecular and neurophysiological changes from minutes to days following nonfatal injury.

While in vitro TBI models are a strong tool to test detailed aspects of biological mechanism, they generally have not been exploited for discriminating between the different types of TBI (e.g. mild, moderate or severe), long term studies (effect of aging), and for treatment strategies. However, they have been of special interest to elucidate specific mechanisms outside a complex biological environment such as the brain. Such models use a pulse wave or a vacuum pulse to stretch neuronal and glial cells[5,6]. For example Tang et al used a model of dynamic stretch injury of cortical axons to determine the potential mechanisms between microtubule damage, partial transport interruption and axonal varicosities in traumatic axonal

injury[7]. Because the objective of this work is to understand the long term effect of single and repetitive mTBI, an in vivo model will provide critical insights into the evolution of mTBI pathobiology.

Different animal models that have been studied to characterize the consequences of TBI include pigs[8-10] and primates[11], but primarily these studies have been performed using rodents[12-19]. Our choice of a murine model was driven by the future potential to study this mTBI model in mice genetically modified at loci of relevance to TBI such as Apolipoprotein E (APOE) or Tau. The CHI model used in this study is more representative of mTBI/concussive conditions than invasive brain injury models such as fluid percussion injury (FPI) or controlled cortical impact (CCI) that require a craniectomy, which itself can confer profound proinflammatory and behavioral damages[20]. It is also amenable to the study of repeated concussions and, in terms of reproducibility, incorporates an electromagnetic (EM) coil-based delivery device, which delivers consistent strike velocities[21,22]. To date, published mouse models of CHI have typically investigated the effect of a single mTBI or two mTBIs with an inter-injury interval of 24 h[14,18,19,23]. A single mTBI has been shown to cause subtle and transient behavioral and immunohistochemical abnormalities, whereas two such injuries 24 h apart worsened the outcome[14,15,18,19]. Unfortunately, little is known about the cumulative consequence of more than two brain injuries at multiple time intervals, as investigations of this nature are scarce and have predominantly employed the weight drop model[12,13,24,25]. In this study, we addressed this void by examining mice subjected to one mTBI (s-mTBI) or a total of five mTBIs (r-mTBI). Moreover, our interconcussive interval was 48 h, a temporal window

during which the mouse brain is known to be vulnerable to subsequent injuries[15] which mimics human situations (combat or sports) where additional injuries are sustained prior to full recovery from the previous injury. The purpose of these studies was to develop a reliable and robust mouse model of mTBI/concussion to investigate the neurobehavioral and neuropathological consequences of single and repetitive injury, and provide a platform for investigation of the long-term consequences of mTBI, particularly r-mTBI.

2.2. Materials and Methods:

2.2.1. Animals:

Male, C57BL/6J mice (10 weeks, 24–30g, Jackson Laboratories, Bar Harbor, ME) were singly housed under standard laboratory conditions (23°C ±1C, 50% ±5% humidity, and 12 h light/dark cycle) with free access to food and water throughout the study. Mice were allowed to adapt to the vivarium for 1 week prior to experimental procedures. All procedures involving mice were performed under Institutional Animal Care and Use Committee approval and in accordance with the National Institute of Health Guide for the Care and Use of Laboratory Animals.

2.2.2. Optimization of the closed head injury model:

A separate group of 28 animals was used for survival studies and optimization of the mTBI model. All of these mice were euthanized 24h after the single or last injury/anesthesia for pathological analyses.

Group I (n=6): 3 animals with s-mTBI (injury parameter at 5 m/sec, strike depth of 1.3 mm) and 3 control/sham injury animals (3 min anesthesia).

Group II (n=6): 3 animals with s-mTBI (injury parameter at 5 m/sec, strike depth of 1.8 mm) and 3 controls (3 min anesthesia).

Group III (n=6): 3 animals with s-mTBI (injury parameter at 3 m/sec, strike depth of 1.0 mm) and 3 controls (3 min anesthesia). This group was sacrificed 24H post injury and was solely used for pathology.

Group IV (n=10): 5 animals with r-mTBI (injury parameter at 5 m/sec, strike depth of 1.0 mm) over a period of 10h (1 injury every 2h) and 5 control animals (3 min anesthesia every 2 hours).

In addition to these 4 groups, there have been different survival studies to address other injury parameters such as the dwell time (impact duration), frequency of the injury and the stereotaxic positioning of the probe on the skull.

2.2.3. Injury groups and schedules for the novel mTBI model:

For the behavioral analyses, a total of 48 mice were ~~randomly~~ assigned to one of four groups: single injury, single sham (anesthesia alone), repetitive injury (total of five hits with an interconcussion interval of 48 h), and repetitive sham (five anesthesias, 48 h apart); (Table.2.1). The behavior analysis began 24 h after the sole/last mTBI/anesthesia for each group (Fig.2.1). Behavior outcomes were assessed by an experimenter blinded to group assignment. For histological examination, a total of 35 mice were ~~randomly~~ assigned to one of five treatment

groups: single injury, single sham, repetitive injury, repetitive sham (all euthanized at 24 h post sole/ last mTBI/anesthesia), and single injury euthanized at 10 days post mTBI (s-mTBI-10D). The s-mTBI-10D treatment group was included to enable comparison of the consequences of one hit versus five hits at the same time point after the first injury. The mice used for behavior analysis were aged to be further assessed at 6, 12, and 18 months post injury as presented in the following chapter (Chapter 3). Separate cohorts of mice were used for histological analysis at 6, 12 months' time points.

Study	Injury status	n	Survival time
Behavior	s-sham	12	> 1 year
	s-mTBI	12	> 1 year
	r-sham	12	> 1 year
	r-mTBI	12	> 1 year
Histology	s-sham	7	24H
	s-mTBI	7	24H
	s-mTBI	7	10 Days
	r-sham	7	10 Days
	r-mTBI	7	10 Days

Table.2.1: Summary of the injury groups at acute time points.

Figure 1

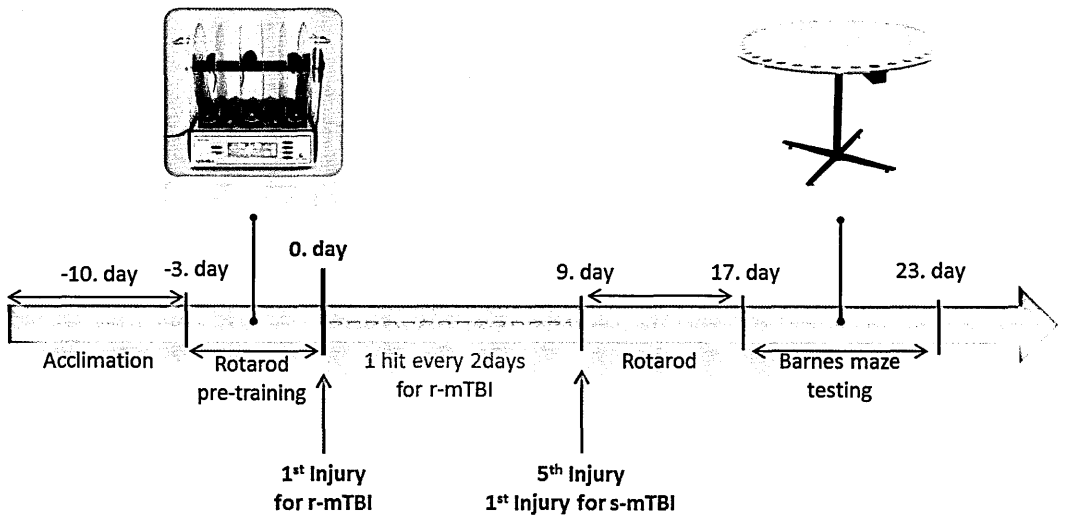

Figure.2.1: Outline of experimental schedule.

2.2.4. Injury protocol:

Mice were anesthetized with 1.5 L/min of oxygen and 3% isoflurane and, after its head was shaved, each mouse was transferred into a stereotaxic frame (Just For Mice Stereotaxic, Stoelting, Wood Dale, IL) mounted with an EM controlled impact device (Impact One^{TM} Stereotaxic Impactor, Richmond, IL), (Fig.2.2). The animals were placed on a heating pad to maintain their body temperature at 37°C and noninvasive rubber pads were adjusted in height to level the skull. The head holders were positioned such that lateral movements would not occur when the head was impacted. A 5 mm blunt metal impactor tip was retracted and positioned above the sagittal suture midway before each impact (Fig. 2.3). The injury was triggered using the myNeuroLab controller at a strike velocity of 5 m/sec, strike depth of 1.0 mm, and dwell time of 200 ms; these parameters selected after pilot experiments revealed that a strike velocity > 5 m/sec and/or strike depth > 1.0 mm resulted in skull fracturing. Based on

the manufacturer's instructions, the force applied to the mouse head at the time of impact is 72N under these conditions. At the end of the procedure, the animal was removed from the stereotaxic table and allowed to recover on a heating pad and, upon becoming ambulatory, was returned to its home cage. No pre-operative or post-operative analgesic administration in addition of the anesthesia was given to the mice. Post-surgery, animals were given soft food and closely monitored for 48 h, and then daily for the following 5 days. For the r-mTBI group, additional injuries were administered at days 3, 5, 7, and 9 after the original injury. Sham injured animals underwent the same procedures and anesthesia duration on each occasion, but did not receive a hit, in order to control for the effects of repeated anesthesia.

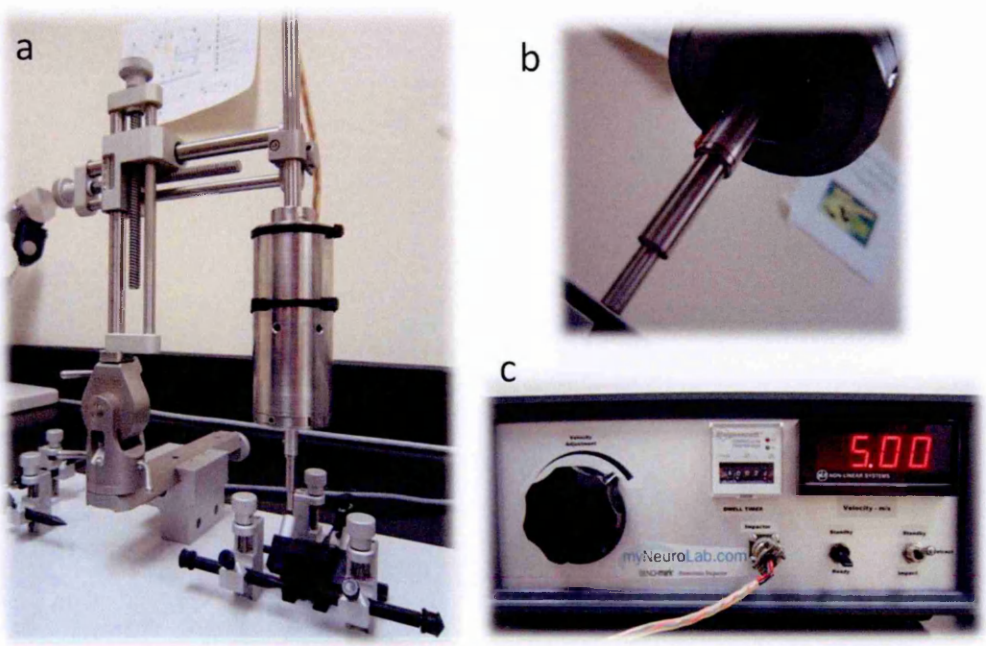

Figure.2.2: Photograph of the EM controlled impact device for mTBI mounted on the Just For Mice™ Stereotaxic table (a), a 5 mm diameter impactor tip (b) and myNeuroLab controller (c).

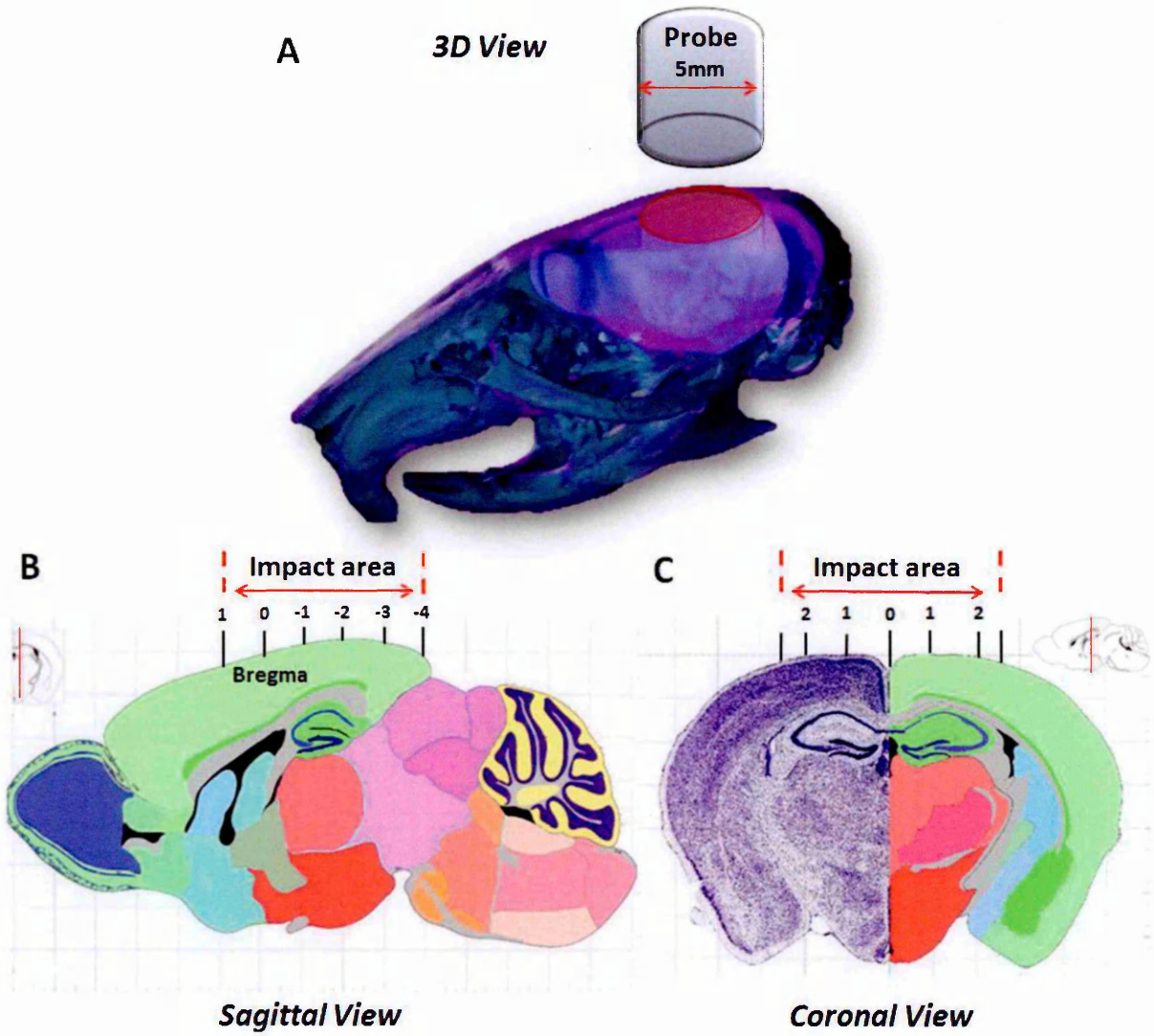

Figure.2.3: Stereotaxic location of the 5 mm impactor tip on the head surface. Three-dimensional view (A) (image adapted with permission from Stephen Larson http://wholebraincatalog.org), sagittal view (B), and coronal view (C) (Images adapted from Franklin et al., 2001)[26].

2.2.5. Assessment of righting reflex and traumatic apnea:

Immediately after termination of anesthesia of both impacted and sham groups, each animal was placed on its back and the latency period to return to an upright position was recorded. Apnea duration was visually measured after each injury as the time to return to

spontaneous breathing. The time taken by injured and sham animals to return to an upright position and the traumatic respiration depression following each injury was recorded as an indicator of restoration of neurological function.

2.2.6. Assessment of motor function:

The rotarod apparatus (Ugo Basile, Varese, Italy) was used to assess motor performance following the injury paradigm, with performance evaluated by measuring the latency to remain on an elevated rotating accelerating rod (3 cm in diameter). Three acclimation trials were performed at a fixed speed of 5 revolutions per minute (RPM) with a 3 min duration. Rotarod pre-training (to establish a performance baseline) was conducted at linear accelerating speed of 5–50 RPM for three trials per day for 3 consecutive days. Each trial lasted a maximum of 5 min with a 3 min rest interval to avoid fatigue. Rotarod testing started 24 h following the sole/last mTBI or anesthesia. For each trial, latency to fall was recorded by an experimenter blinded to group assignment. The trial was also terminated if the animal spun around the rod through three complete revolutions. Testing occurred on days 1, 3, 5, and 7 after the sole/last mTBI/anesthesia.

2.2.7. Assessment of cognitive function:

Two different cognitive-behavioral tests were available to assess spatial memory and learning in rodents. The Morris water maze (MWM), originally designed for rats, uses a pool of water containing an escape platform hidden a few millimeters below the water surface. Visual cues, such as pictures and colored stickers are placed around the pool in sight of the animal to orient themselves. Since its conception the MWM has been widely used in behavioral neuroscience

and optimized to fit neurobehavioral tests in mice. The Barnes Maze (BM) is similar to the Morris water navigation task, but does not utilize a strong aversive stimulus (stress induced by swimming such as in the MWM). If stress is the main driver of MWM performance as suggested by Harrison and colleagues[27], then it may mask spatial memory impairments resulting from mTBI. After the final day of rotarod testing, cognitive function was evaluated using the BM over the MWM. Ethovision XT (Noldus, Wageningen, Netherlands) was used to track and record the movement of each animal. Mice were given 90 sec to locate and enter the target box, and they were required to remain in the target box for 30 sec prior to retrieval, regardless of success. For a period of 6 days, four trials were given per day, with mice starting from one of four cardinal points on each trial. On the 7th day, a single probe trial lasting 60 sec was performed with the mouse starting from the center of the maze and the target box removed. An Ethovision XT system was used to continually record the position of the mouse and measure the distance from the target box 30 times per second for the duration of each trial. The sum of that value was expressed as cumulative distance from target hole. Escape latency was measured as the time taken for the mouse to enter the box.

2.2.8. Tissue processing:

All mice were euthanized 24 h after their last injury/sham injury except for one group that was euthanized 10 days after a single mTBI. All mice were anesthetized with isoflurane perfused transcardially with heparinized PBS, pH 7.4 followed by PBS containing 4% paraformaldehyde. After perfusion, the brains were postfixed in a solution of 4% paraformaldehyde at 4°C for 48 h. The intact brains were then blocked and processed in

paraffin using Tissue-Tek VIP (Sakura, USA). The processing schedule was 1.5 h in each graded ethanol bath (70%, 80%, 95% and three 100%), followed by three xylene baths of 2 h each, and finally four paraffin baths at 60 °C of 2h each. Sagittal (n = 4 brains/group) and coronal (n = 3 brains/group) 6 µm sections were cut with a microtome (2030 Biocut, Reichert/Leica, Germany) and mounted on positively charged glass slides (Fisher, Superfrost Plus).

2.2.9. Histology:

Prior to staining, sections were deparaffinized in xylene, and rehydrated in an ethanol to water gradient. For each group, sets of sagittal (lateral 0.2–0.4 mm) and coronal (- 1.5 and - 3.0 mm relative to bregma) sections were cut. Each slide was visualized with a bright field microscope (Leica, Germany) and digital images were scanned without zoom and with a resolution of 16896 x 26624 pixels for further analysis with a NanoZoomer (Hamamatsu, Japan). The slides were viewed using Slidepath Digital Image Hub software. As a negative control, one section was incubated with all reagents except the primary antibody. Tissue sections were subjected to antigen retrieval with either heated tris-ethylenediaminetetraacetic acid (EDTA) buffer (pH 8.0) or modified citrate buffer (Dako, Glostrup, Denmark, S1699) under pressure. Endogenous peroxidase activity was quenched with a 15 min H_2O_2 treatment (3% in water). Each section was rinsed and incubated with the appropriate blocking buffer (ABC Elite kit, MOM kit, Vector Laboratories, CA) for 20 min, before applying the appropriate primary antibody overnight at 4°C. Then, the diluted biotinylated secondary antibody from the ABC Elite Kit was applied on each glass slide. Antibodies were detected using the avidin-peroxidase complex, and labeling was revealed after incubating the sections in 3,3'-diaminobenzidine (DAB) peroxidase

solution (0.05% DAB - 0.015% H_2O_2 in 0.01M PBS, pH 7.2) for 6–7 min and counterstained with hematoxylin.

2.2.9.1. Haemotoxylin and Eosin staining

A series of sections, mounted on glass slides, were dried for 30 min at 60°C before being stained with Haemotoxylin and Eosin (H&E). Each slide was re-hydrated with Histo-clear (10 min), and alcohol (100% x2 and 95% x2 30 sec each). Following a 30 sec rinse in running tap water, sections were transferred in a solution of Mayer's Haematoxylin for 5 min. Sections were then rinsed a second time followed by a 5 to 10 sec dipping in 1% acid alcohol to differentiate the nuclei. Sections were rinsed again in running tap water followed by a differentiation step in Scott tap water substitute until sections turned blue. After another wash in tap water, the slides were finally immersed in a solution of eosin for 1 minute. The slides were dehydrated with ethanol (95% x2 30 sec each, then 100%x2 30 sec each) followed by two baths of xylene for 3 minutes each. Mounting medium was applied to coverslip and sections were viewed by light microscope.

2.2.9.2. Luxol fast blue staining

A series of sections, mounted on glass slides, were dried for 30 min at 60°C before being stained with luxol fast blue (LFB) and cresyl violet. Each slide was re-hydrated with Histo-clear (10 min), and alcohol (100% x2 and 95% x2 30 sec each). Following a 30 sec rinse in running tap water, sections were transferred in a solution of LFB for 4 h in an oven at 60°C. The excess of stain was then removed with a bath of 95% ethanol. Following a 2 minutes wash in running tap water, the sections were dipped (5-15 sec) in a differentiator bath of 0.05% aqueous lithium

carbonate until the grey matter could be distinguished from white matter. This step was repeated until the nuclei were discolored and sections were then rinsed in running tap water for one minute and transferred to 0.1% cresyl violet solution for 5 minutes. Sections were differentiated in 95% acidic alcohol and rinsed in fresh 95% alcohol followed by dehydration and mounting.

2.2.9.3. Amyloid precursor protein:

A series of sections, mounted on glass slides, were dried for 30 min at 60°C before being stained with amyloid precursor protein (APP) primary antibody (1:40,000 in super sensitive wash buffer, Biogenex, Fremont, CA; monoclonal antibody to the N-terminus, Millipore, Billerica, MA, MAB348.) by overnight incubation at 4°C. Tissue sections were subjected to antigen retrieval with heated tris-ethylenediaminetetraacetic acid (EDTA) buffer (pH 8.0). After three washes (10 min each) in PBS, sections were then incubated as described in the MOM kit (Vector Laboratories). After applying the Avidin/Biotin HRP complex for 30 min, each slide was stained for 7 min with the Vector DAB kit (Vector Laboratories).

2.2.9.4. Glial fibrillary acidic protein:

A series of sections, mounted on glass slides, were dried for 30 min at 60°C before being stained with GFAP antibody (GFAP, 1:20,000 in super sensitive wash buffer, Biogenex, Fremont, CA; Dako, Glostrup, Denmark, ZO334) by overnight incubation at 4°C. After three washes (10 min each) in PBS, sections were then incubated as described in the ABC kit (Vector Laboratories). After applying the Avidin/Biotin HRP complex for 30 min, each slide was stained for 7 min with the Vector DAB kit (Vector Laboratories).

2.2.9.5. Ionized calcium binding adaptor molecule 1:

A series of sections, mounted on glass slides, were dried for 30 min at 60°C before being stained with Iba-1 antibody (Anti-Iba1, 1:5000 in super sensitive wash buffer, Biogenex, Fremont, CA; Abcam, Cambridge, MA, ab5076) by overnight incubation at 4°C. Tissue sections were subjected to antigen retrieval with a solution of citrate buffer (Dako, Glostrup, Denmark, S1699) under pressure. After three washes (10 min each) in PBS, sections were then incubated as described in the ABC kit (Vector Laboratories). After applying the Avidin/Biotin HRP complex for 30min, each slide was stained for 7 min with the Vector DAB kit (Vector Laboratories).

2.2.10. Immunohistochemical quantification:

For each animal, sets of sagittal (n = 4) and coronal (n = 3) sections were stained and analyzed by an observer blinded to experimental conditions using ImageJ software (US National Institutes of Health, Bethesda, MD). Using this software, images were separated into individual color channels (hematoxylin counter stain and DAB chromagen) using the color deconvolution algorithm[28]. While a semi-automated program allowed the threshold setting to be applied as a constant to all images, this was not done due to immunostaining intensity variation between batches of immunostaining. Therefore, each slide had unique parameters set to determine the optimal segmentation (threshold setting) based on the intensity of immunostaining for each antibody. Immunoreactive profiles discriminated in this manner were used to determine the ratio between the area of the counted object (the immunostained area) to the defined field (areas of interest). Two non-overlapping areas of 200 μm^2 in the CA1 region (Fig.2.4A) and two non-overlapping areas of 150 μm^2 in the body of the corpus callosum (CC) were selected within

which the area of GFAP immunoreactivity was calculated and expressed as a percentage of the field of view. Two non-overlapping areas of 200 μm^2 in the cortex underlying the impact site and three non-overlapping areas of 100 μm^2 in the body of the CC were selected within which the area of anti-Iba1 immunoreactivity was calculated and expressed as a percentage of the field of view. APP-immunohistochemistry was quantified in discrete areas, namely the CC and the brainstem (BS) (lateral 0.2–0.4 mm). The numbers of APP-positive profiles were counted in three non-overlapping areas of 100 μm^2 within the body of the CC (Fig.2.4B), and two non-overlapping areas of 200 μm^2 within the BS. Immunoreactive axonal profile counts from the four sections from each animal (n = 4) were then averaged, and all were combined for each group to determine a mean value. Overt cell death was determined by assessing the density of degenerating neurons (acidophilic with shrunken perikarya and pyknotic nuclei) per μm^2 in H&E stained sections (lateral 0.2–0.4 mm). The percentage of degenerating neurons in CA1 regions in the ipsilateral and contralateral hippocampus was then averaged across four sections to evaluate histological changes in each group.

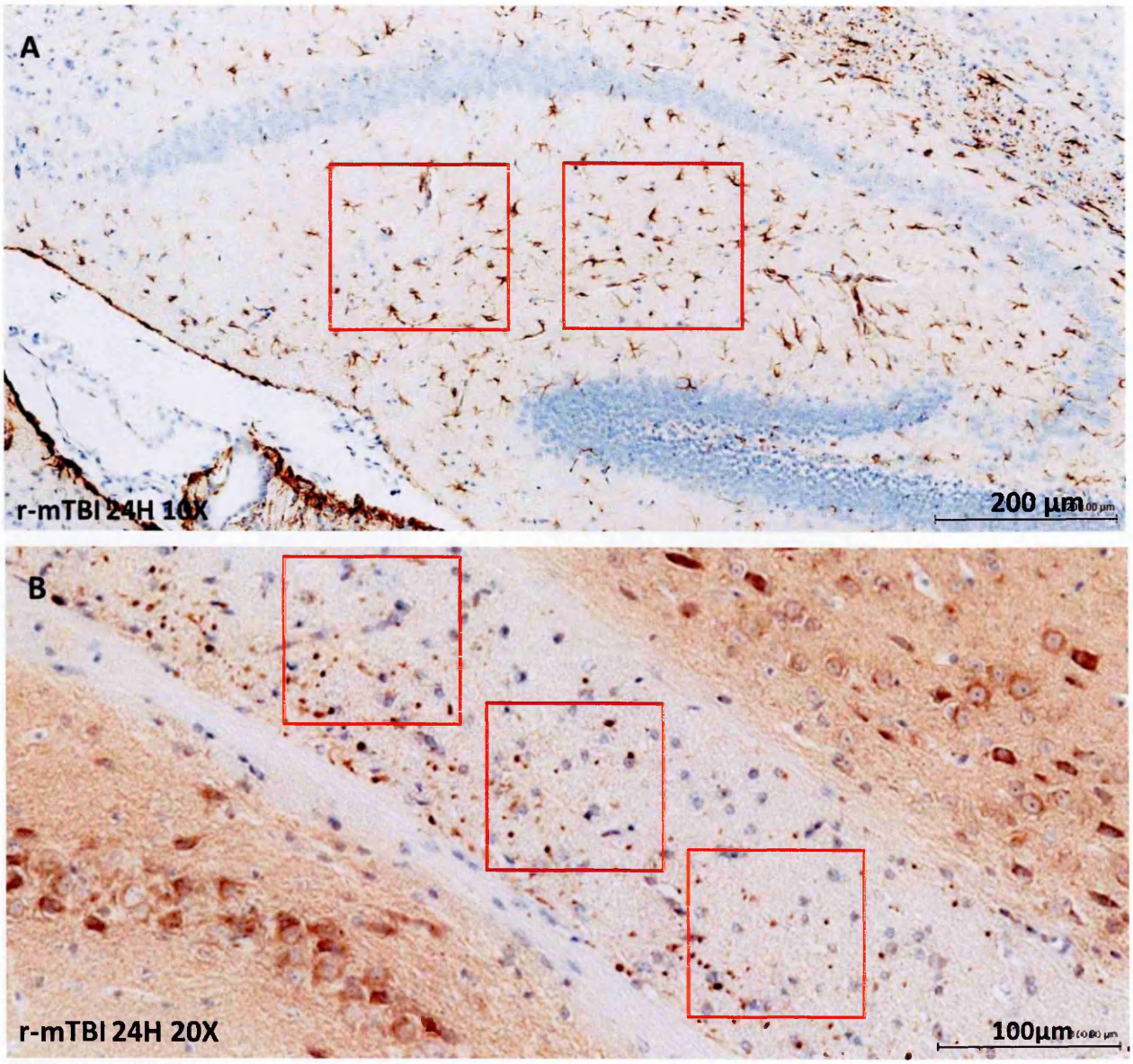

Figure.2.4: Examples of quantitative assessment techniques used to calculate the area of GFAP immunoreactivity in the hippocampus (A) and the number of numbers of APP-positive profiles in the corpus callosum (B).

2.2.11. Statistical analysis:

All data were analyzed using JMP 8.0 (SAS, Cary, NC). Data were tested for normality using the Shapiro–Wilk W test; when not normally distributed, the data were transformed using

square root or natural log transformation. If the data were still not normal after transformation, they were analyzed using nonparametric methods. Normally distributed data were analyzed using parametric methods such as analysis of variance (ANOVA) followed by Tukey's post-hoc correction for multiple comparisons. Repeated measures ANOVA were used to compare performance between cohorts for both rotarod and BM experiments. Only p values < 0.05 were considered to be statistically significant (indicated by an asterisk in the figures).

2.3. Results:

2.3.1. Optimization of the closed head injury model:

Using the cohort of mice for survival studies and optimization of my CHI model, I found that an impact with a depth greater than 1 mm, and faster than 5m/sec, although non-lethal, increased the amount of skull fractures. As illustrated in Figure 2.6, the extent of injury was significantly worse when the mice were injured 5 times in a 10 hours period rather than a period of 9 days. 30% of the mice who received 5 hits over a 10 hours period showed mild hemorrhage at various locations such as the cortical layer (Fig.2.5A), olfactory bulb (Fig.2.5B), cerebellum (Fig.2-6C), and brainstem. After these observations, I determined the standardized setting to induce an mTBI to be at a strike velocity of 5m/sec at 1 mm depth with a 48 h injury interval for the r-mTBI.

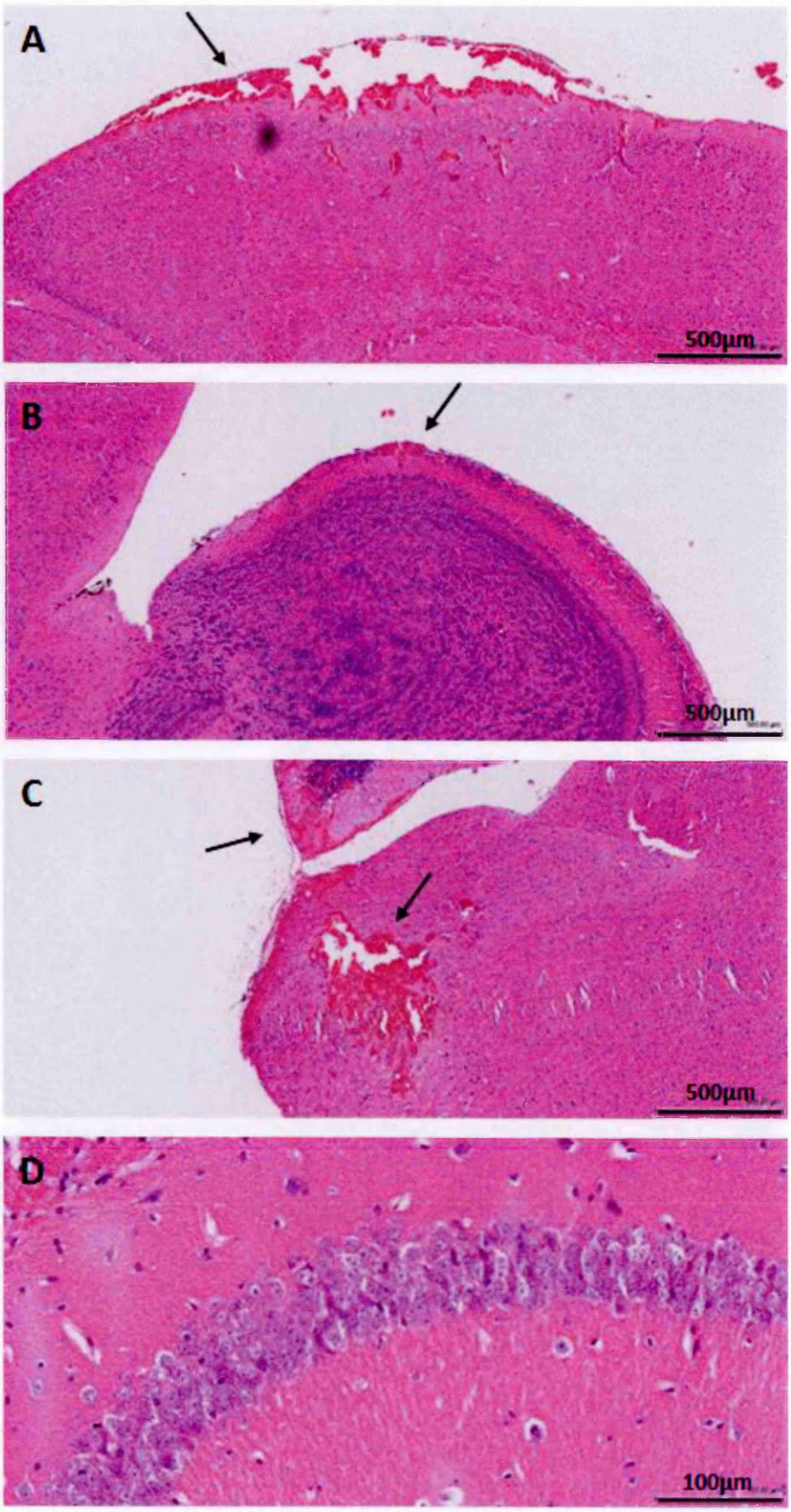
A
500µm
B
500µm
C
500µm
D
100µm

Figure.2.5: Histological images of H&E stained sagittal sections following 5 r-mTBI within 10 h and sacrificed 24 h post last injury. Repetitive-mTBI caused hemorrhages (pointed by arrows) on the cortical surface at the injury site (A), on the surface of the olfactory bulb (B) and within the brain stem (C) at 24h post injury. No damage was observed in the pyramidal cell layer of the hippocampus (D).

2.3.2. Acute neurological response:

Having optimized the conditions for mTBI, single or r-mTBI paradigm or anesthesia control was administered to the study cohort (see section 2.2.3 above). Following CHI, all injured animals demonstrated a period of apnea ranging from 3 to 30 sec followed by a prolonged period of unresponsiveness (3–6 min), (Fig.2.6A). There were no significant differences among impact apneas across injury groups, although the time of apnea did decrease with each mTBI in the r-mTBI group (repeated measures ANOVA). However, we observed significant differences in righting between sham and injured groups (***$p < 0.0001$) (Fig.2.6B). Similar to apnea, the righting reflex recovery duration slightly decreased with each mTBI, although this was not significant (repeated measures ANOVA), (Fig.2.6B). Therefore, regardless of the number of injuries, the traumatic apnea and the time required for recovery of the righting reflex was similar, and did not increase with increasing number of injuries.

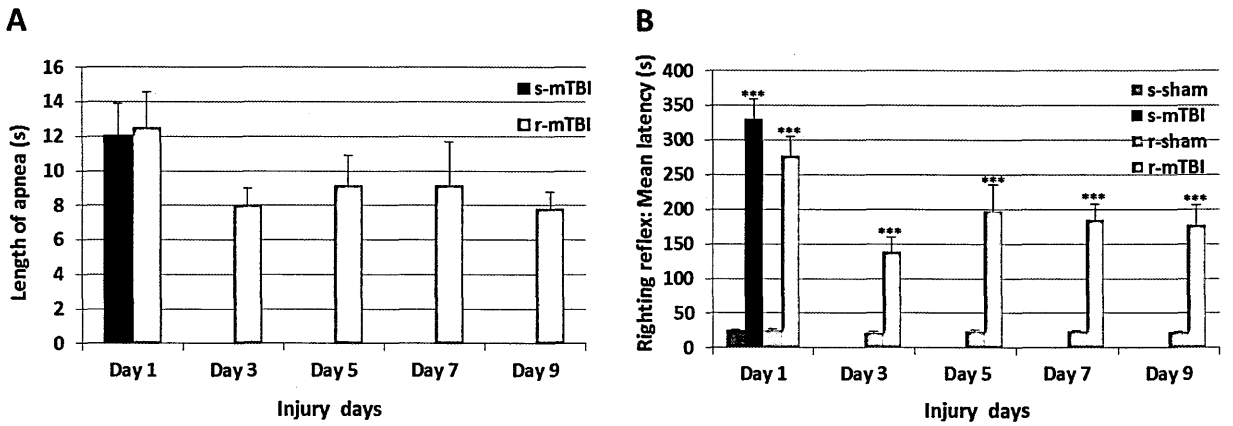

Figure.2.6: Length of traumatic apnea (A) and latency of right reflex (B) were recorded following each anesthesia (n=12 per group). The main effect of injury on traumatic apnea and recovery of the righting reflex was significant (***$p < 0.0001$). The within group effect of days was not significant for either group. Values are presented as mean ± SEM.

2.3.3. Sensorimotor function:

Motor function was evaluated 24 h following the sole/last mTBI/anesthesia. Overall, all animals exhibited a decreased rotarod performance when compared to their last day of pre-training (Fig.2.7). By the last day of rotarod, the s-mTBI and r-mTBI fall latency was shorter than that of their sham controls, 9% and 19% less, respectively (s-mTBI, $p = 0.005$; r-mTBI, $p < 0.001$; repeated measures ANOVA). Mice with a single mTBI improved over the testing period from 90 ± 13% of pre-injury level on day 1 to 95 ± 12% on day 7 (interaction "Injury and test day"; $p < 0.05$; repeated measures ANOVA). In contrast, the r-mTBI mice did not return to an uninjured baseline level; 84 ± 9% of pre-injury level on day 1 to 82 ± 15% on day 7 (interaction "Injury and test day"; $p > 0.05$; repeated measures ANOVA). Rotarod testing was also conducted at 24 and 30 days after the final injury, but by this extended time point the performance of singly or

repetitively injured animals was not different from that of controls, demonstrating the transient nature of the motor deficits.

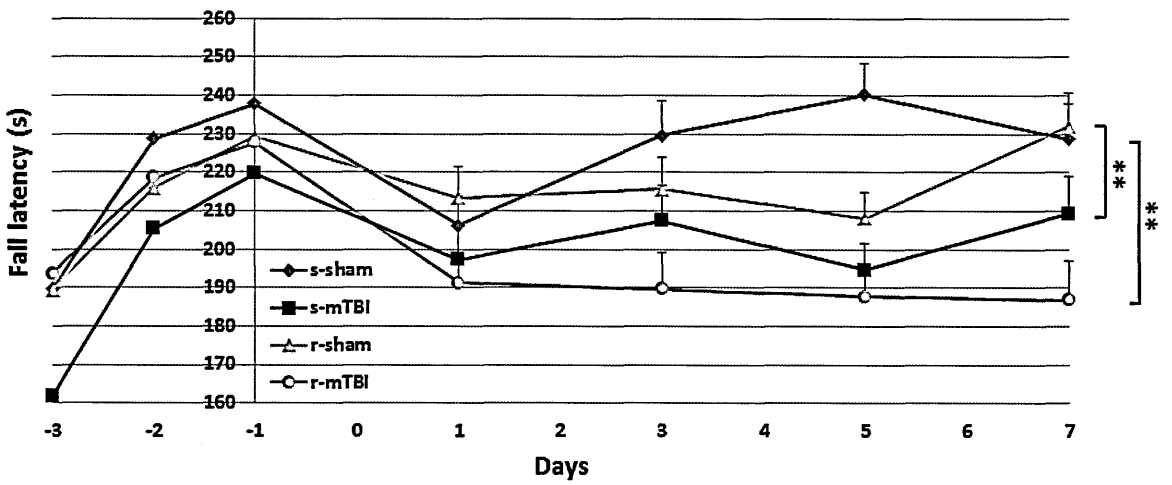

Figure.2.7: Effect of mild traumatic brain injury on rotarod performance. Values were recorded on 7 separate days with three 5 min accelerating trials. Results are the mean ± SEM of the time animals remained on the rotarod before falling. There was a gradation of impairment with multiply injured animals remaining less time on the rod between days 1 and 7 after sole/last mTBI or anesthesia (s-mTBI vs. s-sham [**p = 0.005]; r-mTBI vs. r-sham [**p < 0.001]; [n = 12 per group]).

2.3.4. Cognitive deficits after single and repetitive injury:

Acquisition deficits were observed in brain-injured mice relative to their sham controls (Fig.2.8A and B). Again, we found that the repetitively injured animals were performing worse than the singly injured mice. Although both sham and injured mice were able to find the correct hole by the last day of the acquisition period, both singly and repetitively injured mice had a greater cumulative distance from the hole than their sham controls (52% and 73% further, respectively) (s-mTBI, $p < 0.005$; r-mTBI, $p < 0.0001$; repeated measures ANOVA). Their ability to find a previously learned location of the escape hole was also assessed and all groups

showed improvement in escape latency, but with the r-mTBI group performing worse than controls and the s-mTBI group. Only day 6 from this dataset passed normality testing, and analyzing that day alone, the r-mTBI group was found to be significantly different from the other three groups ($p < 0.0001$). The velocity across each group was similar, (s-sham, 6.3 ± 0.34 cm/s; r-sham, 6.6 ± 0.60 cm/s; s-mTBI, 5.9 ± 0.34 cm/s; r-mTBI, 6.4 ± 0.31 cm/s) indicating that differences in BM performance were not a function of motor deficits.

The probe trial analysis of the average time to reach the target zone, (defined by the target escape hole and its adjacent north and south holes) revealed that the r-mTBI mice performed the worst, requiring on average 15 sec to reach the target zone, followed by the s-mTBI (8.3 sec), the r-sham (4.8 sec), and the s-sham (2.9 sec). For both injury groups, the time to reach the target or adjacent holes was significantly longer than for their sham controls ($p < 0.02$ for both injury groups; ANOVA) (Fig.2.8C). As with the acquisition trials, the average velocity was not significantly different across all four groups ($p > 0.05$).

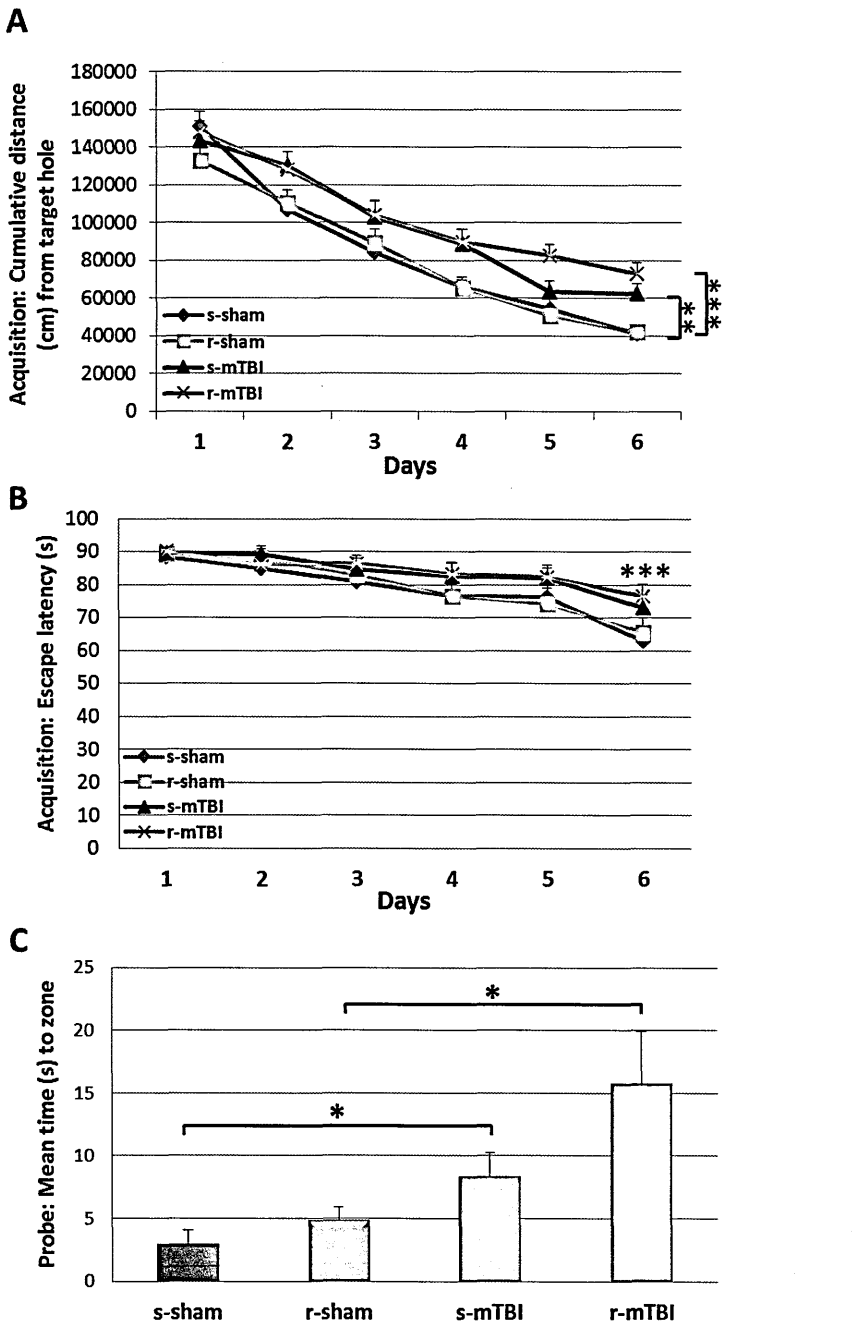

Figure.2.8: Evaluation of learning (acquisition) and spatial memory retention (probe) using the Barnes maze on days 8–14 after sole/ last mild traumatic brain injury (mTBI). Mice were tested in the Barnes maze for their ability to locate a black box at the target hole. During the acquisition testing, both injured groups traveled a greater cumulative distance before escaping to the target hole compared with their respective anesthesia controls, with the r-mTBI groups versus the r-sham group showing a greater significant difference than the s-mTBI groups versus the s-sham group (**s-mTBI, $p < 0.005$; r-mTBI, ***$p < 0.0001$) (A). The mean time to escape to the target hole was longer for the r-mTBI group. On

day 6 of the acquisition trial, the r-mTBI group spent significantly more time escaping to the target hole than did their sham control, r-sham (***$p < 0.0001$) (B). For the probe trial (1 day following the 6 days of acquisition testing), the target box was removed and mice were placed in the middle of the table for a single, 60 sec trial. Although both mTBI groups had a greater latency to reach the target zone than their respective shams (*$p < 0.02$), there was a clear trend for the r-mTBI mice to take longer to reach the target zone (C). The mean velocity for acquisition phase and probe test was similar across all groups. Data are presented as mean ± SEM.

2.3.5. Pathology of single and repetitive injury:

Macroscopic examination of fixed brains revealed focal architectural disturbance with evidence of hemorrhage (<1mm^2) in the inferior surface of the cerebellum in all animals subjected to r-mTBI. These were also evident, but to a lesser extent, in every singly injured mouse at 10 days after injury. Otherwise, there were no focal macroscopic lesions in any of the animals subjected to injury. Specifically, there were no skull fractures, cerebral hemorrhages, or contusions identified using this injury model. Further, examining sections stained for H&E or LFB/CV revealed no evidence of focal structural pathology in the cortex, hippocampus, or hilus of the dentate gyrus (Fig.2.9), with quantification of hippocampal neurons demonstrating no overt cell loss in either the ipsi- or contralateral hippocampi of the injured groups. Animals subjected to s-mTBI displayed no evidence of cerebellar injury at 24 h post- injury (Fig.2.9F). However, at 10 days after single injury, a focal, superficial region of architectural disruption associated with a glial response was observed in the inferior surface of the cerebellum (Fig.2.9I). In the r-mTBI group, this lesion was extensive and extended into underlying white matter (Fig.2.9O).

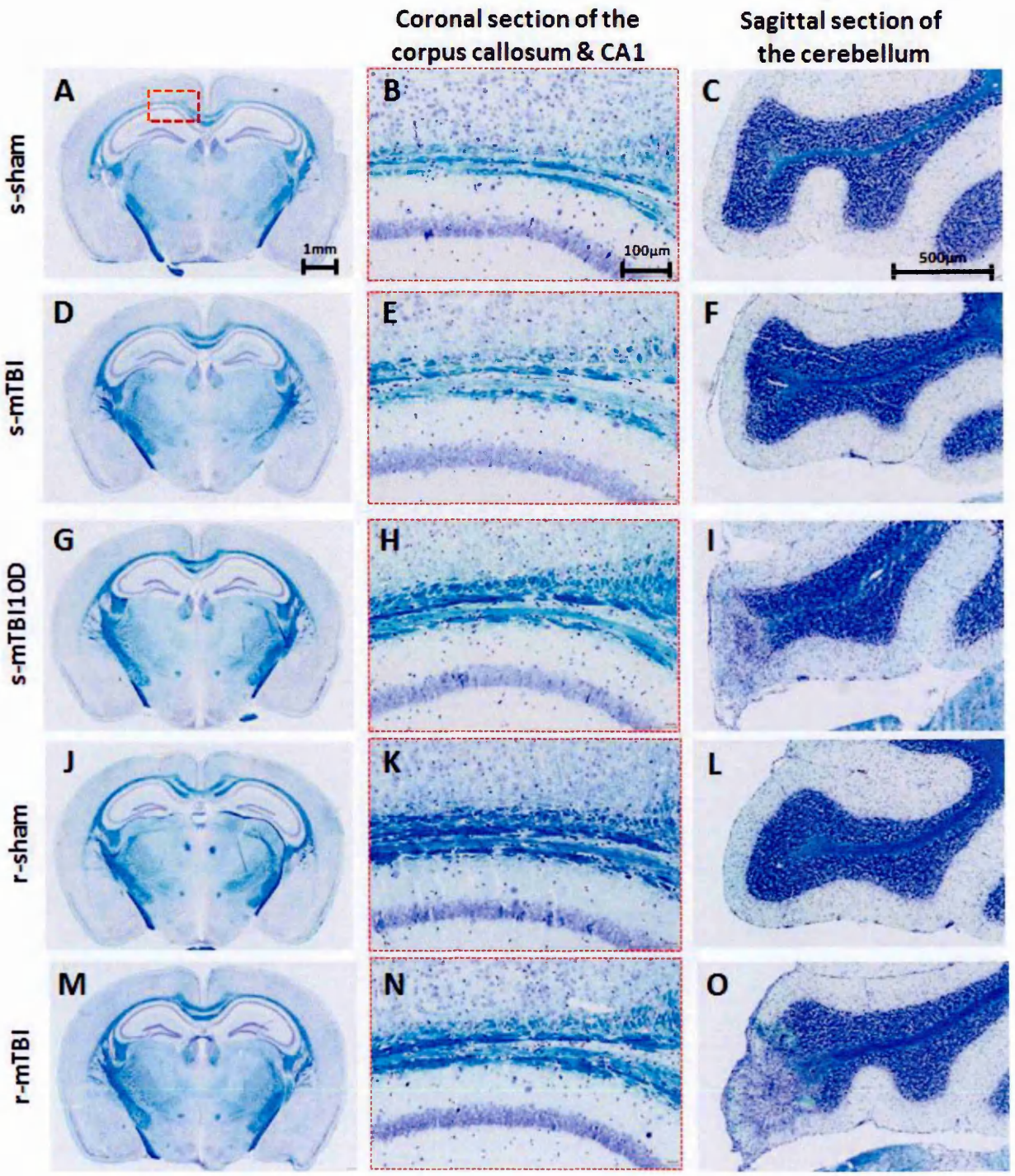

Figure.2.9: Luxol fast blue/cresyl violet staining revealed no overt abnormalities in the cerebral cortex of the injured or non-injured mice. Coronal sections of mouse brain at ≈1.9 mm posterior to bregma (A, D, G, J, M). The red box indicates the region of interest, which is shown at a higher magnification (B, E, H, K, N). Sagittal sections of the cerebellum (0.26 mm lateral to midline) (C, F, I, L, O). A focal region of

architectural disturbance in the inferior surface of the cerebellum was observed in the r-mTBI group (O), which was less extensive in the s-mTBI-10D group (I).

2.3.6. Amyloid precursor protein immunostaining:

Numerous APP-immunoreactive axonal profiles were identified in sections from injured animals (Fig.2.10A and B). These APP immunoreactive axonal profiles were observed as either granular or more elongated, fusiform swellings in the white matter of the parasagittal cortex, the CC, and the spinal trigeminal tracts of the BS. Unique to the r-mTBI group, there was also evidence of cytoplasmic staining in neurons of the primary and secondary motor cortex (Fig.2.10C). APP-immunoreactive axonal profiles were observed 24 h post-injury in the CC of the s-mTBI (Fig.2.11G) and r-mTBI groups (Fig.2.11S) but not in their controls (Fig.2.11C–O). The numbers of APP-immunoreactive profiles in the CC of the s-mTBI was greater than in the r-mTBI group (s-mTBI group 14.4 ± 2.26 vs. r-mTBI 6.0 ± 0.8 axonal profiles/100 μm2; $p < 0.001$; Fig.2.12A). Axonal damage in the BS was minimal in the s-mTBI, whereas greater numbers of punctate immunoreactive swellings were present in the r-mTBI group (s-mTBI 0.4 ± 0.2 vs. r-mTBI 5.2 ± 1 axonal profiles/200 μm^2; $p < 0.001$; Fig.2.12B). By 10 days post-mTBI, no immunoreactive profiles were observed after s-mTBI (Fig.2.11J and K).

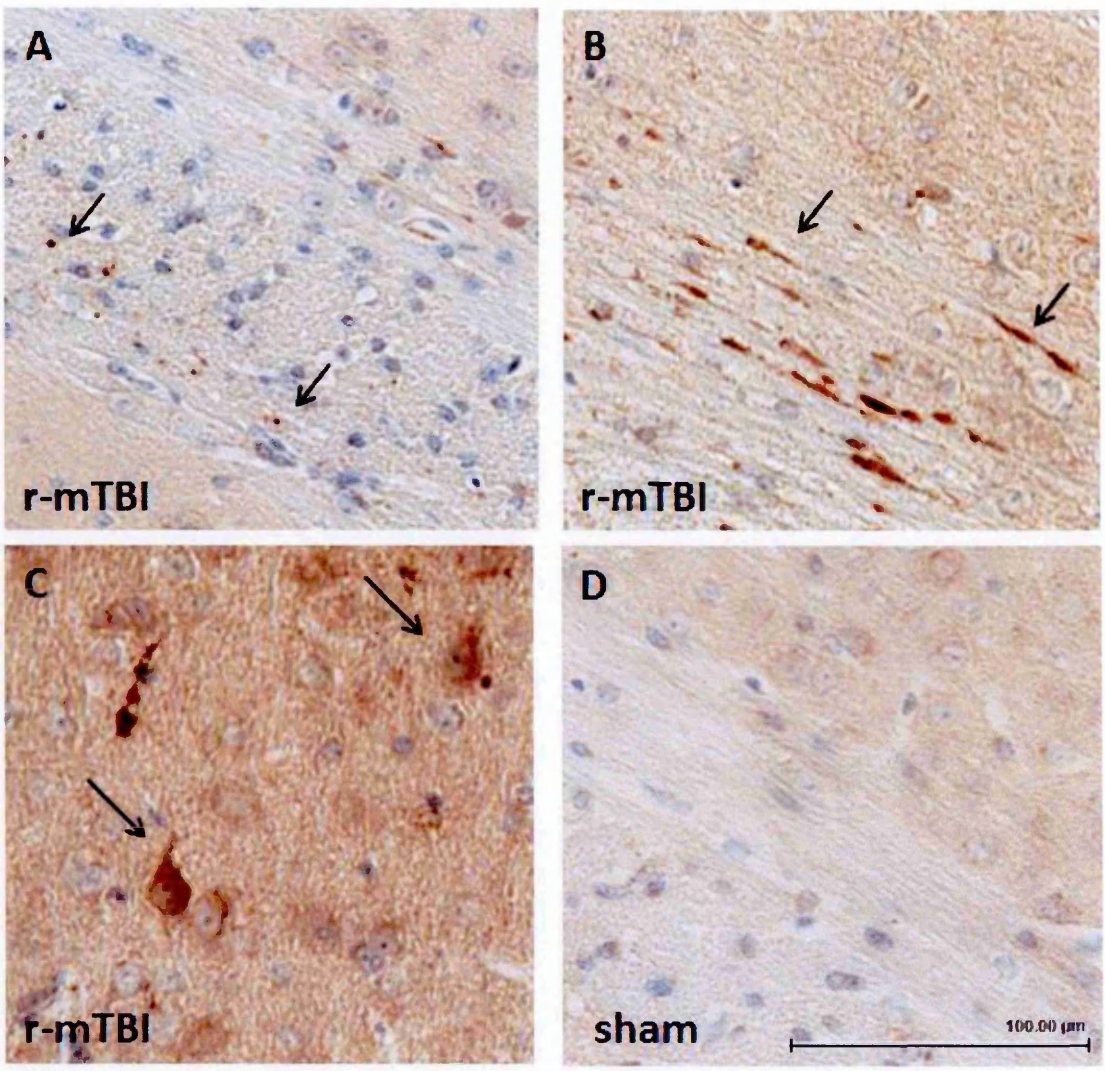

Figure.2.10: Photomicrographs of sagittal sections stained with APP. Immunoreactive axonal profiles were observed as either granular (A) or more elongated, fusiform (B) swellings in both s-mTBI and r-mTBI groups (only the r-mTBI group is displayed). APP immunoreactive neurons were only present in the r-mTBI group, and occasionally observed in the cortex underneath the impact site (C). No APP staining was observed in the sham animals (D). Tissue sections were counterstained with hematoxylin. Scale bar, 100 µm.

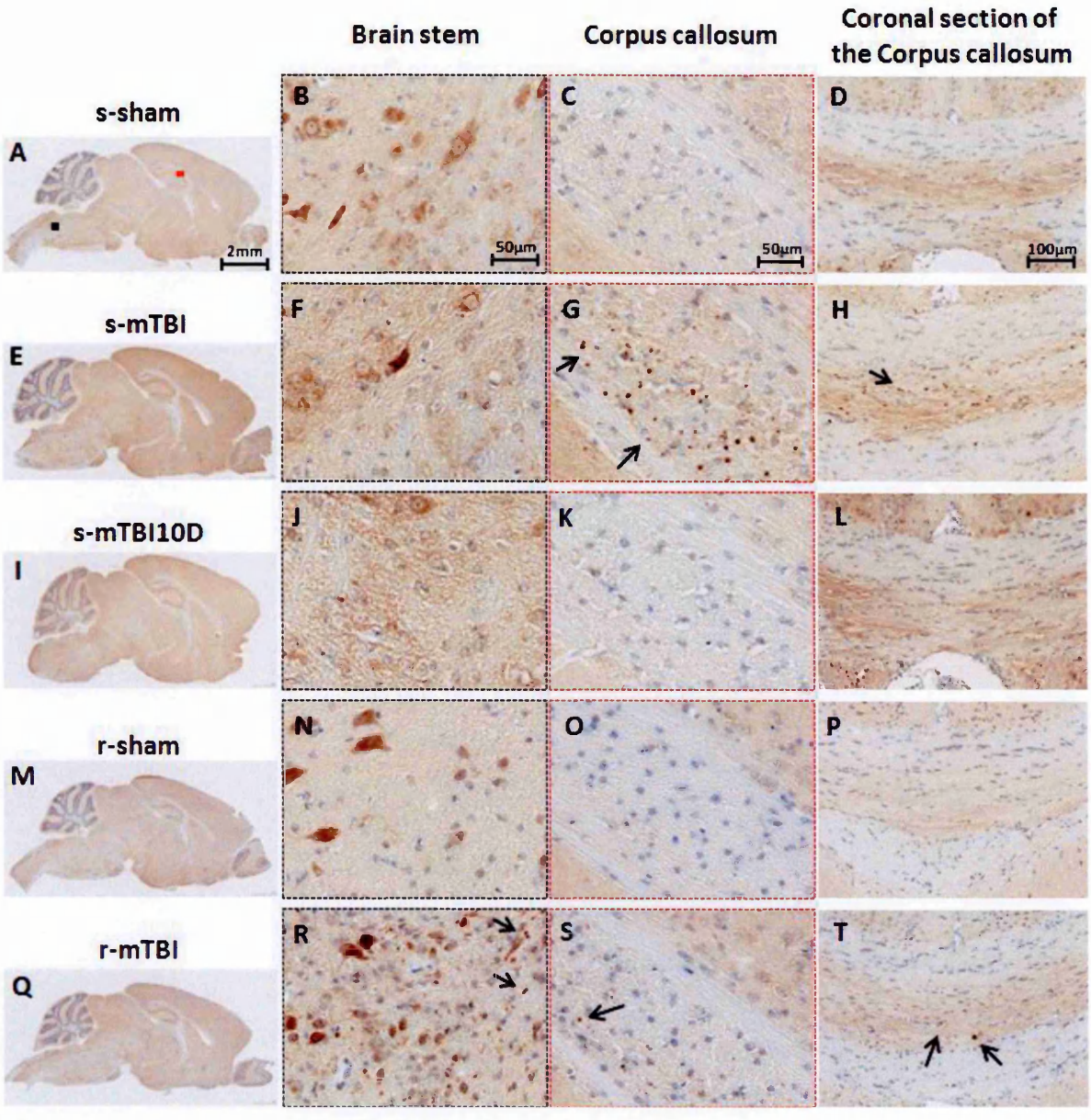

Figure.2.11: Amyloid precursor protein immunohistochemistry of sagittal sections of mouse brain at ≈0.4 mm lateral to the midline in the brainstem (B, F, J, N, R), in the corpus callosum (C, G, K, O, S), and coronal sections ≈2.1 mm posterior to bregma (D, H, L, P, T). Colored boxes indicate areas of interest shown at higher magnification in the right hand panels. Tissue staining from s-sham (A–D), s-mTBI-10D (I–L), and r-sham animals (M–P) was negative for APP immunostaining. Immunoreactive axonal profiles were observed the brainstem in an area underlying the cerebellum in the r-mTBI (R), whereas few such profiles were detected in the s-mTBI group (F). Extensive accumulation of APP was observed as discrete axonal profiles in the corpus callosum of the s-mTBI (G, H), and less in the r-mTBI animals ($p < 0.001$) (S, T). Tissue sections were counterstained with hematoxylin.

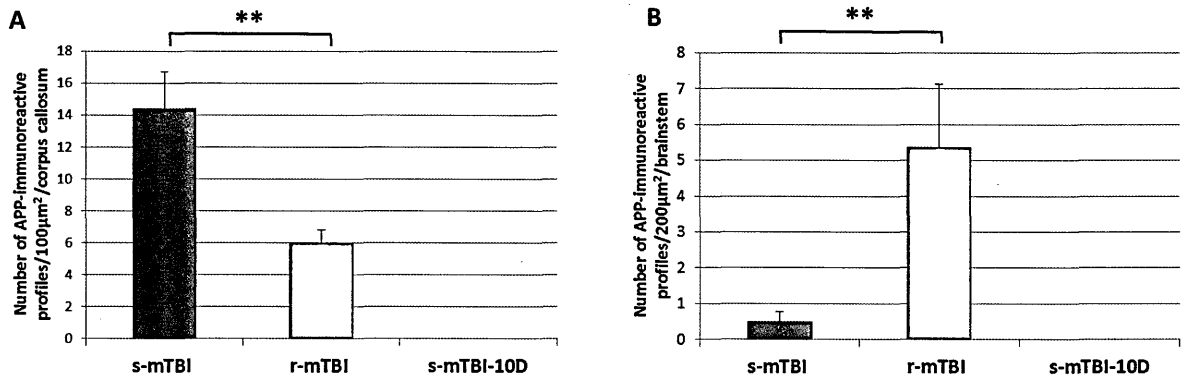

Figure.2.12: Average counts of APP-immunoreactive axonal profiles per μm^2 in the corpus callosum (A) and in the brainstem (B) (n = 4). Fewer axonal profiles were observed in the corpus callosum of the r-mTBI group than in the s-mTBI group (**p < 0.001). APP immunoreactive axonal profiles in the brainstem were observed in the r-mTBI group, whereas only a few were detected in the s-mTBI group (**p < 0.001). Tissue staining from s-sham and s-mTBI-10D animals was negative for APP immunostaining. Data are presented as mean ± SEM.

2.3.7. Glial fibrillary acidic protein immunostaining:

For mice subjected to r-mTBI, immunostaining for GFAP revealed evidence of a mild reactive astrogliosis in regions of the cortex underlying the impact site (Fig.2.13R), the CC (Fig.2.13S), and the hippocampus (Fig.2.13T). In contrast, no gliosis was observed in the cortex at the impact site in shams (Fig.2.13B) or 24 h after a single injury (Fig.2.13F). In the CC, the r-mTBI (Fig.2.13S) and s-mTBI-10D (Fig.2.13K) groups showed a notable increase in the area of GFAP immunoreactivity compared with their respective sham controls, with the magnitude of this increase greater in the r-mTBI than in the s-mTBI-10D group (s-sham 0% vs. s-mTBI-10D 1.8 ± 0.7%; p < 0.0001; r-sham 0.6.1 ± 0.2% vs. r-mTBI 5.0 ± 0.7%; p < 0.0001; Fig.2.14A). In the CA1 region, there was no evidence of increased immunoreactivity in mice subjected to s-sham (Fig.2.13D), or in the singly injured animals at either time point (Fig.2.14H–L), (s-sham1.5 ± 0.2% vs. s-mTBI 1.2 ± 0.2%, vs. s-mTBI-10D 1.9 ± 0.3%; p > 0.05). By contrast, increased GFAP

immunoreactivity was observed in the CA1 region of the r-mTBI group (Fig.2.13T) compared with its sham (Fig.2.139P), (r-mTBI 5.7 ± 0.4% vs. r-sham 3.8 ± 0.5%; Fig.2.14B; $p < 0.005$). Interestingly, we also observed an increase in GFAP-immunoreactivity in the CA1 region of the r-sham animals (Fig.2.13P) when compared with the s-mTBI (Fig.2.13H) and the s-sham animals (Fig.2.13D, $p < 0.01$).

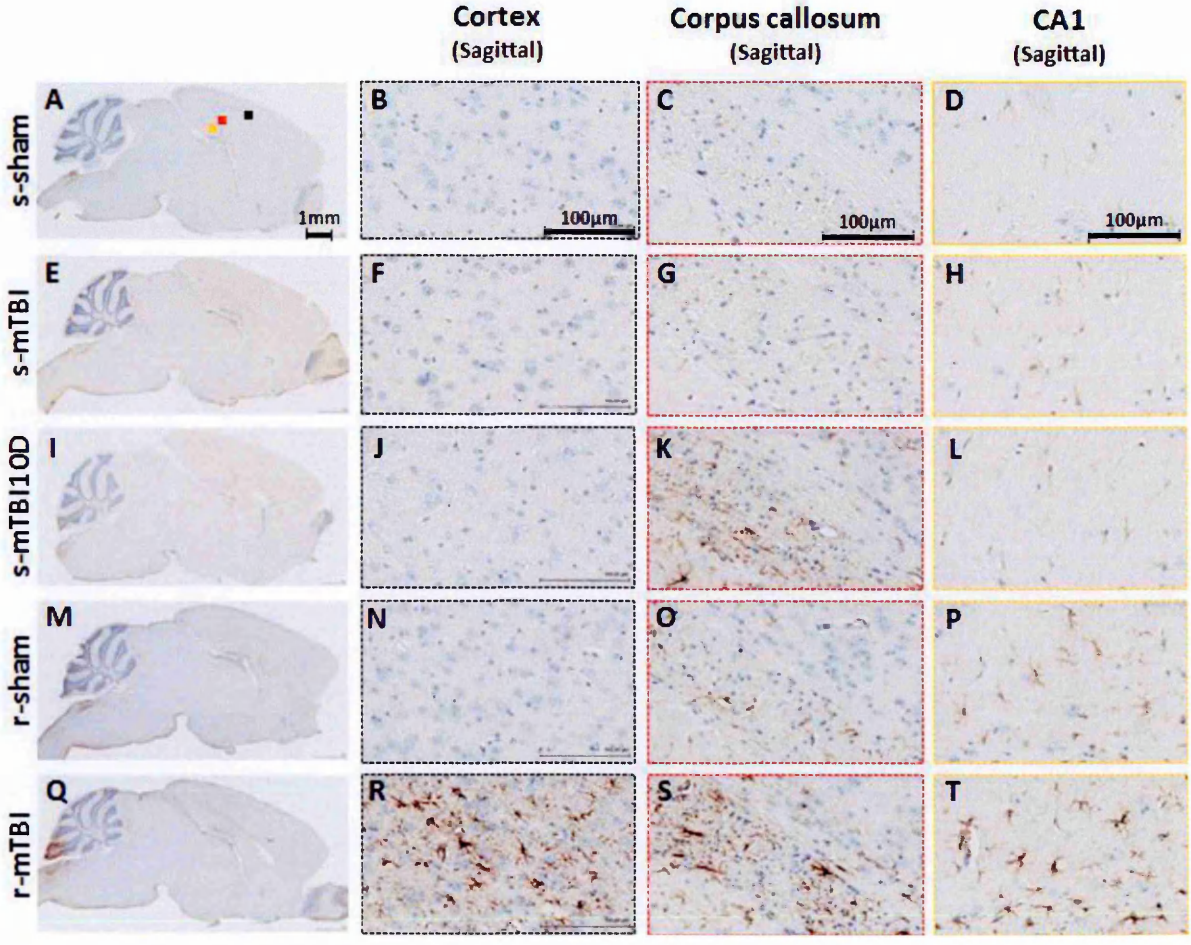

Figure.2.13: Glial fibrillary acid protein immunohistochemistry of sagittal sections of the mouse brain at ± 0.4 mm lateral to midline in the cortex (B, F, J, N, R), corpus callosum (C, G, K, O, S), and the CA1 sub region of the hippocampus (D, H, L, P, T). Colored boxes indicate areas of interest shown at higher magnification in the right panels. There were no changes in the s-mTBI group (E–H) compared with their respective sham group (A–D) at 24 h post-injury. An increase in the area of GFAP staining was observed in the corpus callosum at 10 days post s-mTBI (K). An increased area of GFAP immunoreactivity was observed in the CA1 region of the r-sham group (P). GFAP immunohistochemistry shows extensive

staining in the r-mTBI at 24 h after final injury in the cortex, corpus callosum, and hippocampus (R–T). Tissue sections were counterstained with hematoxylin.

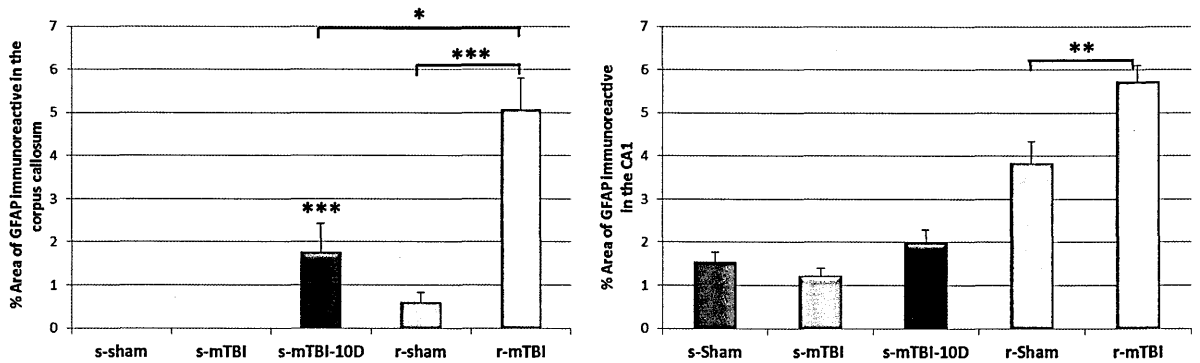

Figure.2.14: Quantitative analysis of GFAP staining intensity in two 150 μm^2 areas of the corpus callosum (A) and two 200 μm^2 areas of the CA1 region (B) (n = 4). Data are presented as mean ± SEM, (*$p < 0.05$; **$p < 0.001$; ***$p < 0.0001$).

2.3.8. Ionized calcium binding adaptor molecule 1 immunostaining:

In the sham animals, none of the regions of interest showed cells with structural characteristics of activated microglia (hypertrophic and bushy morphology); (Fig.2.15A–C; J–L). In the singly injury animals, microglial activation in the BS and in the cortex was not noticeable at either 24 h or 10 days post injury (Fig.2.15D–I). However, in the CC, the s-mTBI and the s-mTBI-10D showed a notable increase in Iba1-immunoreactivity (s-sham 1.34 ± 0.2% vs. s-mTBI 2.5 ± 0.3%, vs. s-mTBI-10D 2.9 ± 0.9%; $p < 0.005$; Fig.11E–H and Fig.2.16A). For mice subjected to r-mTBI, immunostaining for anti-Iba-1 revealed clusters of activated microglia in the BS (Fig. 12.15M), the CC (r-sham 1.5 ± 0.3% vs. s-mTBI 8.5 ± 0.8%; $p < 0.0001$; Fig.2.16N), and microglia with a bushy morphology in the region of the cortex underlying the impact site (r-sham 0.3 ± 0.09% vs. r-mTBI 4.0 ± 1.1%; $p < 0.0001$; Fig.2.16O).

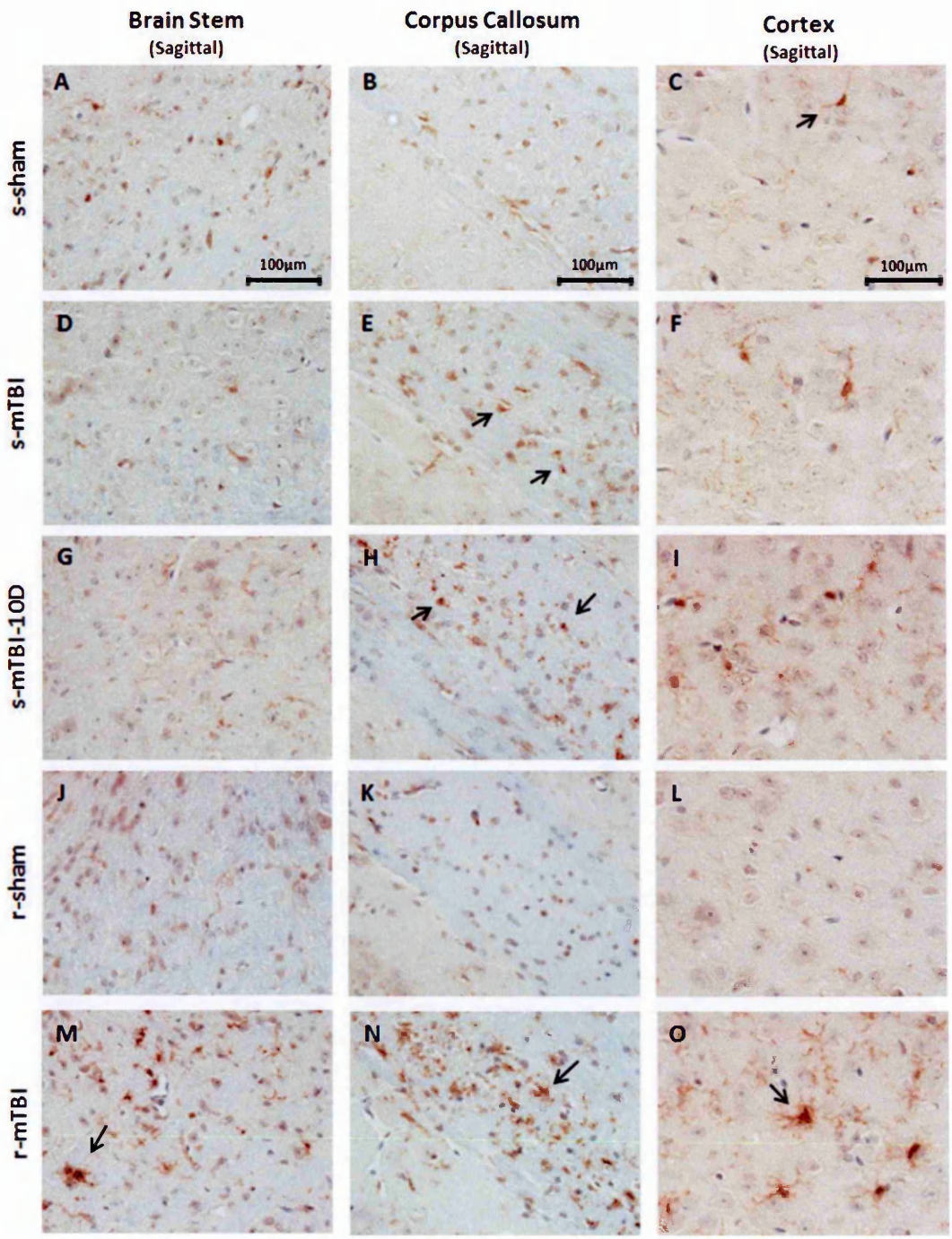

Figure.2.15: Immunohistochemical labeling for microglia with anti-Iba1. Sagittal sections of the mouse brain at ≈ 0.4 mm lateral to midline in the brainstem (A, D, G, J, M), in the corpus callosum (B, E, H, K, N), and in the cortex (C, F, I, L, O). There was no microglial activation in the sham (A–C) and r-sham (J–L) groups. An increased area of anti-Iba1 immunoreactivity was observed in the corpus callosum at 24 h (E) and 10 days (H) post s-mTBI. Anti-Iba1 immunohistochemistry indicates multifocal microglial

activation after r-mTBI in the brainstem (M), corpus callosum (N), and cortex (O). Tissue sections were counterstained with hematoxylin.

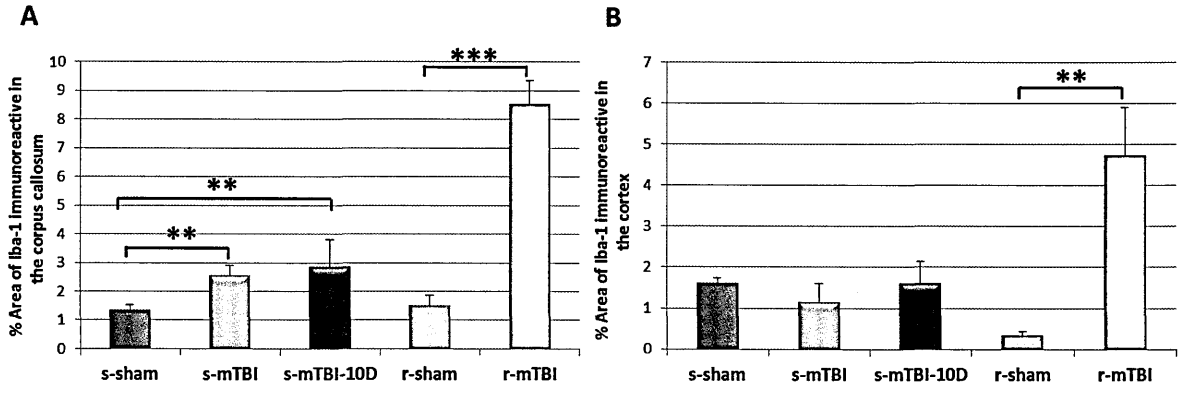

Figure.2.16: Quantitative analysis of anti-Iba1 staining intensity in three 100 μm^2 areas of the corpus callosum (A) and two 200 μm^2 areas of the cortex (B) (n = 4). Data are presented as mean ± SEM, (**p < 0.001; ***p < 0.0001).

In summary, our results demonstrate that animals exposed to s-mTBI have short-term behavioral abnormalities that manifest as transient deficits in motor function and spatial memory, which are accompanied by reactive astrocytosis and sparse APP-immunoreactive axonal pathology in the CC. By contrast, animals subjected to r-mTBI with an inter-injury interval of 48 h demonstrated greater cognitive impairment, microglial activation, more widespread and marked reactive astrocytosis, multifocal axonal pathology, and focal injury in the cerebellum (Table 2.2).

	s-sham	s-mTBI	s-mTBI-10D	r-sham	r-mTBI
Cortex	-	-	-	-	A
	-	-	-	G	G G G
	-	-	-	-	M M
Corpus callosum	-	A A A	-	-	AA
	-	-	G G	G	G G G
	M	M M	M M	M	M M M
CA1	-	-	-	-	-
	G	G	G	G G	G G G
	M	M	M	M	M
Brain stem	-	A	-	-	A A
	-	-	-	-	-
	-	-	-	-	M

Table.2.2: Summary of the location and relative intensity of immunohistochemical data for APP **(A)**, GFAP **(G)** and anti-Iba1 **(M)**. Present (X), moderate staining (XX), and intense staining (XXX).

2.4. Discussion:

Following the development and optimization of mTBI in a non-invasive CHI model, the influence of single and r-mTBI on cognitive performance and the resulting neuropathology was assessed in mice. Results from our study indicated that a single injury a 5m/sec velocity strike and 1mm impact depth, or r-mTBI with the same parameter but spaced every 48h met mild injury criteria (i.e. 0% mortality, no hemorrhage, short period of traumatic apnea, and no skull fracture).

We achieved our goal by successfully developing and characterizing a new mouse model of CHI produced by using an EM controlled impact device. The purpose in developing this model was to establish an easily implemented, robust, and highly replicable animal model to address the consequences of mTBI and understand the cumulative and chronic effects of repetitive mild

injury. Moreover, to our knowledge, this is the first study of its kind to examine the consequences of more than two repetitive hits at an interconcussive interval of 48 h.

Rodent models of CHI that predominate the field use either an electromagnetic impactor or the weight drop model to model r-mTBI. Since the publication of our model, two other independent groups have confirmed and replicated our observations using similar settings on the same injury device (EM controlled impactor). In these studies, r-mTBI caused exacerbated acute spatial learning, memory deficits, inflammation, and axonal injury when compared to single mTBI[18,29]. The study of Hylin and colleague[29] uses the same impactor tip (5 mm in diameter) driven at a velocity of 5.0 m/sec to a depth of 1.0 mm. At these settings, they delivered 2 impacts within 24h or 4 impacts within 24 h. In a second study, Shitaka and colleague[18], used the same injury apparatus but incorporated a larger rubber tip (9 mm in diameter) delivering 2 impacts within 24 h at 5.0 m/sec to a deeper depth: 3.3 mm. Likewise, studies using a weight drop model report that 4 to 5 injuries within 24 h produced acute deficits in spatial memory[13,30]. Overall, while differences exist across laboratories in term of the injury setting, there is a consensus on the consequences of r-mTBI. This is of specific importance for the continuing development and the translation of animal models to clinical settings.

Consistent with other mouse models of r-mTBI and evidence from athletes who have experienced repeated mild concussive injuries, our model shows acute postural equilibrium impairment post-injury as assessed by the rotarod motor task[24,31]. Whereas the performance of the s-mTBI group improved over time, the r-mTBI group was unable to recover their sensorimotor function up to 7 days post-injury, which was the latest day tested in this study.

Over this time period, each injury group performed worse than their respective shams with a rank order of performance of r-mTBI < s-mTBI < r-sham = s-sham. When tested for cognitive performance in the BM, both injury groups showed cognitive impairment consistent with findings in previous animal models of brain injury[13,17,18,32-34]. There was a worsening trend for r-mTBI compared with s-mTBI during the acquisition trials as well as on time to zone in the probe trial, and on the final day of acquisition training the r-mTBI group performed significantly worse than the other three groups.

From a neuropathological perspective, the only macroscopic abnormality observed was a focal contusion injury on the inferior surface of the cerebellum away from the site of injury in the r-mTBI and s-mTBI-10D groups. In addition, we observed an evolving cerebellar injury in the s-mTBI-10D group that is likely the result of secondary injury processes that develop over a period of days after the initial trauma. Aside from this observation, there was no evidence of structural damage to the brain based on routine morphological assessment with H&E and LFB/CV staining, including no signs of neuronal loss.

Axonal injury can be detected by immunohistochemistry for the APP, a member of the homologous type-I transmembrane protein[35]. APP is found in neurons and conveyed along the axon by fast anterograde transport[36,37]. In case of axonal damage or transection, the transport is interrupted and APP has been shown to accumulate in the damage areas indicative of dysfunction or in the proximal axonal ends if transected[38]. As a consequence, so-called APP-positive varicose followed by spheroids (bulbs) are formed. APP has been hypothesized to function as a receptor in intracellular axonal transport and may interact with kinesin and the

microtubule cytoskeleton enabling the transport of cargo to the synaptic terminal[39]. Several studies have also hypothesized the role of this protein to be involved in tissue maintenance[40], brain development[41] and in response to injury[42].

In this study, axonal injury following trauma results in swollen and tortuous axons that can be detected by the accumulation of APP as early as 35 min after brain injury[43], and in our model, a single impact resulted in APP-immunoreactive axons localized to the CC, evident at 24 h after injury. By 10 days postinjury (s-mTBI-10D) there was no evidence for APP immunoreactivity, consistent with the current literature for animal models in that strong APP staining is present at 24 h post-injury[8,17,44], which diminishes by 14 days post-injury[33,43]. In the r-mTBI group, more widespread damage was observed, with immunoreactive axons also evident in the spinal trigeminal tracts of the BS and beneath the impact site in the form of APP immunoreactive neuronal perikaryas.

However, in the r-mTBI group, the APP immunoreactive axonal swellings were less frequent and less robustly stained in the CC than those observed at 24 h after s-mTBI. These observations may be consistent with a deleterious effect of repetitive versus single injury on the ability of the brain to efficiently catabolize and clear APP, facilitating amyloidogenic processing and contributing to later evolution of amyloid plaque pathology[3,45]. More work is required to explain why no increase in APP immunoreactivity was observed in r-mTBI versus s-mTBI. Nevertheless, the comparison of r-mTBI with s-mTBI-10D (where both groups are matched for time since the first/single injury) clearly demonstrates that repetitive injury

sustains an APP immunoreactive axonal profile over the 10-day period following the initial injury.

As stated above, the cohort of r-mTBI also showed multifocal injury in various brain regions but the extent of axonal damage represented by the number of APP immunoreactive profiles were significantly reduced when compared to the s-mTBI group. This apparent decrease in the density of APP-immunoractive profiles may arise for a number of reasons. These include cleavage enzymes, inflammatory response, or/and axoplasmic leakage after axonal rupture. For example, axonal swellings may either dissipate as axonal homeostasis is restored and/or cleared by enhanced activation of macrophage/microglial cells and increased astrocytosis. It was also reported that following experimental head injury in rodents, resident microglia and macrophages are recruited in both focal and diffuse TBI[46-48]. After injury, the axonal membranes break apart stimulating cytokine/chemokine release by neurons followed by degradation of the myelin sheath and macrophage infiltration[49,50]. Then, macrophages clear APP and the cell debris significantly decreasing the amount of APP by the time of the fifth injury. Ultimately, these disconnected axons are cleared by microglia and macrophage which in turn triggers Wallerian degeneration within days after injury[51]. As expected, our data show co localization of astrogliosis and APP profiles which is correlated with a lower magnitude of APP staining in the corpus callosum in the r-mTBI group as well as 10 days post s-mTBI. Further studies are required to determine if the decrease of APP pathology could be the consequence of reactive astrocytes and/or microglial activation.

A simpler mechanism may also explain the decrease in APP immunostaining in the r-mTBI. By 10 days post initial injury, the axons could be significantly damaged by both primary and secondary injuries impairing axonal transport, and thus be perceived as a decreased APP accumulation. APP staining was strongly visible at 24H after injury, and then disappeared by 10 days. Consistent with the literature, in rodent, APP is evident between 6 and 24 h before gradually decreasing and completely disappearing by 14 days. Identifying the impact of axonal injury is an important determinant of sensorimotor, behavioral and cognitive impairments after mTBI. Damage to white matter tracts by the primary injury cannot solely explain cognitive problems[52]. This is likely because the cognitive memory, executive function and processing speed largely rely on the coherent activity of the brain network.

In addition to the white matter damage, the r-mTBI group was associated with a notable reactive astrocytosis, with a distinct pattern of GFAP-positive reactive astrocytes localized to the medium and deep layers of the cortex beneath the impact site. As observed in the s-mTBI-10D group, our model produced a measurable reactive astrocytosis at 10 days after initial mTBI. These results are consistent with other studies that showed astrocytosis peaking between 10 and 14 days following concussion in rodents[33,53,54]. This increase in gliosis is also believed to coincide with macrophage accumulation, which has also been shown to peak at 10 days post-injury. Our data demonstrate that repetitive, noninvasive mTBI in the mouse resulted in a graded injury response, with the extent of reactive astrocytosis increased in animals exposed to repetitive impacts. Whereas a single impact produced moderate reactive astrocytosis at 10 days post-injury and was isolated to the CC, five impacts over 9 days showed increased staining

in the CC as well as cortical and hippocampal involvement. As well as axonal injury and astrogliosis, microgliosis was also detected in the CC of injured animals as early as 24 h and up to at least 10 days post-mTBI, whereas the r-mTBI group revealed clusters of activated microglia in multiple brain regions (CC, BS, and cortex). The time course of microglial activation observed in this study was similar to that noted in previous reports[18,55-57]. Depending mainly upon injury severity and the duration of the ensuing inflammatory cascade, microgliosis can be either beneficial or detrimental with respect to tissue preservation[58]. Known as the first line of defense in both focal and diffuse TBI[59], microglial activation has been reported to play a beneficial role by secreting brain-derived neurotrophic growth factors and insulin-like growth factor[60-62]. They have also been shown to have a detrimental role at an acute time point by secreting inflammatory cytokines such as interleukin (IL)-1β and tumor necrosis factor (TNF)-α[63,64]. Moreover, in several TBI models, minocycline, which has anti-inflammatory properties, has been shown to reduce histopathological consequences after mTBI in mice[65,66]. Of particular interest is a recent study by Siopi and collaborators which demonstrated that reducing neuroinflammation post-injury attenuated memory impairment in a mouse model of CHI[67,68], however more work is required to address the impact of microglial activation on cognitive function after TBI.

The main limitation of this model is a function of interspecies physiological differences. The murine skull has a greater deformability than that of the rat, and its relatively small mass compared to that of humans complicates biomechanical studies, as it cannot simulate a true human rotational/angular injury induced by the brain inertia[69,70]. Consequently, the lack of

head movement is a common issue of brain concussion in sub-primate animals, as this is inconsistent with human brain concussion. Nonetheless, the key elements of brain trauma neuropathology remain similar across species. For example, the pathological consequences of axonal injury (axonal varicosities, axonal bulbs) have been observed in humans, pigs, rats, and mice[3,8,18,33]. The other advantages of mouse models (genetic manipulability, ease of protocol implementation, and cost) make this an appropriate platform in which to identify molecular consequences of repetitive versus single injury for exploration in higher mammals.

In conclusion, we have developed a simple and reproducible mouse model of mTBI, which induces pathological and behavioral features comparable to those observed in the human condition. Moreover, by recapitulating the pathological alterations observed in human TBI patients, this model is also suitable for studying various mechanisms of post-traumatic injury such as axonal injury, cell death, or apoptosis. Our intent was that future application of this model of mTBI could be used to investigate the long term consequences of r-mTBI (see Chapter 3), the influence of different numbers of injuries and different inter-injury intervals, and the impact of r-mTBI in mice genetically modified at loci of relevance to human TBI such as Tau (see Chapter 4) or APOE, aspects currently lacking in the literature. An increased understanding of mTBI and its cumulative effects will enable identification of molecular targets specific to mTBI and ultimately the development of novel, effective therapeutics, which are desperately needed. Furthermore, the acute phase following traumatic brain injury is associated with a complex and mixed neuroinflammatory response involving polymorphs, microglia and T lymphocytes amongst others [59,71]. Whilst this acute phase response has long

been recognized as contributing to immediate pathology, more recently attention has been drawn to the role persistent inflammation beyond this acute phase response might have in respect of longer-term neurodegenerative consequences. The next chapter lays out the foundation for prospective longitudinal studies in mTBI by characterizing the chronic pathological and behavioral outcomes following s-mTBI and r-mTBI in this mouse model of mTBI. We believe this work promises to be instrumental to the field of TBI research, we will be the first to provide an extensive timeline of TBI sequelae after s-mTBI and r-mTBI, as well as potential pre-clinical platform in which to investigate therapeutic opportunities in TBI and wider neurodegenerative diseases.

2.5. References:

1 Forstl, H., Haass, C., Hemmer, B., Meyer, B. & Halle, M. Boxing-acute complications and late sequelae: from concussion to dementia. *Deutsches Arzteblatt international* **107**, 835-839, doi:10.3238/arztebl.2010.0835 (2010).

2 Gavett, B. E., Stern, R. A., Cantu, R. C., Nowinski, C. J. & McKee, A. C. Mild traumatic brain injury: a risk factor for neurodegeneration. *Alzheimer's research & therapy* **2**, 18, doi:10.1186/alzrt42 (2010).

3 Johnson, V. E., Stewart, W. & Smith, D. H. Traumatic brain injury and amyloid-beta pathology: a link to Alzheimer's disease? *Nature reviews. Neuroscience* **11**, 361-370, doi:10.1038/nrn2808 (2010).

4 Van Den Heuvel, C., Thornton, E. & Vink, R. Traumatic brain injury and Alzheimer's disease: a review. *Progress in brain research* **161**, 303-316, doi:10.1016/S0079-6123(06)61021-2 (2007).

5 Tang-Schomer, M. D., Patel, A. R., Baas, P. W. & Smith, D. H. Mechanical breaking of microtubules in axons during dynamic stretch injury underlies delayed elasticity, microtubule disassembly, and axon degeneration. *FASEB journal : official publication of the Federation of American Societies for Experimental Biology* **24**, 1401-1410, doi:10.1096/fj.09-142844 (2010).

6 Morrison, B., 3rd, Cater, H. L., Benham, C. D. & Sundstrom, L. E. An in vitro model of traumatic brain injury utilising two-dimensional stretch of organotypic hippocampal slice cultures. *Journal of neuroscience methods* **150**, 192-201, doi:10.1016/j.jneumeth.2005.06.014 (2006).

7 Tang-Schomer, M. D., Johnson, V. E., Baas, P. W., Stewart, W. & Smith, D. H. Partial interruption of axonal transport due to microtubule breakage accounts for the formation of periodic

varicosities after traumatic axonal injury. *Experimental neurology* **233**, 364-372, doi:10.1016/j.expneurol.2011.10.030 (2012).

8 Browne, K. D., Chen, X. H., Meaney, D. F. & Smith, D. H. Mild traumatic brain injury and diffuse axonal injury in swine. *Journal of neurotrauma* **28**, 1747-1755, doi:10.1089/neu.2011.1913 (2011).

9 Raghupathi, R. & Margulies, S. S. Traumatic axonal injury after closed head injury in the neonatal pig. *Journal of neurotrauma* **19**, 843-853, doi:10.1089/08977150260190438 (2002).

10 Raghupathi, R., Mehr, M. F., Helfaer, M. A. & Margulies, S. S. Traumatic axonal injury is exacerbated following repetitive closed head injury in the neonatal pig. *Journal of neurotrauma* **21**, 307-316, doi:10.1089/089771504322972095 (2004).

11 Gennarelli, T. A. *et al.* Diffuse axonal injury and traumatic coma in the primate. *Annals of neurology* **12**, 564-574, doi:10.1002/ana.410120611 (1982).

12 Creeley, C. E., Wozniak, D. F., Bayly, P. V., Olney, J. W. & Lewis, L. M. Multiple episodes of mild traumatic brain injury result in impaired cognitive performance in mice. *Academic emergency medicine : official journal of the Society for Academic Emergency Medicine* **11**, 809-819 (2004).

13 DeFord, S. M. *et al.* Repeated mild brain injuries result in cognitive impairment in B6C3F1 mice. *Journal of neurotrauma* **19**, 427-438, doi:10.1089/08977150252932389 (2002).

14 Laurer, H. L. *et al.* Mild head injury increasing the brain's vulnerability to a second concussive impact. *Journal of neurosurgery* **95**, 859-870, doi:10.3171/jns.2001.95.5.0859 (2001).

15 Longhi, L. *et al.* Temporal window of vulnerability to repetitive experimental concussive brain injury. *Neurosurgery* **56**, 364-374; discussion 364-374 (2005).

16 Nakajima, Y. *et al.* Distinct time courses of secondary brain damage in the hippocampus following brain concussion and contusion in rats. *The Tohoku journal of experimental medicine* **221**, 229-235 (2010).

17 Prins, M. L., Hales, A., Reger, M., Giza, C. C. & Hovda, D. A. Repeat traumatic brain injury in the juvenile rat is associated with increased axonal injury and cognitive impairments. *Developmental neuroscience* **32**, 510-518, doi:10.1159/000316800 (2010).

18 Shitaka, Y. *et al.* Repetitive closed-skull traumatic brain injury in mice causes persistent multifocal axonal injury and microglial reactivity. *Journal of neuropathology and experimental neurology* **70**, 551-567, doi:10.1097/NEN.0b013e31821f891f (2011).

19 Uryu, K. *et al.* Repetitive mild brain trauma accelerates Abeta deposition, lipid peroxidation, and cognitive impairment in a transgenic mouse model of Alzheimer amyloidosis. *The Journal of neuroscience : the official journal of the Society for Neuroscience* **22**, 446-454 (2002).

20 Cole, J. T. *et al.* Craniotomy: true sham for traumatic brain injury, or a sham of a sham? *Journal of neurotrauma* **28**, 359-369, doi:10.1089/neu.2010.1427 (2011).

21 Albert-Weissenberger, C. & Siren, A. L. Experimental traumatic brain injury. *Experimental & translational stroke medicine* **2**, 16, doi:10.1186/2040-7378-2-16 (2010).

22 Brody, D. L. *et al.* Electromagnetic controlled cortical impact device for precise, graded experimental traumatic brain injury. *Journal of neurotrauma* **24**, 657-673, doi:10.1089/neu.2006.0011 (2007).

23 Conte, V. *et al.* Vitamin E reduces amyloidosis and improves cognitive function in Tg2576 mice following repetitive concussive brain injury. *Journal of neurochemistry* **90**, 758-764, doi:10.1111/j.1471-4159.2004.02560.x (2004).

24 Kane, M. J. *et al.* A mouse model of human repetitive mild traumatic brain injury. *Journal of neuroscience methods* **203**, 41-49, doi:10.1016/j.jneumeth.2011.09.003 (2012).

25 Yoshiyama, Y. *et al.* Enhanced neurofibrillary tangle formation, cerebral atrophy, and cognitive deficits induced by repetitive mild brain injury in a transgenic tauopathy mouse model. *Journal of neurotrauma* **22**, 1134-1141, doi:10.1089/neu.2005.22.1134 (2005).

26 Franklin, K. B. J., and Paxinos, G. The Mouse Brain in Stereotaxic Coordinates, 2nd ed. *Elsevier/Academic Press: San Diego, London* (2001).

27 Harrison, F. E., Hosseini, A. H. & McDonald, M. P. Endogenous anxiety and stress responses in water maze and Barnes maze spatial memory tasks. *Behavioural brain research* **198**, 247-251, doi:10.1016/j.bbr.2008.10.015 (2009).

28 Ruifrok, A. C. & Johnston, D. A. Quantification of histochemical staining by color deconvolution. *Analytical and quantitative cytology and histology / the International Academy of Cytology [and] American Society of Cytology* **23**, 291-299 (2001).

29 Hylin, M. J. *et al.* Repeated mild closed head injury impairs short-term visuospatial memory and complex learning. *Journal of neurotrauma*, doi:10.1089/neu.2012.2717 (2013).

30 Meehan, W. P., 3rd, Zhang, J., Mannix, R. & Whalen, M. J. Increasing recovery time between injuries improves cognitive outcome after repetitive mild concussive brain injuries in mice. *Neurosurgery* **71**, 885-891, doi:10.1227/NEU.0b013e318265a439 (2012).

31 Guskiewicz, K. M. Balance assessment in the management of sport-related concussion. *Clinics in sports medicine* **30**, 89-102, ix, doi:10.1016/j.csm.2010.09.004 (2011).

32 Eakin, K. & Miller, J. P. Mild traumatic brain injury is associated with impaired hippocampal spatiotemporal representation in the absence of histological changes. *Journal of neurotrauma* **29**, 1180-1187, doi:10.1089/neu.2011.2192 (2012).

33 Huh, J. W., Widing, A. G. & Raghupathi, R. Midline brain injury in the immature rat induces sustained cognitive deficits, bihemispheric axonal injury and neurodegeneration. *Experimental neurology* **213**, 84-92, doi:10.1016/j.expneurol.2008.05.009 (2008).

34 Shultz, S. R. *et al.* Repeated mild lateral fluid percussion brain injury in the rat causes cumulative long-term behavioral impairments, neuroinflammation, and cortical loss in an animal model of repeated concussion. *Journal of neurotrauma* **29**, 281-294, doi:10.1089/neu.2011.2123 (2012).

35 Gentleman, S. M., Nash, M. J., Sweeting, C. J., Graham, D. I. & Roberts, G. W. Beta-amyloid precursor protein (beta APP) as a marker for axonal injury after head injury. *Neuroscience letters* **160**, 139-144 (1993).

36 Koo, E. H. *et al.* Precursor of amyloid protein in Alzheimer disease undergoes fast anterograde axonal transport. *Proceedings of the National Academy of Sciences of the United States of America* **87**, 1561-1565 (1990).

37 Sisodia, S. S., Koo, E. H., Hoffman, P. N., Perry, G. & Price, D. L. Identification and transport of full-length amyloid precursor proteins in rat peripheral nervous system. *The Journal of neuroscience : the official journal of the Society for Neuroscience* **13**, 3136-3142 (1993).

38 Yam, P. S., Takasago, T., Dewar, D., Graham, D. I. & McCulloch, J. Amyloid precursor protein accumulates in white matter at the margin of a focal ischaemic lesion. *Brain research* **760**, 150-157 (1997).

39 Kamal, A., Almenar-Queralt, A., LeBlanc, J. F., Roberts, E. A. & Goldstein, L. S. Kinesin-mediated axonal transport of a membrane compartment containing beta-secretase and presenilin-1 requires APP. *Nature* **414**, 643-648, doi:10.1038/414643a (2001).

40 Breen, K. C., Bruce, M. & Anderton, B. H. Beta amyloid precursor protein mediates neuronal cell-cell and cell-surface adhesion. *Journal of neuroscience research* **28**, 90-100, doi:10.1002/jnr.490280109 (1991).

41 Trapp, B. D. & Hauer, P. E. Amyloid precursor protein is enriched in radial glia: implications for neuronal development. *Journal of neuroscience research* **37**, 538-550, doi:10.1002/jnr.490370413 (1994).

42 Mattson, M. P. *et al.* Cellular signaling roles of TGF beta, TNF alpha and beta APP in brain injury responses and Alzheimer's disease. *Brain research. Brain research reviews* **23**, 47-61 (1997).

43 Pierce, J. E., Trojanowski, J. Q., Graham, D. I., Smith, D. H. & McIntosh, T. K. Immunohistochemical characterization of alterations in the distribution of amyloid precursor proteins and beta-amyloid peptide after experimental brain injury in the rat. *The Journal of neuroscience : the official journal of the Society for Neuroscience* **16**, 1083-1090 (1996).

44 Huh, J. W., Widing, A. G. & Raghupathi, R. Basic science; repetitive mild non-contusive brain trauma in immature rats exacerbates traumatic axonal injury and axonal calpain activation: a preliminary report. *Journal of neurotrauma* **24**, 15-27, doi:10.1089/neu.2006.0072 (2007).

45 Sivanandam, T. M. & Thakur, M. K. Traumatic brain injury: a risk factor for Alzheimer's disease. *Neuroscience and biobehavioral reviews* **36**, 1376-1381, doi:10.1016/j.neubiorev.2012.02.013 (2012).

46 Oehmichen, M., Theuerkauf, I. & Meissner, C. Is traumatic axonal injury (AI) associated with an early microglial activation? Application of a double-labeling technique for simultaneous detection of microglia and AI. *Acta neuropathologica* **97**, 491-494 (1999).

47 Bye, N. *et al.* Transient neuroprotection by minocycline following traumatic brain injury is associated with attenuated microglial activation but no changes in cell apoptosis or neutrophil infiltration. *Experimental neurology* **204**, 220-233, doi:10.1016/j.expneurol.2006.10.013 (2007).

48 Czigner, A. *et al.* Kinetics of the cellular immune response following closed head injury. *Acta neurochirurgica* **149**, 281-289, doi:10.1007/s00701-006-1095-8 (2007).

49 Aloisi, F. Immune function of microglia. *Glia* **36**, 165-179 (2001).

50 Hansson, E. & Ronnback, L. Glial neuronal signaling in the central nervous system. *FASEB journal : official publication of the Federation of American Societies for Experimental Biology* **17**, 341-348, doi:10.1096/fj.02-0429rev (2003).

51 Povlishock, J. T. & Becker, D. P. Fate of reactive axonal swellings induced by head injury. *Laboratory investigation; a journal of technical methods and pathology* **52**, 540-552 (1985).

52 Bigler, E. D. Neuropsychological testing defines the neurobehavioral significance of neuroimaging-identified abnormalities. *Archives of clinical neuropsychology : the official journal of the National Academy of Neuropsychologists* **16**, 227-236 (2001).

53 Hamberger, A., Viano, D. C., Saljo, A. & Bolouri, H. Concussion in professional football: morphology of brain injuries in the NFL concussion model--part 16. *Neurosurgery* **64**, 1174-1182; discussion 1182, doi:10.1227/01.NEU.0000316855.40986.2A (2009).

54 Hellewell, S. C., Yan, E. B., Agyapomaa, D. A., Bye, N. & Morganti-Kossmann, M. C. Post-traumatic hypoxia exacerbates brain tissue damage: analysis of axonal injury and glial responses. *Journal of neurotrauma* **27**, 1997-2010, doi:10.1089/neu.2009.1245 (2010).

55 Chen, S., Pickard, J. D. & Harris, N. G. Time course of cellular pathology after controlled cortical impact injury. *Experimental neurology* **182**, 87-102 (2003).

56 Haselkorn, M. L. *et al.* Adenosine A1 receptor activation as a brake on the microglial response after experimental traumatic brain injury in mice. *Journal of neurotrauma* **27**, 901-910, doi:10.1089/neu.2009.1075 (2010).

57 Kelley, B. J., Lifshitz, J. & Povlishock, J. T. Neuroinflammatory responses after experimental diffuse traumatic brain injury. *Journal of neuropathology and experimental neurology* **66**, 989-1001, doi:10.1097/NEN.0b013e3181588245 (2007).

58 Neumann, H., Kotter, M. R. & Franklin, R. J. Debris clearance by microglia: an essential link between degeneration and regeneration. *Brain : a journal of neurology* **132**, 288-295, doi:10.1093/brain/awn109 (2009).

59 Morganti-Kossmann, M. C., Rancan, M., Stahel, P. F. & Kossmann, T. Inflammatory response in acute traumatic brain injury: a double-edged sword. *Current opinion in critical care* **8**, 101-105 (2002).

60 Lalancette-Hebert, M., Gowing, G., Simard, A., Weng, Y. C. & Kriz, J. Selective ablation of proliferating microglial cells exacerbates ischemic injury in the brain. *The Journal of neuroscience : the official journal of the Society for Neuroscience* **27**, 2596-2605, doi:10.1523/JNEUROSCI.5360-06.2007 (2007).

61 Neumann, J. *et al.* Microglia provide neuroprotection after ischemia. *FASEB journal : official publication of the Federation of American Societies for Experimental Biology* **20**, 714-716, doi:10.1096/fj.05-4882fje (2006).

62 Thored, P. *et al.* Long-term accumulation of microglia with proneurogenic phenotype concomitant with persistent neurogenesis in adult subventricular zone after stroke. *Glia* **57**, 835-849, doi:10.1002/glia.20810 (2009).

63 Lloyd, E., Somera-Molina, K., Van Eldik, L. J., Watterson, D. M. & Wainwright, M. S. Suppression of acute proinflammatory cytokine and chemokine upregulation by post-injury administration of a novel small molecule improves long-term neurologic outcome in a mouse model of traumatic brain injury. *Journal of neuroinflammation* **5**, 28, doi:10.1186/1742-2094-5-28 (2008).

64 Schmidt, O. I., Heyde, C. E., Ertel, W. & Stahel, P. F. Closed head injury--an inflammatory disease? *Brain research. Brain research reviews* **48**, 388-399, doi:10.1016/j.brainresrev.2004.12.028 (2005).

65 Homsi, S. *et al.* Blockade of acute microglial activation by minocycline promotes neuroprotection and reduces locomotor hyperactivity after closed head injury in mice: a twelve-week follow-up study. *Journal of neurotrauma* **27**, 911-921, doi:10.1089/neu.2009.1223 (2010).

66 Siopi, E. *et al.* Minocycline restores sAPPalpha levels and reduces the late histopathological consequences of traumatic brain injury in mice. *Journal of neurotrauma* **28**, 2135-2143, doi:10.1089/neu.2010.1738 (2011).

67 Siopi, E., Calabria, S., Plotkine, M., Marchand-Leroux, C. & Jafarian-Tehrani, M. Minocycline restores olfactory bulb volume and olfactory behavior after traumatic brain injury in mice. *Journal of neurotrauma* **29**, 354-361, doi:10.1089/neu.2011.2055 (2012).

68 Siopi, E. *et al.* Evaluation of late cognitive impairment and anxiety states following traumatic brain injury in mice: the effect of minocycline. *Neuroscience letters* **511**, 110-115, doi:10.1016/j.neulet.2012.01.051 (2012).

69 LaPlaca, M. C., Simon, C. M., Prado, G. R. & Cullen, D. K. CNS injury biomechanics and experimental models. *Progress in brain research* **161**, 13-26, doi:10.1016/S0079-6123(06)61002-9 (2007).

70 Park, H. K., Fernandez, I. I., Dujovny, M. & Diaz, F. G. Experimental animal models of traumatic brain injury: medical and biomechanical mechanism. *Critical reviews in neurosurgery : CR* **9**, 44-52 (1999).

71 Helmy, A., De Simoni, M. G., Guilfoyle, M. R., Carpenter, K. L. & Hutchinson, P. J. Cytokines and innate inflammation in the pathogenesis of human traumatic brain injury. *Progress in neurobiology* **95**, 352-372, doi:10.1016/j.pneurobio.2011.09.003 (2011).

Chapter 3

3. Chronic evaluation of neurobehavioral and neuropathological changes in the novel mouse model of mTBI

3.1. Introduction:

As already described, epidemiological studies indicate that repetitive traumatic brain injury (TBI) is associated with increased risk of neurodegenerative diseases[1-5]. Chronic neuropathological studies on autopsied human TBI tissue have demonstrated a variety of pathologies typically described in neurodegenerative disorders, suggesting that a history of repetitive mild TBI (r-mTBI) could act as a substrate for future dementia[6]. Descriptions thus far include pathologies in amyloid beta (Aβ)[7-10], tau[9-11], TAR DNA binding protein 43 (TDP-43)[9,10,12], and neuroinflammation[10,13,14]. Historical data on 'dementia pugilistica'[15], together with recent descriptions of the pathology of athletes[10,11,16-18] and military personnel[9,13,19] exposed to r-mTBI, which includes the features now often described as chronic traumatic encephalopathy (CTE) support an association between TBI and neurodegeneration.

In humans, as observed in our mouse model, the acute phase following TBI is associated with a complex and mixed neuroinflammatory response involving activation of resident microglia and astrocytes that express inflammatory mediators locally[20,21]. Whilst this acute phase response has long been recognized as contributing to immediate pathology, more recently attention has been drawn to the role persistent inflammation might have in relation to longer term neurodegenerative consequences[22]. In support of this, autopsy-derived tissues from athletes[10,13,14] demonstrate persistent neuroinflammation many years after TBI.

Increasingly, neuroinflammation is proposed as contributing to development of neurodegenerative diseases[23], perhaps representing an early event in their pathogenesis.

My development and acute phase characterization of a novel mTBI mouse model, described in Chapter 2[24], laid the foundation for evaluation of the long term consequences of mTBI, in particular r-mTBI, using the same paradigm. This, we anticipated, would be of most significance to the translation of our preclinical efforts to human populations. It has recently been suggested that CHI animal models may more closely approximate clinical mTBI than fluid percussion or cortical impact models[25]. To date, few CHI models have examined the long term consequences of r-mTBI[26,27] with neuropathological changes and neurobehavioral deficits being reported up to 3 months post injury in mice. To our knowledge the only study with a time point of analysis greater than 3 months post injury comes from the work of Mannix and colleagues who reported neurobehavioral deficits at 12 months post injury in mice, with little accompanying neuropathology[28,29].

In our model we observe behavioral deficits at up to 18 months post-injury in repetitively versus singly injured mice that is accompanied by characteristic neuropathological features including progressive neuroinflammation supporting the potential for this model to serve as a pre-clinical platform in which to investigate therapeutic opportunities in TBI.

3.2. Materials and Methods:

3.2.1. Animals:

Male, C57BL/6J mice (aged 9-15 months, 32-42g, Jackson Laboratories, Bar Harbor ME) were housed singly under standard laboratory conditions (23°C ± 1°C, 50±5% humidity, and 12-hour light/dark cycle) with free access to food and water throughout the study. All procedures were carried out under Institutional Animal Care and Use Committee approval and in accordance with the National Institute of Health Guide for the Care and Use of Laboratory Animals.

3.2.2. Injury groups and schedule:

For the behavioral analyses we evaluated the same groups of mice on which we previously published (Chapter 2) the results from an acute time point post injury[24] (Fig.3.1). A total of 48 mice were randomly assigned to one of four groups: single injury, single sham, repetitive injury (total of 5 hits with an inter-concussion interval of 48 h), and repetitive sham (5 anesthesias, 48 h apart). For this current study these mice were tested again at 6 (n=12 per group), 12 (n=12 per group) and 18 (n=9 per group) months after mTBI/anesthesia. This cohort of mice was not euthanized at the 18 month timepoint, as we are aging them for a later final timepoint of analyses, and therefore we do not have histological data for the 18 month time point. Separate cohorts of mice for the histological examination and biochemical analyses were randomly assigned to each of the 4 treatment groups as follows: 6 months post injury histology cohort (n=5/treatment group), biochemistry cohort (n=4/treatment group); 12 months post injury histology cohort (n=4/treatment group), biochemistry cohort (n=4/treatment group).

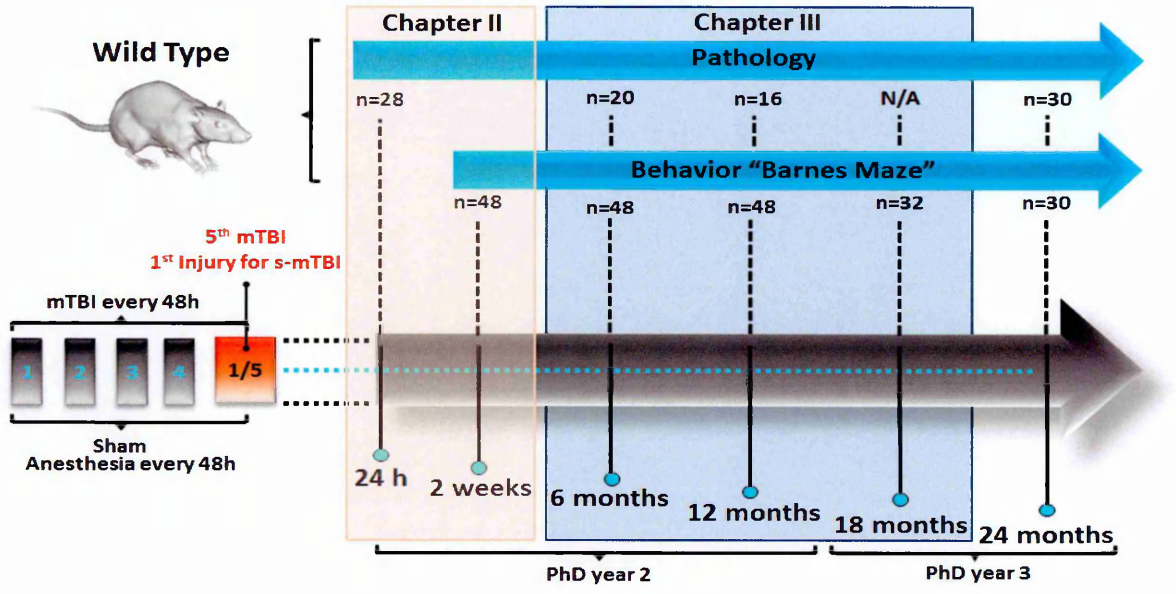

Figure.3.1: Outline of experimental schedule.

3.2.3. Injury protocol:

The mTBI was administered to mice as described in Chapter 2.

3.2.4. Assessment of cognitive function:

Cognitive function was evaluated at 6 and 12 months post-injury/anesthesia using the Barnes maze (BM) as described previously in Chapter 2. The experiments were run blindly to grouping, and the Ethovision XT system (Noldus, Wageningen, NL) was used to track and record the movement of each animal. In addition, at the 12 months post injury time point, following the probe trial (day 8), we performed a reverse behavioral test in which the escape box was switched to the opposite side of the table to test the ability of mice to learn a new spatial contingency. Mice were pre-trained for 4 consecutive days to learn the location of the new hole and tested again with a single probe trial as described above.

3.2.5. Assessment of Anxiety:

Anxiety-like behavior was assessed using an elevated-plus maze which relies on the animal preference for dark enclosed arms over bright open arms[30]. This task assesses the willingness of the mouse to explore the open arms of the maze which are fully exposed and at an elevated height. Time spent in the open arm is decreased in mice that exhibit anxiety-like behaviors. The maze consisted of a plexiglass plus-shaped platform elevated 50 cm from the floor with 4 arms intersecting at a 90° angle, creating 4 individual arms each 55 cm long and 5 cm wide[31]. Closed and open arms were orthogonal to each other; the two closed arms were shielded by 25 cm high side and end walls, whereas the two open arms had no walls. The experimental procedure was initiated by the placement of the mouse into the center zone (intersection point) of the maze, facing one of the open arms. The mouse was allowed to explore the maze for a 5-minute period while an overhead video camera recorded the movements of each mouse. Another student blind to grouping of the mice scored the number of entries in each of the arms. All four paws of the mouse had to enter an arm for it to be considered an entry, as the percentage score for the time spent in the open arm was calculated as follows: (time spent in the open arms/ [time spent in the open arms + time spent in closed arms]) x 100.

3.2.6. Histology:

At 6 and 12 months post-mTBI mice assigned to histological studies were anesthetized with isoflurane and perfused transcardially with phosphate-buffered saline (PBS), pH 7.4 followed by PBS containing 4% paraformaldehyde. After perfusion, the brains were postfixed in a solution of 4% paraformaldehyde at 4°C for 48 h. Immunohistochemistry for GFAP, Iba1 and

APP was carried out as described in Chapter 2. Sets of adjacent sections were stained with a panel of antibodies (Table.3.1) for immunohistochemical analyses. Each slide was visualized with a bright field microscope (BX60), and digital images were visualized and acquired using an Olympus MagnaFire SP camera.

Protein Target	Antibody	Epitope	IHC-Dilution	Source	Assay
Amyloid Precursor Protein	22C11	aa* 66-81	1:40,000	Millipore	IHC[₮]
Glial Fibrillary Acidic Protein	GFAP	GFAP	1:20,000	Millipore	IHC
Anti Iba-1	Iba-1	Iba-1	1:5,000	Dako	IHC
Total-tau	DA31	aa 150-190	N/A	Dr. P. Davies	ELISA[¥]
Phospho-tau	CP13	pS202	1:400	Dr. P. Davies	ELISA/IHC
Phospho-tau	PHF1	pS396/404	1:400	Dr. P. Davies	ELISA/IHC
Phospho-tau	RZ3	pT231	1:400	Dr. P. Davies	ELISA/IHC
Phospho-tau	MC1	Conformational	1:200	Dr. P. Davies	IHC
Beta Amyloid (Aβ)	4G8	aa17-24	1:750	Covance	IHC

*aa, amino acid; [₮]IHC, Immunohistochemistry; [¥]ELISA, Enzyme-Linked Immuno-Sorbent Assay

Table.3.1: Summary of antibodies used in chapter 3.

3.2.7. Immunohistochemical quantification:

All quantifications were done as previously described in Chapter 2. For each animal, (n=5 per group at 6 months post mTBI; n=4 per group at 12 months post mTBI), sagittal sections were stained and analyzed by another student blinded to experimental conditions using ImageJ software (US National Institutes of Health, Bethesda, MD, USA). The atrophy of the corpus callosum was calculated using ImageJ. The "freehand" selection tool was selected to outline the surface area of the body of the corpus callosum as illustrated in Figure3.2. For each experimental group, 14 sagittal brain sections of same area located between the splenium and the body of the corpus callosum was measured and averaged. The scale was set based on the

known distance revealed by the scale of a 10x magnification photomicrograph. For our measurements, 100 pixels represented 100 µm.

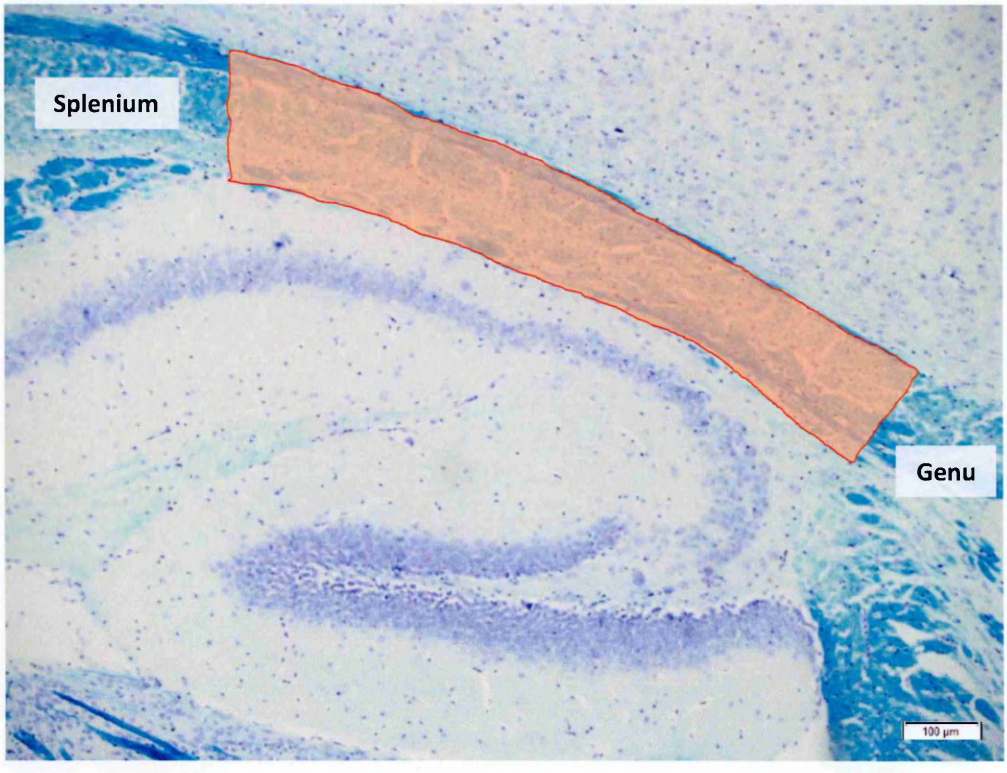

Figure.3.2: Sagittal view of a 10x photomicrograph stained with LFB/CV. Example of an outline highlighted in red used to calculate the surface area for each brain section. Scale bar represents 100µm.

3.2.8. Quantitative assessment of soluble $A\beta_{40}$, phosphorylated and total tau protein:

Analyses of soluble $A\beta_{40}$, phosphorylated tau and total tau protein were carried out on the left hemisected brain obtained from PBS-perfused mice at 6 and 12 months post s/r-mTBI (n=4/group) or s/r-sham exposure (n=4/group). Snap-frozen hemisected cortices and hippocampi were sonicated in 0.5 ml and 0.3 ml of chilled M-PER buffer solution (Thermo Fisher Scientific, Waltham, MA) supplemented with protease and phosphatase inhibitor cocktail (Roche, Indianapolis, IN). For tau biochemistry, tissue homogenates were coded and sent to Peter Davies' group at Albert Einstein College of Medicine, for blinded quantitative

assessments. Sample preparation for the Low-Tau level sandwich ELISA and quantitation of murine-specific tau protein was performed as previously described[32]. Antibodies to detect total and phospho tau (p-tau) (Table.3.1) were used as capture antibodies in the Low-Tau, Sandwich ELISA. Soluble $A\beta_{40}$ was assessed using a sandwich ELISA (WAKO, Richmond, VA) as per the manufacturer's directions. Total protein content was determined by the bicinchonic acid (BCA) method (Thermo Scientific, Waltham, MA) and data were expressed as pmol/g protein ($A\beta_{40}$) and ng tau/mg protein (tau and phosphorylated tau).

3.2.9. Statistics:

All behavioral and pathological data were analyzed using JMP 8.0 (SAS, Cary, NC). Scores were analyzed separately for groups of animals assigned to survival groups for each time points post-injury. Data were tested for normality using the Shapiro-Wilk W Test; when not normally distributed, the data were transformed using square root or natural log transformation. If the data were still not normal after transformation, they were analyzed using non-parametric methods were used for analysis. Repeated-measures ANOVA was used to compare performance during the 6 days of acquisition of the Barnes maze between the matching injury groups when the data were normally distributed. Potential sphericity violations were corrected by adjusting degrees of freedom for all repeated-measures effects by using the Greenhouse-Geisser estimate for epsilon. Probe dataset and quantitative histologic parameters were analyzed with one-way ANOVA, with a Tukey's post-hoc correction for multiple comparisons, unless indicated. ELISA data were plotted and analyzed using Graph-Pad Prism (Prism 6.01, GraphPad Software Inc, La Jolla, CA). One way ANOVA followed by Tukey's post-hoc test was

used for comparison of soluble tau and $A\beta_{40}$ levels between the four groups. Only p values < 0.05 were considered to be statistically significant and are indicated by an asterisk in the figures. Error bars represent the standard error of the mean (SEM).

3.3. Results:

3.3.1. Barnes Maze: acquisition:

At all-time points, both of the injured groups demonstrated a longer cumulative distance to the target in the Barnes maze than their respective sham groups (Fig.3.3A-C), (r-mTBI vs. r-sham, $p < 0.0001$; s-mTBI vs. s-sham, $p < 0.0001$ repeated-measures ANOVA). At 12 and 18 months post injury (Fig.3.3B and C) the deficit in performance of the r-mTBI group became even more apparent in comparison to the s-mTBI group (r-mTBI vs. s-mTBI, $p < 0.005$; repeated-measures ANOVA). The mean cumulative distance over the 6 days acquisition period in the s-mTBI mice was 17%, 36% and 30% longer, respectively, than the s-sham mice at 6, 12 and 18 months post injury. At the same time point the r-mTBI had a greater and progressive separation on cumulative distance travelled (34%, 49% and 55% respectively) when compared to the r-sham. Specifically at 18 months post injury, the r-mTBI group not only travelled longer distances than any other group (r-mTBI vs. s-mTBI, $p < 0.005$; r-mTBI vs. s-sham, r-sham $p < 0.0001$ repeated-measures ANOVA), but was also the only group to show a lack of learning throughout the acquisition trial (Fig.3.3C). There was no difference between the s-sham and r-sham groups at any time point ($p > 0.05$ repeated-measures ANOVA).

The dataset for latency to escape was not normally distributed and thus did not satisfy the assumptions required for a repeated-measure ANOVA. The Wilcoxon signed rank test was

used to test for the daily correlation between each group. No difference in escape latency performance was observed at 6 months post injury between the s-mTBI and s-sham (day 6 of acquisition; $p > 0.05$) (Fig.3.3D). However, when tested at 12 and 18 months post injury, the s-mTBI group showed a progressive decline in escape latency performance. At 6 months post injury, the mean escape latency of the s-mTBI mice improved from 89.18±0.9 s on the first day of acquisition and 52.4 ± 4.0 s on their last day of acquisition. By 12 months post injury, they spent on average 75.8 ± 2.6 s on the first day of acquisition and 59.9±4.4 s by their last acquisition day. There was no improvement observed at 18 months post injury (77.3 ± 2.7 s on day 1 to 73.1 ± 4.4 s on day 6). In contrast, even at the 6 month time point the r-mTBI mice exhibited less improvement over the 6 days than the other groups (Fig.3.3D; days 1 and 6 of acquisition; r-mTBI, 87.94±0.9 s to 69.17±1.0 s; r-sham 88.4±1.1s to 45.1±4.5 s; $p<0.0002$); this lack of improvement during acquisition persisted at 12 months, (79.5 ± 2.1 s to 66.6 ± 4.1 s) and 18 months (79.7 ± 2.8 s to 78.2 ± 4.2 s) post injury. The average velocity was similar across all groups and all time points with a trend for the r-mTBI to be faster than the three other groups ($p > 0.05$; data not shown).

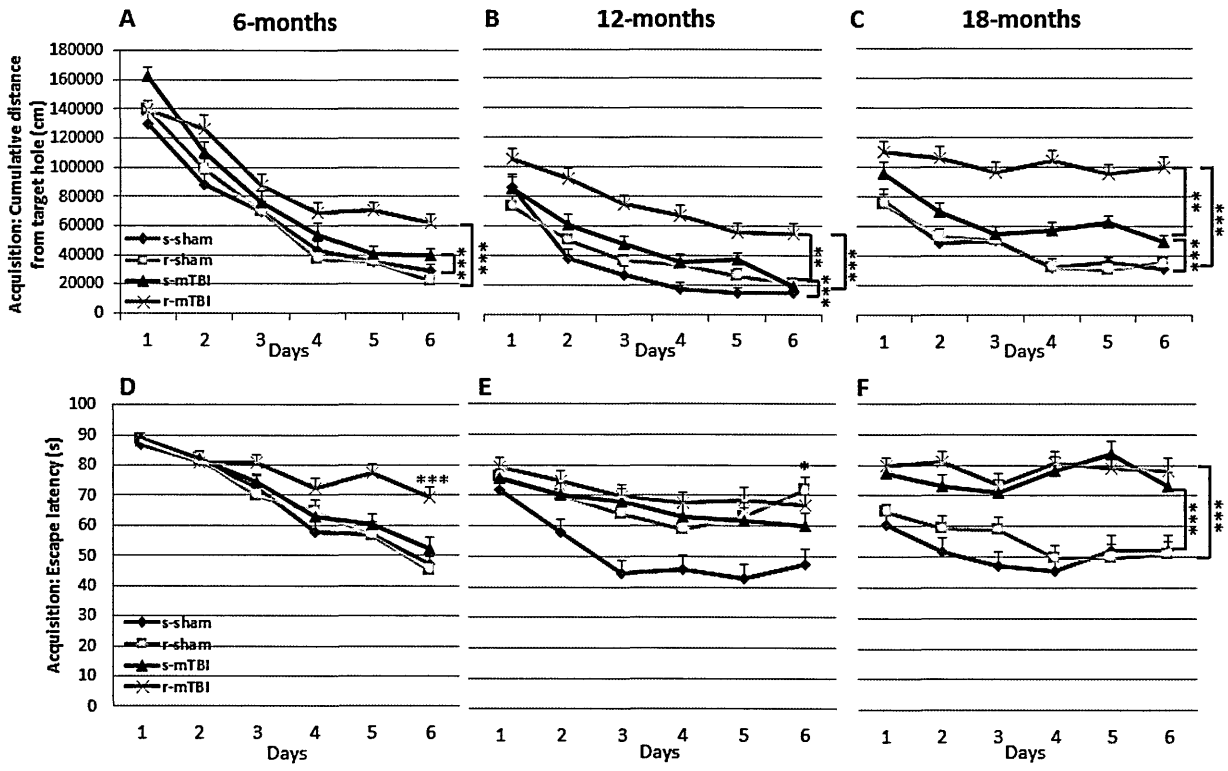

Figure.3.3: Evaluation of learning (acquisition) using the Barnes maze at 6, 12 and 18 months post mTBI. Mice were tested in the Barnes maze for their ability to locate a black box at the target hole. During the acquisition testing at 6 and 12 months, both injured groups traveled a greater cumulative distance before escaping to the target hole compared to their respective anesthesia controls (s-sham vs. s-mTBI; r-sham vs. r-mTBI ***$p < 0.0001$) (A-C), with a trend for the r-mTBI travelling a greater distance than the three other groups. At 12 and 18 months post injury the performance of the r-mTBI group was worse than the s-mTBI (s-mTBI vs. r-mTBI, **$p < 0.005$) (B, C). On day 6 of the acquisition trial at 6 months post injury, the r-mTBI group spent significantly more time escaping to the target hole when compared to the r-sham (red asterisks; ***$p < 0.0001$) (D). On day 6 of the acquisition trial at 12 months post injury, the s-mTBI group spent significantly more time escaping to the target hole when compared to the s-sham (black asterisk; *$p < 0.05$) (E). At 18 months post injury, both injured group spent significantly more time escaping to the target hole when compared to their sham control at every single day of training (***$p < 0.0001$) (F). The mean velocity for the acquisition phase was similar across all groups (data not shown). Data are presented as mean ± SEM; n=12 per group at 6 and 12 months and n=9 per group at 18 months post injury.

3.3.2. Barnes Maze: probe:

Probe test performance was markedly impaired in the r-mTBI mice compared to other groups at each time point (Fig.3.4), requiring on average 12s, 11s and 27s to reach the target

zone at 6 ($p < 0.01$), 12 ($p < 0.05$), and 18 months ($p = 0.055$) respectively (ANOVA). At each time point the s-mTBI, s-sham and r-sham groups had similar performance to each other, which progressively declined as they aged (Fig.3.4A-C). Similar to the acquisition trials, the average velocity was not different across all groups ($p>0.05$; data not shown).

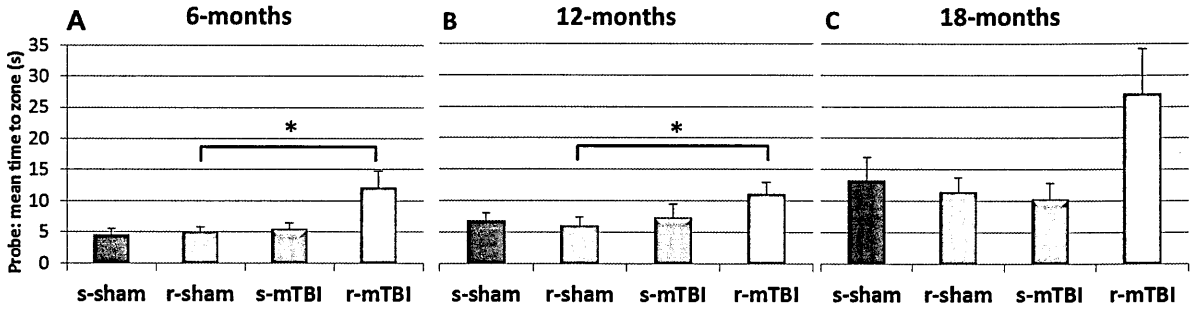

Figure.3.4: Evaluation of spatial memory retention (probe) using the Barnes maze at 6, 12 and 18 months post mTBI. For the probe trial (1 day following the 6 days of acquisition testing), the target box was removed and mice were placed in the middle of the table for a single, 60-sec trial. Probe test performance was markedly impaired in the r-mTBI mice across each time point (A*$p < 0.01$ at 6 months, B *$p < 0.05$ at 12 months, and C $p = 0.05$ at 18 months; as determined by ANOVA). The mean velocity for acquisition phase and probe test was similar across all groups (data not shown). Data are presented as mean ± SEM; n=12 per group at 6 and 12 months and n=9 per group at 18 months post injury.

3.3.3. Reversal Barnes maze and elevated plus maze at 12 months post mTBI:

Following probe testing at 12 months post injury, reversal testing in the Barnes maze was carried out to examine the ability of mice to learn a new location of the target hole. For the r-mTBI group the mean distance travelled to the hidden box was longer compared to the three other groups (r-mTBI vs. r-sham, $p < 0.02$; s-mTBI vs. r-mTBI, $p < 0.0001$; s-mTBI vs. s-sham, $p > 0.05$; repeated-measures ANOVA) (Fig.3.5A). Similarly, the mean escape latency of the s-mTBI mice was not different to their respective shams with performance improving over the four trials from 78.1 ± 3.7 to 50.4 ± 4.8 s, compared to 81.8 ± 3.8 s to 57.5 ± 5.6 s in s-sham animals (Fig.3.5B). In contrast, the r-mTBI group had a higher mean escape latency than the r-sham group in their ability to learn the new target location (r-mTBI, 87.8 ± 1.1 s to 67.2 ± 4.6 s;

s-sham, 82.9 ± 2.3 s to 51.7 ± 5.3 s; $p < 0.004$ at day 4; The Wilcoxon signed rank test) (Fig.3.5B). Probe testing revealed no difference between any of the groups (Fig.3.5C; $p > 0.05$). The day following reversal testing, the anxiety of each animal was tested with the elevated-plus maze (Fig.3.6). Both sham groups (s-sham, 10.19 ± 2 %; r-sham, 9.70 ± 2.7 %) spent a smaller percent of time in the open arm than the s-mTBI (s-mTBI, 14.9 ± 3.3 %) or the r-mTBI (r-mTBI, 13.4 ± 4.7 %; $p > 0.05$).

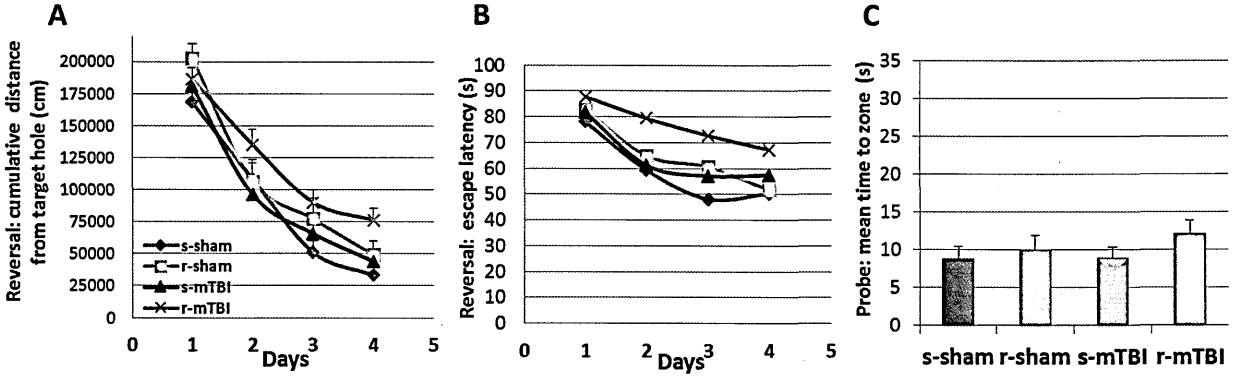

Figure.3.5: Reversal represents learning to find the box when moved to the opposite quadrant. During reversal training, search time decreased in all groups as indicated by a significant effect of trial (***$p < 0.0001$; AB). The r-mTBI group performance was impaired during reversal acquisition (cumulative distance, *$p < 0.05$; A; escape latency, **$p < 0.001$ at day 4; B), while no deficits were observed between the s-mTBI and s-sham group ($p > 0.05$). There was no group differences in probe trials ($p > 0.05$; C). The mean velocity for acquisition phase and probe test was similar across all groups (data not shown). Data are presented as mean ± SEM; n=12 per group.

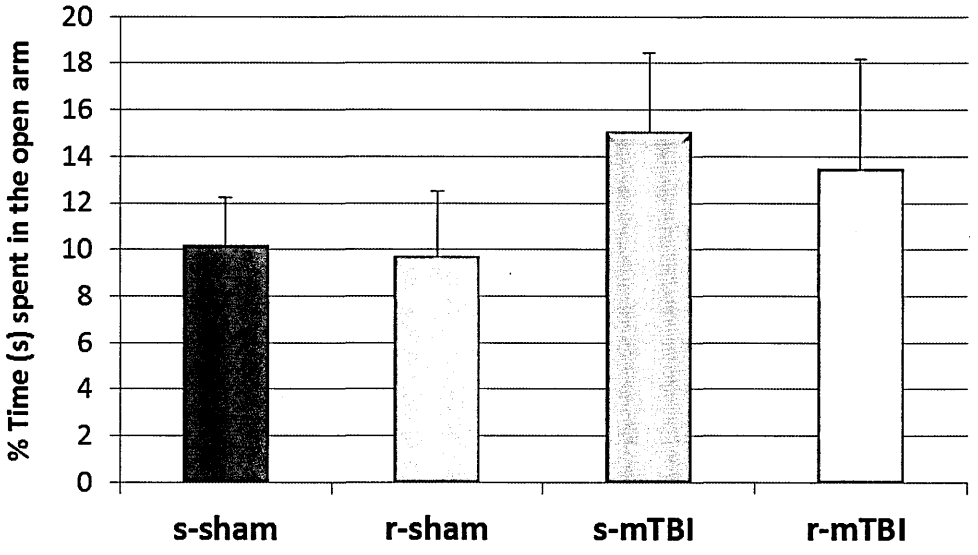

Figure.3.6: Anxiety-like behavior measuring the willingness of the animal to explore exposed arm at a specific height was assessed using an elevated-plus maze. There was a trend for both injured groups to spend more time in the open arms compared to the sham groups. ($p > 0.05$). Data are presented as mean ± SEM; n=12 per group.

3.3.4. White matter integrity:

Changes in the white matter integrity and thickness of the corpus callosum were assessed in sections stained for LFB/CV. Following s-mTBI there was a 12% (+/- 9.2 μm; $p < 0.0001$) reduction in thickness of the body of the corpus callosum at 6 months compared to s-sham (Fig.3.7A-B). This reduction in thickness remained static at 12 months, where the body of the callosum showed a 10% (+/- 4.6 μm; $p < 0.0001$) reduction in thickness compared to sham animals (Fig.3.7C-D). The repetitively injury animals also showed a thinning of the body of the CC at 6 months, with a decrease of 21% (+/- 7.8 μm; $p < 0.0001$) compared to the r-sham group (Fig.3.7E-F). In contrast to the s-mTBI, there was continued loss of callosal white matter between the 6 and 12 month time points where by 12 months post injury the r-mTBI showed a further reduction of 5% ($p < 0.002$) in callosal thickness compared to the 6 month r-mTBI

animals, representing a 26% reduction in CC thickness compared to (Fig.3.6G-H) (+/- 4.0 µm; p < 0.0001) to the r-sham.

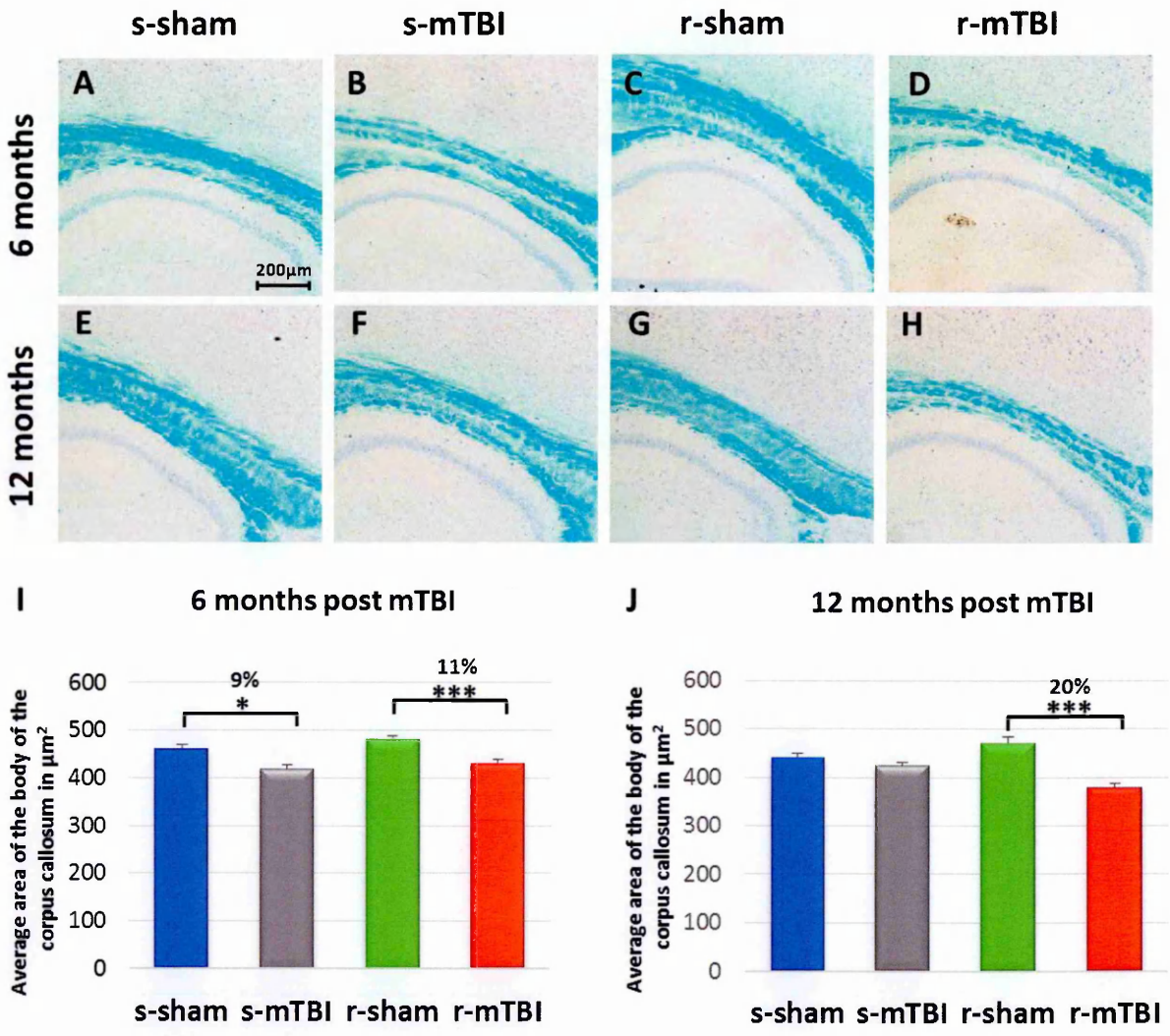

Figure.3.7: Sagittal sections of the mouse brain stained with LFB/CV. LFB/CV staining indicated changes in white matter integrity in the injured animals at both 6 and 12 months post injury (**B, D, F, H**). At 6 months, the thickness of the corpus callosum was decreased on average by 9% after s-mTBI, and by 11% in the r-mTBI **(I)**. By 12 months post injury the average decrease of thickness in the corpus callosum of the s-mTBI was similar to the 6 month timepoint with a 4% decrease, while the r-mTBI showed a progressive reduction by approximately 20% **(J)**. Data are presented as mean ± SEM,*p<0.05, ***p<0.0001.

3.3.5. Amyloid precursor protein immunostaining:

APP-immunoreactive profiles were scattered diffusely throughout the corpus callosum in both injury groups at 6 and 12 months post injury. Typically these were observed as sparse rounded to granular immunoreactive axonal profiles (Fig.3.8B, D). In contrast, save for sparse, single APP-immunoreactive profiles, sham animals showed no evidence of axonal pathology. The number of APP-immunoreactive profiles in the body of the CC of the r-mTBI group was greater than the s-mTBI group at 6 months post mTBI (s-mTBI group 1.2 ± 0.2 vs. r-mTBI 3.6 ± 0.1 axonal profiles/body of CC $p < 0.001$) and 12 months post mTBI (s-mTBI group 3.3 ± 0.5 vs. r-mTBI 9.3 ± 0.8 axonal profiles/body of CC, $p < 0.0001$) (Fig.3.8I-J). Notably, the degree of axonal pathology increased from 6 to 12 months for both the s-mTBI ($p < 0.05$) and r-mTBI groups ($p < 0.001$).

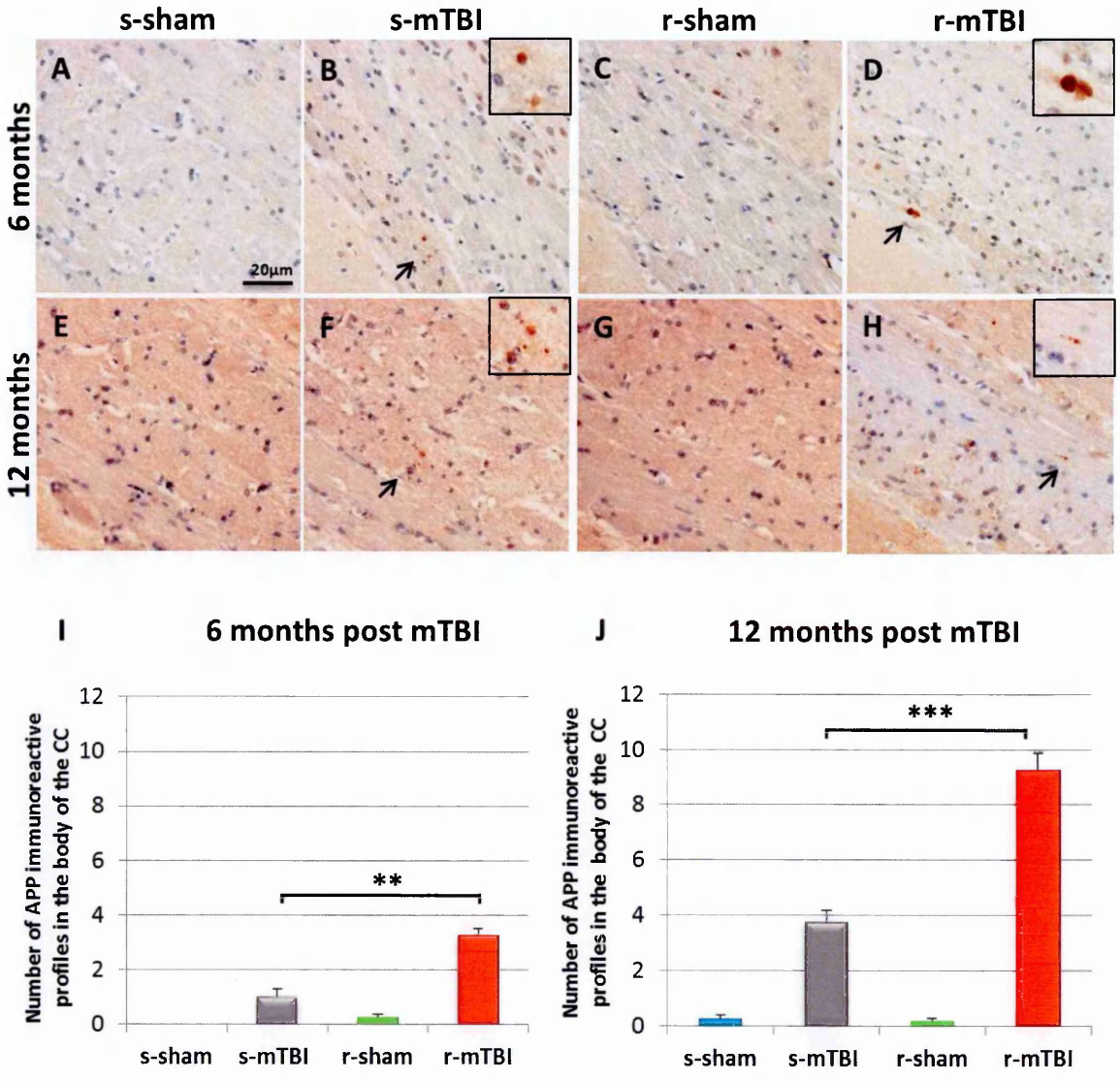

Figure.3.8: Axonal injury within the corpus callosum at 6 and 12 months post mTBI. APP immunoreactive profiles, predominantly observed as axonal bulbs, were seen after s-mTBI and r-mTBI at both time points (B, D, F, H). Tissue staining from sham animals was negative for APP immunostaining. For each image, magnifications of the boxed insets are areas pointed by an arrow. Tissue sections were counter-stained with hematoxylin. Quantitative analysis of APP-immunoreactive profile quantified from the caudal to the dorsal area of the body of the CC at 6 and 12 months post mTBI; n=5 and n=4 respectively. The numbers of APP-immunoreactive profiles in the body of the CC of the r-mTBI group was greater than the s-mTBI group at 6 months post mTBI (s-mTBI group 1.2 ± 0.2 vs. r-mTBI 3.6 ± 0.1 axonal profiles/body of CC $p < 0.001$) and 12 months post mTBI (s-mTBI group 3.3 ± 0.5 vs. r-mTBI 9.3 ± 0.8 axonal profiles/body of CC, $p < 0.0001$) (I-J). Notably, the extent of axonal pathology progressively worsened from 6 to 12 months for both the s-mTBI ($p < 0.05$) and r-mTBI groups ($p < 0.001$). Data are presented as mean ± SEM, (**$p < 0.005$).

3.3.6. Gial fibrillary acidic protein immunostaining:

For all groups, the cortical region underlying the impact site (somatosensory and primary motor cortices), the CC, and the hippocampal regions were assessed in sections stained for GFAP. No astrocytes with morphological appearances of reactive glia, manifest as GFAP-immunoreactive astrocytes with thickened cell processes and hypertrophied cell soma, were observed in the cortex or in hippocampal sector CA1 at 6 or 12 months following s-mTBI (Fig.3.8A-D) or in the single or repetitive anesthesia controls (Fig.3.9E, G), nor was any quantitative difference detected in area of immunopositivity in these regions. Similarly, there was no measurable increase in GFAP immunoreactivity at 6 months in the r-mTBI group in hippocampal sector CA1 (Fig.3.9G). However, increased GFAP-immunoreactivity was observed in this region at 12 months following r-mTBI (r-mTBI 4.2 ± 0.7% vs. r-sham 2.5 ± 0.9%; $p < 0.005$) (Fig.3.9H-J).

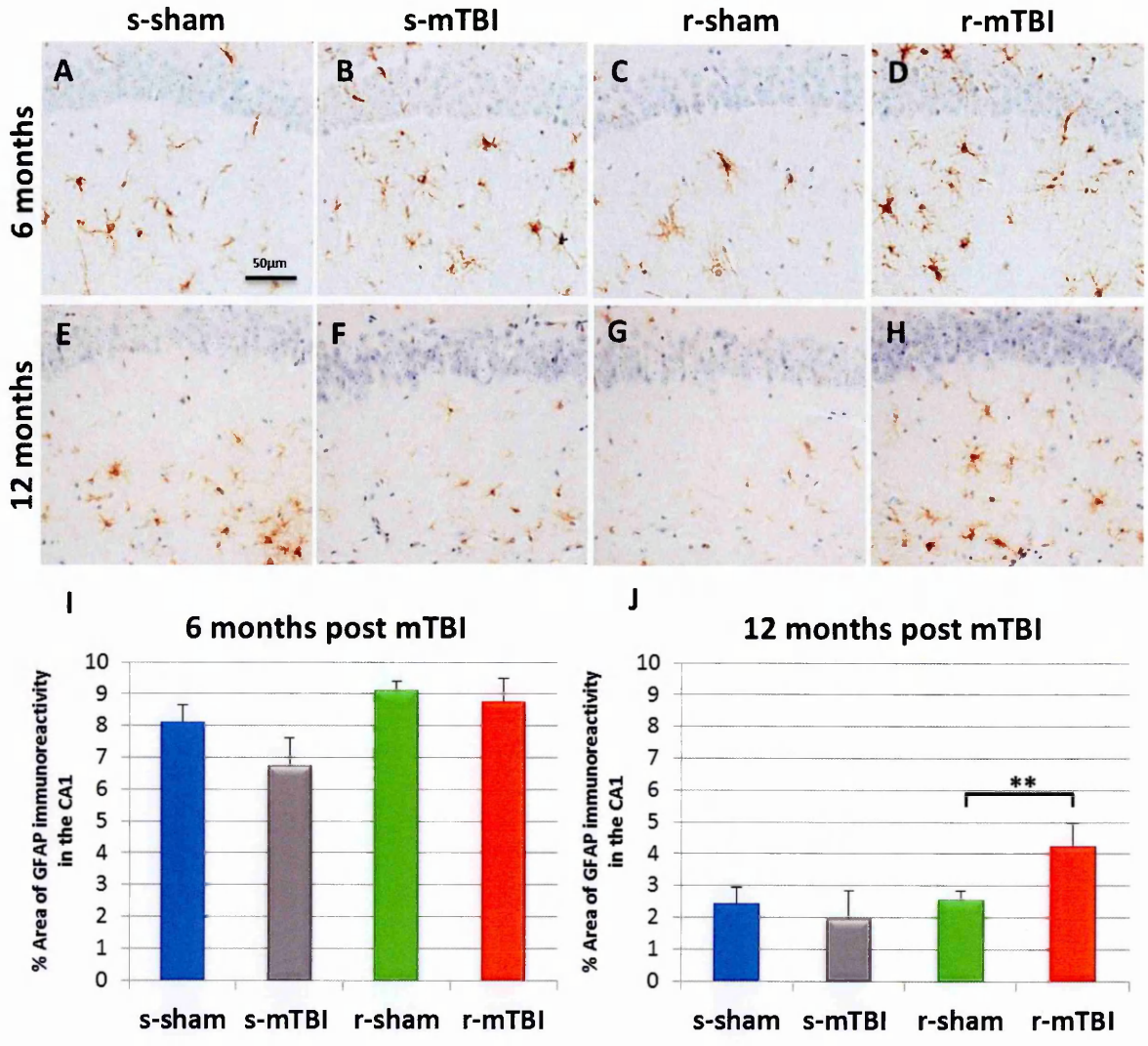

Figure.3.9: GFAP immunohistochemistry of the mouse brain at approximately 0.4 mm lateral to midline in the CA1 subregion of the hippocampus. There were no changes between sham (A, C) and injured (B, D) animals at 6 months post injury. A decrease of GFAP immunoreactivity was observed at 12 months post injury in all groups. An increased area of GFAP immunoreactivity was observed in the r-mTBI (H) when compared to the r-sham (G) at 12 months post injury. Tissue sections were counter-stained with hematoxylin. Quantitative analysis of GFAP staining in two area of 200 μm^2 areas of CA1 subregion of the hippocampus at 6 months (I) and 12 months (J); n=5 and n=4 respectively. Data are presented as mean ± SEM, (**$p < 0.005$).

As regards the corpus callosum, the r-mTBI group showed increased GFAP immunoreactivity at 6 (Fig.3.10D) and 12 months (Fig.3.10H) in the body of the corpus callosum when compared to their shams (Fig.3.10C-G), (6 months: r-sham 3.8 ± 0.6% vs. r-mTBI 7.95 ±

1.2%; $p < 0.01$; 12 months: r-sham 6.25±0.4% vs. r-mTBI 15.4±1.9%; $p < 0.0001$) (Fig.3-10I). Of note, while there was no measurable increase in GFAP immunoreactivity at 6 months in the s-mTBI group (Fig.3-910F), there was an increase in immunoreactivity at 12 months post injury compared to its sham (Fig.3-10E), (Fig.3-10I; 12 months: s-sham 3.0 ± 0.4% vs. s-mTBI 6.6 ± 0.8%; $p < 0.0001$).

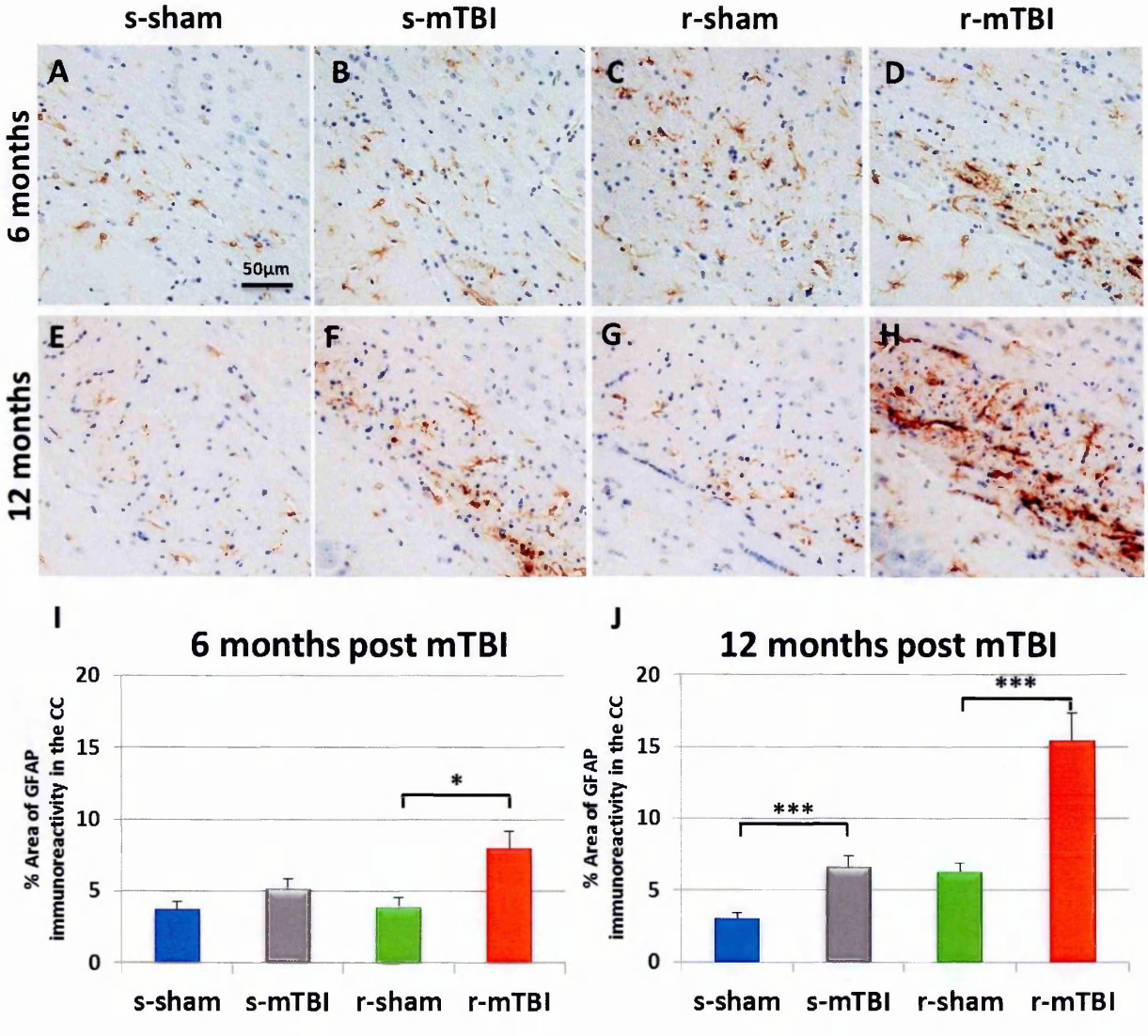

Figure.3.10: GFAP immunohistochemistry of sagittal sections of the mouse brain at approximately 0.4 mm lateral to midline in the corpus callosum. Healthy astrocytes were observed in sham animals at both time points (A, C, E, G). At 6 months post injury, the s-mTBI animals exhibited normal GFAP

inmmunoreactivity (B). By 12 months post injury the s-mTBI group showed mild reactive astrogliosis with variable degrees of thickened cell processes and hypertrophied cell soma (F). These changes were observed in the r-mTBI group as early as 6 months post mTBI (D). By 12 months post injury, severe reactive astrogliosis with disruption of individual domains was observed in the r-mTBI group (H). Tissue sections were counter-stained with hematoxylin. Quantitative analysis of GFAP staining in three 100 μm2 fields of the CC at 6 months (I) and 12 months (J); n=5 and n=4 respectively. Data are presented as mean ± SEM, (*$p < 0.05$; ***$p < 0.0001$).

3.3.7. Ionized calcium binding adaptor molecule 1 immunostaining:

The pattern and distribution of activated microglia revealed that staining for Iba-1 was similar to GFAP. For all groups, there was no appreciable evidence of microglial activation in the retrosplenial, sensorifrontal and motor cortex at 6 or12 months post injury (Fig.3.11A-H). In the corpus callosum, the s-mTBI showed a notable increase in anti-Iba1 reactivity at 12 months (Fig.3.12F-H; s-sham 4.8 ± 0.4% vs. s-mTBI 6.8 ± 0.5%; $p < 0.0001$). For mice subjected to r-mTBI, immunostaining for Iba-1 revealed a markedly increased expression at both 6 and 12 months (Fig.3.12D-H) when compared to their sham groups (Fig.3-6C-G), (6 months: r-sham 4.45 ± 0.6% vs. r-mTBI 11.6 ± 0.8%; $p < 0.01$; 12 months: r-sham 4.3 ± 0.6% vs. r-mTBI 11.9 ± 0.6%; $p < 0.0001$).

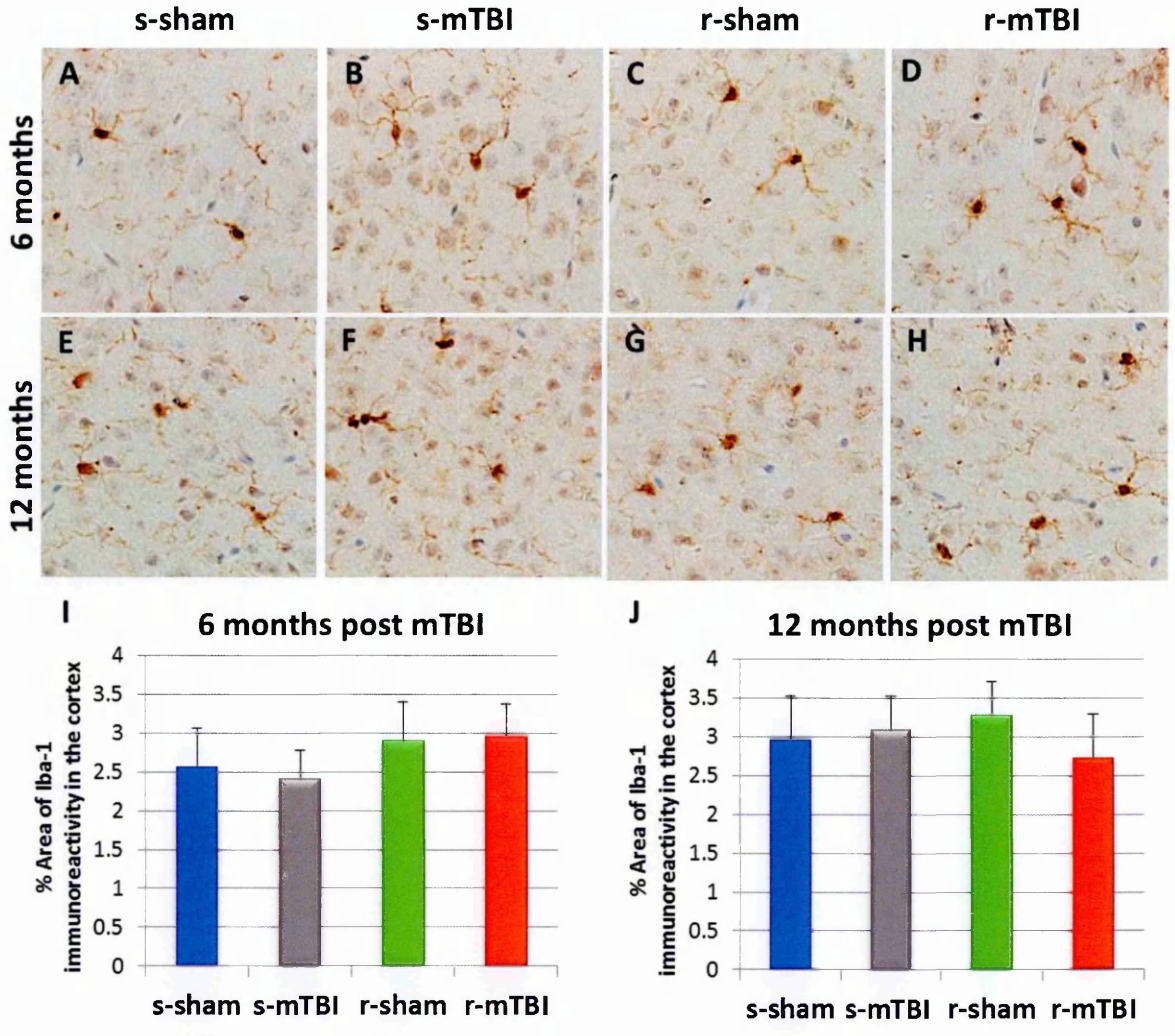

Figure.3.11: Immunohistochemical labeling for microglia with Iba-1. Sagittal sections of the mouse brain approximately 0.4 mm lateral to midline in layer III/IV of the cortex. There was no difference in the expression of Iba-1 with respect to the sham animals at 6 months (A-D), and 12 months (E-H) post injury. Tissue sections were counter-stained with hematoxylin. Quantitative analysis of Iba-1 staining in four 150 μm^2 fields between layer III and V of the cortex at 6 months (I) and 12 months (J); n=5 and n=4 respectively. Data are presented as mean ± SEM, ($p > 0.005$).

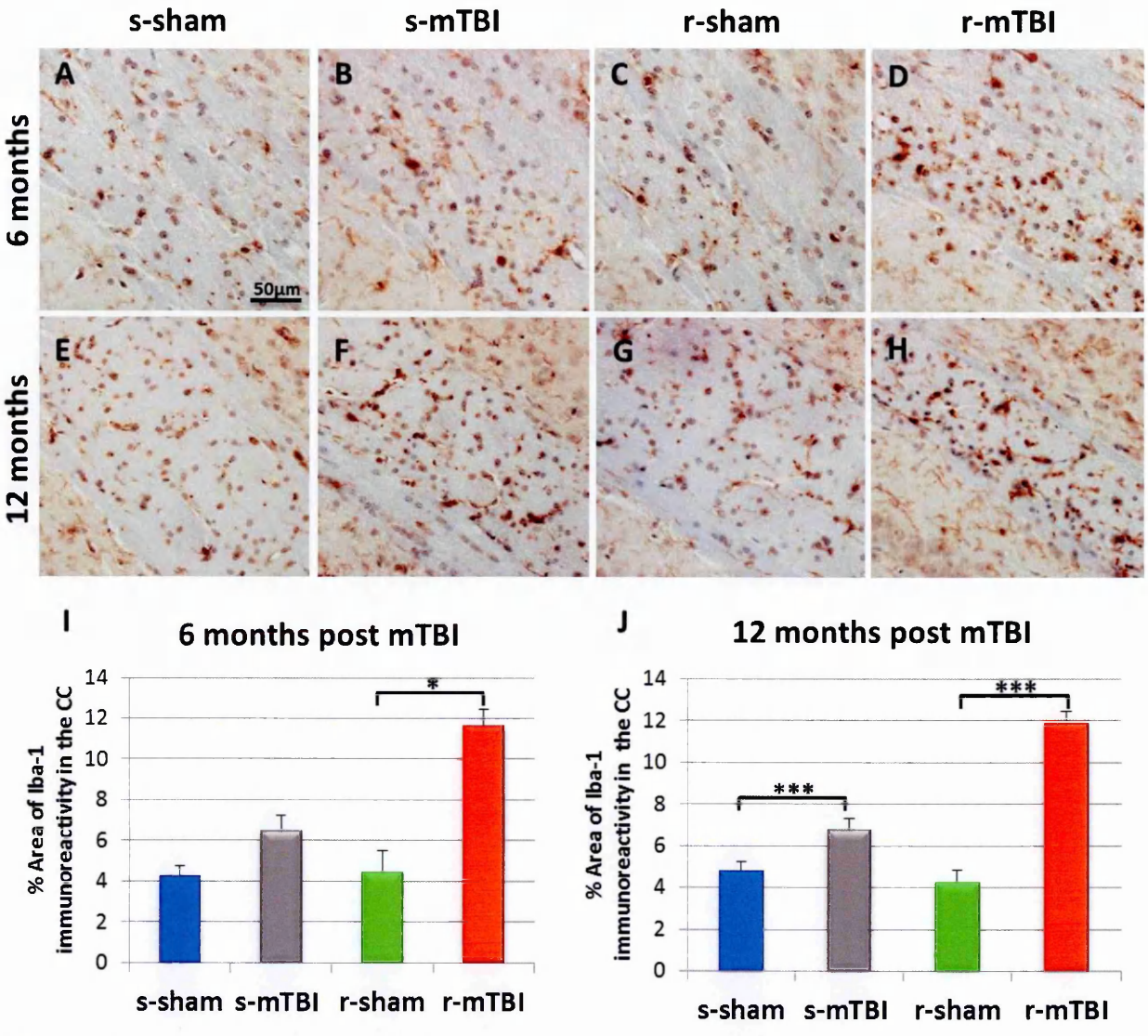

Figure.3.12: Immunohistochemical labeling for microglia with anti-Iba1. Sagittal sections of the mouse brain approximately 0.4 mm lateral to midline in the corpus callosum. Iba-1 immunoreactivity was two-fold greater in the CC following r-mTBI (D) when compared to the s-mTBI (B) and three fold greater when compared to sham controls (A, C). At 6 months post injury, Iba-1 immunoreactivity was markedly increased in both injured groups (F, H) at 12 months post mTBI when compared to sham animals (E, G). Tissue sections were counter-stained with hematoxylin. Quantitative analysis of Iba-1 staining in three 100 μm^2 fields in the corpus callosum at 6 months (I) and 12 months (J); n=5 and n=4 respectively. Data are presented as mean ± SEM, (*$p < 0.05$; *** $p < 0.0001$).

3.3.8. Amyloid and tau biochemistry:

To investigate any pathological effect of TBI on tau in this model, we used our recently developed Low-Tau ELISAs that quantitatively assess different epitopes of tau relevant to various tauopathies: DA31 (total tau; amino acids 150–190), CP13 (pSer-202), RZ3 (pThr-231), and PHF1 (pSer-396/404), To corroborate the biochemical findings, we also carried out immunohistochemical analyses using CP13, RZ3, PHF1 and MC1, an antibody that recognizes only tau in a pathological conformation.

In all experimental groups, at both 6 and 12 months post mTBI/anesthesia, there was no TBI-dependent increase in cortical or hippocampal soluble total or p-tau (Fig.3.13, Fig.3.14, Fig.3.15, $p>0.05$). An age-dependent increase in soluble p-tau was observed between 6 and 12 months in the hippocampi and cortices of all experimental groups ($p<0.0001$). In addition, p-tau was also quantitated as a ratio of phosphorylated tau protein to total tau protein. Again there was no injury effect on these ratios at either time points and in either brain region (cortex; Fig.3.14B, E, H; hippocampus; Fig.3.15B, E, H).

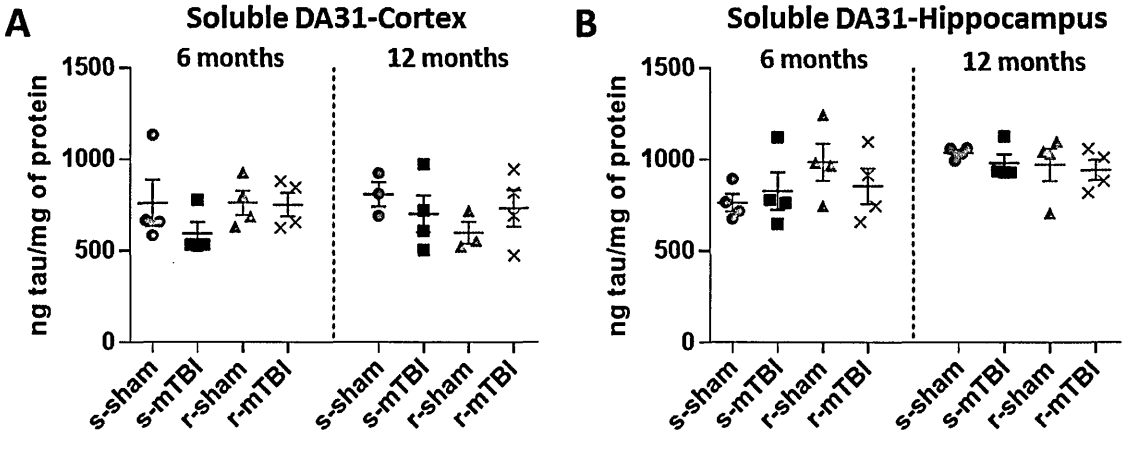

Figure.3.13: DA31 (Total tau) ELISAs measuring the soluble tau level of each group at 6 and 12 months post mTBI/anesthesia. One way ANOVA was used to calculate significance of tau in the cortex (A) and in

the hippocampus (B) between the four groups for each time point. Each data point indicates an individual animal (n=4 per group). No difference was observed between each groups; p>0.05.

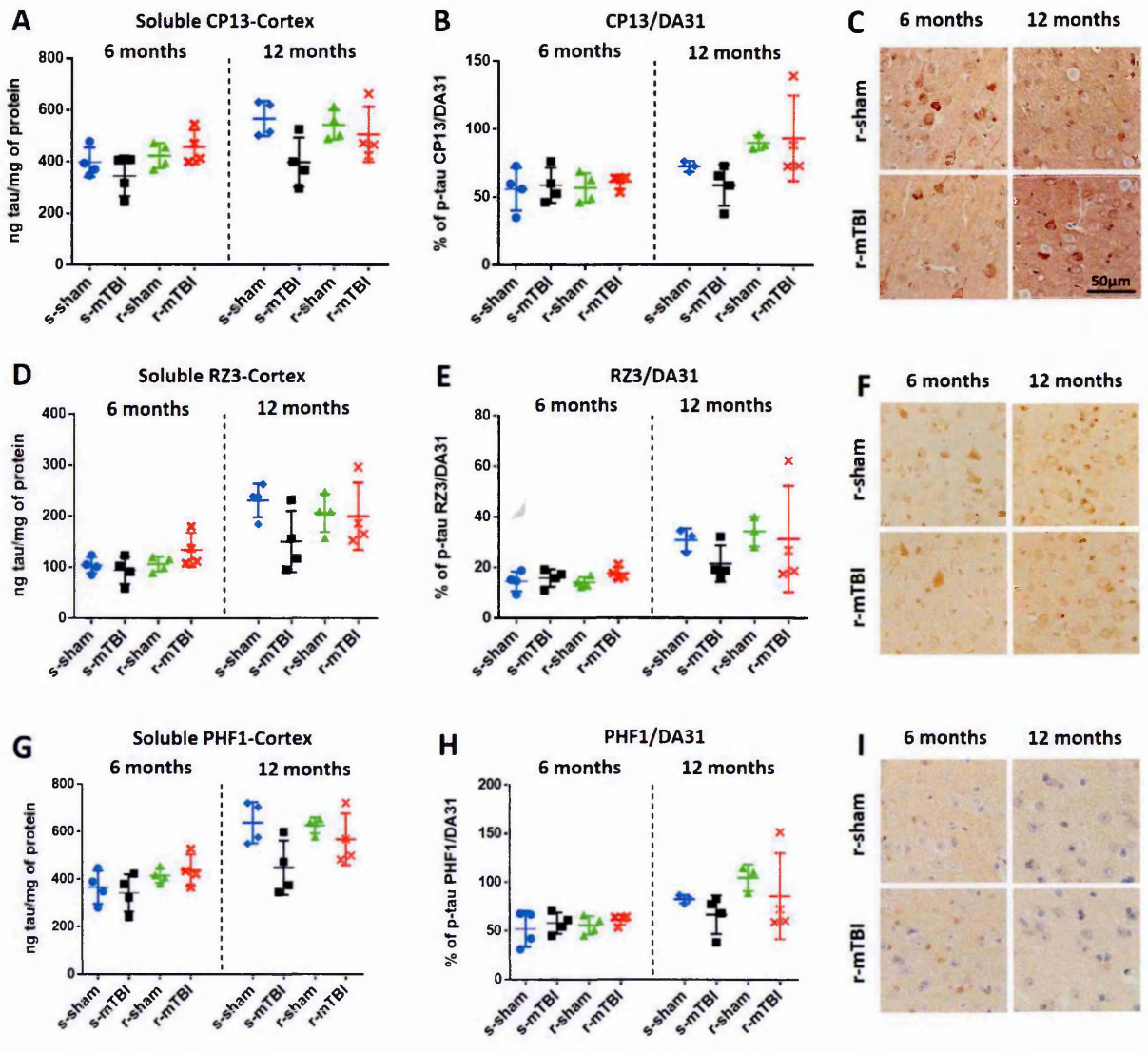

Figure.3.14: Biochemical (ELISA) and IHC assessment of different soluble p-tau species in the neocortex at 6 and12 months post injury. There was no TBI-dependent increase in cortical soluble p-tau pSer-202 (CP13), pThr-231 (RZ3) and pSer-396/404 (PHF1) at 6 or 12 months post mTBI (A, D, G) (p>0.05; one-way ANOVA,). An age-dependent increase for each soluble p-tau was observed between 6 and 12 months post mTBI in the cortices of all groups (p<0.0001; one-way ANOVA followed by Tukey's *post hoc* t-test). Each data point indicates an individual animal (B, E, H) (n=4 per group). Similar to the quantitative analysis of each p-tau epitopes, there was no increase of p-tau when quantitated as a ratio of p-tau protein to total tau protein. P-tau immunohistochemistry of mouse brain at approximately 0.5 mm lateral to midline in the superficial layers of the cerebral cortex (C, F, I). All experimental groups exhibited somatodendritic localization accumulation of CP13 and RZ3 immunoreactivity in neurons of

the superficial layer of the cerebral cortex (C, F). No PHF1 immunoreactivity was observed in injured or sham animals at 6 and 12 months post injury (I). Qualitative assessment of tau immunohistochemistry revealed no change between sham and injured animals at 6 and 12 months post injury in all groups. Tissue sections were counter-stained with hematoxylin.

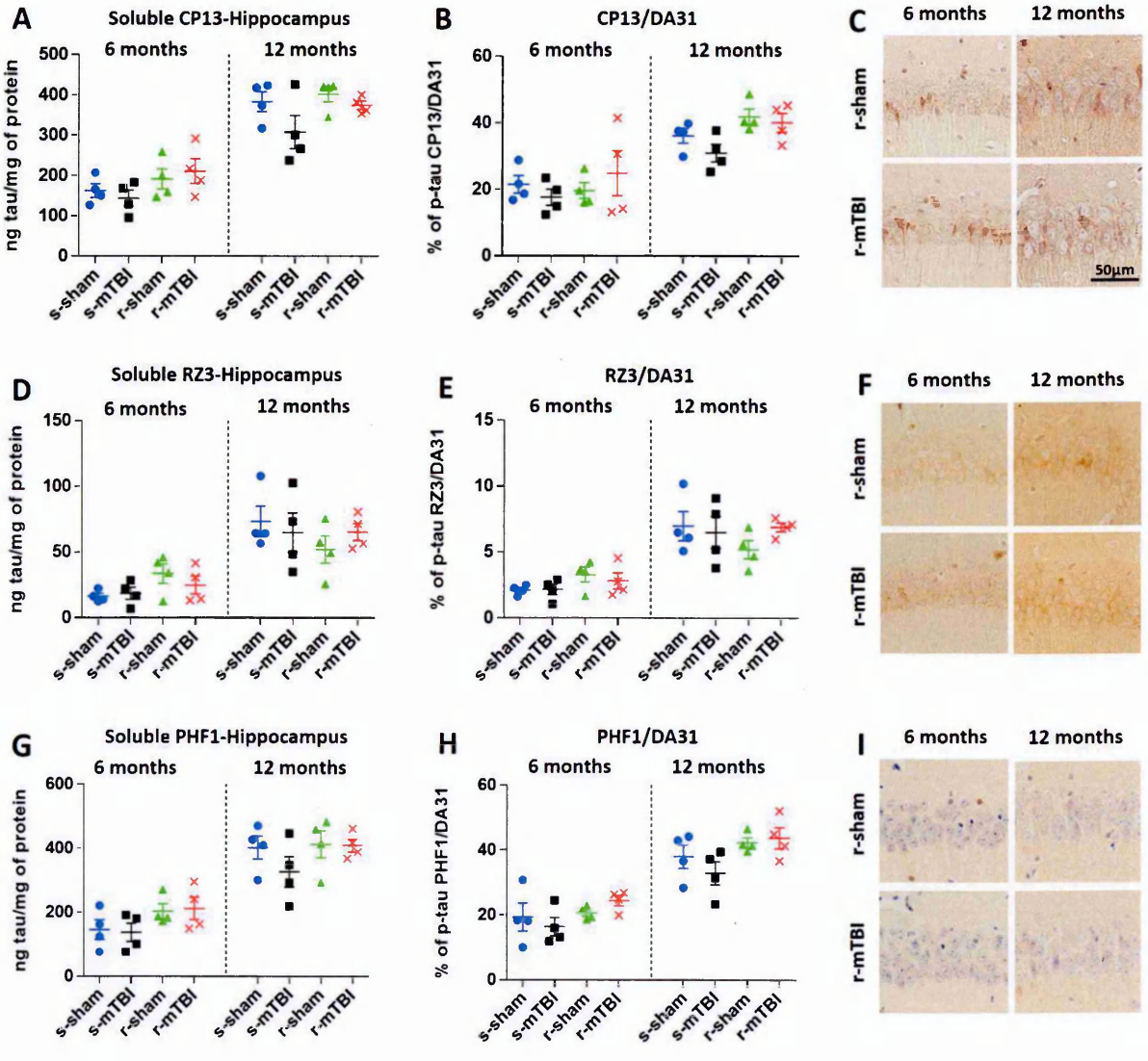

Figure.3.15: Biochemical (ELISA) and IHC assessment of different soluble p-tau species in the hippocampus at 6 and12 months post injury. There was no TBI-dependent increase in hippocampal soluble p-tau pSer-202 (CP13), pThr-231 (RZ3) and pSer-396/404 (PHF1) at 6 or 12 months post mTBI (A, D, G) ($p>0.05$; one-way ANOVA). Each data point indicates an individual animal (n=4 per group). An age-dependent increase in soluble p-tau was observed between 6 and 12 months post mTBI in the hippocampus of all groups ($p<0.0001$; one-way ANOVA followed by Tukey's *post hoc* t-test). Similar to the quantitative analysis of each individual p-tau epitope, there was no increase in p-tau when quantitated as a ratio of p-tau protein to total tau protein (B, E, H). P-tau immunohistochemistry of mouse brain at approximately 0.5 mm lateral to midline in the CA1 region of the hippocampus. All

experimental groups exhibited somatodendritic accumulation of CP13 and RZ3 immunoreactivity in the pyramidal cell layer of the hippocampus (C, F, I). There were no change between sham and injured animals at 6 and 12 months post injury in all groups. Tissue sections were counter-stained with hematoxylin.

Immunohistochemical analyses revealed no injury effects in the localization or accumulation for the p-tau epitopes CP13 and RZ3. All experimental groups exhibited somatodendritic accumulation of CP13 and RZ3 immunoreactivity in neurons of the superficial layer of the cerebral cortex (Fig.3.14C, F, I), CA1 (Fig.3.15C, F, I). The same brain regions were devoid of PHF1 (Fig.3.14, 15I) and MC1 (Fig.3.16) positive neurons regardless of the injury status.

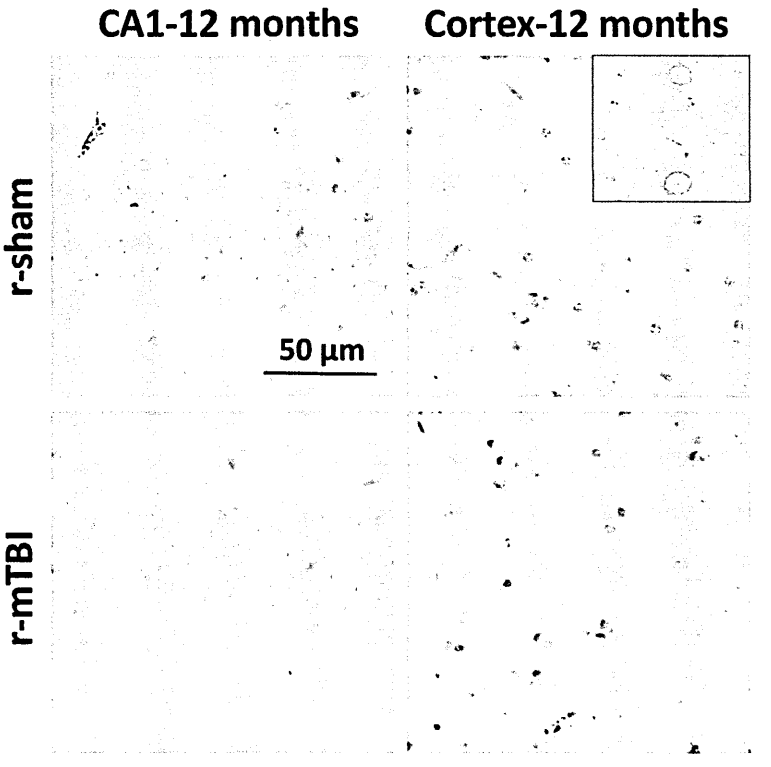

Fig.3.16: MC1-positive cells, an early pathological tau conformation produced by the intramolecular association between the extreme N-terminus and the third microtubule repeat domain of tau observed in positive control (top right corner inset) were not detected in both the neocortex and the hippocampus at 6 and 12 months post injury/anesthesia in all groups; n=5 and n=4 respectively. Tissue sections were counter-stained with hematoxylin.

ELISA analysis of soluble murine $A\beta_{40}$ showed no TBI or age-dependent increases (Fig.3.17A, C). Aβ deposition with 4G8 (Fig.3.17B, D) was not detected in the cerebral cortex or in the hippocampus of any group at 6 and 12 months post injury.

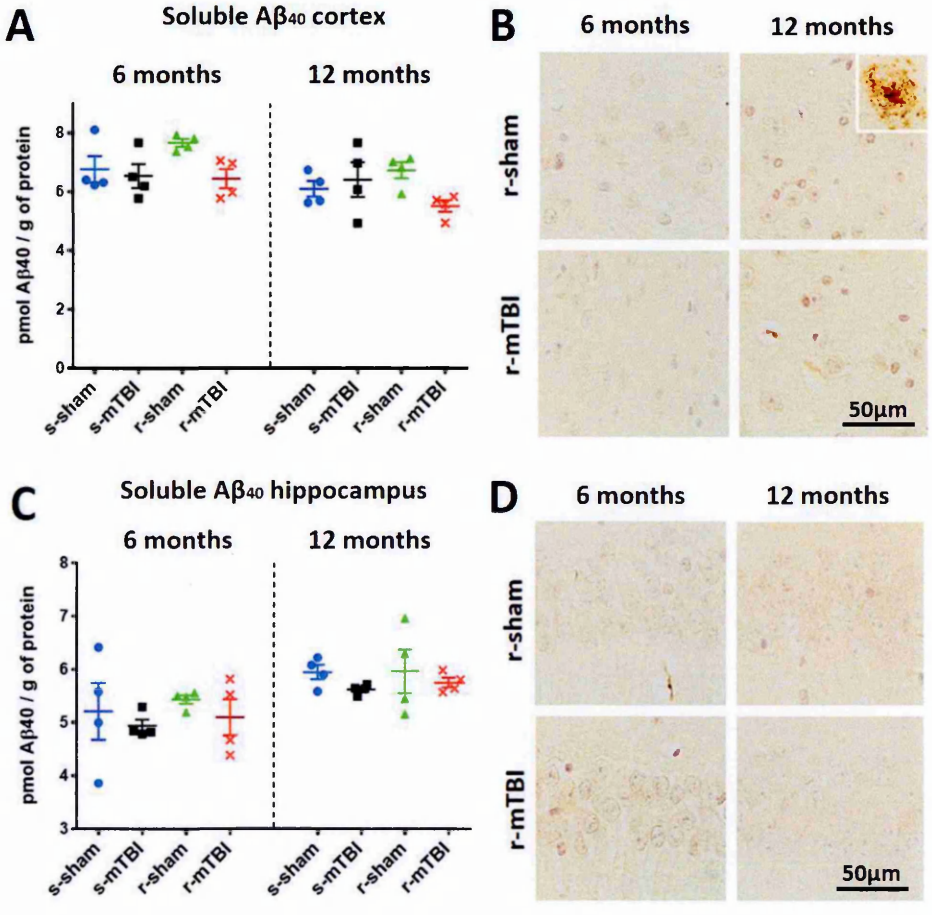

Figure.3.17: Quantification (ELISAs) of soluble $A\beta_{40}$ and its associated IHC staining in the cortex and hippocampus at 6 and12 months post injury. Analysis of soluble murine $A\beta_{40}$ showed no TBI or age-dependent increases (A, C). Aβ deposition with 4G8 was not detected in the cerebral cortex and hippocampus in any group at 6 and 12 months post injury (B, D). Top right inset represent a positive control animal for 4G8.

3.4. Discussion:

With this extension of our original work on the acute phase characteristics of single and r-mTBI in our mouse model (Chapter 2) we have now demonstrated that there are measurable behavioral and neuropathological consequences which persist and evolve for some considerable time after injury, particularly following repetitive injury. This is manifest as continued and developing behavioral deficits up to 18 months following injury and as evolving neuropathological changes up to 12 months from the initial injury, characterized by persistent neuroinflammation associated with ongoing white matter degradation independent of $A\beta_{40}$ or tau accumulation. Importantly, the findings provide evidence that our mouse model recapitulates many aspects of TBI described in human studies[4,9,10,18,33,34].

The neurobehavioral analyses were carried out in the same cohort of mice that were previously evaluated at an acute (24 h) time point after injury (Chapter 2) in which both s-mTBI and r-mTBI injury resulted in cognitive deficits. From the current data we demonstrate that for the probe trial (cognitive performance) the single injury animals have recovered to the same level of performance as their sham animals by 6 months post injury, remaining at comparable levels at subsequent 12 and 18 month evaluations. These findings are consistent with observations in the human population in which those suffering from mild head injury often return to their pre-concussive status within one week[35-37]. In contrast, following repetitive injury, where animals are subjected to a total of 5 mild TBI with an inter-concussion interval of 48 h, the acute cognitive deficit persisted at six months and, indeed, continued to evolve through the 12 and 18 month time points. Altogether, these data provide evidence that cognitive impairments following a single mTBI may be transient, while cognitive deficits

following repetitive injury not only persist but continue to evolve up to 18 months after injury. Moreover, with regard to repetitive injury, Guskiewicz and colleagues[5] suggest that the effects of a concussion far outlast the acute phase. Indeed, the prevalence of mild cognitive impairment and significant memory problems is 5-times greater in former athletes who suffered multiple concussions compared with retirees without a history of concussion[5].

At all-time points examined, the behavioral performance of repetitively-injured animals was diminished when compared to the other groups. The main difference between both injury groups at 18 months was in the average distance travelled to reach the target hole. Animals from the r-mTBI group were unable to learn and were continually distant from the target, reinforcing the fact that repetitive insults worsen cognitive performance at chronic time points post injury. Overall, these results are consistent with observations in human patients, where residual impairments in learning strategy and/or a lack of executive function have also been reported post injury[38-40].

Interestingly, in the elevated plus maze, there was a trend for the injured mice to spend more time in the open arm than the sham controls, demonstrating a mild behavioral disinhibition. This trend is also consistent with human studies where disinhibition has been reported as a consequence of mTBI[10,41-43].

Accompanying these neurobehavioral deficits, we observed comparable concordant neuropathologies in the various injury models. In particular, the single injury animals displayed evident pathology, manifest as a degree of neuroinflammation and white matter loss (corpus callosum thinning), which peaked at six months and remained static at the 12 month evaluation. This suggests that the pathological disturbance following a single mTBI may be

transient in nature, potentially due to the action of intrinsic mechanisms that restore axonal membrane and reorganize the fiber tracts. Indeed, activated microglia can promote neural plasticity[44-46] and repair[47]. Similar to microglia, activated astrocytes have also been involved in facilitating repair[48] in the mature brain via the release of neurotrophic factors[49] such as brain-derived neurotrophic factor (BDNF). In contrast, not only did the repetitively injured mice show greater pathological changes at all-time points when compared to the single injury animals, there was also evidence of a continued progression of neuropathology up to 12 months post injury. White matter degradation appeared to continue some considerable months from the original injuries, with evidence of further callosal thinning between 6 and 12 months corresponding to evidence of ongoing axonal degradation manifest as APP-immunoreactive axonal profiles. The sequence of these chronic changes remain unclear, however, secondary mechanisms initiated after trauma such as chronic microglial activation and reactive astrogliosis may contribute to the ongoing axonal pathology and eventually lead to the progressive loss of axons following r-mTBI. Post-traumatic neuroinflammatory responses possess both beneficial and detrimental effects, and these likely differ in the acute and delayed phases after mTBI[45,50].

Imaging studies have demonstrated white matter integrity is correlated with executive function, attention and memory[34,51-53]. Given that the most significant pathological changes were observed in the corpus callosum rather than the hippocampus, it appears likely that the white matter pathology is responsible for the neurobehavioral deficits. Behavioral performance depends on a broad array of circuits/brain systems including afferent (sensory) pathways, and sensorimotor integration in which the corpus callosum is involved. The pattern of white matter injury could very well be the underlying cause of these widespread deficits, although it is

impossible to ascertain the specificity of any particular lesion/mechanism to any one deficit. For example, a multitude of diverse secondary injury mechanisms could cause the neurological deficits observed months to years after r-mTBI. Among these, oxidative stress[54], lipid peroxidation[54], mitochondrial dysfunction[54], cytoskeletal degradation[55-57], depolarization and disturbances of ionic homeostasis[58] have long been implicated in the pathophysiology of TBI. These events release toxic and pro-inflammatory chemokines, cytokines, prostaglandins and oxidative metabolites which in turn could contribute to the ongoing neuroinflammation. Of note, the crosstalk between proinflammatory cytokines and glutamates receptors, a process defined as "immunoexcitotoxicity" may also play a central role in the prolonged progression of neurodegenerative changes after r-mTBI[22]. This correlates with the impairments in strategy learning which are frequently observed in human subjects in the absence of overt lesions in grey matter following TBI[59-61].

The results of this study also support the contention that r-mTBI may also prevent normal microglial switching from an activated to resting state, which was specific to the subcortical white matter regions, particularly the corpus callosum. As time elapses post injury, our results indicate that the level on inflammation observed at acute time point post injury remains elevated in corpus callosum while it recovered in the cortical grey matter.

Although inflammation is a consistent pathological feature in our model, there may be other pathologies that contribute to the observed cognitive deficits, such as dendritic[62,63] and/or synaptic loss[63,64]. As such, additional biochemical, electrophysiological and pathological examinations are warranted.

The chronic inflammation we observe is in line with autopsy reports from former athletes with history of r- mTBI[10,13,14]. Given the proposed pathophysiological role for chronic neuroinflammation in neurodegenerative disease[23], our data suggest that the progressive neuroinflammation in the r-mTBI model may be a key contributor to the neurobehavioral deficits. Our data also suggest that the cognitive deficits observed occurred independently of $A\beta_{40}$ or tau accumulation. Recently, Mannix and colleagues used a weight drop model to deliver r-mTBI to wild type mice and to APOE transgenic mice expressing the human E4 allele (which confers risk for development of Alzheimer's disease, and also risk of poor outcome after TBI). They reported no change in tau phosphorylation and $A\beta_{40}$ accumulation at 6 months post injury[28]. Consistent with that study, we observed no evidence for involvement of tau or amyloid beta pathology in this model at the 6 and 12 month timepoints. Use of genetically modified animals, expressing human forms of these proteins, may be necessary in order to mimic these pathological features, but in our wild type mouse model these results further underscore the significance of the neuroinflammatory processes as contributory toward the neurobehavioral dysfunction we observe.

Despite the limitations when translating from laboratory TBI models to human populations[25,65], in this model we describe components that are clinically relevant. The white matter degradation, axonal injury and neuroinflammation we observed in the corpus callosum in our injury groups at 6 and 12 months post injury are now recognized to be important aspects of human long term TBI sequelae, observed after both repetitive mTBI[4,6,10,34] and single moderate to severe injury[66-69]. This may suggest that the neurodegenerative consequences of a

single moderate to severe injury and of r-mTBI are on the same spectrum, with a phenotype influenced by severity and frequency of TBI, but this has yet to be demonstrated.

The acute cognitive deficits and accompanying neuropathology reported in Chapter 2 are thus demonstrated to persist and progress at extended time points in repetitively injured mice. Our demonstration of cognitive deficits at 18 months post injury, and progressive neuropathological changes at 12 months post injury, emphasize the relevance of our model for translational studies to elucidate the pathophysiology of these TBI-associated neurobehavioral and neuropathological changes. Together these acute and chronic evaluations support our contention that this model is a relevant preclinical model for human mTBI, and will serve as a valuable tool with which to explore TBI sequelae at the molecular level which in turn should identify therapeutic targets. For example, since glial activation endure over time, it seems that controlling it could be beneficial and may lead to behavioral improvements. Moreover, as originally intended, the development of this mTBI paradigm in a mouse model facilitates the investigation of the role of genes and proteins known or hypothesized to be of significance in human TBI; the influence of one such protein "tau" is investigated in the work described in the following Chapter.

3.5. References:

1 Goldman, S. M. *et al.* Head injury and Parkinson's disease risk in twins. *Annals of neurology* **60**, 65-72, doi:10.1002/ana.20882 (2006).

2 Chen, H., Richard, M., Sandler, D. P., Umbach, D. M. & Kamel, F. Head injury and amyotrophic lateral sclerosis. *American journal of epidemiology* **166**, 810-816, doi:10.1093/aje/kwm153 (2007).

3 Lehman, E. J., Hein, M. J., Baron, S. L. & Gersic, C. M. Neurodegenerative causes of death among retired National Football League players. *Neurology*, doi:10.1212/WNL.0b013e31826daf50 (2012).

4 Elder, G. A. *et al.* Blast exposure induces post-traumatic stress disorder-related traits in a rat model of mild traumatic brain injury. *Journal of neurotrauma* **29**, 2564-2575, doi:10.1089/neu.2012.2510 (2012).

5 Guskiewicz, K. M. *et al.* Association between recurrent concussion and late-life cognitive impairment in retired professional football players. *Neurosurgery* **57**, 719-726; discussion 719-726 (2005).

6 Smith, D. H., Johnson, V. E. & Stewart, W. Chronic neuropathologies of single and repetitive TBI: substrates of dementia? *Nature reviews. Neurology*, doi:10.1038/nrneurol.2013.29 (2013).

7 Roberts, G. W., Gentleman, S. M., Lynch, A. & Graham, D. I. beta A4 amyloid protein deposition in brain after head trauma. *Lancet* **338**, 1422-1423 (1991).

8 Costanza, A. *et al.* Review: Contact sport-related chronic traumatic encephalopathy in the elderly: clinical expression and structural substrates. *Neuropathology and applied neurobiology* **37**, 570-584, doi:10.1111/j.1365-2990.2011.01186.x (2011).

9 McKee, A. C. *et al.* The spectrum of disease in chronic traumatic encephalopathy. *Brain : a journal of neurology* **136**, 43-64, doi:10.1093/brain/aws307 (2013).

10 Sosa, M. A. *et al.* Blast overpressure induces shear-related injuries in the brain of rats exposed to a mild traumatic brain injury. *Acta Neuropathologica Communications* **1**, 51 (2013).

11 Omalu, B. I., Fitzsimmons, R. P., Hammers, J. & Bailes, J. Chronic traumatic encephalopathy in a professional American wrestler. *Journal of forensic nursing* **6**, 130-136, doi:10.1111/j.1939-3938.2010.01078.x (2010).

12 King, A. *et al.* Abnormal TDP-43 expression is identified in the neocortex in cases of dementia pugilistica, but is mainly confined to the limbic system when identified in high and moderate stages of Alzheimer's disease. *Neuropathology : official journal of the Japanese Society of Neuropathology* **30**, 408-419, doi:10.1111/j.1440-1789.2009.01085.x (2010).

13 Goldstein, L. E. *et al.* Chronic traumatic encephalopathy in blast-exposed military veterans and a blast neurotrauma mouse model. *Science translational medicine* **4**, 134ra160, doi:10.1126/scitranslmed.3003716 (2012).

14 Corsellis, J. A., Bruton, C. J. & Freeman-Browne, D. The aftermath of boxing. *Psychological medicine* **3**, 270-303 (1973).

15 Millspaugh, J. A. Dementia pugilistica. *US Naval Med Bulletin* **35**, 297-261 (1937).

16 Omalu, B. I. *et al.* Chronic traumatic encephalopathy in a national football league player: part II. *Neurosurgery* **59**, 1086-1092; discussion 1092-1083, doi:10.1227/01.NEU.0000245601.69451.27 (2006).

17 Omalu, B. I., Hamilton, R. L., Kamboh, M. I., DeKosky, S. T. & Bailes, J. Chronic traumatic encephalopathy (CTE) in a National Football League Player: Case report and emerging medicolegal practice questions. *Journal of forensic nursing* **6**, 40-46, doi:10.1111/j.1939-3938.2009.01064.x (2010).

18 McKee, A. C. *et al.* Chronic traumatic encephalopathy in athletes: progressive tauopathy after repetitive head injury. *Journal of neuropathology and experimental neurology* **68**, 709-735, doi:10.1097/NEN.0b013e3181a9d503 (2009).

19 Omalu, B. *et al.* Chronic traumatic encephalopathy in an Iraqi war veteran with posttraumatic stress disorder who committed suicide. *Neurosurgical focus* **31**, E3, doi:10.3171/2011.9.FOCUS11178 (2011).

20 Morganti-Kossmann, M. C., Rancan, M., Stahel, P. F. & Kossmann, T. Inflammatory response in acute traumatic brain injury: a double-edged sword. *Current opinion in critical care* **8**, 101-105 (2002).

21 Helmy, A., De Simoni, M. G., Guilfoyle, M. R., Carpenter, K. L. & Hutchinson, P. J. Cytokines and innate inflammation in the pathogenesis of human traumatic brain injury. *Progress in neurobiology* **95**, 352-372, doi:10.1016/j.pneurobio.2011.09.003 (2011).

22 Blaylock, R. L. & Maroon, J. Immunoexcitotoxicity as a central mechanism in chronic traumatic encephalopathy-A unifying hypothesis. *Surgical neurology international* **2**, 107, doi:10.4103/2152-7806.83391 (2011).

23 Perry, V. H., Nicoll, J. A. & Holmes, C. Microglia in neurodegenerative disease. *Nature reviews. Neurology* **6**, 193-201, doi:10.1038/nrneurol.2010.17 (2010).

24 Mouzon, B. C. *et al.* Repetitive mild traumatic brain injury in a mouse model produces learning and memory deficits accompanied by histological changes. *Journal of neurotrauma*, doi:10.1089/neu.2012.2498 (2012).

25 Tang-Schomer, M. D., Johnson, V. E., Baas, P. W., Stewart, W. & Smith, D. H. Partial interruption of axonal transport due to microtubule breakage accounts for the formation of periodic varicosities after traumatic axonal injury. *Experimental neurology* **233**, 364-372, doi:10.1016/j.expneurol.2011.10.030 (2012).

26 Shitaka, Y. *et al.* Repetitive closed-skull traumatic brain injury in mice causes persistent multifocal axonal injury and microglial reactivity. *Journal of neuropathology and experimental neurology* **70**, 551-567, doi:10.1097/NEN.0b013e31821f891f (2011).

27 Hylin, M. J. *et al.* Repeated mild closed head injury impairs short-term visuospatial memory and complex learning. *Journal of neurotrauma*, doi:10.1089/neu.2012.2717 (2013).

28 Mannix R, M. W., Mandeville J, Grant PE, et al. Clinical Correlates in an Experimental Model of Repetitive Mild Brain Injury. *Annals of neurology*, doi:doi: 10.1002/ana.23858 (2013).

29 Meehan, W. P., 3rd, Zhang, J., Mannix, R. & Whalen, M. J. Increasing recovery time between injuries improves cognitive outcome after repetitive mild concussive brain injuries in mice. *Neurosurgery* **71**, 885-891, doi:10.1227/NEU.0b013e318265a439 (2012).

30 Lister, R. G. Ethologically-based animal models of anxiety disorders. *Pharmacology & therapeutics* **46**, 321-340 (1990).

31 Walf, A. A. & Frye, C. A. The use of the elevated plus maze as an assay of anxiety-related behavior in rodents. *Nature protocols* **2**, 322-328, doi:10.1038/nprot.2007.44 (2007).

32 Alder, J., Fujioka, W., Lifshitz, J., Crockett, D. P. & Thakker-Varia, S. Lateral fluid percussion: model of traumatic brain injury in mice. *Journal of visualized experiments : JoVE*, doi:10.3791/3063 (2011).

33 Weber, J. T. Experimental models of repetitive brain injuries. *Progress in brain research* **161**, 253-261, doi:10.1016/S0079-6123(06)61018-2 (2007).

34 Kraus, M. F. *et al.* White matter integrity and cognition in chronic traumatic brain injury: a diffusion tensor imaging study. *Brain : a journal of neurology* **130**, 2508-2519, doi:10.1093/brain/awm216 (2007).

35 Lovell, M. R. *et al.* Functional brain abnormalities are related to clinical recovery and time to return-to-play in athletes. *Neurosurgery* **61**, 352-359; discussion 359-360, doi:10.1227/01.NEU.0000279985.94168.7F (2007).

36 Lovell, M. R. *et al.* Recovery from mild concussion in high school athletes. *Journal of neurosurgery* **98**, 296-301, doi:10.3171/jns.2003.98.2.0296 (2003).

37 McCrea, M. *et al.* Incidence, Clinical Course, and Predictors of Prolonged Recovery Time Following Sport-Related Concussion in High School and College Athletes. *Journal of the International Neuropsychological Society : JINS*, 1-12, doi:10.1017/S1355617712000872 (2012).

38 Brooks, J., Fos, L. A., Greve, K. W. & Hammond, J. S. Assessment of executive function in patients with mild traumatic brain injury. *The Journal of trauma* **46**, 159-163 (1999).

39 Lipton, M. L. *et al.* Diffusion-tensor imaging implicates prefrontal axonal injury in executive function impairment following very mild traumatic brain injury. *Radiology* **252**, 816-824, doi:10.1148/radiol.2523081584 (2009).

40 Ozen, L. J. & Fernandes, M. A. Slowing down after a mild traumatic brain injury: a strategy to improve cognitive task performance? *Archives of clinical neuropsychology : the official journal of the National Academy of Neuropsychologists* **27**, 85-100, doi:10.1093/arclin/acr087 (2012).

41 Baugh, C. M. *et al.* Chronic traumatic encephalopathy: neurodegeneration following repetitive concussive and subconcussive brain trauma. *Brain imaging and behavior* **6**, 244-254, doi:10.1007/s11682-012-9164-5 (2012).

42 Gavett, B. E., Stern, R. A. & McKee, A. C. Chronic traumatic encephalopathy: a potential late effect of sport-related concussive and subconcussive head trauma. *Clinics in sports medicine* **30**, 179-188, xi, doi:10.1016/j.csm.2010.09.007 (2011).

43 Koliatsos, V. E. *et al.* A mouse model of blast injury to brain: initial pathological, neuropathological, and behavioral characterization. *Journal of neuropathology and experimental neurology* **70**, 399-416, doi:10.1097/NEN.0b013e3182189f06 (2011).

44 Walton, N. M. *et al.* Microglia instruct subventricular zone neurogenesis. *Glia* **54**, 815-825, doi:10.1002/glia.20419 (2006).

45 Block, M. L., Zecca, L. & Hong, J. S. Microglia-mediated neurotoxicity: uncovering the molecular mechanisms. *Nature reviews. Neuroscience* **8**, 57-69, doi:10.1038/nrn2038 (2007).

46 Ziv, Y., Avidan, H., Pluchino, S., Martino, G. & Schwartz, M. Synergy between immune cells and adult neural stem/progenitor cells promotes functional recovery from spinal cord injury. *Proceedings of the National Academy of Sciences of the United States of America* **103**, 13174-13179, doi:10.1073/pnas.0603747103 (2006).

47 Aarum, J., Sandberg, K., Haeberlein, S. L. & Persson, M. A. Migration and differentiation of neural precursor cells can be directed by microglia. *Proceedings of the National Academy of Sciences of the United States of America* **100**, 15983-15988, doi:10.1073/pnas.2237050100 (2003).

48 Kumar, A. & Loane, D. J. Neuroinflammation after traumatic brain injury: Opportunities for therapeutic intervention. *Brain, behavior, and immunity* **26**, 1191-1201, doi:10.1016/j.bbi.2012.06.008 (2012).

49 Zhao, Z. *et al.* Overexpression of glial cell line-derived neurotrophic factor in the CNS rescues motoneurons from programmed cell death and promotes their long-term survival following axotomy. *Experimental neurology* **190**, 356-372, doi:10.1016/j.expneurol.2004.06.015 (2004).

50 Loane, D. J. & Byrnes, K. R. Role of microglia in neurotrauma. *Neurotherapeutics : the journal of the American Society for Experimental NeuroTherapeutics* **7**, 366-377, doi:10.1016/j.nurt.2010.07.002 (2010).

51 Kinnunen, K. M. *et al.* White matter damage and cognitive impairment after traumatic brain injury. *Brain : a journal of neurology* **134**, 449-463, doi:10.1093/brain/awq347 (2011).

52 Sharp, D. J. & Ham, T. E. Investigating white matter injury after mild traumatic brain injury. *Current opinion in neurology* **24**, 558-563, doi:10.1097/WCO.0b013e32834cd523 (2011).

53 Kumar, R. *et al.* Serial changes in the white matter diffusion tensor imaging metrics in moderate traumatic brain injury and correlation with neuro-cognitive function. *Journal of neurotrauma* **26**, 481-495, doi:10.1089/neu.2008.0461 (2009).

54 Ji, J. *et al.* Lipidomics identifies cardiolipin oxidation as a mitochondrial target for redox therapy of brain injury. *Nature neuroscience* **15**, 1407-1413, doi:10.1038/nn.3195 (2012).

55 Hall, E. D., Detloff, M. R., Johnson, K. & Kupina, N. C. Peroxynitrite-mediated protein nitration and lipid peroxidation in a mouse model of traumatic brain injury. *Journal of neurotrauma* **21**, 9-20, doi:10.1089/089771504772695904 (2004).

56 Mustafa, A. G., Singh, I. N., Wang, J., Carrico, K. M. & Hall, E. D. Mitochondrial protection after traumatic brain injury by scavenging lipid peroxyl radicals. *Journal of neurochemistry* **114**, 271-280, doi:10.1111/j.1471-4159.2010.06749.x (2010).

57 Mustafa, A. G., Wang, J. A., Carrico, K. M. & Hall, E. D. Pharmacological inhibition of lipid peroxidation attenuates calpain-mediated cytoskeletal degradation after traumatic brain injury. *Journal of neurochemistry* **117**, 579-588, doi:10.1111/j.1471-4159.2011.07228.x (2011).

58 Gentile, N. T. & McIntosh, T. K. Antagonists of excitatory amino acids and endogenous opioid peptides in the treatment of experimental central nervous system injury. *Annals of emergency medicine* **22**, 1028-1034 (1993).

59 Sterr, A., Herron, K. A., Hayward, C. & Montaldi, D. Are mild head injuries as mild as we think? Neurobehavioral concomitants of chronic post-concussion syndrome. *BMC neurology* **6**, 7, doi:10.1186/1471-2377-6-7 (2006).

60 Henry, L. C. *et al.* Metabolic changes in concussed American football players during the acute and chronic post-injury phases. *BMC neurology* **11**, 105, doi:10.1186/1471-2377-11-105 (2011).

61 Daneshvar, D. H. *et al.* Long-term consequences: effects on normal development profile after concussion. *Physical medicine and rehabilitation clinics of North America* **22**, 683-700, ix, doi:10.1016/j.pmr.2011.08.009 (2011).

62 Chen, Y. *et al.* Correlated memory defects and hippocampal dendritic spine loss after acute stress involve corticotropin-releasing hormone signaling. *Proceedings of the National Academy of Sciences of the United States of America* **107**, 13123-13128, doi:10.1073/pnas.1003825107 (2010).

63 Gao, X., Deng, P., Xu, Z. C. & Chen, J. Moderate traumatic brain injury causes acute dendritic and synaptic degeneration in the hippocampal dentate gyrus. *PloS one* **6**, e24566, doi:10.1371/journal.pone.0024566 (2011).

64 Ding, J. Y. *et al.* Synapse loss regulated by matrix metalloproteinases in traumatic brain injury is associated with hypoxia inducible factor-1alpha expression. *Brain research* **1268**, 125-134, doi:10.1016/j.brainres.2009.02.060 (2009).

65 Tang-Schomer, M. D., Patel, A. R., Baas, P. W. & Smith, D. H. Mechanical breaking of microtubules in axons during dynamic stretch injury underlies delayed elasticity, microtubule disassembly, and axon degeneration. *FASEB journal : official publication of the Federation of American Societies for Experimental Biology* **24**, 1401-1410, doi:10.1096/fj.09-142844 (2010).

66 Farbota, K. D. *et al.* Longitudinal volumetric changes following traumatic brain injury: a tensor-based morphometry study. *Journal of the International Neuropsychological Society : JINS* **18**, 1006-1018, doi:10.1017/S1355617712000835 (2012).

67 Gale, S. D., Johnson, S. C., Bigler, E. D. & Blatter, D. D. Nonspecific white matter degeneration following traumatic brain injury. *Journal of the International Neuropsychological Society : JINS* **1**, 17-28 (1995).

68 Johnson, V. E. *et al.* Inflammation and white matter degeneration persist for years after a single traumatic brain injury. *Brain : a journal of neurology* **136**, 28-42, doi:10.1093/brain/aws322 (2013).

69 Tomaiuolo, F. *et al.* Memory and anatomical change in severe non missile traumatic brain injury: approximately 1 vs. approximately 8 years follow-up. *Brain research bulletin* **87**, 373-382, doi:10.1016/j.brainresbull.2012.01.008 (2012).

Chapter 4

4. Exploration of the effects of single and repetitive mTBI on tau phosphorylation in hTau transgenic animals

4.1. Introduction:

With TBI affecting approximately 20% of the 2.3 million deployed U.S. military personnel[1] and the unprecedented wave of suicide and death among NFL players has drawn public concern on mTBI. The constant media focus on veterans and athletes struggling with the consequences of TBI has raised concerns among parents as to their children's safety if they participate in high-TBI-risk sports such as American football or ice hockey. The potential medical consequences of r-mTBI have been known for some time, but were previously restricted mostly to the aftermath of boxing, and the neurobehavioral disorder termed "dementia pugilistica"[2]. Recently, this term was replaced by chronic traumatic encephalopathy (CTE) to describe the negative pathological sequelae resulting from a wider range of exposure situations[3,4] (football, wrestling, hockey, and rugby). CTE is a progressive neurodegeneration characterized by prominent neuropsychiatric features and a neuropathological profile that includes: brain atrophy, cavum septum pellucidum, amyloid-β, TDP-43 and a widespread evidence for hyperphosphorylated tau (p-tau) and neurofibrillary tangles[5] (Fig.4.1).

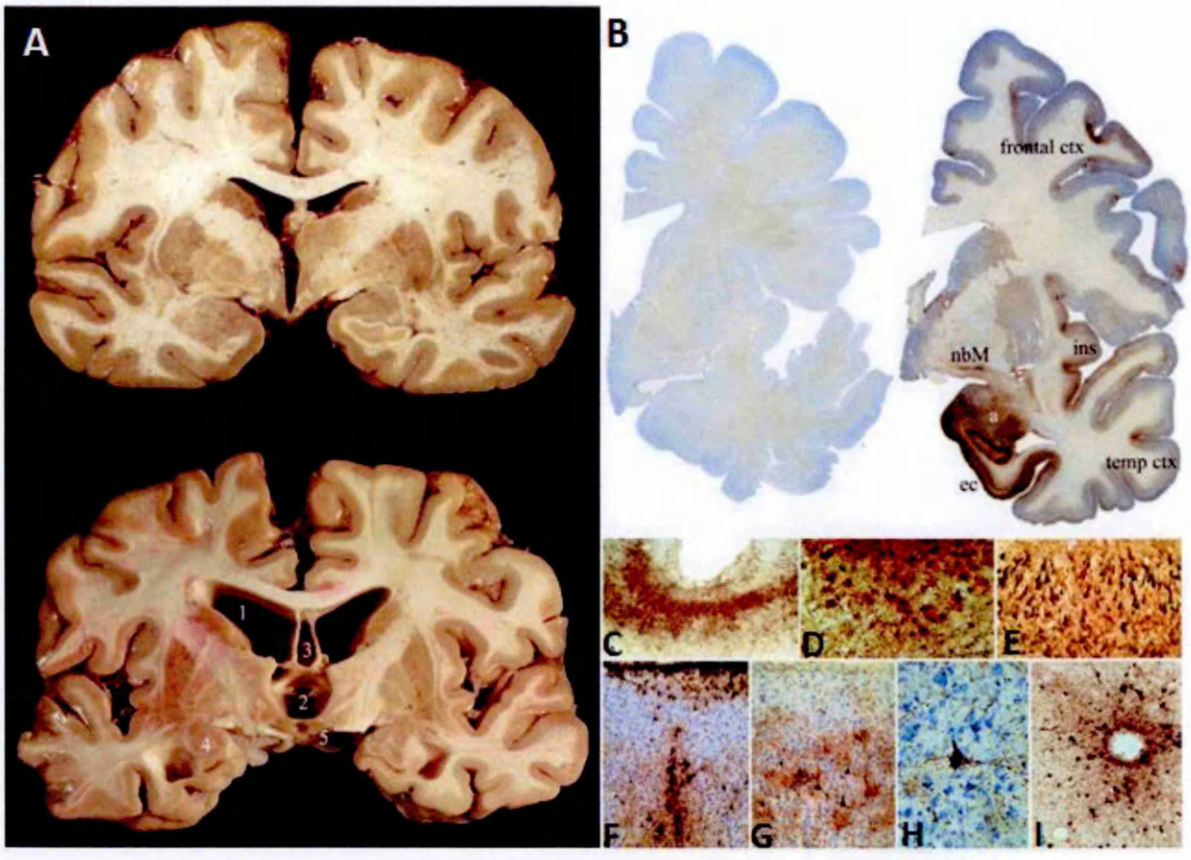

Figure.4.1: Gross pathology of chronic traumatic encephalopathy.
Left Panel: The coronal section of normal brain (top left), showing the expected size and relationship of the cerebral cortex and ventricles. The brain from a retired professional football player (bottom left), showing the characteristic gross pathology of CTE with severe dilatation of ventricles II (1) and III (2), cavum septum pellucidum (3), marked atrophy of the medial temporal lobe structures (4), and shrinkage of the mammillary bodies (5).Microscopic pathology of chronic traumatic encephalopathy.
Right Panel: (Top) Phosphorylated tau (AT8) immunostained coronal hemisections of a normal brain (left) and a brain from a retired professional football player with CTE (right). The brain with CTE, showing severe neurofibrillary degeneration of the amygdala (a), entorhinal cortex (ec), temporal cortex, insular cortex (ins), nucleus basalis of Meynert (nbM), and frontal cortex. The cortical changes are most severe at the depths of the sulci. Right Panels (Bottom): (C) Tau neurofibrillary tangles (NFT) are often prominent at depths of the sulci (AT8 immunostain, original magnification 60). (D) Subpial tau immunoreactive tangles are found in both neurons and astrocytes (double immunostained section for GFAP [red] and AT8 [brown], showing colocalization of tau and GFAP; original magnification 350). (E) Extremely dense NFTs are found in the medial temporal lobe structures, including CA1 of the hippocampus, shown here. Senile plaques are absent (AT8 immunostain, original magnification 150). (F) NFTs and astrocytic tangles tend to be centered around small blood vessels and in subpial patches (AT8 immunostain, original magnification 150). (G) NFTs characteristically involve cortical layers II and III (AT8 immunostain, original magnification 150). (H) NFT in a Betz cell of primary motor cortex (AT8 immunostain, original magnification 350). (I) Perivascular tau immunoreactive NFTs are a characteristic feature of CTE (original magnification 150). Reprinted from PM&R, Volume 3, Issue 10, Supplement 2,

Recent autopsy reports reveal similar pathologies found years after single blast injury[1] and in a few cases at acute time points post r-mTBI[5,6]. CTE can only be definitively diagnosed post-mortem, and because the symptoms begin insidiously and are clinically confounded with other neurodegenerative diseases with aging, the incidence of CTE is likely underestimated. Because the pathological presentation of CTE depicts abnormal accumulation of tau protein, this illness has been classified as a tauopathy[1,4,5,7]. Tauopathies are characterized by tau aberrations: abnormal and hyperphosphorylation[8], misfolding[6], and aggregation[9]. The best known tauopathy is Alzheimer disease, others include progressive supranuclear palsy, Pick's Disease, frontotemporal dementia and Parkinsonism linked to chromosome 17 (human location of the tau gene), among others[10].

To study the specific contribution of tau pathology to the pathogenesis of CTE, we used our head injury model to compare and characterize the consequences of single and r-mTBI in genetically modified mice that express the 6 human tau isoforms. Tau has already being extensively characterized owing to its critical involvement in AD and other neurodegenerative disorders[10-12]. We do not know to what extent the pathobiology of tau in TBI may relate to the pathobiology of tau in AD or other tauopathies, but we assume that it will derive from a disruption of normal tau function so a brief overview of tau biology is outlined below.

In this chapter we will test the following hypotheses:

1. Single or r-mTBI is associated with an acute increase of Aβ deposition and p-tau accumulation in hTau transgenic animals.
2. The increase of p-tau and Aβ deposition is associated with worse behavioral performance compared to the wild type animals.

To this end, we will use our previously characterized CHI model and repeat the same experimental procedures including behavioral, pathological, and biochemical analyses in hTau transgenic mice.

4.1.1. Tau Background:

The microtubule-associated protein tau (MAPT) was identified as a microtubule-assembly factor in 1975 in Marc Kirschner's laboratory[13]. Tau proteins are expressed in the peripheral and central nervous system (CNS) but are also present at a lower level in kidney, lung and testis[14]. In the CNS, Tau proteins are mostly found in the distal portions of axons where they provide stability and flexibility to the microtubule[15]. Tau also plays a physiological role in dendritic function in postsynaptic targeting of the Src kinase Fyn in dendrites[16] and by promoting morphological differentiation of oligodendrocytes[17]. Tau has also been shown to have a role in axonal transport[18-20], to be an enzyme inhibitor[21,22] and to bind to mitochondria leading to cell death[23].

4.1.2. Tau isoforms in humans:

In the human CNS a total of 6 Tau isoforms are produced by alternative mRNA splicing of the MAPT gene on chromosome 17q21.31[9] (Fig.4.1). These isoforms are named according to whether 3 or 4 microtubule binding repeat (MTBs) sequences are expressed and by the presence or absence of two exons at the N-Terminus (termed N) (Fig.4.2). The exclusion of exon

10 leads to the production of tau isoform with three repeats (3R), and its inclusion leads to tau isoforms with four repeats (4R). Tau isoforms can include no N-terminal exons (0N), tau exon 2 (1N), or tau exons 2 and 3 (2N), resulting in six human tau isoforms as represented in Figure 4.1. Alternative mRNA splicing of MAPT is similar across brain regions and equal amounts of 3R and 4R tau are found in the cortex of healthy adults[24]. Expression of these isoforms is developmentally regulated, the shortest isoform (3R0N) is highly expressed in the brain during development and rapidly decreases after birth[25].

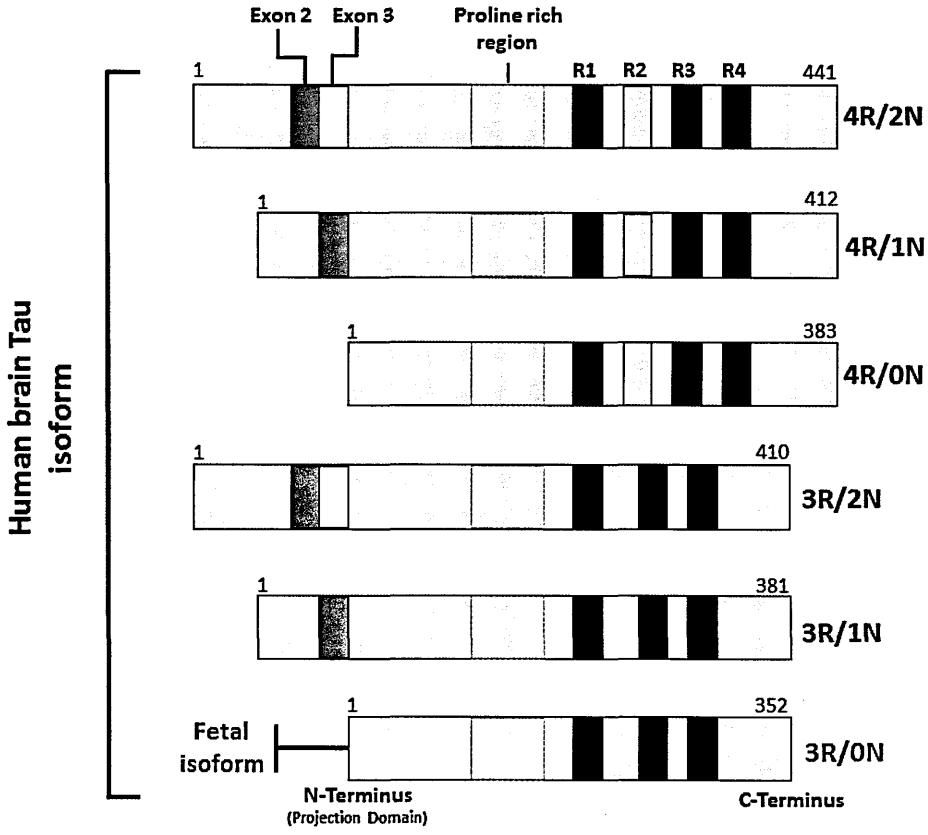

Figure.4.2: Structural domains of the 6 tau isoforms (amino acids 352–441) expressed in the adult human brain after alternative mRNA splicing of Exon 2 (dark blue), Exon 3 (light blue) and Exon 10 (light grey)[26]. The isoforms can differ from each other in the number of microtubule bindings domains (MTBs) (three or four repeats located in the C-terminal), and are referred to as 3R or 4R tau isoforms, respectively. Each repeat is 31 or 32 amino acids in length. They can also differ in the presence or absence of either one or two 29 amino acid long, highly acidic inserts (shown in blue) at the N-terminal

portion of the protein (the projection domain). Between the projection domain and the MTBs lies a basic proline-rich region (shown in red). The exons and introns are not drawn to scale.

4.1.3. Tau isoforms in animal models:

Since various animal models have been established to investigate the physiological role of tau, it is important to consider the differences between the adult profiles of tau isoforms in both humans and animals. To date, in all vertebrates examined, tau is produced by similar developmentally regulated alternative mRNA splicing, but the number of expressed tau isoforms in adult brain varies between species. In contrast with humans, most adult wild type rodents almost exclusively express isoforms with four repeats (Fig.4.3). In the rat, the protein expression of 4R isoforms is nine fold higher than 3R isoforms[27], and mice also express predominantly 4R isoforms[28]. Goedert and colleagues showed that isoforms with up to 5 MTBs repeats are expressed in the brains of adult chickens[29]. Invertebrates such as Caenorhabditis elegans and Drosophila melanogaster are also well established model organisms that have been used successfully to explore many aspects of human neurodegenerative diseases, including tauopathies[30-32]. However, unless genetically altered, their genomes each encode only one tau isoform[32-34]. The species divergences and the complex nature of tau regulation in normal brains and in brains exhibiting tauopathy makes modeling of tau pathogenesis difficult.

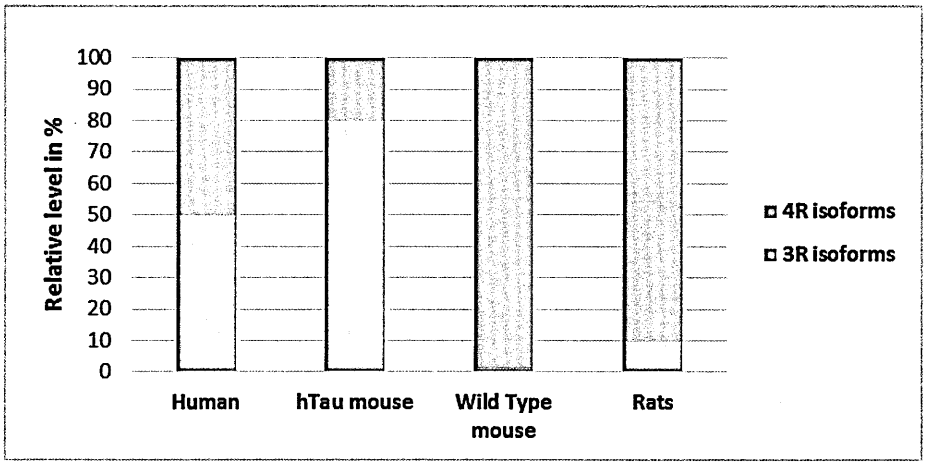

Figure.4.3: Relative distribution of 3R and 4R tau isoforms in adult human, mouse and rat brain. In healthy adult human brain, the ratio of expression level of 4R to 3R is approximately 1. While all 6 human isoforms are produced in the hTau transgenic mouse, only 20% of the total Tau is 4R (80% are 3R; 2:8). In the wild-type mouse, tau exists almost exclusively in the 4R form, while isoforms in the adult rat consist of a 4R:3R ratio of approximately 9:1.

4.1.4. Tau structure:

From a structural standpoint, tau can be subdivided into three regions (Fig.4.2). The N-terminal domain is associated with the cell membrane and regulates the spacing between the microtubules[35-37]. Between the C and N-terminal domain, a basic proline-rich region includes many phosphorylation sites[26,37]. The C-terminal region contains the positively-charged microtubule domains that interact with the negatively-charged microtubule[38,39]. The ability of tau to bind to the microtubule depends on the MTBs, with 4 MTBs isoforms demonstrating greater microtubule stabilization than isoforms with three repeat domains[40]. Interestingly, the region between repeats 1 and 2 is unique to 4R tau and is responsible for a 40-fold difference in the binding affinities between 3R and 4R tau[41,42].

4.1.5. Tau Phosphorylation and Tauopathies:

In many cases, tau phosphorylation under physiological conditions regulates the binding of tau to microtubules, or to other structures such as the membrane[43] or the actin cytoskeleton[44]. In tauopathies such as AD, Pick's disease, progressive supranuclear palsy (PSP), and CTE, tau is hyperphosphorylated and, as a result, is unable to interact with microtubules[10,45-48] (Fig.4.4). The microtubule (MT) binding ability of tau is regulated primarily by serine/threonine-directed phosphorylation, which can effectively modulate the binding affinity of tau for MTs, although other post translational modifications such as glycosylation, ubiquitinylation, deamidation, oxidation, and nitration have been described[48]. The hyperphosphorylation of tau is the most studied modification and seems to be an early and crucial event to precede filament assembly. Other causes of abnormal disengagement of tau from the MTs include imbalance in the activity levels or regulation of tau kinases and phosphatases, and mutation of the MAPT gene that directly affect the MTB domain[10,49] (e.g. inclusion or exclusion of exon 10). Under these pathological conditions, the equilibrium of tau binding to the MTs is perturbed, which results in an increase in the levels of unbound tau. Abnormally phosphorylated tau protein becomes dissociated from neuronal microtubules and accumulates and aggregates in an insoluble form. These aggregates are made of hyperphosphorylated tau and are also referred to as paired helical filaments (PHFs). These PHFs will form elongated inclusions or eventually develop in neurofibrillary tangles (NFTs). Similar to AD, CTE can be classified in phases defined by Braak staging. Braak stages I and II are used when NFTs are confined mainly to the transentorhinal region of the brain, stages III and IV indicate involvement of limbic regions such as the hippocampus, and stages V and VI are when

there is extensive neocortical involvement[50]. Mutations in the tau gene, which give rise to frontotemporal dementia with Parkinsonism linked to chromosome 17 (FTDP-17), alter the proportion of tau isoforms or the ability of tau to bind microtubules and to promote microtubule assembly[51,52]. Although phosphorylation of tau is a major early characteristic of tau aggregation, dysregulation of the MAPT gene splicing is enough to cause neurodegeneration by altering the tau isoform ratio[12]. For example, all six tau isoforms are usually present in equimolar concentration in AD patients, whereas a shift toward an increase of 4R isoforms is observed in patients with PSP or argyrophilic grain dementia (AGD). In contrast, a shift toward an increase of 3R is associated with Pick's disease. Together these apparent differences in tau pathogenic mechanisms in different diseases underscore the significance of tau homeostasis and the complexity of tau pathogenesis. Interestingly Tau hyperphosphorylation may not necessarily always be detrimental as the process happens reversibly in state of hibernation[53], hypothermia[54] and during the period of development[55].

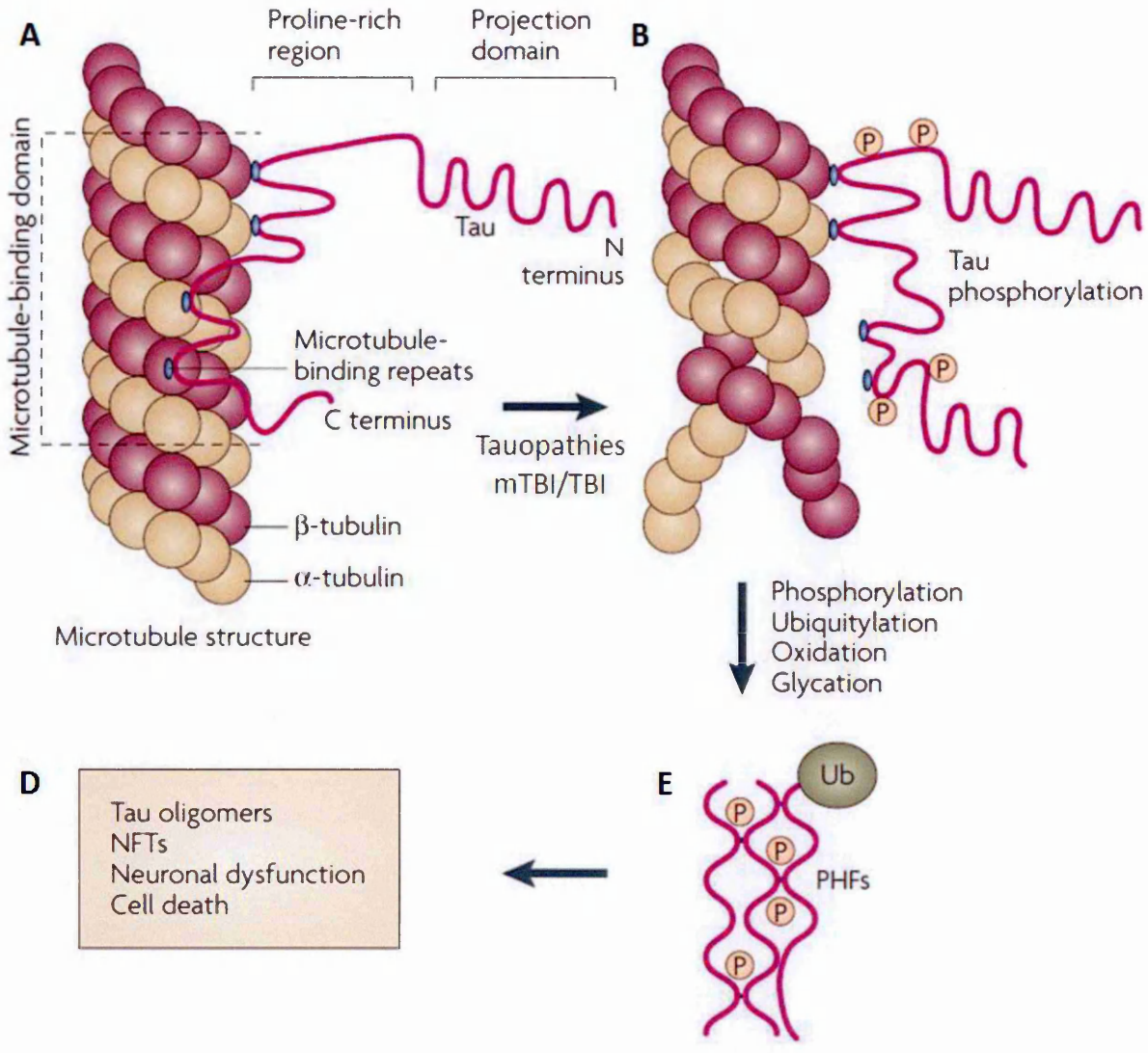

Figure.4.4: Intracellular neuronal aggregates in tauopathies. Microtubules are strong cylindrical polymers composed of α- and β-tubulin that provide structural support to neurons (A). Phosphorylation (by kinases such as GSK3-β, CDK5 and ERK2) at a number of serine/threonine sites flanking the microtubule-binding repeats, as well as sites in the repeat region, attenuates tau binding, which results in destabilization of microtubules (B). Abnormally phosphorylated tau protein becomes dissociated from neuronal microtubules and accumulates as PHFs (C). Proteolytic processing leads to the formation of tau oligomers and NFTs (D). Tau in these aggregates is heavily phosphorylated at several sites and crosslinked by disulphide bonds. The decrease in the association of tau with microtubules and other physiologically relevant proteins, together with the formation of PHFs, is thought to contribute to neuronal dysfunction and eventually cell death. Modified by permission from Macmillan Publishers Ltd: Nature Reviews, Mazanets M.P, Fisher P.M. "Untangling tau hyperphosphorylation in drug design for neurodegenerative diseases".6(6):464, copyright 2007.

4.1.6. Tau and TBI:

Since traumatic brain injury has long been recognized as risk factor for later development of neurodegenerative disease[56,57], numerous studies have sought to uncover the association between these events[5,58-67]. Although the epidemiological data are quite strong, very little is known about the mechanistic link between repeated mTBI and the development of either AD or CTE, and there are no published experimental models showing that multiple episodes of TBI induce specific neurodegenerative conditions. Although recently some research groups have produced animal models of mTBI[1,61,68-71], studies on repetitive mTBI in laboratory models are few[61,65,66,68,71], and studies of chronic time points after single or repetitive mTBI are lacking altogether. Only two studies have reported tau involvement in an mTBI model[1,68]. In these studies, an increased amount of p-tau without evidence of tau aggregates was found in brain homogenates of wild-type (WT) mice after 14 days post single blast injury[1], or 30 days post repetitive mTBI[68] but not at 6 months post mTBI[61]. As the hallmark AD pathological features of amyloid plaques and NFTs have been reported in TBI patients, the use of transgenic models of AD and mutated tau have been proposed to investigate TBI pathogenesis. In this regard, Brody and colleagues showed that AD (3xTg-AD) and mutated Tau (P301L) mouse models demonstrate an acute increase in tau immunoreactivity and tau phosphorylation up to 2 weeks after controlled cortical impact (CCI) injury[64]. However, the caveats of these models are that tau mutations are very rare in the general population, tau is not present at physiological levels in the mutant mice (p301L) and the models investigated thus far (e.g. WT, Tg44, p301L) do not express each human tau isoform. Consequently, we hypothesized that none of these models could adequately model the human response to TBI. Therefore for our

investigation of the role of tau in TBI pathogenesis following our novel mTBI paradigm we decided to use hTau transgenic mice, which expresses 6 isoforms of human non-mutated tau on a null murine tau background[72,73].

4.2. Materials and Methods:

4.2.1. Animals:

Male mice expressing human tau (hTau) on a C57BL/6 and null murine tau background[72,73] (aged 10-12 weeks, 20-24g, Jackson Laboratories, Bar Harbor ME) were housed singly under standard laboratory conditions (23˚C ± 1˚C, 50 ± 5% humidity, and 12-hour light/dark cycle) with free access to food and water throughout the study. These hTau mice were generated by crossing mice that express a tau transgene derived from a human PAC, H1 haplotype, known as 8c mice[74], with tau knockout (KO) mice in which cDNA for the enhanced green fluorescent protein (EGFP) was inserted into exon one of tau. The resulting hTau mice express all 6 human tau isoforms, but do not express mouse tau[72]. Of note, the physiological tau isoform ratio (3R/4R) in the hTau mice is not 1:1 as in human, rather it is 4:1 (Peter Davies, *pers. comm.*) but they are still closer to mimicking physiological occurrence of human tau than wild type mice (see Figure 4.3) or other tau transgenic models which express single isoforms of either mutated or wild type tau[75]. All procedures were carried out under Institutional Animal Care and Use Committee approval and in accordance with the National Institute of Health Guide for the Care and Use of Laboratory Animals.

4.2.2. Injury groups and schedule:

For the behavioral analyses a total of 36 mice were randomly assigned to one of four treatment groups as described in Chapter 2, single injury, single sham, repetitive injury, repetitive sham. The behavior analysis began 24 h after the sole/last mTBI/anesthesia for each group. Behavior outcomes were assessed blinded to group assignment. In this study, less animals were assigned for each group than with the wild type studies (n=9/group as compared to 12/group for wild type mice) as we encountered difficulty in breeding these animals. On discussion with our colleagues and collaborators in the field, including the original creator of this mouse, Dr. Peter Davies, we find that this is a common problem. The breeding performance was mostly affected by a high rate of cannibalism by the mothers. Most of the litters comprised only 1 or 2 animals, and as we only used male transgenic animals it was very hard to generate groups of 6 to 12 animals with the matching ages for behavioral studies.

Following the acute time point of behavioral analyses, this cohort of mice was then allowed to survive for analyses at a later time point (see Chapter 5). Separately from this behavioral cohort, two other cohorts of hTau animals were assigned for pathological (n=12) and biochemical (n=12) examination. As before, the animals were randomly assigned to one of the 4 treatment groups, with 3 mice per group for pathology and 3 mice per group for biochemistry. All mice for pathological and biochemical analyses were euthanized at 24 h post sole/last mTBI/anesthesia.

4.2.3. Injury protocol:

The mTBI was administered to mice as previously described in Chapter 2. Mice were anesthetized with 1.5 L/min of oxygen and 3% isoflurane prior to anesthesia or mTBI. A 5 mm blunt metal impactor tip was retracted and positioned midway relative to the sagittal suture before each impact. The injury was triggered using the myNeuroLab controller at a strike velocity of 5m/s, strike depth of 1.0 mm, and dwell time of 200 ms. Sham injured animals underwent the same procedures and were exposed to anesthesia for the same length of time as the mTBI animals.

4.2.4. Assessment of motor function:

Assessment of motor function was evaluated by monitoring the time a mouse could remain on an accelerating rod using the rotarod apparatus (Ugo Basile, Varese, Italy) in the same manner we described previously in Chapter 2.

4.2.5. Assessment of Cognitive Function:

Learning and memory were evaluated by monitoring the distance and time taken to find an escape hole over a period of 6 training days (learning) and a final probe trial (memory) the same manner we described in Chapter 2.

4.2.6. Histology:

At 24 h after their last injury/anesthesia the mice assigned to histological studies were anesthetized with isoflurane and perfused transcardially with phosphate-buffered saline (PBS), pH 7.4 followed by PBS containing 4% paraformaldehyde. After perfusion, the brains were post fixed in a solution of 4% paraformaldehyde at 4°C for 48 h. The intact brains were then blocked

and processed as previously described Chapter 2. Immunohistochemistry for GFAP, Iba1 and APP was carried out as described in Chapter 2. Each slide was visualized with a bright field microscope (BX60), and digital images were visualized and acquired using an Olympus MagnaFire SP camera.

For Tau immunohistochemistry sections were stained with the following monoclonal antibodies at a 1:400 dilution: CP13[73,76] [pS202]; PHF1[77,78] [pS396/404]; RZ3[79] [pT231] (Fig.4.5A). MC1 is a conformation dependent antibody that reacts with both the N terminus (amino acids 7–9), and an amino acid sequence of tau in the third MTB (amino acids 313–322) that is necessary for *in vitro* formation of filamentous aggregates of tau similar to those seen in AD[80] (Fig.4.5B). These Tau antibodies and protocols were generously provided by Dr. Peter Davies, The Feinstein Institute for Medical Research, Bronx, NY. A summary of antibodies used for these neuropathological analyses is showed in table 4.1.

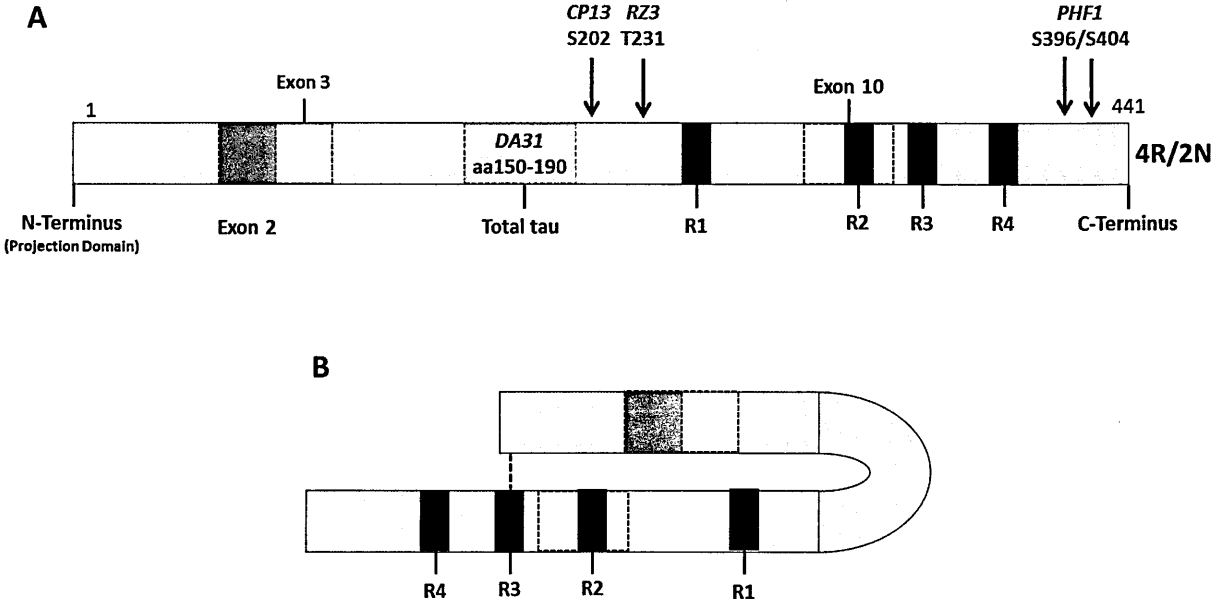

Figure.4.5: Tau phosphorylation sites for the antibodies used in this study (A)[38].These phosphorylation sites are found both in normal brain and AD brains. MC1 recognizes a very specific early pathological

tau conformation produced by the intramolecular association between the extreme N-terminus (aa7-9) and the third microtubule repeat domain (aa1313-322) of tau (B).

For terminal deoxynucleotidyl transferase dUTP nick end labeling (TUNEL) staining, the in situ cell death detection kit (Roche Diagnostics, Indianapolis, IN) was used following the manufacturer's guidelines. Labeling was performed with DAB as the chromogen. To avoid bias, positive and negative controls were included to show nonspecific binding/reaction.

Protein Target	Antibody	Epitope	Type	Source
Amyloid Precursor Protein	22C11	aa66-81	Mouse mAb	Millipore
Glial Fibrillary Acidic Protein	GFAP	GFAP	Polyclonal Rabbit	Dako
Anti Iba-1	Iba-1	Iba-1	Polyclonal Goat	Abcam
Phospho-Tau	CP-13	pS202/Pt205	Mouse mAb	Dr. P. Davies
Phospho-Tau	MC-1	C & N Termi	Mouse mAb	Dr. P. Davies
Phospho-Tau	PHF-1	pS396/404	Mouse mAb	Dr. P. Davies
Phospho-Tau	RZ3	pT231	Mouse mAb	Dr. P. Davies

Table.4.1: Summary of antibodies used in chapter 4.

4.2.7. Immunohistochemical quantification:

Immunoreactivity for cell markers was measured by quantitative optical segmentation as previously described in Chapter 2. Immunoreactivity for each cell marker was assessed within the superficial layer of the cortex, in the CA1 sub region of the hippocampus, and in the corpus callosum. For each animal, (n=3/group), sagittal sections were stained and analyzed blinded to the study grouping using ImageJ software (US National Institutes of Health, Bethesda, MD, USA). Changes in CP13 and RZ3 immunoreactivity was calculated and expressed as a percentage of the field of view within the pyramidal cell layer of the CA1 and CA3 sub-regions of the hippocampus.

4.2.8. Biochemical assessment of phosphorylated and total tau protein:

Mice were exsanguinated via aortic puncture using a wide-bore needle to prevent hemolysis of red blood cells. Immediately after cardiac puncture, mouse brains were perfused with chilled 1X PBS for 1 min to eliminate the confounding effects of blood proteins present in the brain vasculature. Brains were dissected at 4°C into hemispheres, then cortices, hippocampi and cerebella, and then snap frozen in liquid nitrogen.

Phosphorylated tau and total tau protein were analyzed in the hemisected hippocampi and cortices obtained from all groups (n=3/group). Snap-frozen hemisected cortices and hippocampi were sonicated in 0.5 ml and 0.3 ml of chilled M-PER buffer solution (Thermo Fisher Scientific, Waltham, MA) supplemented with protease inhibitor cocktail (Roche, Indianapolis, IN). Biochemical analyses were carried out by our collaborators at the Feinstein Institute for Medical Research, Bronx, NY, to whom we sent coded tissue homogenates for quantitative assessments. Sample preparation for low-tau sandwich ELISA and quantitation of murine-specific tau protein was performed as previously described[81]. Total tau DA31, CP13, PHF1 and RZ3 were used as capture antibodies in the low-tau, Sandwich ELISA as described in Chapter 3. Data were expressed as μg tau/mg protein (tau and phosphorylated tau).

4.2.9. Statistics:

Behavioral data were analyzed using JMP 8.0 (SAS, Cary, NC) as previously detailed in Chapter 2. Quantitative histologic parameters were analyzed with one-way ANOVA, with a Tukey's post-hoc correction for multiple comparisons, unless indicated. ELISA data were plotted and analyzed using Graph-Pad Prism (Prism 6.01, GraphPad Software Inc. La Jolla, CA). One way ANOVA followed by Tukey's post-hoc test was used for comparison of soluble tau and

$A\beta_{40}$ levels between the four groups. Only p values < 0.05 were considered to be statistically significant and are indicated by an asterisk in the figures. Error bars represent the standard error of the mean (SEM).

4.3. Results:

4.3.1. Barnes maze : acquisition:

Acute acquisition deficits were only observed in the repetitively injured group relative to their sham controls (r-mTBI vs. r-sham, $p < 0.05$ repeated-measures ANOVA) (Fig.4.6A). The mean distance travelled over the 6 days acquisition period in the r-mTBI mice was 24% longer than the r-sham mice. There was no difference between the s-mTBI, s-sham and r-sham groups at any time point ($p > 0.05$ repeated-measures ANOVA).

The dataset for latency to escape was not normally distributed and thus did not satisfy the assumptions required for a repeated-measure ANOVA. The Wilcoxon signed rank test was used to test for the daily correlation between each group. No difference in escape latency performance was observed across all groups ($p > 0.05$) (Fig.4-6B). The average velocity was similar across all groups and all time points with a trend for the r-mTBI to be faster than the three other groups ($p > 0.05$; Fig.4.6C).

4.3.2. Barnes maze: probe:

The probe trial analyses determined the average time to reach either one of the three holes of the target zone, (defined by the target escape hole and its adjacent north and south holes). The analyses revealed that the r-mTBI mice performed the worst, requiring on average 21 sec to reach the target zone, followed by the r-sham (15 sec), the s-mTBI (12 sec), and the s-

sham (9 sec) (Fig.4.6D). While there was a trend for both injured groups to perform worse than their respective sham groups, the time to reach the target or adjacent holes did not reach statistical significance ($p > 0.05$ for both injury groups; ANOVA). The mean velocity for the probe trial was similar across all groups ($p > 0.05$).

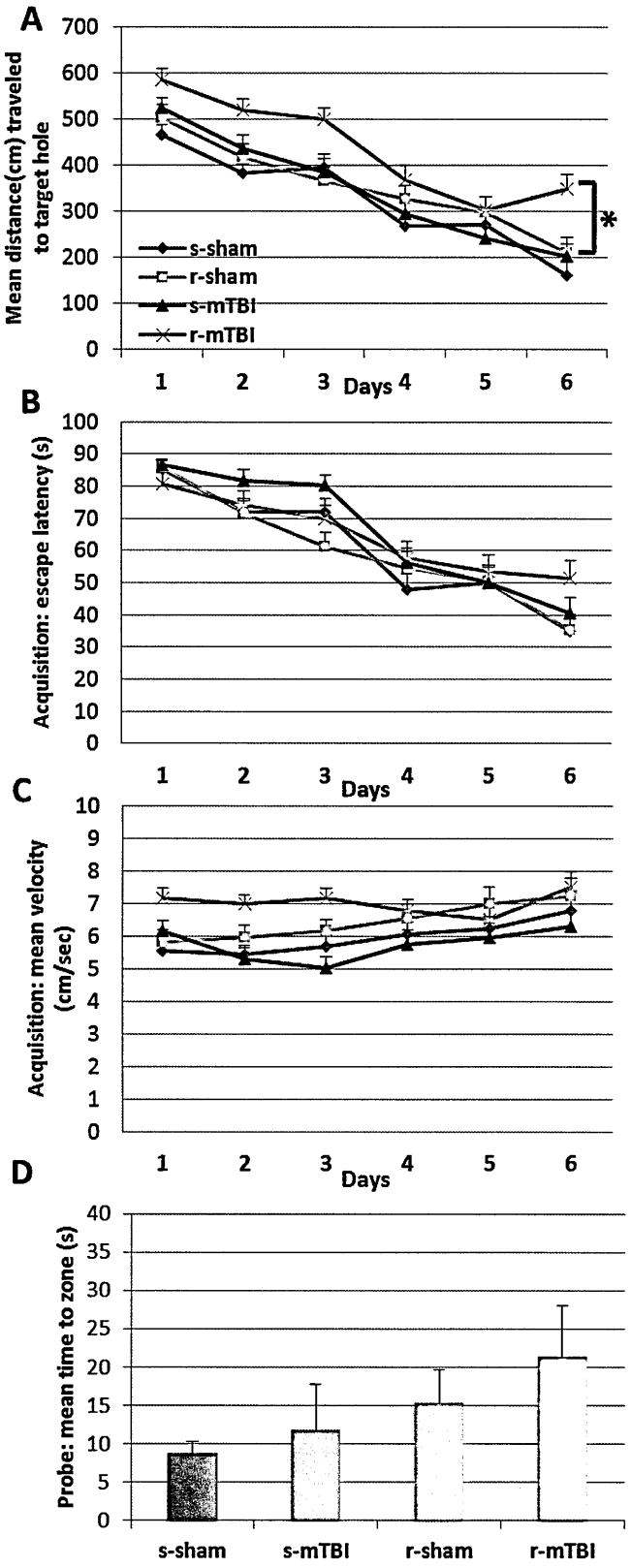

Figure. 4.6: Evaluation of learning (acquisition) and spatial memory retention (probe) using the Barnes maze on days 8–14 after sole/ last mTBI. Mice were tested in the Barnes maze for their ability to locate a black box beneath the target hole. During the acquisition testing, the r-mTBI group traveled a greater distance before escaping to the target hole compared with their respective anesthesia controls,(*r-mTBI, $p < 0.05$; r-mTBI) (A). The mean time to escape to the target hole (B) and the mean velocity (C) for acquisition phase was similar across all groups. For the probe trial (1 day following the 6 days of acquisition testing), the target box was removed and mice were placed in the middle of the table for a single, 60 sec trial. There was a trend for both mTBI groups to take longer to reach the target zone when compared to their respective control group ($p > 0.05$) (D). Data are presented as mean ± SEM.

4.3.3. Rotarod:

Motor function was evaluated 24 h following the sole/last mTBI/ anesthesia. Overall, all animals exhibited increased rotarod performance when compared to their last day of pre-training (Fig. 4.7). The performance of singly or repetitively injured animals was not different from that of their controls ($p > 0.05$; repeated measures ANOVA).

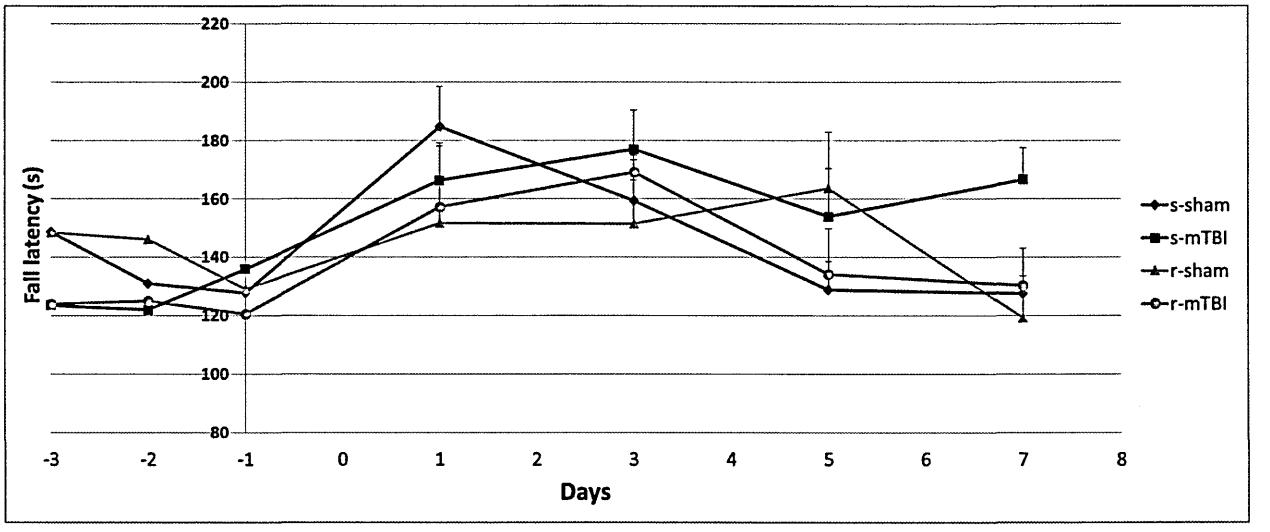

Figure. 4.7: Effect of mild traumatic brain injury on rotarod performance. Values were recorded on 7 separate days with three 5 min accelerating trials. Results are the mean ± SEM of the time animals remained on the rotarod before falling. There were no differences between injured and sham groups ($p > 0.05$) repeated measures ANOVA; ($n = 9$ per group).

4.3.4. Pathology of single and repetitive mild injury in hTau mice:

The brains of the hTau animals had no gross macroscopic differences when compared to the wild type animals. Macroscopic examination of fixed brains revealed evidence of focal microhemorrhage (<1 mm^2) in the inferior surface of the cerebellum in all animals subjected to r-mTBI. Otherwise, there were no focal macroscopic lesions in any of the animals subjected to injury. Furthermore, as was intended with the original design of this paradigm, and

demonstrated in the studies with wild type mice (Chapter 2), there were no skull fractures, cerebral hemorrhages, or contusions identified using this injury model in hTau mice.

4.3.5. Gial fibrillary acidic protein immunostaining:

For mice subjected to r-mTBI, immunostaining for GFAP revealed evidence of a mild reactive astrogliosis in the corpus callosum (Fig.4.8A-D;I-L) and regions of the cortex underlying the impact site. In contrast, no gliosis was observed in the cortex at the impact site in sham animals or singly injured mice. In the CC, the r-mTBI group (Fig.4.8L) showed a notable increase in the area of GFAP immunoreactivity compared with r-sham, whereas no difference was observed between the s-mTBI and the s-sham (s-mTBI 3.0 ± 0.9% vs. s-sham 3.6% ± 0.45%; $p > 0.05$; r-mTBI 11.2 ± 2.5% vs. r-sham 2.3 ± 0.4%; $p < 0.05$; Fig. 4.8M-N). In the CA1 region, there was no evidence of increased immunoreactivity across all groups (Fig.4.8E-H, N $p > 0.05$).

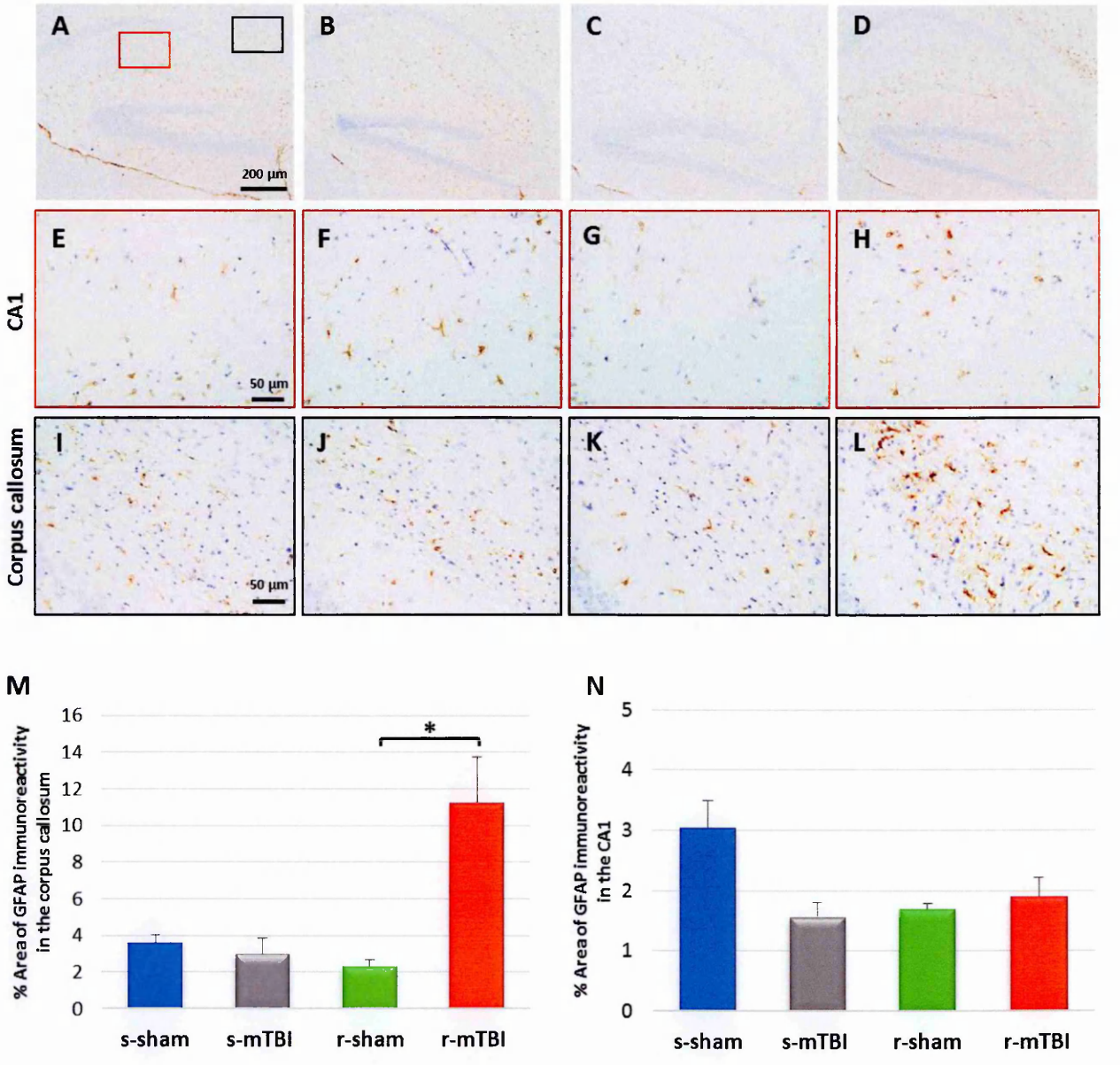

Figure.4.8: Glial fibrillary acid protein (GFAP) immunohistochemistry of sagittal sections of hTau mouse brain at ≈ 0.4 mm lateral to midline in the hippocampal region (A-L). Colored boxes indicate areas of interest, CA1 sub-region of the hippocampus (E-H) and corpus callosum (I-L) shown at higher magnification in the bottom two rows. There were no changes in the s-mTBI group (B) compared with their respective sham group (A). However, an increase in the area of GFAP staining was observed in the r-mTBI at 24 h after final injury in the corpus callosum (D, L). Quantitative analysis of GFAP staining in three 100 μm^2 areas of the splenium of the corpus callosum at 24 h post last mTBI (r-mTBI 11.2 ± 2.5% vs. r-sham 2.3 ± 0.4%; $p < 0.05$) (M). Quantitative analysis of GFAP staining intensity in two 200 μm^2 areas of the CA1 region ($p > 0.05$) (N). Tissue sections were counterstained with hematoxylin. Data are presented as mean ± SEM, (*$p < 0.05$) (n=3 per group).

4.3.6. Amyloid precursor protein immunostaining:

Numerous APP-immunoreactive axonal profiles were identified in sections from both injury groups (Fig.4.9B, D). These APP immunoreactive axonal profiles were observed as either granular or more elongated, fusiform swellings in the white matter of the parasagittal cortex, the CC, and the spinal trigeminal tracts of the brain stem (BS). APP-immunoreactive axonal profiles were observed 24 h post-injury in the CC of the s-mTBI (Fig.4.9B) and r-mTBI groups (Fig.4.9D) but not in their controls (Fig.4.9A, C). The numbers of APP-immunoreactive profiles in the CC of the s-mTBI was greater than in the r-mTBI group (s-mTBI group 18 ± 2.26 vs. r-mTBI 14 ± 0.8 axonal profiles/100 μm^2; $p < 0.001$; Fig. 9A). Overall, the APP immunohistochemistry observed in the hTau mice was similar to our initial study in WT mice (Chapter 2) in terms of number of immunoreactive axonal profiles per brain region (e.g. CC, BS). Axonal damage in the BS was minimal in the s-mTBI, whereas greater numbers of punctate immunoreactive swellings were present in the r-mTBI group. In the r-mTBI group, there was also evidence of cytoplasmic staining in neurons of the primary and secondary motor cortex.

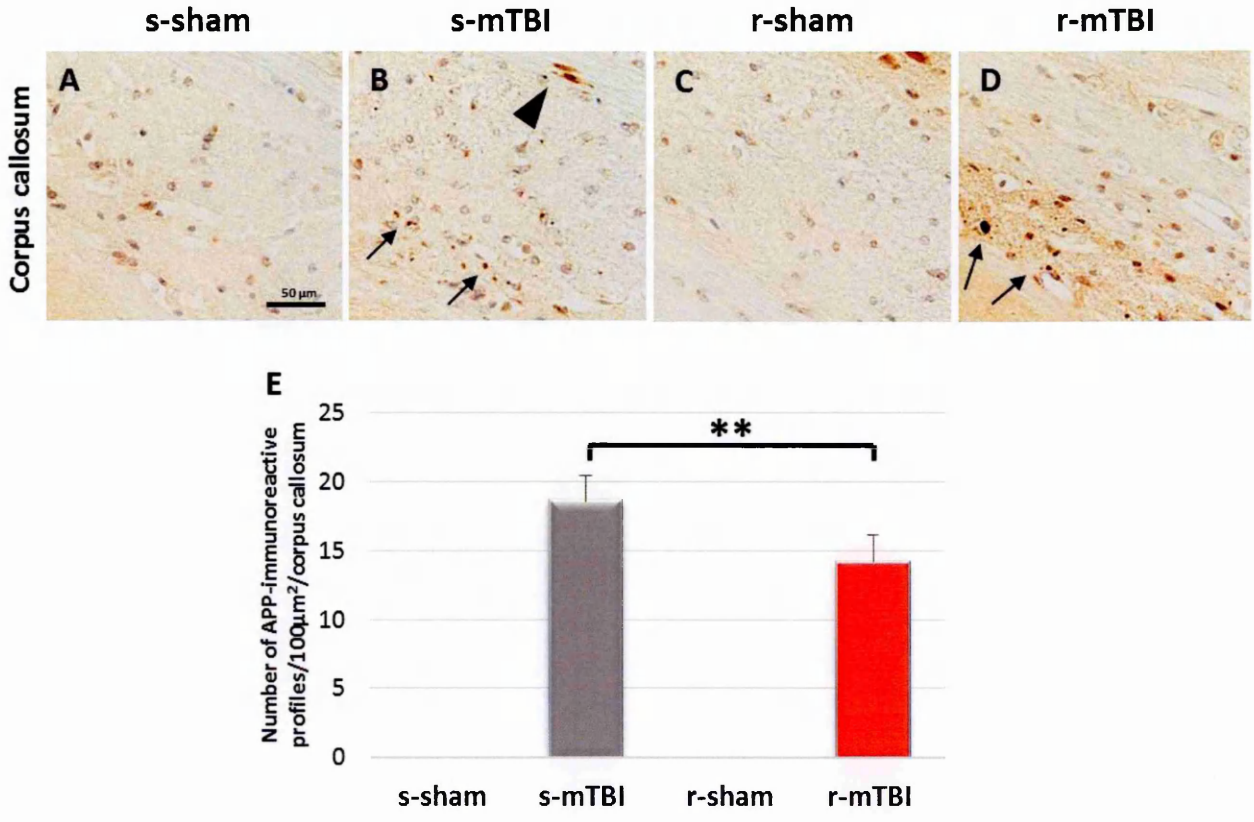

Figure.4.9: Amyloid precursor protein immunohistochemistry of sagittal sections of hTau mouse brain at 24 h after sole/ last mTBI of sagittal sections of mouse brain at ≈ 0.4 mm lateral to the midline. Immunoreactive axonal profiles were observed in the corpus callosum as either granular (arrow) or more elongated, fusiform (arrow head) swellings in both s-mTBI (B) and r-mTBI groups (D). Tissue staining from s-sham (A), and r-sham animals (C) was negative for APP immunostaining. Average counts of APP-immunoreactive axonal profiles per 100 μm^2 in the corpus callosum (s-mTBI group 18.5 ± 1.8 vs. r-mTBI 14.1 ± 1.9 axonal profiles/ 100 μm^2 (E). Data are presented as mean ± SEM (**p < 0.001) (n=3 per group).

4.3.7. Ionized calcium binding adaptor molecule 1 immunostaining:

As with the sham wild type animals previously reported in Chapter 2, we found no evidence for inflammation with Iba1 staining in the hTau sham animals (Fig.4.10A, C, E, G). In the singly injured animals, both resting and activated microglia (with a bushy morphology) were observed at 24h post injury in the CC (Fig4.10B) (s-mTBI 6.22 ± 0.9% vs. s-sham 3.22 ± 0.9%; p <

0.05; Fig.4.10I) and in the cortex (Fig4.10D) (s-mTBI 6.2 ± 0.9% vs. s-sham 4.01 ± 0.3%; p < 0.001; Fig.4.10J). For mice subjected to r-mTBI, immunostaining for anti-Iba-1 revealed clusters of activated microglia in the CC (Fig.4.10D) (r-mTBI 13.7 ± 1.3% vs. r-sham 2.21 ± 0.6%; p < 0.0001; s-mTBI 6.22 ± 0.9% vs. r-mTBI 13.7 ± 1.3%; p < 0.05; Fig.4.10H), and microglia with a bushy morphology in the region of the cortex underlying the impact site (r-mTBI 10.4 ± 1.3% vs. r-sham 2.01± 0.5%; p < 0.0001; s-mTBI 6.2 ± 0.9% vs. r-mTBI 10.4 ± 1.3%; p < 0.05; Fig.4.10J).

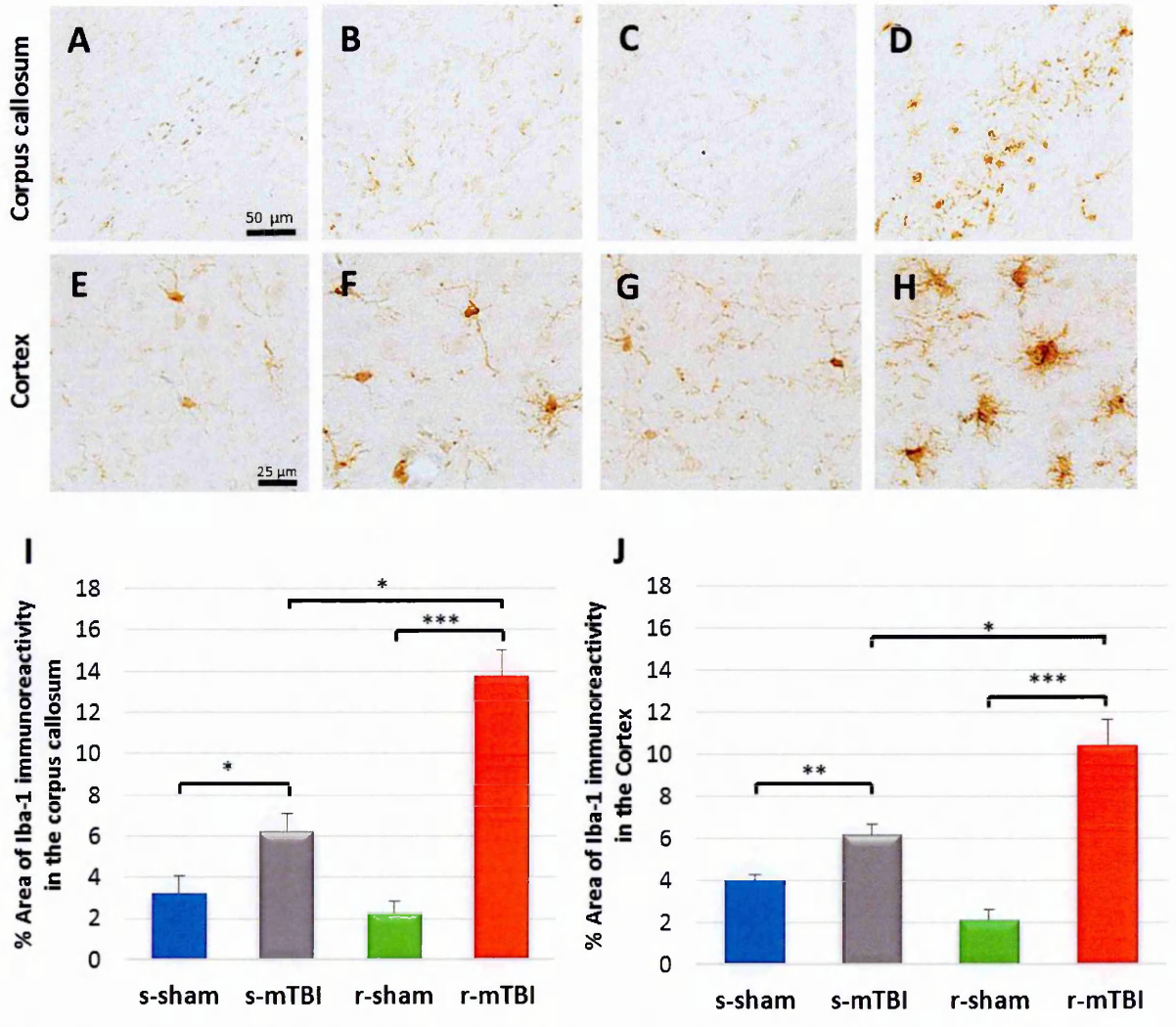

Figure.4.10: Immunohistochemical labeling for microglia with anti-Iba1 at 24 h after sole/ last mTBI of sagittal sections of mouse brain at ≈ 0.4 mm lateral to the midline. There was no microglial activation in the s-sham (A, E) and r-sham (C, G) groups. A mild increase in the area of Iba-1 immunoreactivity was

observed in the region of the corpus callosum (B), and with a bushy morphology (arrow) in the cortex (F) beneath the impact site at 24 h post s-mTBI. For mice subjected to r-mTBI, immunostaining for anti-Iba-1 revealed clusters of activated microglia with hypertrophic and bushy morphology in the region of the corpus callosum and in the cortex underlying the impact site (H). Quantitative analysis of Iba-1 staining intensity in three 100 μm^2 areas of the corpus callosum (I) and in two 200 μm^2 fields between layer III and V of the cortex (J) at 24h post sole/last mTBI. Data are presented as mean ± SEM, (*p<.05; **p<.005; ***p<.0005) (n=3 per group).

4.3.8. Qualitative assessment of Tau immunohistochemistry:

To determine the intraneuronal distributions of tau immunostaining, when reviewing the tau immunohistochemistry we partitioned the stained neurons into three subcellular segments as represented in Fig.4.11.

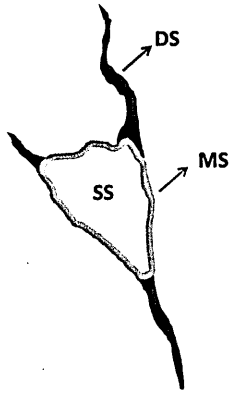

Figure.4.11: Subcellular partitioning of neuronal contours divided into three sub-regions: the somatic segment (SS), the dendritic segment (DS), and the membranous segment (MS).

4.3.9. CP13 immunohistochemistry in the hippocampus:

Mouse brains exposed to single and repetitive mTBI exhibited enhanced somatodendritic phosphorylated tau CP13, a marker of the p-tau epitope at serine residue 202. CP13 is an early tau phosphorylation marker that also detects pretangles and late-stage NFT

accumulation characteristic of several neurodegenerative diseases[37,72,82]. Within the CA1 (Fig.4.12A-D) and CA3 (Fig.4.12E-H) sub-region of the hippocampus, but not in the dentate gyrus, robust CP13 immunostaining was observed in most of the single (Fig.4.12B, F) and repetitive mTBI groups (Fig.4.12D, H) compared to their respective shams (Fig.4.12A, E, C, G). Qualitatively, the magnitude of this increase was greater in the somatic and dendritic segment of the r-mTBI (Fig.4.12D, H) than in the s-mTBI (Fig.4.12B, F). CP13 was also evident in the membranous segment of the neurons of sham animals with increased CP13 staining observed in the r-sham (Fig.4.12C, G) group compared with the s-sham group (Fig.4.12A, E). Quantitatively, CP13 immunostaining in the CA1 of both injured groups was not different compared with their respective sham group (s-mTBI 12.5 ± 1.7% vs. s-sham 12.2 ± 1.6%; $p > 0.05$; Fig.4.12I). Within the CA3 sub-region, more CP13 immunoreactivity was evident in the r-mTBI compared to the r-sham group (r-mTBI 34.1.4 ± 4.8% vs. r-sham 18.9 ± 3.3%; $p < 0.05$) while only a small increase was observed between the s-sham and s-mTBI group (s-mTBI 25.5 ± 3.2% vs. s-sham 23.9 ± 3.9%; $p < 0.05$; Fig.4.12J).

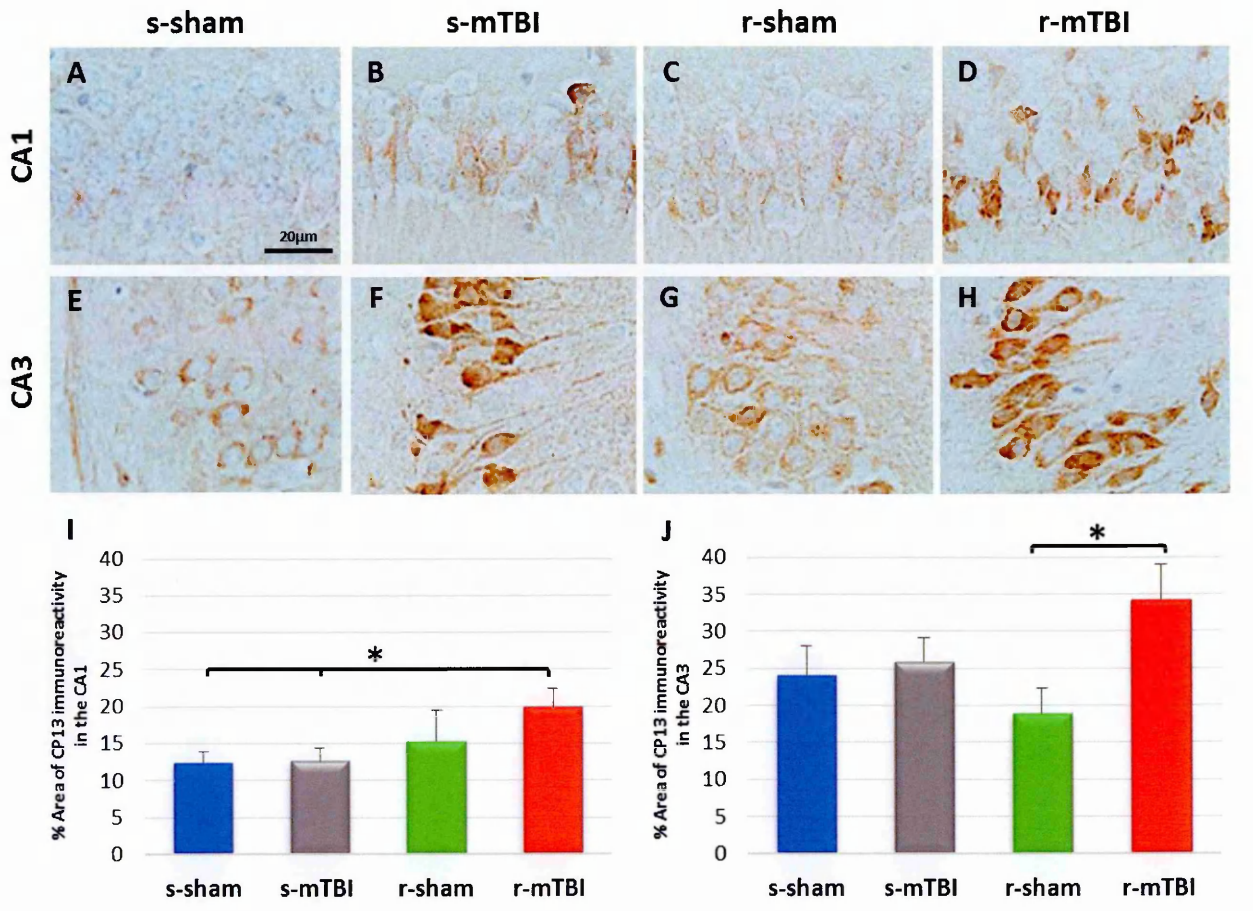

Figure.4.12: Tau pathology using CP13 (p202) in the hippocampus of the hTau mice. There was enhanced phosphorylated tau immunoreactivity in the CA1 and CA3 of hTau mice at 24hrs after s-mTBI and r-mTBI compared with their respective sham controls (A-H). CP13 immunoreactivity revealed minimal staining in the membranous segment of the s-sham group (A) while a trend for an increase in immunoreactivity was observed in the r-sham (C). There was an intraneuronal progression of CP13 immunoreactivity in the CA1 sub region of the hippocampus from the membranous segment as observed in s-mTBI (B) to the somatic segment in the r-mTBI (D). There was also an increase of CP13 immunoreactivity in the CA3 sub region of all groups, again, with a trend for the r-sham (G) to have a stronger membranous segment staining than the s-sham (E). Both single and r-mTBI had amplified membranous and somatic staining (F, H).). Quantitative analysis of CP13 staining in the pyramidal cell layer of hippocampal regions CA1 (I) and CA3 (J) at 24h post sole/last mTBI (O). Tissue sections were counter-stained with hematoxylin. n =3/group respectively. Data are presented as mean ± SEM, (*$p < 0.05$).

4.3.10. RZ3 immunohistochemistry in the hippocampus:

Mouse brains exposed to single and repetitive mTBI also exhibited enhanced somatodendritic phosphorylated tau RZ3, a marker of the p-tau epitope at threonine residue 231. This marker is used to detect phosphorylated tau protein accumulation in AD patients. Similar to CP13, a stronger RZ3 immunostaining was observed within the CA1 (Fig.4.13A-D) and CA3 (Fig.4.13E-H) sub-region of the hippocampus, but not in the dentate gyrus of the single (Fig.4.13B, F) and multiple mTBI groups (Fig.4.13D, H) when compared to their respective sham controls (Fig.4.13A, E, C, G). As with CP13, RZ3 immunostaining in the injured group was more pronounced in the r-mTBI (Fig.4.13D, H) than the s-mTBI group (Fig.4.13B, F). RZ3 in the r-sham (Fig.4.13C, G) animals was evident in the membranous and in a few somatic segments of the neurons while only the membranous segment was stained in the s-sham group (Fig.4.13A, E). RZ3 quantitation showed that immunoreactivity levels were significantly greater in the CA1 sub-region of the r-mTBI animals than in the other groups (r-mTBI 36.1 ± 2.8% vs. r-sham 17.9 ± 4.6%; $p < 0.001$; s-mTBI 24.9 ± 3.7% vs. s-sham 17.7 ± 1.6%; $p > 0.05$; Fig.4.13I). The RZ3 immunoreactivity pattern in the CA3 was relatively similar in all groups (Fig.4.13), with a trend for a small increase in immunoreactivity observed in the injured groups (Fig.4.13J).

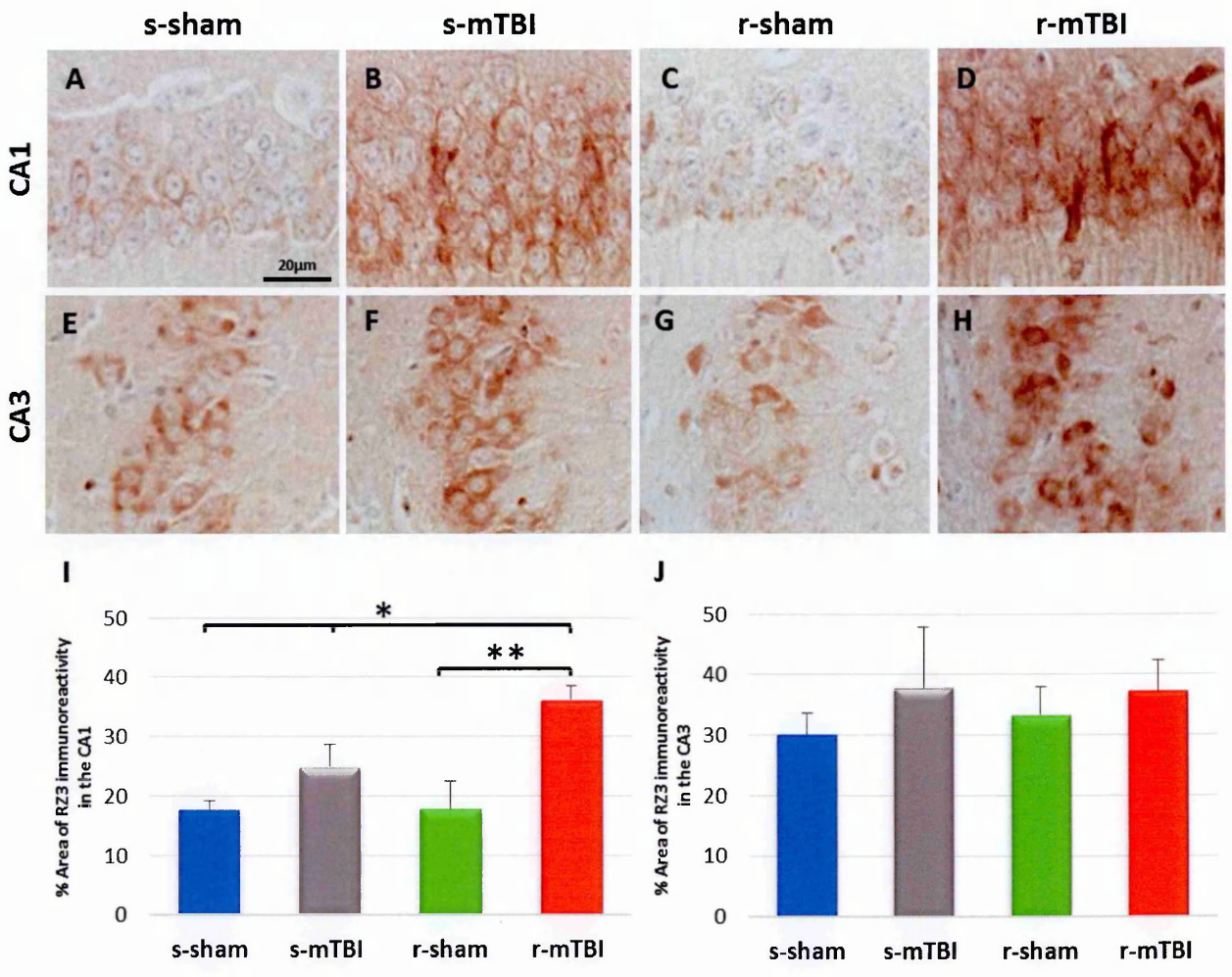

Figure.4.13: Tau pathology using RZ3 (p231) in the hippocampus of the hTau mice. There was enhanced phosphorylated tau immunoreactivity in the CA1 and CA3 of hTau mice at 24hrs after s-mTBI and r-mTBI compared with their respective sham groups (A-H). RZ3 immunoreactivity revealed minimal staining in the membranous segment of the s-sham group (A) while a few neurons had strong membranous segment immunoreactivity in the r-sham (C). Membranous accumulation of RZ3 was observed in the s-mTBI (B) and with a stronger staining in the r-mTBI (D). RZ3 immunoreactivity is predominantly localized in the membranous segment of both s-sham and s-mTBI groups (E, F). The r-mTBI (H) show greater dendritic and membranous staining than the r-sham group (G). Quantitative analysis of RZ3 staining in the pyramidal cell layer of hippocampal regions CA1 (I) and CA3 (J) at 24h post sole/last mTBI (O). Tissue sections were counter-stained with hematoxylin. n =3/group respectively. Data are presented as mean ± SEM, (*$p < 0.05$, **$p < 0.001$).

4.3.11. Qualitative analysis of PHF1 and MC1 immunohistochemistry in the hippocampus:

To detect late-stage neurofibrillary-like pathology, we used two different antibodies: PHF1, which recognizes p-tau epitopes at both Serine 396 and Serine 404 and MC1, an AD conformation-specific antibody. The hippocampus was devoid of PHF1 and MC1 immunoreactivity in both control and injured animals.

4.3.12. Tau immunohistochemistry in the cortex:

Abnormal phosphorylation and conformational changes of tau in the neocortex were evaluated with the same panel of monoclonal antibodies; CP13, RZ3, MC1 and PHF1. For hTau mice subjected to single (Fig.4.14B, F) and repetitive mTBI (Fig.4.14D, H), immunostaining for CP13 and RZ3 revealed evidence of increase p-tau in the cell bodies and apical dendrites of cortical neurons underlying the impact site.

As expected given the lack of MC1 immunostaining in the hippocampus, we did not observe noticeable changes across each group (Fig.4.14I-L). Similarly, the cortex was also devoid of PHF1 immunoreactivity in both sham and mTBI animals (Fig.4.14M, N, O) with the exception of one mouse in the r-mTBI group that showed abnormal phosphorylated tau immunoreactivity in the membranous fragment of a few neurons in the neocortex (Fig.4.14P).

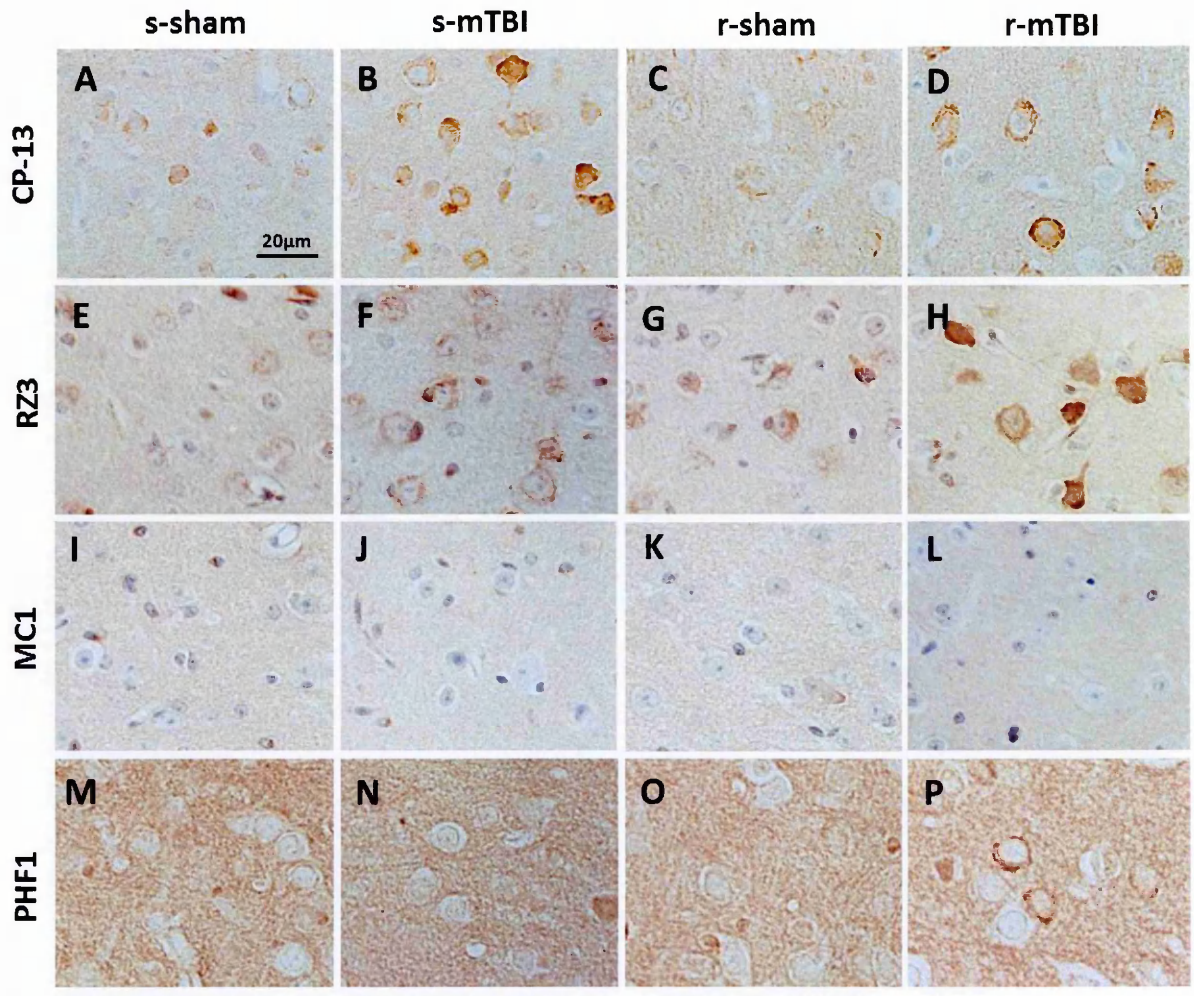

Figure.4.14: Qualitative changes in tau phosphorylation in the neocortex**.** Tau pathology using CP13, RZ3, MC1, PHF1 immunoreactivity in superficial layers of the cerebral cortex at 24h post sole/last mTBI/anesthesia. CP13 and RZ3 immunoreactivity were observed in the cell body and apical dendrites of cortical neurons of both injured groups (B, D, F, H). The immunoreactivity levels were greater than in both sham groups with hyperphosphorylated tau localized in the membranous segments of the neurons (A, C, E, G). There was no MC1 immunostaining observed in any group (I-L). Sporadic PHF1 immunostaining in the membranous segment of the r-mTBI (P) was observed at 24h post injury, while no cortical neurons were labeled in the s-mTBI both sham groups (M-O). Tissue sections (A-L) were counterstained with hematoxylin. (n=3 per group).

4.3.13. TUNEL:

Pyramidal neurons of the hippocampus, and neurons that stained positive for Tau in the cortex, were devoid of TUNEL positive staining, indicating that there was no apoptotic programmed cell death in either sham (Fig.4.15A, B) or injured animals (Fig.4.15C, D).

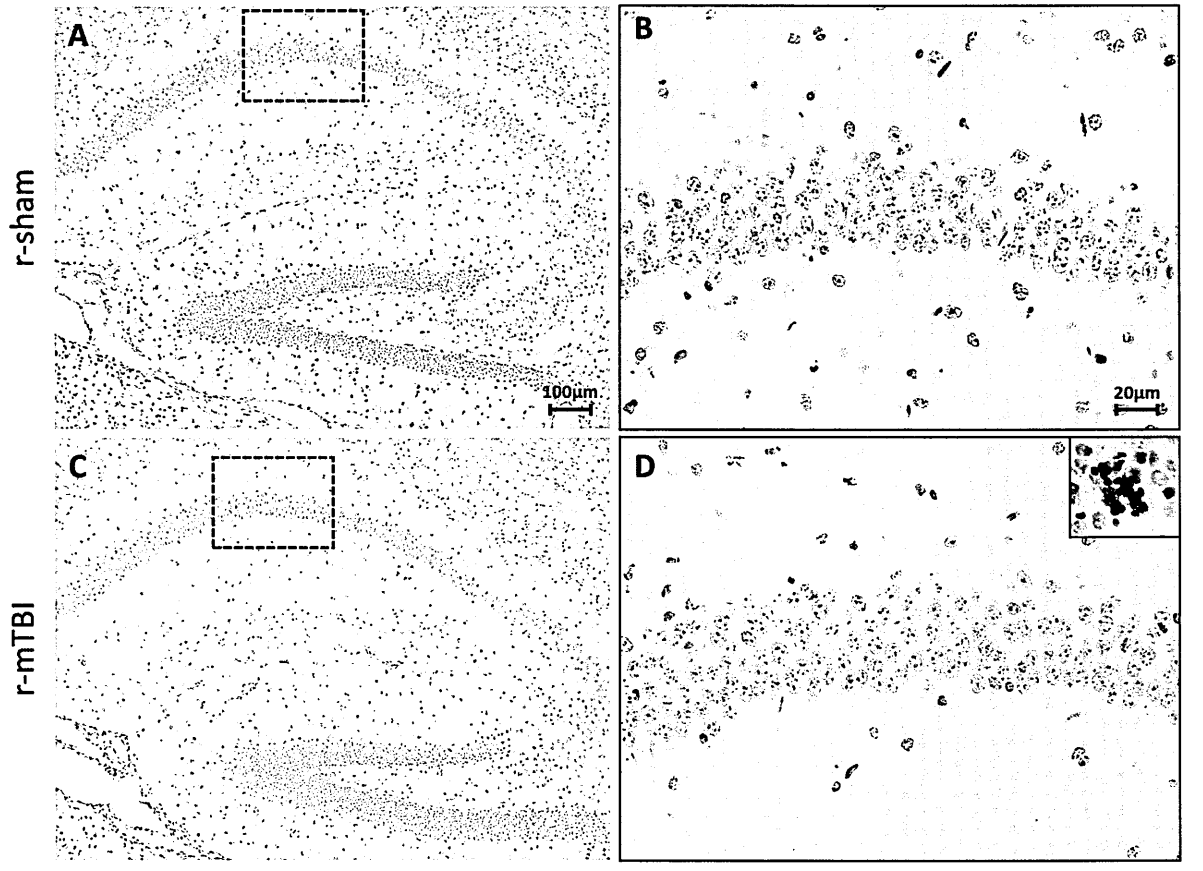

Figure.4.15: There were no TUNEL positive neurons in any group in any brain region. TUNEL-positive neurons in the hippocampal CA1 sector in the r-sham (A, B) and the r-mTBI (C, D) at 24h post last anesthesia/injury. The black boxes in A and C (20x) indicate the regions of interest which are then shown at a higher magnification (40x) in panels B and D. The inset in the top right corner (D) represent an image of a control TUNEL-positive nuclei with condensed chromatin and apoptotic bodies. Tissue sections were counterstained with hematoxylin (n=3 per group).

4.3.14. ELISA to detect low levels of mouse Tau:

To further confirm the histological findings, separate groups of injured and sham hTau mice were euthanized at 24 h post injury for biochemical analyses. Each brain region homogenate (cortices and hippocampi from one hemisphere) were subjected to low tau Sandwich ELISA coated with total tau DA31, p-tau CP13, PHF1, and RZ3.

We found no marked increases in the amount of soluble total tau DA31 or phosphorylated tau (CP13,RZ3,PH1) in injured compared with sham control groups for either the cortical (Fig.4.16) or hippocampal (Fig.4.17) brain sub-regions. However, a trend for an increase of total tau (DA31) was observed in the s-mTBI (+17%) and the r-mTBI group (+5%) when compared to their respective sham groups (s-sham 9.6 ± 1.2 μg tau/mg protein vs. s-mTBI 11.1 ± 1.8%; r-sham 10.6 ± 1.6 μg tau/mg protein vs. r-mTBI 11.1 ± 1.1%; $p > 0.05$ $p > 0.05$; Fig. 4.16A) . A gradual trend, depending on the number of injuries or anesthesias, was also revealed when the amount of tau present in the brain region homogenates is quantified as a ratio of phosphorylated tau protein (CP13, PHF1 or RZ3) to total tau protein. There is a 17% increase of CP13 in the cortical homogenate between the s-sham and the s-mTBI and a 6% increase between the r-sham and the r-mTBI and a 39% increase of CP13 between the s-sham and r-mTBI group (Fig4.16E).

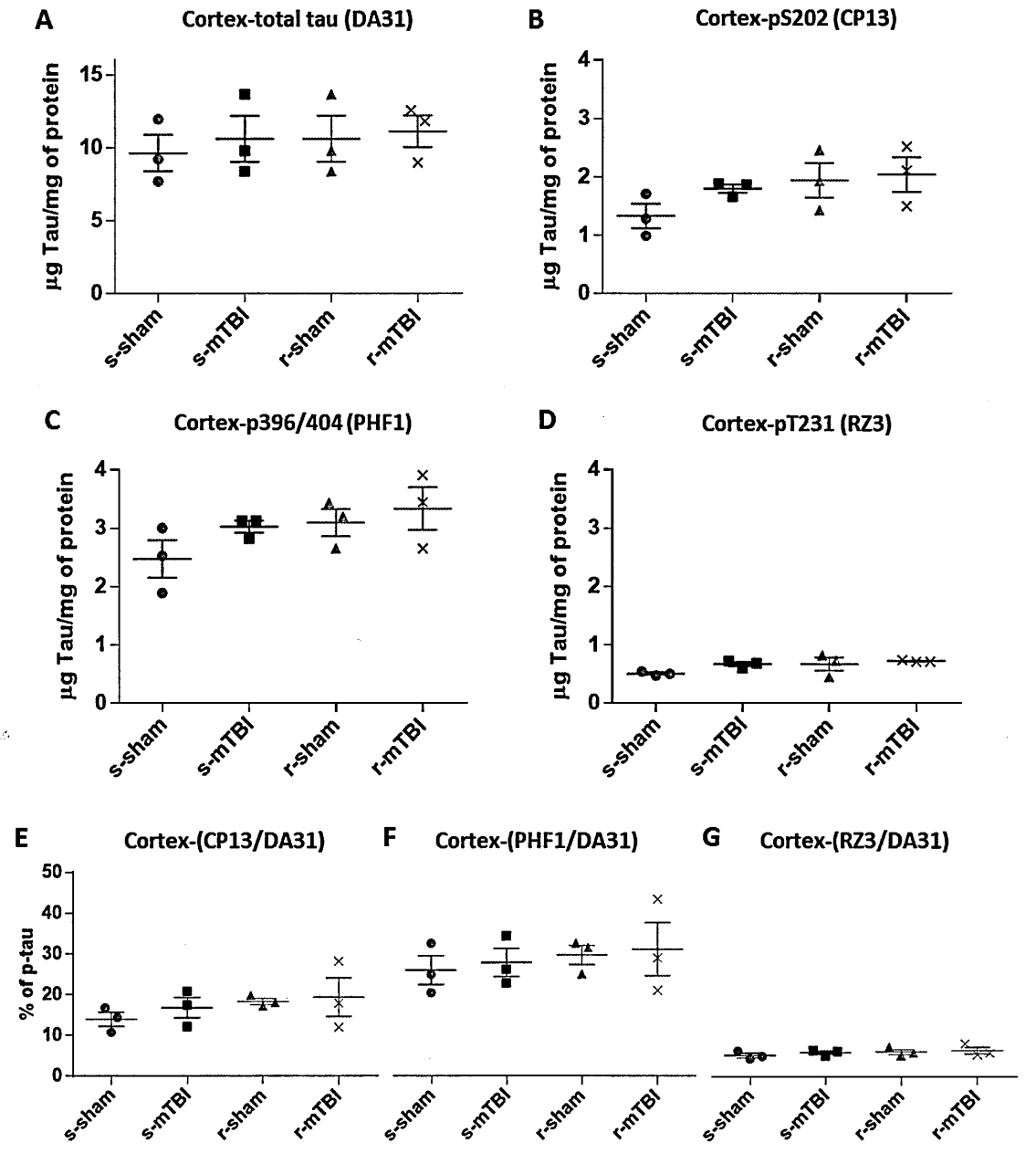

Figure.4.16: Quantitative analysis of cortical homogenate from hTau mice at 24h post sole/last mTBI/anesthesia. Total Tau DA31 (A) p-tau CP13 (B), PHF-1 (C), and RZ3 (D) ELISAs. There was no difference in cortical soluble phosphorylated tau in injured hTau mice vs. sham animals. While not significant, there was always a trend for the injured groups to have a higher amount of phosphorylated-tau when compared to their respective shams. Quantitation of CP13, PHF-1, and RZ3 from cortical homogenates as a percentage of total tau protein (DA31) (E, F, G). Again, analyses revealed a non-significant trend for an increase in the ratio of phospho to total tau in injured and r-sham groups compared to s-sham. Data are presented as mean ± SEM, (n=3/group), ($p>.05$; two-tailed Student's t test).

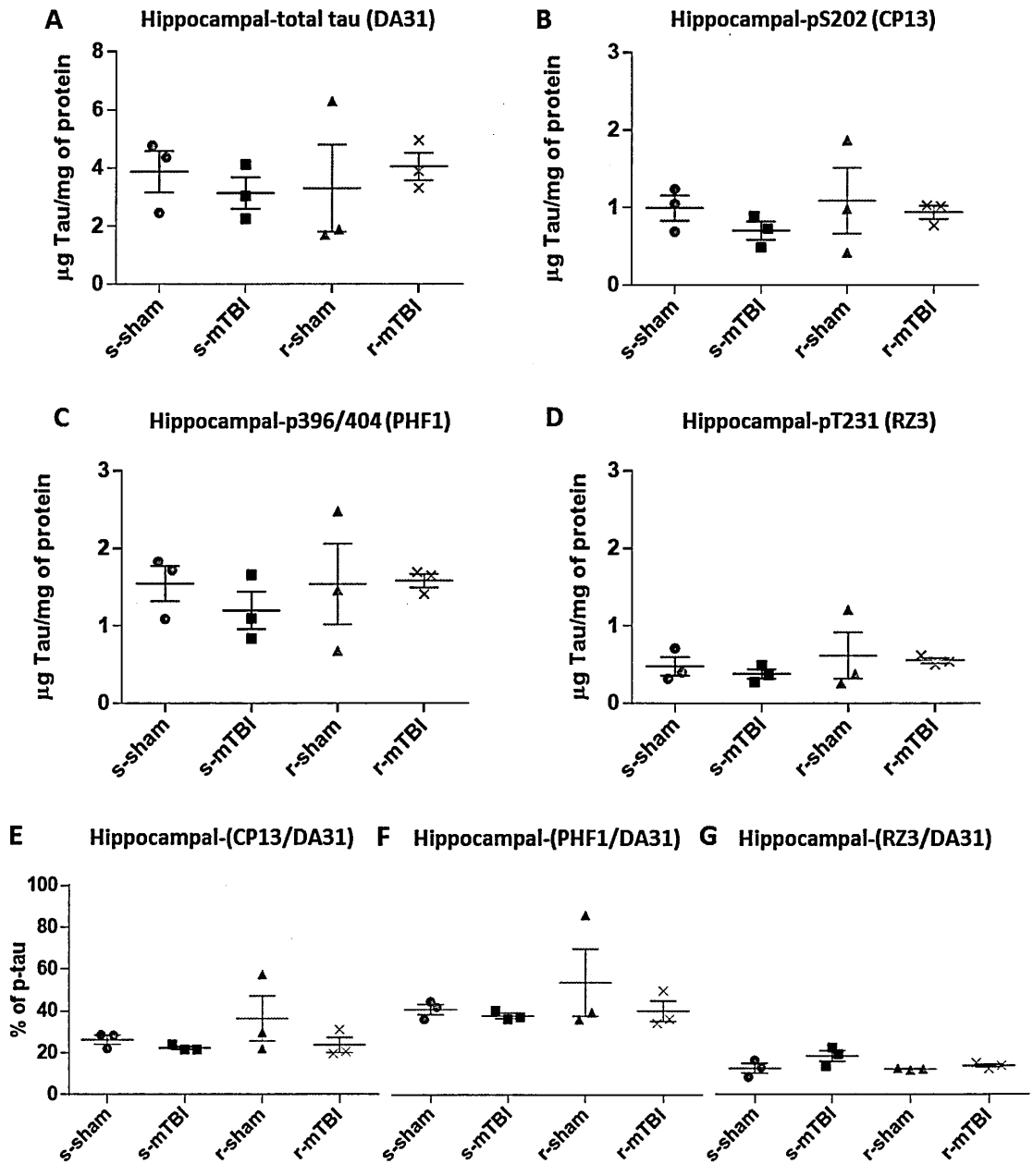

Figure.4.17: Quantitative analysis of hippocampal homogenate of hTau mice at 24h post sole/last mTBI/anesthesia. Total Tau DA31 (A) phospho-tau CP13 (B), PHF1 (C), and RZ3 (D) ELISAs. There was no difference in hippocampal soluble phosphorylated tau in injured hTau mice vs. sham animals. Quantitation of CP13, PHF1, and RZ3 from hippocampal homogenates as a percentage of total tau protein (DA31) (E, F, G). There was no difference in the ratio of phosphorylated tau protein to total tau protein in injured vs. sham animals. Data are presented as mean ± SEM, (n=3 per group), ($p>.05$; two-tailed Student's t test).

4.4. Discussion:

This chapter focused on the acute effects of single and r-mTBI in a transgenic mouse model expressing all 6 isoforms of human tau protein on a null murine background, in order to explore the potential role of tau pathobiology in TBI sequelae. Two major findings were revealed by this study. First we showed that single and r-mTBI induced a modest cortical increase in the soluble fraction of three different p-tau epitopes: CP13, PHF1 and RZ3. Secondly, this increase was not associated with worse behavioral performance when compared to wild type animals. In all groups, there was no evidence of Aβ accumulation and/or MC1 inmmunostaining, a distinct pathological conformation of the tau molecule in Alzheimer's disease. This study provides a direct connection between mTBI and tau pathology and indicates our model can mimic pathology observed in human brains, including neuroinflammation, diffuse axonal injury, behavioral impairments and an increase of tau phosphorylation[1,5,67,68,83,84].

Recently there has been a surge of attention focusing on the neuropathological sequelae of TBI (especially repetitive concussive injury) amongst athletes engaged in contact sports and military personnel exposed to blast injury. Several studies have documented a distinct, slowly progressive tauopathy defined as CTE[4,5,7]. However, despite the growing evidence from postmortem analyses that seemingly link repeated mTBI with CTE, this causal relationship has not yet been firmly established, as autopsy confirmation is required and thus the precise incidence of CTE after repetitive head injury is still unknown[67,85]. The cases which have fueled the surge of interest in CTE, at least in the US, have been high profile cases[3,86-88] (celebrity athletes for example), who have died prematurely, and the incidence of CTE in

individuals living for decades beyond the time of their TBIs remains to be explored. To explore the role and significance of tau in TBI it is therefore critical to utilize longitudinal studies in appropriate animal models that will adequately enable monitoring of the distinct biochemical and pathological changes that occur post-injury, and correlation with any behavioral dysfunction. We choose the hTau mouse model because it expresses all six isoforms of the human tau protein on a null murine background, and as such best recapitulates the relevant human tau background.

Very little is known about the mechanisms involved in the accumulation of tau proteins observed in human cases after TBI. Evidence from a recent animal model of TBI[58] demonstrates rapid formation of neurotoxic oligomeric and p-tau aggregates that may be followed by a toxic gain of function. Whether the increase in soluble p-tau observed in our model at 24 h post injury is a transient, sustained or leads to aggregates remains to be determined. The increase of cellular p-tau may triggers a stepwise process that involves tau aggregation, gain of toxic function and conformational changes that eventually lead to paired helical filaments conformation, and the pathologic features of CTE and other tauopathies. However, while CP13 (pS202) and RZ3 (pT231) are present both in normal and AD brains, in human AD, the increases of p-tau on the pS202 and pT321 motifs (as we observed in our model) could define early events that eventually disrupt tau MT function, precede tangle formation and neurodegeneration. Notably, pT231 phosphorylation has been shown to be the first phospho epitopes that appear during pretangle formation in AD[36]. Further work is required to address the time course and the presence if any, of other tau species such as soluble small oligomers, and insoluble tau species. However, the absence of MC1 immunostaining suggests that mTBI

does not trigger the formation of toxic tau conformational species at 24h post single and r-mTBI. Therefore, this increase of p-tau could reflect various degree of brain neuroplasticity or the establishment of a series of events that may become toxic over time.

In the hTau mouse model of mTBI, injured at 3 months of age (comparable to young adult in humans) we observed key aspects of human mTBI pathology[5,67], and intriguingly similar pathological outcome in many aspects when compared with WT mice at the acute time point[84]. First, consistent with our previous study in WT mice (Chapter 2), neurobehavioral impairments, neuroinflammation, and axonal injury in the absence of macroscopic tissue damage were observed in hTau animals. As anticipated, the major changes observed between the hTau mice and the WT animals were unveiled by the tau pathology and biochemistry. Notably cell body accumulation of CP13 and RZ3 hyperphosphorylated tau is evident at 3 months of age in the hTau mice while the WT were devoid of tau pathology. Since the hTau mice have an age dependent change in the localization and accumulation of tau hyperphosphorylation[72], these features render this model ideally suited to assess whether a single or r-mTBI can accelerate pathological tau burden as seen in humans[5,6,89]. At 24 h post single/last injury an increase in p-tau (CP13, RZ3 and PHF1) was observed after immunohistochemical quantification. However the statistical analysis of the ELISAs reading revealed that this trend was not significant, perhaps owing to the small number of animals per group or due to the variance in levels of tau expression in these hTau mice. hTau mice were extremely difficult to breed compared to WT mice, and as such this precluded the analyses of a larger group for this study. Despite this limitation in sample size (i.e. low power and biological variation) increasing the number of animals per group will give a better representation of a general mouse cohort with a clearer

signal in potentially pathogenic changes to tau protein. For example, the post hoc power analysis on the ratio of CP13/DA31 from the cortical sample at an acute time point showed that the power was low (1%) as it is much lower than the generally accepted 80%. Therefore in order to detect significant changes with a mean difference of 5.5% between the s-sham and the r-mTBI group we should have used 35 animals per group. Interestingly our findings are also seemingly in parallel with the only two relevant models of single or r-mTBI in the literature (in terms of age and injury severity). In this regards, Kane and colleagues reported an increase in p-tau at 30 days post repetitive mTBI injury[68], while Goldstein et al (2012), demonstrate enhanced CP13 somatodendritic phosphorylated tau at two weeks post injury in the cerebral cortex of a single murine blast model[1]. In our recently published work on the effects of mTBI in aged hTau we investigated the effects of our various injury paradigms in 18-month-old hTau mice at 3 weeks post-injury[90]. At 18 months, these mice already exhibit clear tau pathology, with tau hyperphosphorylation and inflammation. However, despite these age-related changes, in parallel with the pattern shown in this current study, we also observed augmented p-tau immunoreactivity along with an increase in astrocyte/microglia activation in the superficial layer of the motor/somatosensory cortex and in the corpus callosum. The comparison of these data (young vs. aged hTau mice) perhaps suggest that antecedent tau pathology, ageing and inflammation may be a significant factor involved in driving the pace of tau pathology in some human cases.

Although attempts have been made to define clinicopathological boundaries for the diagnosis of CTE[5,67,91], with some describing it as a distinct encompassing tauopathy[5,7], it is becoming evident that the presentation and incidence of CTE following repetitive mTBI is complex in nature and involves additional contributory factors as discussed below, which must

be considered when developing mouse models of injury. These are factors that we plan to explore with this model.

In advanced ageing one of the most striking underlying features readily observed especially in the medial temporal limbic regions is tau pathology, as detected by AT8 immunostaining at autopsy[29]. This universal feature of ageing has also been clearly demonstrated as early as 6-30 years of age, in select subcortical areas as AT8 (pS202) positive pretangles[28]. This presentation of abnormal tau material in humans may be considered to be intrinsic to the human brain and its initital appearance and/or propagation may arise as a result of several combinatory factors (such as; sub/concussive head injury, substance abuse in professional athletes, medication/drug history/steroids, ageing, inflammation, vascular damage, comorbid diseases, genetic background (ApoE; MAPT), environmental risk factors and much more). As such, if the staging of antecedent NFT-like pathology already exists in a subset of the young adult human population exposed to such risk factors mentioned above, this may possibly explain why certain individuals may be selectively susceptible to develop augmented CTE-like tauopathy following repetitive mTBI. This will continue to remain a challenge as it is currently impossible to detect or monitor changes in pathological tau profiles in humans before and after mild repetitive injury. Current advances to develop a specific tau biomarker for in vivo neuroimaging, such as has been developed for in vivo amyloid imaging with the (FDDNP) compound[92], will be an invaluable tool to further help to shed some light on the role of tau pathobiology in disease. Such an advance with tau imaging would represent a major step forward to diagnose CTE in live patients. Another possibility will be to identify CSF or blood biomarkers of tau changes that correlate with tau pathobiology in the brain[93,94]. Total and p-

tau measurement in CSF is currently used as an AD diagnostic aid[95-97], but we would suggest that markers for TBI or CTE will need to be of much greater scope (i.e. detecting multiple potentially pathological changes in tau) than what is currently available. Detailed mass-spectrometry characterization of tau in the brain and blood of our mouse models of TBI is currently ongoing in our laboratories, with the goal of providing such biomarker profiles for validation in human samples.

Another important factor that should be considered when developing animal models of injury that best recapitulate the human scenario is to use appropriate mouse models with the same human tau isoform background. In our model we used the hTau mice that expresses all six human tau isoforms on a null murine background. However unlike humans that express 3R:4R tau isoform ratio at (50:50), they have been reported to express a higher ratio of 3R:4R tau isoform ratio at (4:1)[72]. Changes in the tau isoform ratio are associated with distinct tauopathies, for example, a shift toward an increase of 4R isoforms is observed in patients with PSP or AGD whereas a shift toward an increase of 3R is associated with FTDP17[12]. The effects of some of the FTDP-causing mutations in tau (for example; P310L, V337M and G272V) have been extensively studied in transgenic mice that develop widespread NFTs[76,98], and these studies as well as in vitro cell culture models suggest that the 4R tau isoform is a potentially more favorable substrate for aberrant hyperphosphorylation, and also has the propensity to self-aggregate into filaments more readily at a lower phosphorylation stoichiometry[99]. Therefore it is plausible that the significant imbalance in 3R:4R ratio in our hTau model may affect the outcome of tau pathology following injury as compared to humans and as such should be considered in the interpretation of our data.

Our qualitative immunohistochemical observations showed an increase in somatodendritic phosphorylated tau (CP13, PHF1, RZ3) in the superficial layer of the cortex of the injured group, as has been described many years after r-mTBI in CTE cases. Supporting these observations, ELISA of the cortical homogenate also revealed a trend toward an elevation of phosphorylated tau epitopes pS202 and pT231, all associated with early tau filament aggregation and pS396/404, a marker for late stage tau conformation such as NFTs[37]. The mechanisms for translation of mechanical forces into biochemical changes are likely to be complex and include a variety of signaling pathways and genes regulation. However, it is highly probable that the observed increase of soluble p-tau may be a part of a normal cell response caused by tearing the cell membrane and/or the subsequent influx of high calcium concentration into the cells. The resulting increase of calcium-dependent protease and other kinases and phosphatases may in turn, initiate abnormal p-tau on serine and threonine residues. Therefore if the level of phosphorylation is exceeded, the cell is more likely to experience increased cell death or abnormal function that may lead to neurodegenerative diseases. Whether specific phosphorylation sites contribute to the pathogenesis of r-mTBI as previously described in AD patients[37] remain to be addressed.

In the hippocampus however, despite the subtle changes in p-tau levels as determined by ELISA, we observed a dramatic increase in p-tau immunoreactivity via immunohistochemical analysis, but this was localized in the subregions of the CA1 and CA3 hippocampal area.

Another notable observation between immunohistochemistry (IHC) and biochemical analysis surrounds the level of PHF1 immunostaining vs. PHF1 protein levels. Protein assays

using ELISA showed the highest changes between injured and non-injured animals for the ratio of PHF1/DA31 (total tau). However IHC staining with the PHF1 antibody showed that the different brain regions were almost devoid of positive PHF1 immunostaining (this was in contrast to both CP13 and RZ3 antibodies which showed stronger immunostaining intensity). This difference could be attributed to the masking of the PHF1 epitope following fixation with paraformaldehyde, which forms strong cross-links made up of methylene bridges with primary amines of proteins in perfused tissue. The differences may also reflect mouse to mouse variation, which could be addressed as previously explained by increasing the numbers of mice in each group. Further analyses and quantification of both IHC and biochemical data may be needed to address this apparent discrepancy.

Based on these results, it remains unclear and to be determined if the acute increase of cortical tau phosphorylation originates from the endogenous pool of tau from formerly healthy axons damaged by the injury, or from tau newly synthesized as a response to the cytoskeletal damage. While further work is required to answer this question, TUNEL staining revealed no apoptotic neurons in the cortex or hippocampal regions in sham or injured animals. This suggests that neurons that show an enhanced somatodendritic phosphorylated tau staining are not apoptotic. These findings raise the question whether tau hyperphosphorylation is a permanent, progressive, or a reversible component after head injury. In other words, does it become completely resistant to autophagy and other endogenous cellular removal mechanisms? Is phosphorylated tau used to repair the damaged neuron's cytoskeleton? Is tau hyperphosphorylation fully reversible? Owing to its known involvement in AD pathogenesis, tau has been considered as a disease causing agent. However, the potential link between a

transient surge of tau hyperphosphorylation, as observed after TBI, and neurodegeneration has not yet been clearly defined. In fact, evidence suggests that tau phosphorylation at certain sites (e.g. KXGS motifs) may protect against tau aggregation[100]. In addition, Arendt and colleagues revealed that hyperphosphorylation of tau in hibernating animals reverses rapidly upon arousal from torpor[53]. Further works remain to be done, but similar to these observations from hibernating animals, tau hyperphosphorylation resulting from TBI might potentially involve an intrinsic response to protect the neurons from further damage through mechanisms that stabilize the cytoskeleton and synaptic structure[101,102]. These critical questions prompted our design and implementation of another study in order to evaluate the long term consequences of mTBI in hTau. A second cohort of hTau mice, exposed to the same four injury/sham paradigms, was euthanized at 12 months post injury (following behavioral characterization) and will shortly undergo pathological and biochemical analysis.

Other pathological features seen in human CTE cases, such as perivascular tau pathology, neuropil threads and astrocytic tangles that are occasionally observed from post-mortem analysis at chronic time-points post r-mTBI[5], were not observed in our mouse model of mTBI. Gallyas Silver stain, a traditional histopathological method used for the detection of neurofibrillary tangles will be performed to confirm these preliminary observations. It is possible that these differences between human CTE cases and our mouse model may be constrained by time-points of pathological assessment, differences in the severity and frequency of injury, interspecies differences; including the craniospinal angle, the significantly greater deformability of the murine skull, and the white to grey matter ratio in mice and humans. Overall, these data seem to suggest that tau hyperphosphorylation at acute time

points post-injury may be a contributing factor to the mTBI pathology, however axonal injury and inflammation may be more important for TBI pathogenesis.

Moreover our findings herein also raise the question concerning the link between anesthesia exposure and increased tau phosphorylation, which have been reported on several occasions in the literature[54,103,104]. Indeed, a trend for lower spatial memory performance (Probe trial) was observed in the r-sham group. The pathological examination also revealed a tendency for an increase in tau phosphorylation in mice exposed to multiple anesthesias. This trend was not observed in our previous study in aged hTau mice. This could be explained by the transient increase of tau phosphorylation that resorbs within weeks post exposure[105] or by the fact that aged tau mice have such high levels of phosphorylated tau that they supersede that which could be induced by anesthesia.

At the clinical level, repetitive mTBI/CTE can present with behavioral, cognitive, and/or motor-related symptoms. In the few months or years following injury the most common disturbances anecdotally recorded by patients or their relatives include behavioral changes, such as – impulsitvity, depression, aggression, mood swings and suicidality[2,106,107]. With regard to cognitive impairment, patients can exhibit impaired attention and/or concentration, executive function and memory problems as the disease progresses, possibly leading to dementia. Motor disturbances also appear several years after injury, represented as tremors (parkinsonian type), ataxia, dysarthria and impaired co-ordination[5,108]. To further characterize the early neurobehaviroal phenotype of our hTau mouse model post injury, we performed two different tests, Barnes maze (for spatial memory), and rotarod (motor cordination).

When tested for behavioral performance in the Barnes maze, the r-mTBI group showed impaired learning consistent with our mTBI study in WT mice[84]. However, in contrast to our previous study, single injury failed to demonstrate any significant effect on the behavior of the hTau mice as they performed at the same level as their sham control counterparts (in term of escape latency and distance travelled). Alterations in genetic background of the animals could be the cause of such differences, because mice which have been genetically manipulated are known to perform differently for a given behavioral test. It is interesting to note that the overall performance of the hTau mice was superior to the WT groups as they were able to find the hidden box with the shortest distance and time travelled when compared to WT animals over the acquisition trial phase, although they performed worse on probe trial. Results from the rotarod suggest that neither injury nor anesthesia had an effect on the locomotor activity of these mice. There is currently no point of reference in the literature to compare motor related function in hTau mice, however, a direct comparison with our wild type mice suggest a motor coordination and balance deficit in these mice, as their score was 58% lower (overall) than their wild type counterparts at the same age and for the same experimental paradigm.

To date, numerous investigators have consistently reported a strong case for the development of tau pathology several years following repetitive mTBI[5]. However the majority of these studies have been from retrospective studies which have principally focused on biased samples of clinically symptomatic cases. The experimental data presented here suggest that tau pathophysiology along with inflammation and axonal injury (as seen in both wild-type and hTau models) all appears to play somewhat of a significant role in the early events preceding single or repetitive mTBI and strongly correlates with the (acute) behavioral changes post-

injury. Additional longitudinal (prospective) studies in both humans and appropriate animal models that aim to characterize the distinctive pathological and biochemical profile of tau pathophysiology in the brain/CSF before and after injury will be required to evaluate the beneficial and/or detrimental role of tau in TBI sequelae.

4.5. References:

1 Goldstein, L. E. *et al.* Chronic traumatic encephalopathy in blast-exposed military veterans and a blast neurotrauma mouse model. *Science translational medicine* **4**, 134ra160, doi:10.1126/scitranslmed.3003716 (2012).

2 Millspaugh, J. A. Dementia pugilistica. *US Naval Med Bulletin* **35**, 297-261 (1937).

3 Omalu, B. I. *et al.* Chronic traumatic encephalopathy in a national football league player: part II. *Neurosurgery* **59**, 1086-1092; discussion 1092-1083, doi:10.1227/01.NEU.0000245601.69451.27 (2006).

4 McKee, A. C. *et al.* Chronic traumatic encephalopathy in athletes: progressive tauopathy after repetitive head injury. *Journal of neuropathology and experimental neurology* **68**, 709-735, doi:10.1097/NEN.0b013e3181a9d503 (2009).

5 McKee, A. C. *et al.* The spectrum of disease in chronic traumatic encephalopathy. *Brain : a journal of neurology* **136**, 43-64, doi:10.1093/brain/aws307 (2013).

6 Sosa, M. A. *et al.* Blast overpressure induces shear-related injuries in the brain of rats exposed to a mild traumatic brain injury. *Acta Neuropathologica Communications* **1**, 51 (2013).

7 Stern, R. A. *et al.* Long-term consequences of repetitive brain trauma: chronic traumatic encephalopathy. *PM & R : the journal of injury, function, and rehabilitation* **3**, S460-467, doi:10.1016/j.pmrj.2011.08.008 (2011).

8 Morrison, B., 3rd, Cater, H. L., Benham, C. D. & Sundstrom, L. E. An in vitro model of traumatic brain injury utilising two-dimensional stretch of organotypic hippocampal slice cultures. *Journal of neuroscience methods* **150**, 192-201, doi:10.1016/j.jneumeth.2005.06.014 (2006).

9 Gentleman, S. M., Nash, M. J., Sweeting, C. J., Graham, D. I. & Roberts, G. W. Beta-amyloid precursor protein (beta APP) as a marker for axonal injury after head injury. *Neuroscience letters* **160**, 139-144 (1993).

10 Koo, E. H. *et al.* Precursor of amyloid protein in Alzheimer disease undergoes fast anterograde axonal transport. *Proceedings of the National Academy of Sciences of the United States of America* **87**, 1561-1565 (1990).

11 Yam, P. S., Takasago, T., Dewar, D., Graham, D. I. & McCulloch, J. Amyloid precursor protein accumulates in white matter at the margin of a focal ischaemic lesion. *Brain research* **760**, 150-157 (1997).

12 Sisodia, S. S., Koo, E. H., Hoffman, P. N., Perry, G. & Price, D. L. Identification and transport of full-length amyloid precursor proteins in rat peripheral nervous system. *The Journal of neuroscience : the official journal of the Society for Neuroscience* **13**, 3136-3142 (1993).

13 Kamal, A., Almenar-Queralt, A., LeBlanc, J. F., Roberts, E. A. & Goldstein, L. S. Kinesin-mediated axonal transport of a membrane compartment containing beta-secretase and presenilin-1 requires APP. *Nature* **414**, 643-648, doi:10.1038/414643a (2001).

14 Breen, K. C., Bruce, M. & Anderton, B. H. Beta amyloid precursor protein mediates neuronal cell-cell and cell-surface adhesion. *Journal of neuroscience research* **28**, 90-100, doi:10.1002/jnr.490280109 (1991).

15 Trapp, B. D. & Hauer, P. E. Amyloid precursor protein is enriched in radial glia: implications for neuronal development. *Journal of neuroscience research* **37**, 538-550, doi:10.1002/jnr.490370413 (1994).

16 Mattson, M. P. *et al.* Cellular signaling roles of TGF beta, TNF alpha and beta APP in brain injury responses and Alzheimer's disease. *Brain research. Brain research reviews* **23**, 47-61 (1997).

17 Oehmichen, M., Theuerkauf, I. & Meissner, C. Is traumatic axonal injury (AI) associated with an early microglial activation? Application of a double-labeling technique for simultaneous detection of microglia and AI. *Acta neuropathologica* **97**, 491-494 (1999).

18 Bye, N. *et al.* Transient neuroprotection by minocycline following traumatic brain injury is associated with attenuated microglial activation but no changes in cell apoptosis or neutrophil infiltration. *Experimental neurology* **204**, 220-233, doi:10.1016/j.expneurol.2006.10.013 (2007).

19 Aloisi, F. Immune function of microglia. *Glia* **36**, 165-179 (2001).

20 Czigner, A. *et al.* Kinetics of the cellular immune response following closed head injury. *Acta neurochirurgica* **149**, 281-289, doi:10.1007/s00701-006-1095-8 (2007).

21 Povlishock, J. T. & Becker, D. P. Fate of reactive axonal swellings induced by head injury. *Laboratory investigation; a journal of technical methods and pathology* **52**, 540-552 (1985).

22 Hansson, E. & Ronnback, L. Glial neuronal signaling in the central nervous system. *FASEB journal : official publication of the Federation of American Societies for Experimental Biology* **17**, 341-348, doi:10.1096/fj.02-0429rev (2003).

23 Bigler, E. D. Neuropsychological testing defines the neurobehavioral significance of neuroimaging-identified abnormalities. *Archives of clinical neuropsychology : the official journal of the National Academy of Neuropsychologists* **16**, 227-236 (2001).

24 Chen, Y. *et al.* Correlated memory defects and hippocampal dendritic spine loss after acute stress involve corticotropin-releasing hormone signaling. *Proceedings of the National Academy of Sciences of the United States of America* **107**, 13123-13128, doi:10.1073/pnas.1003825107 (2010).

25 Gao, X., Deng, P., Xu, Z. C. & Chen, J. Moderate traumatic brain injury causes acute dendritic and synaptic degeneration in the hippocampal dentate gyrus. *PloS one* **6**, e24566, doi:10.1371/journal.pone.0024566 (2011).

26 Martin, L., Latypova, X. & Terro, F. Post-translational modifications of tau protein: implications for Alzheimer's disease. *Neurochemistry international* **58**, 458-471, doi:10.1016/j.neuint.2010.12.023 (2011).

27 Ding, J. Y. *et al.* Synapse loss regulated by matrix metalloproteinases in traumatic brain injury is associated with hypoxia inducible factor-1alpha expression. *Brain research* **1268**, 125-134, doi:10.1016/j.brainres.2009.02.060 (2009).

28 Braak, H., Zetterberg, H., Del Tredici, K. & Blennow, K. Intraneuronal tau aggregation precedes diffuse plaque deposition, but amyloid-beta changes occur before increases of tau in cerebrospinal fluid. *Acta neuropathologica*, doi:10.1007/s00401-013-1139-0 (2013).

29 Braak, H., Alafuzoff, I., Arzberger, T., Kretzschmar, H. & Del Tredici, K. Staging of Alzheimer disease-associated neurofibrillary pathology using paraffin sections and immunocytochemistry. *Acta neuropathologica* **112**, 389-404, doi:10.1007/s00401-006-0127-z (2006).

30 Balogh, G. *et al.* Lipidomics reveals membrane lipid remodelling and release of potential lipid mediators during early stress responses in a murine melanoma cell line. *Biochimica et biophysica acta* **1801**, 1036-1047, doi:10.1016/j.bbalip.2010.04.011 (2010).

31 Ekroos, K., Janis, M., Tarasov, K., Hurme, R. & Laaksonen, R. Lipidomics: a tool for studies of atherosclerosis. *Current atherosclerosis reports* **12**, 273-281, doi:10.1007/s11883-010-0110-y (2010).

32 Pietilainen, K. H. *et al.* Acquired obesity is associated with changes in the serum lipidomic profile independent of genetic effects--a monozygotic twin study. *PloS one* **2**, e218, doi:10.1371/journal.pone.0000218 (2007).

33 Ji, J. *et al.* Lipidomics identifies cardiolipin oxidation as a mitochondrial target for redox therapy of brain injury. *Nature neuroscience* **15**, 1407-1413, doi:10.1038/nn.3195 (2012).

34 Xiong, Y., Mahmood, A. & Chopp, M. Animal models of traumatic brain injury. *Nature reviews. Neuroscience* **14**, 128-142, doi:10.1038/nrn3407 (2013).

35 Harrison, F. E., Hosseini, A. H. & McDonald, M. P. Endogenous anxiety and stress responses in water maze and Barnes maze spatial memory tasks. *Behavioural brain research* **198**, 247-251, doi:10.1016/j.bbr.2008.10.015 (2009).

36 Luna-Munoz, J., Chavez-Macias, L., Garcia-Sierra, F. & Mena, R. Earliest stages of tau conformational changes are related to the appearance of a sequence of specific phospho-dependent tau epitopes in Alzheimer's disease. *Journal of Alzheimer's disease : JAD* **12**, 365-375 (2007).

37 Augustinack, J. C., Schneider, A., Mandelkow, E. M. & Hyman, B. T. Specific tau phosphorylation sites correlate with severity of neuronal cytopathology in Alzheimer's disease. *Acta neuropathologica* **103**, 26-35 (2002).

38 Acker, C. M., Forest, S. K., Zinkowski, R., Davies, P. & d'Abramo, C. Sensitive quantitative assays for tau and phospho-tau in transgenic mouse models. *Neurobiology of aging* **34**, 338-350, doi:10.1016/j.neurobiolaging.2012.05.010 (2013).

39 Kar, S., Florence, G. J., Paterson, I. & Amos, L. A. Discodermolide interferes with the binding of tau protein to microtubules. *FEBS letters* **539**, 34-36 (2003).

40 Gustke, N., Trinczek, B., Biernat, J., Mandelkow, E. M. & Mandelkow, E. Domains of tau protein and interactions with microtubules. *Biochemistry* **33**, 9511-9522 (1994).

41 Goode, B. L. & Feinstein, S. C. Identification of a novel microtubule binding and assembly domain in the developmentally regulated inter-repeat region of tau. *The Journal of cell biology* **124**, 769-782 (1994).

42 Panda, D., Goode, B. L., Feinstein, S. C. & Wilson, L. Kinetic stabilization of microtubule dynamics at steady state by tau and microtubule-binding domains of tau. *Biochemistry* **34**, 11117-11127 (1995).

43 Brandt, R., Leger, J. & Lee, G. Interaction of tau with the neural plasma membrane mediated by tau's amino-terminal projection domain. *The Journal of cell biology* **131**, 1327-1340 (1995).

44 Fulga, T. A. *et al.* Abnormal bundling and accumulation of F-actin mediates tau-induced neuronal degeneration in vivo. *Nature cell biology* **9**, 139-148, doi:10.1038/ncb1528 (2007).

45 Omalu, B. *et al.* Chronic traumatic encephalopathy in an Iraqi war veteran with posttraumatic stress disorder who committed suicide. *Neurosurgical focus* **31**, E3, doi:10.3171/2011.9.FOCUS11178 (2011).

46 Rajput, A. *et al.* Parkinsonism, Lrrk2 G2019S, and tau neuropathology. *Neurology* **67**, 1506-1508, doi:10.1212/01.wnl.0000240220.33950.0c (2006).

47 Santpere, G. & Ferrer, I. Delineation of early changes in cases with progressive supranuclear palsy-like pathology. Astrocytes in striatum are primary targets of tau phosphorylation and GFAP oxidation. *Brain pathology* **19**, 177-187, doi:10.1111/j.1750-3639.2008.00173.x (2009).

48 Spillantini, M. G. & Goedert, M. Tau pathology and neurodegeneration. *Lancet neurology* **12**, 609-622, doi:10.1016/S1474-4422(13)70090-5 (2013).

49 Mazanetz, M. P. & Fischer, P. M. Untangling tau hyperphosphorylation in drug design for neurodegenerative diseases. *Nature reviews. Drug discovery* **6**, 464-479, doi:10.1038/nrd2111 (2007).

50 Braak, H. & Braak, E. Neuropathological stageing of Alzheimer-related changes. *Acta neuropathologica* **82**, 239-259 (1991).

51 Spillantini, M. G., Bird, T. D. & Ghetti, B. Frontotemporal dementia and Parkinsonism linked to chromosome 17: a new group of tauopathies. *Brain pathology* **8**, 387-402 (1998).

52 Spillantini, M. G. & Goedert, M. Tau protein pathology in neurodegenerative diseases. *Trends in neurosciences* **21**, 428-433 (1998).

53 Arendt, T. *et al.* Reversible paired helical filament-like phosphorylation of tau is an adaptive process associated with neuronal plasticity in hibernating animals. *The Journal of neuroscience : the official journal of the Society for Neuroscience* **23**, 6972-6981 (2003).

54 Planel, E. *et al.* Anesthesia leads to tau hyperphosphorylation through inhibition of phosphatase activity by hypothermia. *The Journal of neuroscience : the official journal of the Society for Neuroscience* **27**, 3090-3097, doi:10.1523/JNEUROSCI.4854-06.2007 (2007).

55 Brandt, R. The tau proteins in neuronal growth and development. *Frontiers in bioscience : a journal and virtual library* **1**, d118-130 (1996).

56 Elder, G. A. *et al.* Blast exposure induces post-traumatic stress disorder-related traits in a rat model of mild traumatic brain injury. *Journal of neurotrauma* **29**, 2564-2575, doi:10.1089/neu.2012.2510 (2012).

57 Lehman, E. J., Hein, M. J., Baron, S. L. & Gersic, C. M. Neurodegenerative causes of death among retired National Football League players. *Neurology*, doi:10.1212/WNL.0b013e31826daf50 (2012).

58 Hawkins, B. E. *et al.* Rapid accumulation of endogenous tau oligomers in a rat model of traumatic brain injury: possible link between traumatic brain injury and sporadic tauopathies. *The Journal of biological chemistry* **288**, 17042-17050, doi:10.1074/jbc.M113.472746 (2013).

59 Johnson, V. E., Stewart, W. & Smith, D. H. Traumatic brain injury and amyloid-beta pathology: a link to Alzheimer's disease? *Nature reviews. Neuroscience* **11**, 361-370, doi:10.1038/nrn2808 (2010).

60 Johnson, V. E., Stewart, W. & Smith, D. H. Widespread tau and amyloid-Beta pathology many years after a single traumatic brain injury in humans. *Brain pathology* **22**, 142-149, doi:10.1111/j.1750-3639.2011.00513.x (2012).

61 Mannix R, M. W., Mandeville J, Grant PE, et al. Clinical Correlates in an Experimental Model of Repetitive Mild Brain Injury. *Annals of neurology*, doi:doi: 10.1002/ana.23858 (2013).

62 Smith, C., Graham, D. I., Murray, L. S. & Nicoll, J. A. Tau immunohistochemistry in acute brain injury. *Neuropathology and applied neurobiology* **29**, 496-502 (2003).

63 Tran, H. T., LaFerla, F. M., Holtzman, D. M. & Brody, D. L. Controlled cortical impact traumatic brain injury in 3xTg-AD mice causes acute intra-axonal amyloid-beta accumulation and independently accelerates the development of tau abnormalities. *The Journal of neuroscience : the official journal of the Society for Neuroscience* **31**, 9513-9525, doi:10.1523/JNEUROSCI.0858-11.2011 (2011).

64 Tran, H. T., Sanchez, L., Esparza, T. J. & Brody, D. L. Distinct temporal and anatomical distributions of amyloid-beta and tau abnormalities following controlled cortical impact in transgenic mice. *PloS one* **6**, e25475, doi:10.1371/journal.pone.0025475 (2011).

65 Uryu, K. *et al.* Repetitive mild brain trauma accelerates Abeta deposition, lipid peroxidation, and cognitive impairment in a transgenic mouse model of Alzheimer amyloidosis. *The Journal of neuroscience : the official journal of the Society for Neuroscience* **22**, 446-454 (2002).

66 Yoshiyama, Y. *et al.* Enhanced neurofibrillary tangle formation, cerebral atrophy, and cognitive deficits induced by repetitive mild brain injury in a transgenic tauopathy mouse model. *Journal of neurotrauma* **22**, 1134-1141, doi:10.1089/neu.2005.22.1134 (2005).

67 Smith, D. H., Johnson, V. E. & Stewart, W. Chronic neuropathologies of single and repetitive TBI: substrates of dementia? *Nature reviews. Neurology*, doi:10.1038/nrneurol.2013.29 (2013).

68 Kane, M. J. *et al.* A mouse model of human repetitive mild traumatic brain injury. *Journal of neuroscience methods* **203**, 41-49, doi:10.1016/j.jneumeth.2011.09.003 (2012).

69 Laurer, H. L. *et al.* Mild head injury increasing the brain's vulnerability to a second concussive impact. *Journal of neurosurgery* **95**, 859-870, doi:10.3171/jns.2001.95.5.0859 (2001).

70 Meehan, W. P., 3rd, Zhang, J., Mannix, R. & Whalen, M. J. Increasing recovery time between injuries improves cognitive outcome after repetitive mild concussive brain injuries in mice. *Neurosurgery* **71**, 885-891, doi:10.1227/NEU.0b013e318265a439 (2012).

71 Shitaka, Y. *et al.* Repetitive closed-skull traumatic brain injury in mice causes persistent multifocal axonal injury and microglial reactivity. *Journal of neuropathology and experimental neurology* **70**, 551-567, doi:10.1097/NEN.0b013e31821f891f (2011).

72 Andorfer, C. *et al.* Hyperphosphorylation and aggregation of tau in mice expressing normal human tau isoforms. *Journal of neurochemistry* **86**, 582-590 (2003).

73 Thompson, H. J. *et al.* Lateral fluid percussion brain injury: a 15-year review and evaluation. *Journal of neurotrauma* **22**, 42-75, doi:10.1089/neu.2005.22.42 (2005).

74 Duff, K. *et al.* Characterization of pathology in transgenic mice over-expressing human genomic and cDNA tau transgenes. *Neurobiology of disease* **7**, 87-98, doi:10.1006/nbdi.1999.0279 (2000).

75 Irene Litvan (Editor), Y. A. F. b. & Atypical Parkinsonian Disorders: Clinical and Research Aspects / Edition 1 *Springer-Verlag New York, LLC* (2005).

76 Lewis, J. *et al.* Neurofibrillary tangles, amyotrophy and progressive motor disturbance in mice expressing mutant (P301L) tau protein. *Nature genetics* **25**, 402-405, doi:10.1038/78078 (2000).

77 Greenberg, S. G., Davies, P., Schein, J. D. & Binder, L. I. Hydrofluoric acid-treated tau PHF proteins display the same biochemical properties as normal tau. *The Journal of biological chemistry* **267**, 564-569 (1992).

78 Otvos, L., Jr. *et al.* Monoclonal antibody PHF-1 recognizes tau protein phosphorylated at serine residues 396 and 404. *Journal of neuroscience research* **39**, 669-673, doi:10.1002/jnr.490390607 (1994).

79 Vingtdeux, V., Davies, P., Dickson, D. W. & Marambaud, P. AMPK is abnormally activated in tangle- and pre-tangle-bearing neurons in Alzheimer's disease and other tauopathies. *Acta neuropathologica* **121**, 337-349, doi:10.1007/s00401-010-0759-x (2011).

80 Jicha, G. A., O'Donnell, A., Weaver, C., Angeletti, R. & Davies, P. Hierarchical phosphorylation of recombinant tau by the paired-helical filament-associated protein kinase is dependent on cyclic AMP-dependent protein kinase. *Journal of neurochemistry* **72**, 214-224 (1999).

81 Alder, J., Fujioka, W., Lifshitz, J., Crockett, D. P. & Thakker-Varia, S. Lateral fluid percussion: model of traumatic brain injury in mice. *Journal of visualized experiments : JoVE*, doi:10.3791/3063 (2011).

82 Kimura, T. *et al.* Sequential changes of tau-site-specific phosphorylation during development of paired helical filaments. *Dementia* **7**, 177-181 (1996).

83 Hylin, M. J. *et al.* Repeated mild closed head injury impairs short-term visuospatial memory and complex learning. *Journal of neurotrauma*, doi:10.1089/neu.2012.2717 (2013).

84 Mouzon, B. C. *et al.* Repetitive mild traumatic brain injury in a mouse model produces learning and memory deficits accompanied by histological changes. *Journal of neurotrauma*, doi:10.1089/neu.2012.2498 (2012).

85 Hazrati, L. N. *et al.* Absence of chronic traumatic encephalopathy in retired football players with multiple concussions and neurological symptomatology. *Frontiers in human neuroscience* **7**, 222, doi:10.3389/fnhum.2013.00222 (2013).

86 Omalu, B. I. *et al.* Chronic traumatic encephalopathy in a National Football League player. *Neurosurgery* **57**, 128-134; discussion 128-134 (2005).

87 Omalu, B. I., Fitzsimmons, R. P., Hammers, J. & Bailes, J. Chronic traumatic encephalopathy in a professional American wrestler. *Journal of forensic nursing* **6**, 130-136, doi:10.1111/j.1939-3938.2010.01078.x (2010).

88 Omalu, B. I., Hamilton, R. L., Kamboh, M. I., DeKosky, S. T. & Bailes, J. Chronic traumatic encephalopathy (CTE) in a National Football League Player: Case report and emerging medicolegal practice questions. *Journal of forensic nursing* **6**, 40-46, doi:10.1111/j.1939-3938.2009.01064.x (2010).

89 DeKosky, S. T., Ikonomovic, M. D. & Gandy, S. Traumatic brain injury--football, warfare, and long-term effects. *The New England journal of medicine* **363**, 1293-1296, doi:10.1056/NEJMp1007051 (2010).

90 Ojo, J. O. *et al.* Repetitive mild traumatic brain injury augments tau pathology and glial activation in aged hTau mice. *Journal of neuropathology and experimental neurology* **72**, 137-151, doi:10.1097/NEN.0b013e3182814cdf (2013).

91 DeKosky, S. T., Blennow, K., Ikonomovic, M. D. & Gandy, S. Acute and chronic traumatic encephalopathies: pathogenesis and biomarkers. *Nature reviews. Neurology* **9**, 192-200, doi:10.1038/nrneurol.2013.36 (2013).

92 Small, G. W. *et al.* PET Scanning of Brain Tau in Retired National Football League Players: Preliminary Findings. *The American journal of geriatric psychiatry : official journal of the American Association for Geriatric Psychiatry* **21**, 138-144, doi:10.1016/j.jagp.2012.11.019 (2013).

93 Zetterberg, H. *et al.* Neurochemical aftermath of amateur boxing. *Archives of neurology* **63**, 1277-1280, doi:10.1001/archneur.63.9.1277 (2006).

94 Ost, M. *et al.* Initial CSF total tau correlates with 1-year outcome in patients with traumatic brain injury. *Neurology* **67**, 1600-1604, doi:10.1212/01.wnl.0000242732.06714.0f (2006).

95 Brunnstrom, H., Hansson, O., Zetterberg, H., Londos, E. & Englund, E. Correlations of CSF tau and amyloid levels with Alzheimer pathology in neuropathologically verified dementia with Lewy bodies. *International journal of geriatric psychiatry* **28**, 738-744, doi:10.1002/gps.3881 (2013).

96 Ertekin-Taner, N. Alzheimer disease: The quest for Alzheimer disease genes-focus on CSF tau. *Nature reviews. Neurology* **9**, 368-370, doi:10.1038/nrneurol.2013.117 (2013).

97 Schoonenboom, N. S. *et al.* Amyloid beta(1-42) and phosphorylated tau in CSF as markers for early-onset Alzheimer disease. *Neurology* **62**, 1580-1584 (2004).

98 Yoshiyama, Y. *et al.* Synapse loss and microglial activation precede tangles in a P301S tauopathy mouse model. *Neuron* **53**, 337-351, doi:10.1016/j.neuron.2007.01.010 (2007).

99 Zhong, Q., Congdon, E. E., Nagaraja, H. N. & Kuret, J. Tau isoform composition influences rate and extent of filament formation. *The Journal of biological chemistry* **287**, 20711-20719, doi:10.1074/jbc.M112.364067 (2012).

100 Schneider, A., Biernat, J., von Bergen, M., Mandelkow, E. & Mandelkow, E. M. Phosphorylation that detaches tau protein from microtubules (Ser262, Ser214) also protects it against aggregation into Alzheimer paired helical filaments. *Biochemistry* **38**, 3549-3558, doi:10.1021/bi981874p (1999).

101 Arendt, T. & Bullmann, T. Neuronal plasticity in hibernation and the role of the microtubule-associated protein tau as a 'master switch' regulating synaptic gain in neuronal networks. *American journal of physiology. Regulatory, integrative and comparative physiology*, doi:10.1152/ajpregu.00117.2013 (2013).

102 Dave, K. R., Christian, S. L., Perez-Pinzon, M. A. & Drew, K. L. Neuroprotection: lessons from hibernators. *Comparative biochemistry and physiology. Part B, Biochemistry & molecular biology* **162**, 1-9, doi:10.1016/j.cbpb.2012.01.008 (2012).

103 Run, X. *et al.* Anesthesia induces phosphorylation of tau. *Journal of Alzheimer's disease : JAD* **16**, 619-626, doi:10.3233/JAD-2009-1003 (2009).

104 Whittington, R. A., Bretteville, A., Dickler, M. F. & Planel, E. Anesthesia and tau pathology. *Progress in neuro-psychopharmacology & biological psychiatry*, doi:10.1016/j.pnpbp.2013.03.004 (2013).

105 Statler, K. D. *et al.* Comparison of seven anesthetic agents on outcome after experimental traumatic brain injury in adult, male rats. *Journal of neurotrauma* **23**, 97-108, doi:10.1089/neu.2006.23.97 (2006).

106 Corsellis, J. A., Bruton, C. J. & Freeman-Browne, D. The aftermath of boxing. *Psychological medicine* **3**, 270-303 (1973).

107 Grahmann, H. & Ule, G. [Diagnosis of chronic cerebral symptoms in boxers (dementia pugilistica & traumatic encephalopathy of boxers)]. *Psychiatria et neurologia* **134**, 261-283 (1957).

108 Hall, R. C., Hall, R. C. & Chapman, M. J. Definition, diagnosis, and forensic implications of postconcussional syndrome. *Psychosomatics* **46**, 195-202, doi:10.1176/appi.psy.46.3.195 (2005).

Chapter 5

5. General discussion

5.1. Overview of the current studies:

1. We developed a simple and reproducible mouse model of mTBI, which induces histopathological changes consistent with other animal models of brain trauma and learning/memory problems comparable to those observed in the human condition[1-4].
2. Animals exposed to a s-mTBI had learning impairments without exhibiting spatial memory retention deficits when compared to their sham controls at 6, 12 and 18 months post-injury.
3. Animals exposed to s-mTBI had transient behavioral impairment, diffuse astrogliosis, neuroinflammation, and axonal damage, whereas r-mTBI results in more significant behavioral deficits and pathological abnormalities.
4. Animals exposed to r-mTBI displayed persistent cognitive deficits, a slower rate of learning and progressive behavioral impairment over time. These deficits arise in parallel with a number of neuropathological abnormalities, including progressive neuroinflammation and continuing white matter degradation up to 12 months following repetitive injury.
5. Neither single nor r-mTBI was associated with elevated brain levels of amyloid beta or abnormal tau phosphorylation at 6 or 12 months post injury.
6. These data provide the first evidence that, whilst an s-mTBI produces neurobehavioral changes and pathology between acute and 6 months post injury, these changes appeared to be static for the 6 and 12 months period post injury.

7. r-mTBI produces behavioral and pathological changes which continue to evolve many months post injury.
8. These findings recapitulate important aspects of human long term TBI sequelae, in particular persistent neuroinflammation, white matter injury, and axonal pathology in the corpus callosum[3,5-9].
9. However, we did not observe the tau pathology which has been the focus of such debate in human TBI cases, particularly in the high profile chronic traumatic encephalpathy (CTE) cases which have been reported primarily in the US.
10. The hTau transgenic mice developed acute pathology (APP axonal profiles, microgliosis, astrogliosis) leading to neurocognitive impairments in a manner similar to our observations following mTBI in wild-type mice[10].

5.2. Implications:

As mild brain injury or concussion does not typically result in death in humans, it is difficult to identify and study the pathological mechanisms of concussion at acute time points in humans. Thus, our current understanding of the consequences of mild brain injury comes almost exclusively from autopsied brains of individuals (typically athletes or military personnel) known to have a history of repeated head injuries. In many of these cases the clinical presentation included failing memory, depression and impulse control problems. In addition, the majority of these brains come from middle-aged patients and therefore the observed pathology does not as clearly represent the consequences of TBI as the effects of age can themselves be a confounding factor but can also present new variables such as genetic influences on long term outcome, the effects of other comorbid conditions, and/or chronic

effects of consumption of substances of abuse. Thus, the establishment of a representative animal model of mTBI in Chapter 2 holds important implications in studying acute histopathological sequelae after single and r-mTBI as human pathological samples are lacking at such short time points post injury.

Our results provided pathological and behavioral evidence that our model of mTBI is particularly suitable to study the effect of both single and multiple injuries as it reproduces traits of human mTBI. In this regard, our model is superior to models of mTBI that subject the animal to some degree of head surgery which results in various level of cranial disturbance[11] (e.g. CCI, FPI). In addition to allowing administration of more than two mTBI, the required time under anesthesia is minimal and thus clinically relevant. The EM coil-based device also delivers reproducible velocities without the need for frequent calibration while reducing the chance of a rebound that can occur with the weight drop head injury model[11,12].

Therefore, we decided to us this model to examine the long-term sequelae following injury. Cause and effect relationships for the delayed sequelae of single and r-mTBI are not well understood, an animal model that translates to the human condition would improve our understanding of the evolution of mTBI pathology that occurs prior to the appearance of neurological and neuropathological dysfunction. The fact that our model of single and r-mTBI induced axonal injury within hours, inflammation and astrogliosis within days, and behavioral impairments within a week, supports evidence that single and multiple concussion can contribute to subsequent and immediate neurological disturbances.

The first study could be an important tool used for medical counseling of patients who have suffered concussions. This study concludes safety guidance should be issued for high risk

groups such as children involved in sports, professional athletes and military personnel. Because neurological disturbances can occur so rapidly, new rules regarding the period of recovery should be implemented, especially after sports injury. Athletes have a high risk for further exposure to trauma which most likely would result in exacerbated deficits as our r-mTBI data indicates. For example, students' academic performance depends largely on memory and processing speed; academic accommodation should be considered until the injured scholar is able to fully recover from the trauma.

The results in Chapter 3 present evidence that animals exposed to multiple injuries have sustained inflammation at 6 months post injury while the singly injured mice recover over the same period of time as s-mTBI mice have the same level of inflammation as their respective shams at 6 months post-injury. This may indicate that the individuals exposed to r-mTBI may have an elevated level of brain inflammation that does not subside with time, even if no additional trauma occurs. While no markers of inflammation were observed at 6 months post s-mTBI, at 12 months post injury, we observed a gradual increase in astrogliosis and inflammation in both the single and r-mTBI groups. While both injured groups had increased inflammation at 12 months post-injury, the r-mTBI group showed more intense pathology. This supports the current hypothesis that a history of mTBI could exacerbate the onset of brain inflammation that typically occurs with aging and is known to play a role in neurodegenerative disease. Further studies are clearly needed to confirm these observations, but this avenue could open the door for potential treatments targeting inflammation in the mTBI brain. The chronic inflammation observed over the many months following repetitive injury suggest that although early treatments for TBI patients (regardless of the injury severity) can minimize

further damage, our data suggests that a chronic treatment paradigm may also be needed to mitigate the long term consequences of repetitive brain injury. Overall, our mouse model of head injury provides a platform for future studies that will have important implications in identifying molecular targets and testing therapeutic agents to alleviate the early and long term brain damage induced by mTBI.

In chapter 4 the short-term behavioral and pathological changes after a single and r-mTBI in hTau mice were consistent with those we observed in wild type mice. This may suggest that inflammation and axonal injury, rather than tau pathophysiology, play a significant role in the early events after single or r-mTBI and better correlate with the acute behavioral changes post-injury. The question of whether tau pathology may gradually appear over the days or months post injury remains to be addressed.

Taken together, the findings from these studies support the hypothesis that mTBI should be regarded as a chronic disease, not a one-time event. This concept holds important implications for the management and treatment of traumatic brain injury in humans as it often does not clinically present in the immediate aftermath of trauma, but rather months, or even years, post injury[7,9,13-16].

5.3. Ongoing work:

5.3.1. Characterization of our model of head injury at 24 months post injury:

The findings in Chapter 3 are key to understanding the evolution over time of a single and r-mTBI. However, the late life consequences of single and r-mTBI are still lacking as laboratory wild-type mice typically live only 2 to 3 years, and to our knowledge, this is the only study to

examine such extended time points in an experimental model of head injury. As such, this study also provides an opportunity to evaluate mTBI coupled with the effects of aging as there is no information in animal or human autopsied brain on the impact of mTBI in the context of aging. Accordingly, the same cohort of mice in which we performed neurobehavioral testing at 24h, 6, 12, 18 months post mTBI was tested for subsequent neurobehavioral impairments. When we designed this study we received skepticism over the fact that many mice might die before reaching this final time point for the study, but as expected based on the average life expectancy of mice in our vivarium, and the deliberately mild nature of the inflicted injury, only 3 mice died (2 r-sham and 1 s-sham).

The remaining cohort of mice were thus tested for the 5th time in the Barnes Maze at 24 months after injury/anesthesia, and were then euthanized for neuropathological and biochemical analyses (ongoing). The cohort was then separated for further ongoing pathological and biochemical analysis. Other parts of the central nervous system (spinal column, optic nerve) were also collected and fixed for further pathological examination. As observed at 18 months post injury the r-mTBI group had strong cognitive and learning impairment. In fact this last time point confirmed the trend observed at 18 months post injury where injured groups plateau and revealed the expected progressive decline in the sham group as they aged. Additionally, cerebral blood flow was also measured prior to euthanatization as the association of cerebral hypoperfusion and TBI is well established[17,18]. Cerebral blood flow analysis of this cohort (24 months post mTBI) illustrates a decrease of blood flow of about 10% in r-mTBI mice, however these results were not statistically significant, when compared to the

r-sham. As this line of investigation is currently lacking in the field, examination of the blood brain barrier and the cerebrovasculature following brain trauma is necessary.

5.3.2. Chronic consequences of single and repetitive mTBI in hTau mice:

Although we do not intend to follow a cohort of hTau mice to the same extensive timepoints that we have for wild type mice, we have 36 male hTau mice which were subjected to the same injury/sham paradigms as the wild type mice (s-sham, s-mTBI, r-sham, r-mTBI, N=9/group) that have now been aged to 12 months post mTBI/anesthesia. As described in Chapter 4, sub-optimal breeding with the hTau mice has necessitated our use of smaller numbers of mice per study group. Preliminary analysis in the Barnes maze reveals age and time dependent spatial learning deficits in the r-mTBI group compared to r-sham animals. Moreover, the hTau mice presented a trend for worse learning and spatial deficits when compared with the wild type cohort at 12 months post injury, as indicated by their impaired performance. While no pathological analyses have yet been carried out, the soluble fraction of the hTau brain homogenate is ongoing. Preliminary results revealed no changes overall in the soluble fraction, but a trend for an increase of tau aggregate in the injured group at 12 months post injury. Because of the high degree of variation of tau levels in these mice, further analyses are needed to fully interpret these data. We are currently characterizing and measuring the amount of total and phospho-tau in the insoluble fraction as well as its associated pathology. These preliminary data suggest that r-mTBI produce long term deficits in learning and cognitive function independent of tau accumulation in the soluble fraction of the brain homogenate.

5.4. Future studies:

The findings described in this thesis will be extended to investigate the mechanisms driving other cognitive/behavioral alterations associated with TBI. For example, mTBI can increase the risk of post-traumatic stress disorder (PTSD), an anxiety disorder caused by a violent/traumatic event. PTSD and TBI often coexist because brain injuries are often sustained in traumatic experiences. To further understand and untangle the specific changes in PTSD's brain diagnosed patients, we are using our r-mTBI model to investigate how a stressful event at the time of injury could lead to PTSD.

Lipid metabolism and oxidation in TBI are of particular interest due their high concentration in the CNS and the chronic changes (inflammation, cell loss) observed in the major white matter tracks of the injured animals. We aim to use mass-spectrometry-based lipidomic platforms to identify and isolate a few lipid molecules out off hundreds lipid species as biomarkers for diagnosis of mTBI. Lipidomics has been demonstrated to be a useful tool in the study of mechanisms and biomarkers in many diseases such as cancer[19], atherosclerosis[20] and obesity[21] and thus could become a powerful tool to diagnose and scale the injury status of a patient.

Identification of an effective treatment for TBI is a major challenge for the neuroscience research community as all clinical trials evaluating potentially neuroprotective compounds have failed in demonstrating clinical efficacy. These disappointing results may be due to the fact that most therapeutic strategies target a single pathophysiological mechanism despite the fact that many mechanisms are involved in secondary injury after mTBI. Testing multifunctional therapies is now considered an important research direction in animal models of TBI. Previous

studies in animals have provided a proof-of-principle for improvement of functional recovery at an acute time point after cortical injury but this effect failed to be translated clinically. We are currently tackling the problem with a different approach by focusing our treatment not only on the acute effect of mTBI but on a delayed neurorestorative treatment that would reduce the chronic inflammation cause by the injury observed in our mouse model. If correct, this approach could spark a new treatment strategy, one in which TBI patients must be treated not only for their primary injury but also for the long-term consequences that may last for years resulting from secondary injuries. The last major barrier of the translational gap between human and rodent model would be narrowed if the use of higher species with brains that are more anatomically and functionally closer to human were further developed. While we can't recapitulate all aspects of a human TBI in a mouse, we can identify and screen potentially relevant molecular mechanisms without the cost and ethical hurdles that comes with research using higher order species.

In addition, more research should explore different injury paradigms. As it is not unusual for athletes to experience more than five concussions in a career[22,23], studies that incorporate a greater frequency of mTBI over longer period of time would better replicate the pathology observed in CTE patients. This area has, for the most part, been ignored by the research and medical communities until recently. There is no good way to assess when a brain is moderately injured, nor do we understand how the brain heals. Accordingly, further animal models should include additional variables such as the number, the severity and the frequency of mTBI to accomplish a better translation between animal experiments and the heterogeneity of human mTBI. The identification of common mechanisms of TBI sequelae across a wide range of

laboratory models may represent our best hope of identifying therapeutics for broad application in the TBI patient population. Finally, further studies are needed to determine the relevance of mTBI to the future development of neurodegenerative disease.

5.5. Conclusions:

The work presented in this thesis has three key components: 1) the development and characterization of an animal model of mTBI, 2) the identification of sustained white matter inflammation and axonal damage after repeated mTBI, 3) tau hyperphosphorylation appears to have a contributory, but not primary role in the acute phase post-injury.

The results described in this thesis characterize both acute and long term (24 month) consequences of single and repetitive injury. This work represents a unique and critical contribution to the TBI research field, as until now, the majority of the TBI research has focused on the acute consequences of TBI, and until very recently neither mild nor repetitive injury was a focus. Major research and clinical efforts should emphasize the long term consequences of TBI and the development of reliable biomarkers for single and repetitive mTBI. TBI is not typically a single event from which we recover, but if untreated, can be the beginning of a series of events that we may have to deal with for years. In other words, this suggests that while early intervention (e.g. surgery, drug therapy) is the most desirable approach, there is a large therapeutic window in which interventions may prove efficacious. However, our data also suggest that the time post-injury may dictate the type of therapy that is needed for the greatest effect. As pointed out in this thesis, our results provide the first evidence that, whilst an s-mTBI produces transient neurobehavioral changes and pathology which remains static in the period following injury, r-mTBI produces behavioral and pathological changes which continue to

evolve many months post injury. These findings collectively recapitulate important aspects of human long term TBI sequelae, in particular persistent neuroinflammation, white matter injury, and axonal pathology in the corpus callosum[7,16]. The relationships between the history of mTBI(s) and the progressive neuroinflammation are likely to be complex and warrant further work to elucidate their association with neurodegenerative disease. Although tau is clearly a component of CTE, not everyone who has tau pathology has CTE[24]. Indeed, owing to the lack of large-scale controlled studies, there are also no compelling epidemiological data currently available to estimate the incidence or prevalence of CTE after r-mTBI. Long-term follow-up of multiple cohorts of individuals, such as American football players and soldiers, with consideration of the influence of risk factors such as mechanism, frequency and severity of injury, gender, life style and potential genetic predisposition is required to clearly define CTE as a disease entity both pathologically and clinically. Experimental TBI models like the one presented in this thesis should facilitate elucidation of the cellular and molecular changes underlying these phenomena. Translation from these preclinical studies to clinical application in human TBI populations will result in effective treatment for TBI and its chronic neurodegenerative sequelae.

5.6. References:

1 Guskiewicz, K. M. *et al.* Association between recurrent concussion and late-life cognitive impairment in retired professional football players. *Neurosurgery* **57**, 719-726; discussion 719-726 (2005).

2 Kinnunen, K. M. *et al.* White matter damage and cognitive impairment after traumatic brain injury. *Brain : a journal of neurology* **134**, 449-463, doi:10.1093/brain/awq347 (2011).

3 Weber, J. T. Experimental models of repetitive brain injuries. *Progress in brain research* **161**, 253-261, doi:10.1016/S0079-6123(06)61018-2 (2007).

4 Ozen, L. J. & Fernandes, M. A. Slowing down after a mild traumatic brain injury: a strategy to improve cognitive task performance? *Archives of clinical neuropsychology : the official journal of the National Academy of Neuropsychologists* **27**, 85-100, doi:10.1093/arclin/acr087 (2012).

5 Kraus, M. F. *et al.* White matter integrity and cognition in chronic traumatic brain injury: a diffusion tensor imaging study. *Brain : a journal of neurology* **130**, 2508-2519, doi:10.1093/brain/awm216 (2007).

6 McKee, A. C. *et al.* Chronic traumatic encephalopathy in athletes: progressive tauopathy after repetitive head injury. *Journal of neuropathology and experimental neurology* **68**, 709-735, doi:10.1097/NEN.0b013e3181a9d503 (2009).

7 McKee, A. C. *et al.* The spectrum of disease in chronic traumatic encephalopathy. *Brain : a journal of neurology* **136**, 43-64, doi:10.1093/brain/aws307 (2013).

8 Elder, G. A. *et al.* Blast exposure induces post-traumatic stress disorder-related traits in a rat model of mild traumatic brain injury. *Journal of neurotrauma* **29**, 2564-2575, doi:10.1089/neu.2012.2510 (2012).

9 Sosa, M. A. *et al.* Blast overpressure induces shear-related injuries in the brain of rats exposed to a mild traumatic brain injury. *Acta Neuropathologica Communications* **1**, 51 (2013).

10 Mouzon, B. C. *et al.* Repetitive mild traumatic brain injury in a mouse model produces learning and memory deficits accompanied by histological changes. *Journal of neurotrauma*, doi:10.1089/neu.2012.2498 (2012).

11 Xiong, Y., Mahmood, A. & Chopp, M. Animal models of traumatic brain injury. *Nature reviews. Neuroscience* **14**, 128-142, doi:10.1038/nrn3407 (2013).

12 Kane, M. J. *et al.* A mouse model of human repetitive mild traumatic brain injury. *Journal of neuroscience methods* **203**, 41-49, doi:10.1016/j.jneumeth.2011.09.003 (2012).

13 Johnson, V. E. *et al.* Inflammation and white matter degeneration persist for years after a single traumatic brain injury. *Brain : a journal of neurology* **136**, 28-42, doi:10.1093/brain/aws322 (2013).

14 Johnson, V. E., Stewart, W. & Smith, D. H. Traumatic brain injury and amyloid-beta pathology: a link to Alzheimer's disease? *Nature reviews. Neuroscience* **11**, 361-370, doi:10.1038/nrn2808 (2010).

15 Johnson, V. E., Stewart, W. & Smith, D. H. Widespread tau and amyloid-Beta pathology many years after a single traumatic brain injury in humans. *Brain pathology* **22**, 142-149, doi:10.1111/j.1750-3639.2011.00513.x (2012).

16 Smith, D. H., Johnson, V. E. & Stewart, W. Chronic neuropathologies of single and repetitive TBI: substrates of dementia? *Nature reviews. Neurology*, doi:10.1038/nrneurol.2013.29 (2013).

17 DeWitt, D. S. & Prough, D. S. Traumatic cerebral vascular injury: the effects of concussive brain injury on the cerebral vasculature. *Journal of neurotrauma* **20**, 795-825, doi:10.1089/089771503322385755 (2003).

18 Golding, E. M., Robertson, C. S. & Bryan, R. M., Jr. The consequences of traumatic brain injury on cerebral blood flow and autoregulation: a review. *Clinical and experimental hypertension* **21**, 299-332 (1999).

19 Balogh, G. *et al.* Lipidomics reveals membrane lipid remodelling and release of potential lipid mediators during early stress responses in a murine melanoma cell line. *Biochimica et biophysica acta* **1801**, 1036-1047, doi:10.1016/j.bbalip.2010.04.011 (2010).

20 Ekroos, K., Janis, M., Tarasov, K., Hurme, R. & Laaksonen, R. Lipidomics: a tool for studies of atherosclerosis. *Current atherosclerosis reports* **12**, 273-281, doi:10.1007/s11883-010-0110-y (2010).

21 Pietilainen, K. H. *et al.* Acquired obesity is associated with changes in the serum lipidomic profile independent of genetic effects--a monozygotic twin study. *PloS one* **2**, e218, doi:10.1371/journal.pone.0000218 (2007).

22 Maroon, J. C. & Bost, J. Concussion management at the NFL, college, high school, and youth sports levels. *Clinical neurosurgery* **58**, 51-56 (2011).

23 Pellman, E. J., Lovell, M. R., Viano, D. C. & Casson, I. R. Concussion in professional football: recovery of NFL and high school athletes assessed by computerized neuropsychological testing--Part 12. *Neurosurgery* **58**, 263-274; discussion 263-274, doi:10.1227/01.NEU.0000200272.56192.62 (2006).

24 Hazrati, L. N. *et al.* Absence of chronic traumatic encephalopathy in retired football players with multiple concussions and neurological symptomatology. *Frontiers in human neuroscience* **7**, 222, doi:10.3389/fnhum.2013.00222 (2013).

Appendix 1: Trace of Barnes maze performance in wild type animals.

Trace of Barnes maze performance 2 weeks post injury

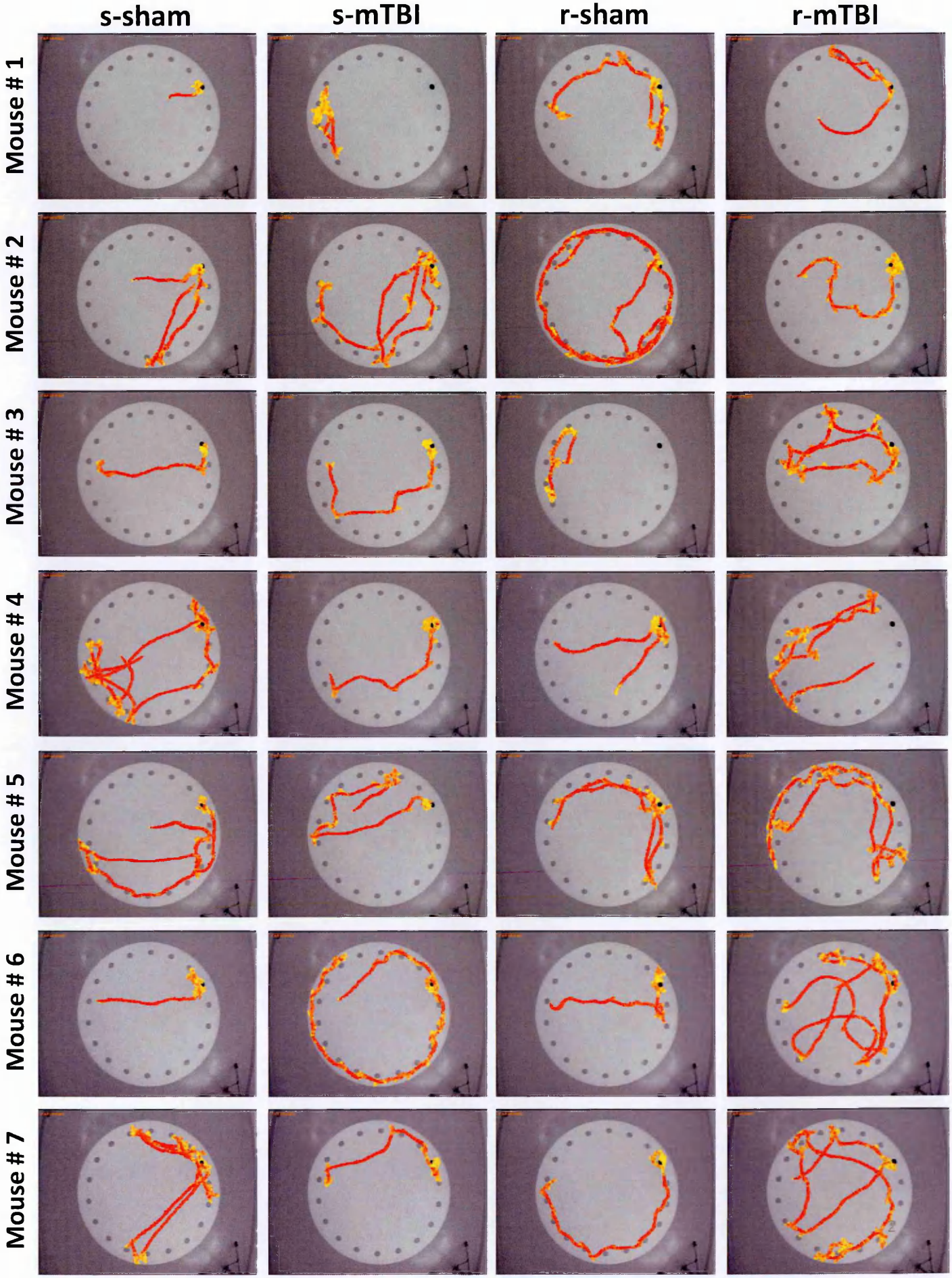

Trace of Barnes maze performance 2 weeks post injury

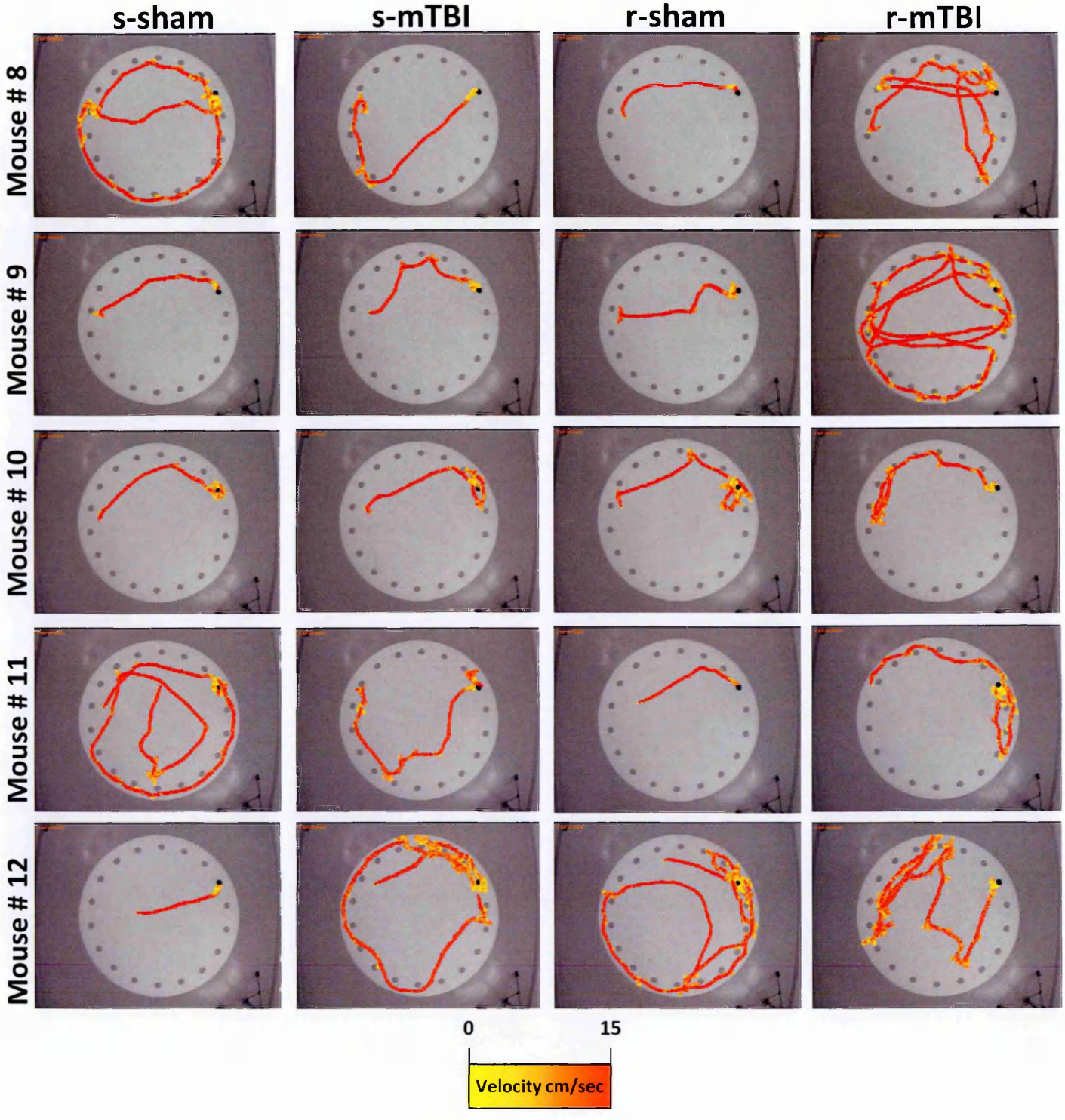

Traces of Barnes maze performance from each wild type animal in each group during the last day of acquisition starting on the west side of the table. Only 1 of the 4 starting points (East, West, North, South) is represented. The path of the mice until their escape into the target hole (arrow head) or the end of the 90 sec trial is represented by a gradient color line. The gradient color line indicates the velocity (cm/sec) of the tested animal. A yellow line indicate a mice travelling at a slow velocity (0-5m/sec), orange at a medium velocity (5-10 m/sec) or red at a high velocity (10-15m/sec).

Trace of Barnes maze performance at 6 months post injury

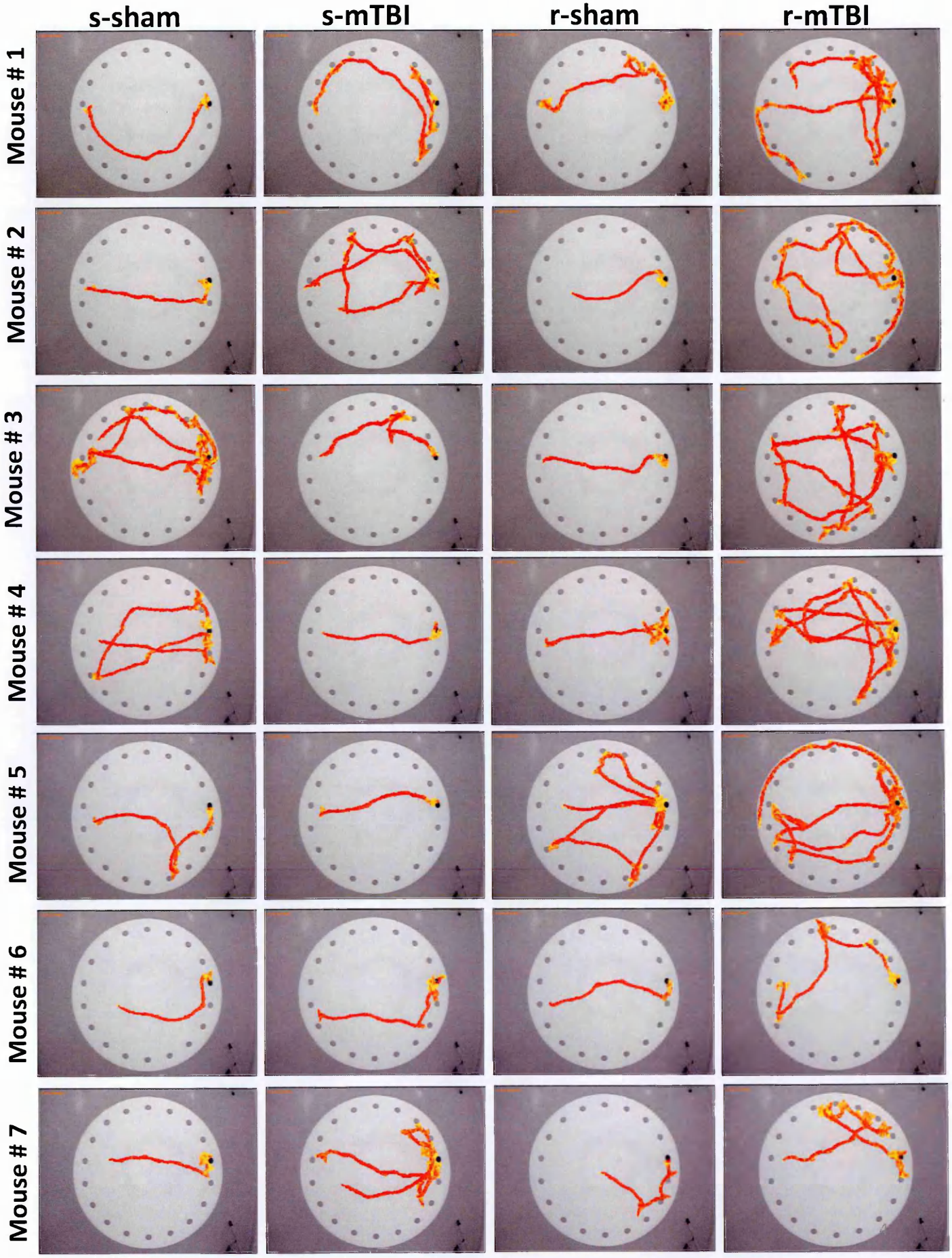

Trace of Barnes maze performance 6 months post injury

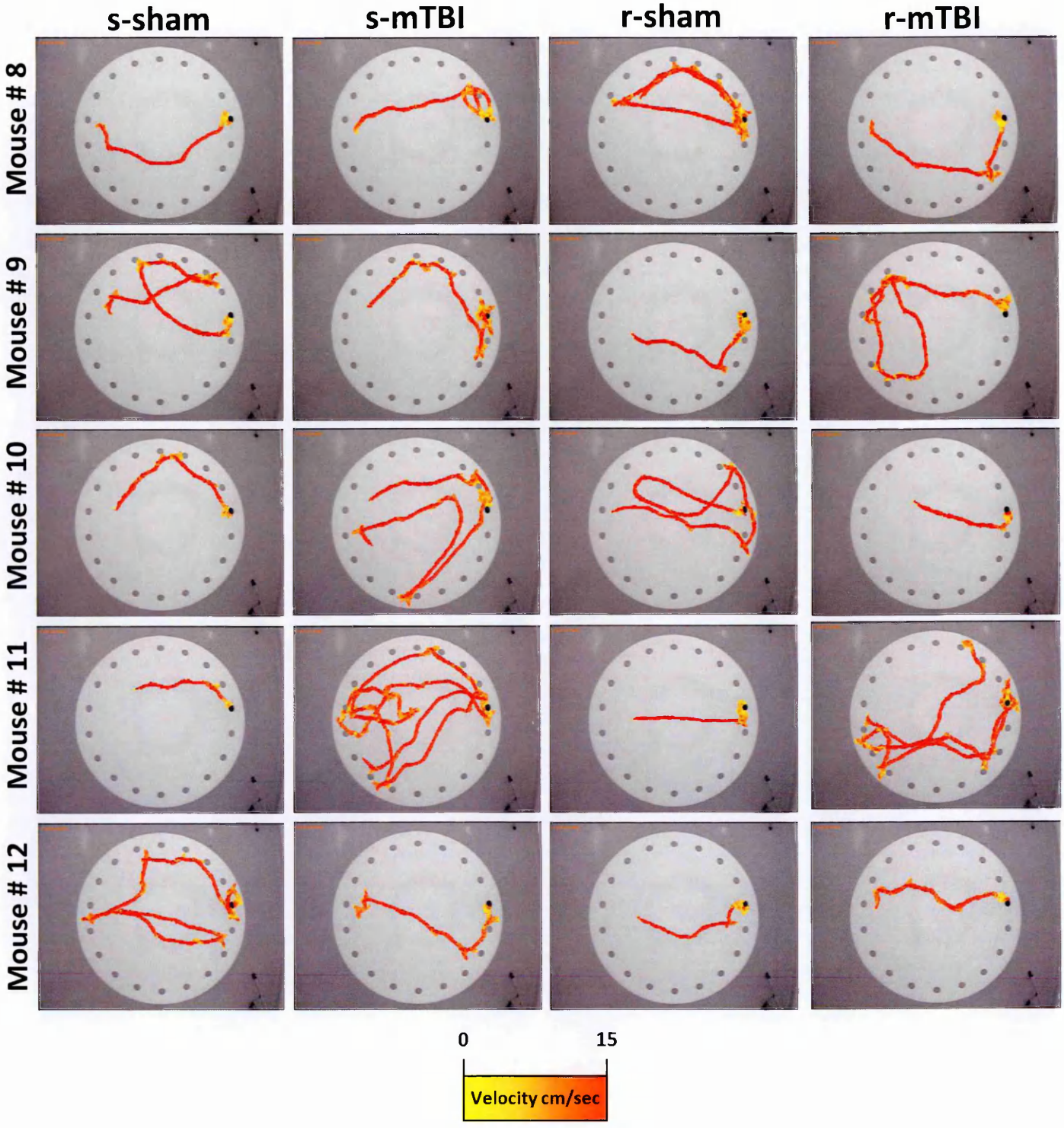

Traces of Barnes maze performance from each wild type animal in each group during the last day of acquisition starting on the west side of the table. Only 1 of the 4 starting points (East, West, North, South) is represented. The path of the mice until their escape into the target hole (arrow head) or the end of the 90 sec trial is represented by a gradient color line. The gradient color line indicates the velocity (cm/sec) of the tested animal. A yellow line indicate a mice travelling at a slow velocity (0-5m/sec), orange at a medium velocity (5-10 m/sec) or red at a high velocity (10-15m/sec).

Trace of Barnes maze performance 12 months post injury

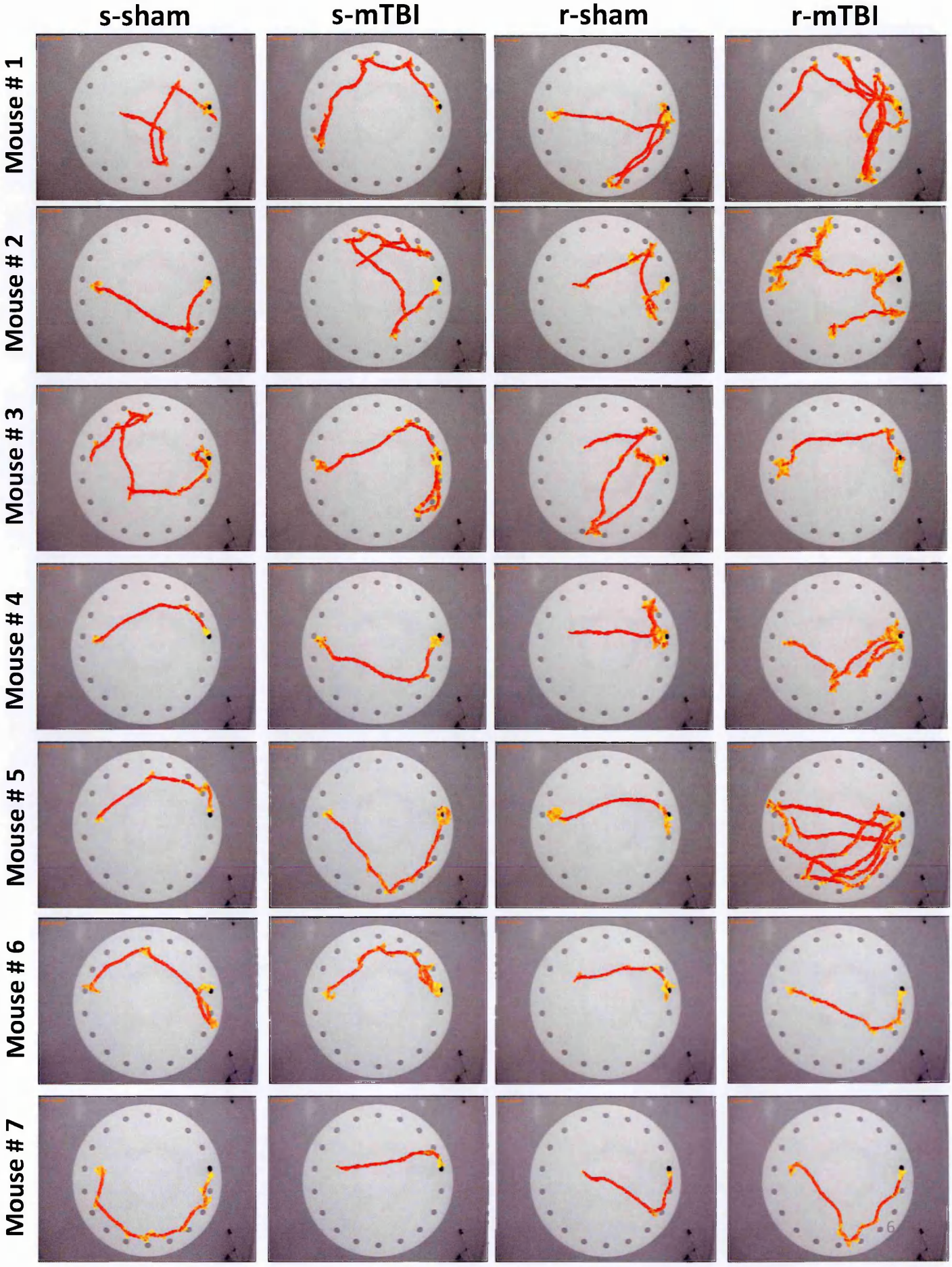

Trace of Barnes maze performance 12 months post injury

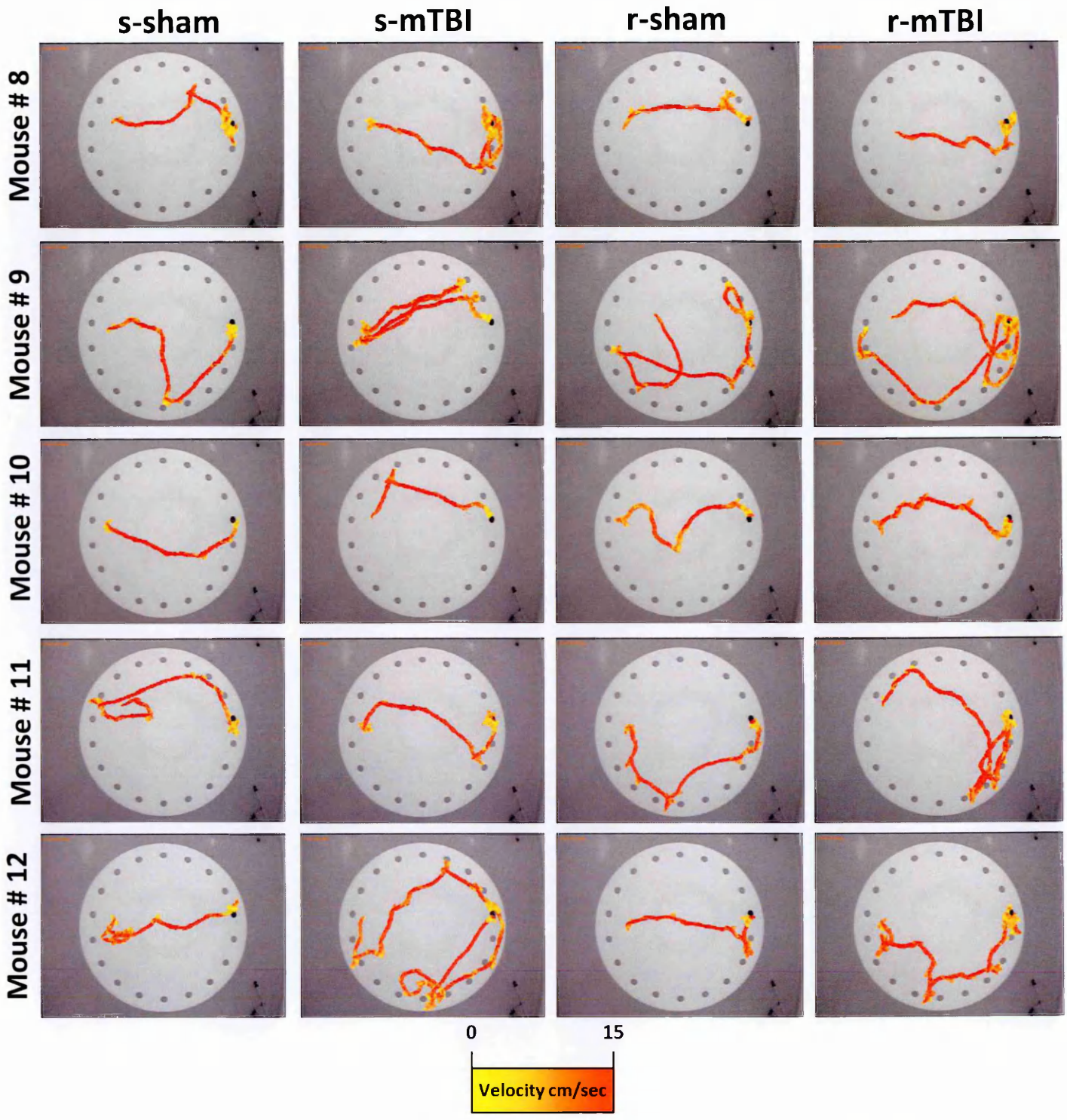

Traces of Barnes maze performance from each wild type animal in each group during the last day of acquisition starting on the west side of the table. Only 1 of the 4 starting points (East, West, North, South) is represented. The path of the mice until their escape into the target hole (arrow head) or the end of the 90 sec trial is represented by a gradient color line. The gradient color line indicates the velocity (cm/sec) of the tested animal. A yellow line indicate a mice travelling at a slow velocity (0-5m/sec), orange at a medium velocity (5-10 m/sec) or red at a high velocity (10-15m/sec).

Trace of Barnes maze performance 18 months post injury

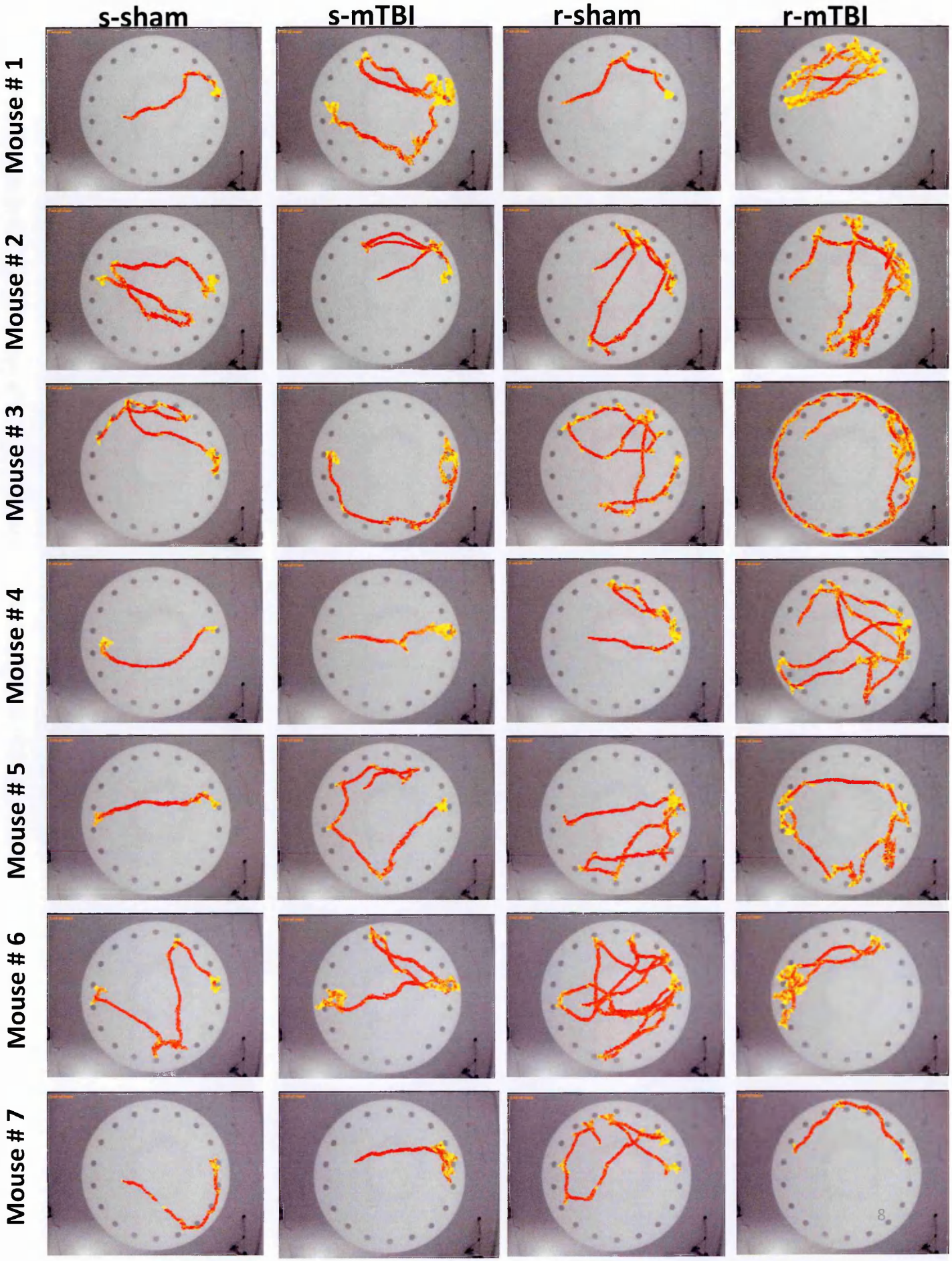

Trace of Barnes maze performance 18 months post injury

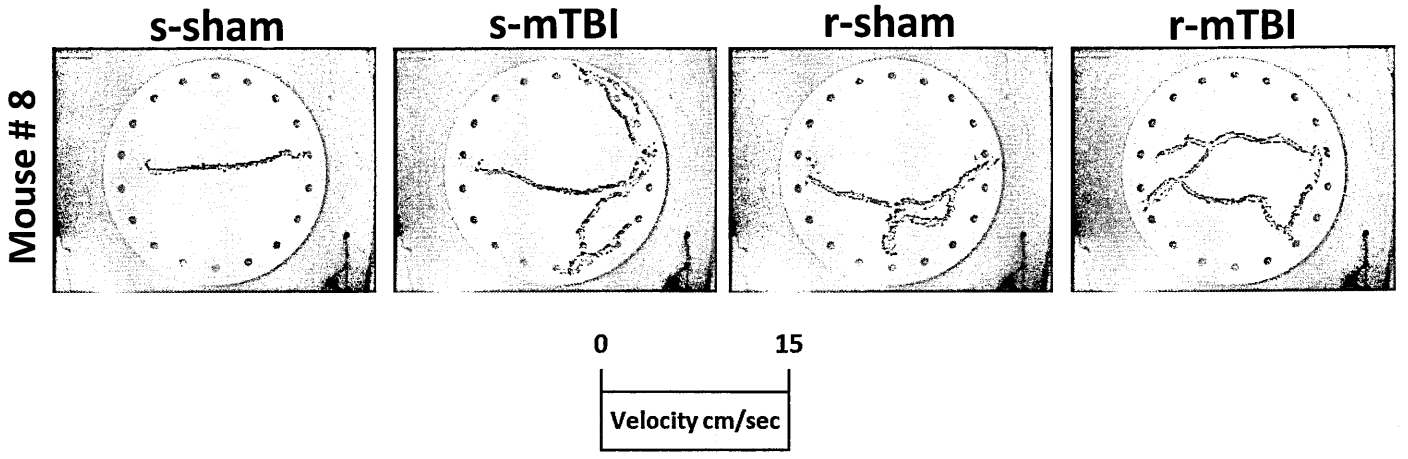

Traces of Barnes maze performance from each wild type animal in each group during the last day of acquisition starting on the west side of the table. Only 1 of the 4 starting points (East, West, North, South) is represented. The path of the mice until their escape into the target hole (arrow head) or the end of the 90 sec trial is represented by a gradient color line. The gradient color line indicates the velocity (cm/sec) of the tested animal. A yellow line indicate a mice travelling at a slow velocity (0-5m/sec), orange at a medium velocity (5-10 m/sec) or red at a high velocity (10-15m/sec).

Appendix 2: Trace of Barnes maze performance in hTau animals.

Trace of Barnes maze performance 2 weeks post injury

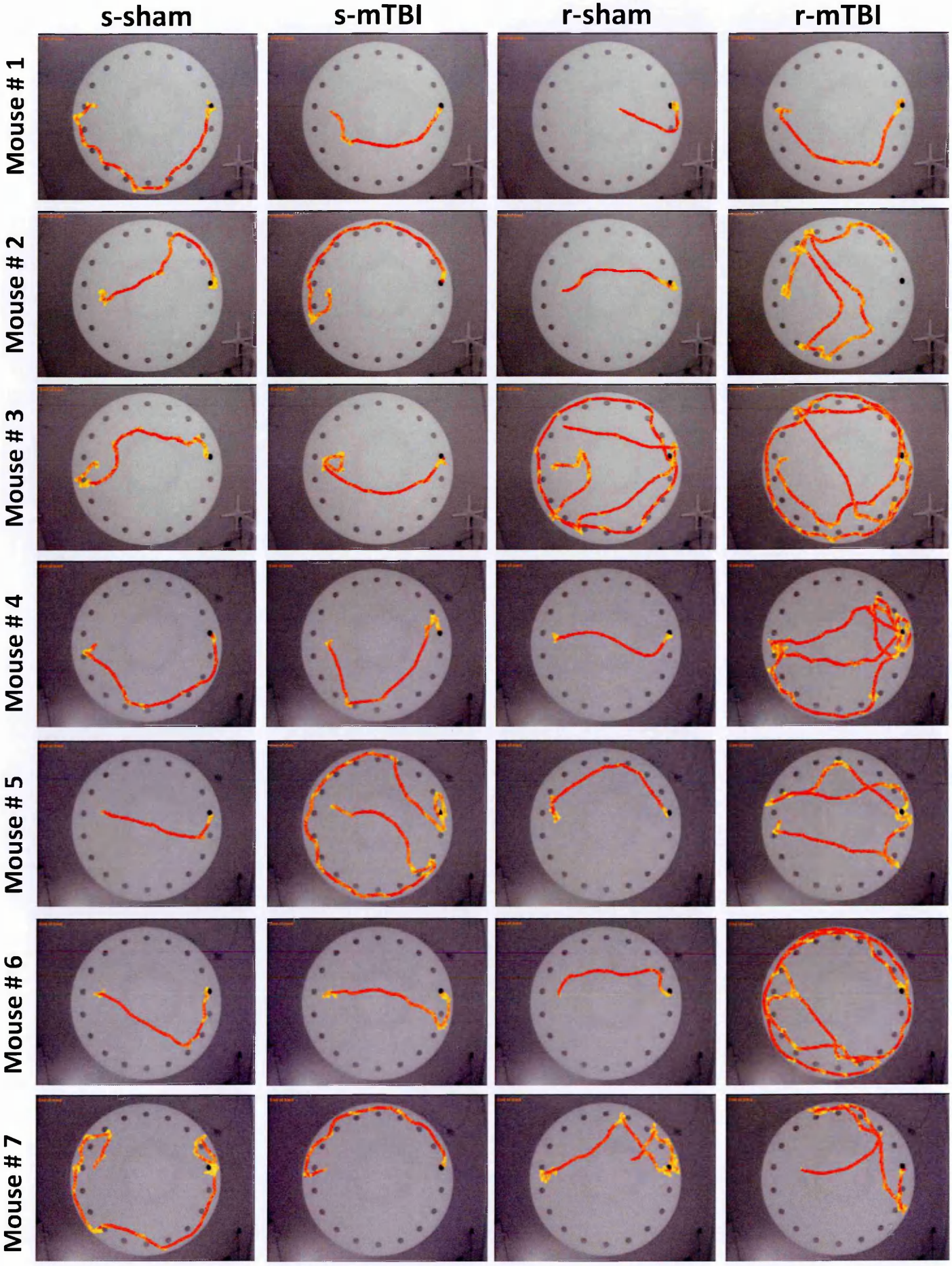

Trace of Barnes maze performance 2 weeks post injury

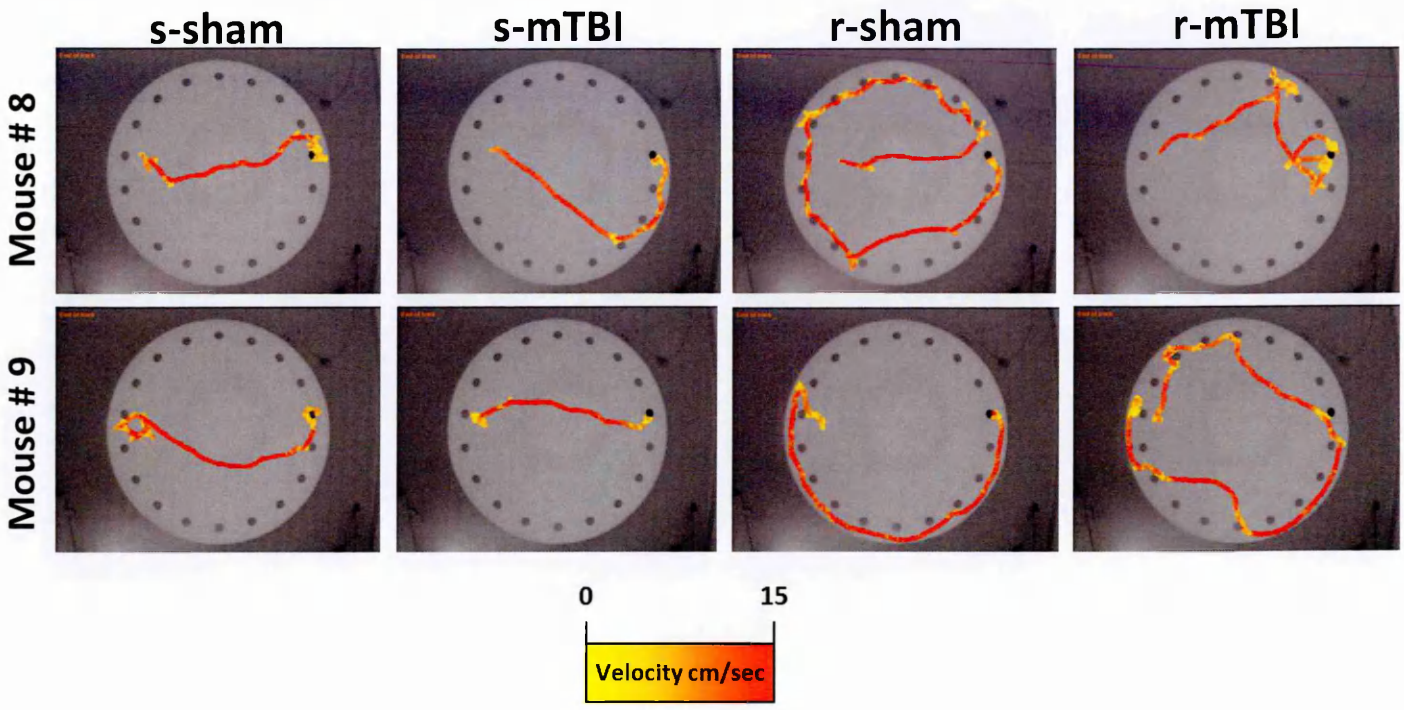

Traces of Barnes maze performance from each hTau animal in each group during the last day of acquisition starting on the west side of the table. Only 1 of the 4 starting points (East, West, North, South) is represented. The path of the mice until their escape into the target hole (arrow head) or the end of the 90 sec trial is represented by a gradient color line. The gradient color line indicates the velocity (cm/sec) of the tested animal. A yellow line indicate a mice travelling at a slow velocity (0-5m/sec), orange at a medium velocity (5-10 m/sec) or red at a high velocity (10-15m/sec).

Appendix 3

Publications:

1. Olubunmi J, **Mouzon B**, Greenberg MG, Bachmeier C, Mullan M, Crawford F. Repetitive mild traumatic brain injury augments tau pathology and glial activation in aged h-Tau mice: a pathological study. J Neuropathol Exp Neurol. Feb;72(2):137-51. 2013.

2. **Mouzon B**, Chaytow H, Crynen G, Bachmeier C, Stewart J, Mullan M, Stewart W, Crawford F. Repetitive mild traumatic brain injury in a mouse model produces learning and memory deficits accompanied by histological changes. J. Neurotrauma. December 10 2012; 29(18).

3. Bachmeier C, Paris D, Beaulieu-Abdelahad D, **Mouzon B**, Mullan M, Crawford F. A Multifaceted Role for apoE in the Clearance of Beta-Amyloid across the Blood-Brain Barrier. Neuro-degenerative diseases. 2012; 11(1):13-21.

4. Abdullah L, Crynen G, Reed J, Bishop A, Phillips J, Ferguson S, **Mouzon B**, Mullan M, Mathura V, Mullan MJ, Ait-Ghezala G, Crawford F. Proteomic-based identification of a CNS biological profile of delayed cognitive impairment in mice exposed to Gulf War agents. Mol. Medicine. 2011; 13(4):275-88.

5. Crawford, F, Crynen G, Reed J, **Mouzon B**, Bishop A, Katz, B, Ferguson S, Phillips J, Ganapathi V, Mathura V, Roses A, Mullan M. Identification of plasma biomarkers of TBI outcome using proteomic approaches in an APOE mouse model. J. Neurotrauma. 2011; 29(2):246-60.

6. Luis CA, Abdullah L, Ait-Ghezala G, **Mouzon B**, Keegan AP, Crawford F, Mullan M. Feasibility of Predicting MCI/AD Using Neuropsychological Tests and Serum β-Amyloid. Int J Alzheimers Dis. 2011;2011:786264.

7. Kennelly S, Abdullah L, Kenny RA, Mathura V, Luis CA, **Mouzon B**, Crawford F, Mullan M, Lawlor B. Apolipoprotein E genotype-specific short-term cognitive benefits of treatment with the antihypertensive nilvadipine in Alzheimer's patients-an open-label trial. Int J Geriatr Psychiatry. 2011 May 10.

8. Ferguson S, **Mouzon B**, Kayihan G, Wood M, Poon F, Doore S, Mathura V, Humphrey J, O'Steen B, Hayes R, Roses A, Mullan M, Crawford F. Apolipoprotein E genotype and oxidative stress response to traumatic brain injury. Neuroscience. 2010 Jul 14;168(3):811-9.

9. Kayihan GC, Wood M, **Mouzon B**, Ferguson S, Mullan M and Crawford F. Gulf War agents trigger discrete transcriptional changes in cultured human neurons. (2009, submitted to Journal of Toxicology and Environmental Health, Part A: Current Issues).

10. Abdullah L, Luis C, Paris D, **Mouzon B**, Ait-Ghezala G, Keegan AP, Wang D, Crawford F, Mullan M. Serum Abeta levels as predictors of conversion to MCI/AD in an ADAPT subcohort. Mol Med. 2009 24.

11. Lopez, J.V., **Mouzon, B.**, McCarthy, P.J., Kerr, R. The many faces of gene expression profiling: Transcriptome analyses applied towards elucidating marine organismal interactions and metabolism. Textbook on Molecular Biotechnology. IK International Publishing House Pvt. Ltd Amity University Uttar Pradesh (AUUP), ISBN 978-93-80026-37-4. 2009 287-304.

12. Crawford F, Wood M, Ferguson S, Mathura V, Gupta P, Humphrey J, **Mouzon B**, Laporte V, Margenthaler E, O'Steen B, Hayes R, Roses A, Mullan M. Apolipoprotein E-genotype dependent hippocampal and cortical responses to traumatic brain injury. Neuroscience, 2009 159:1349-62.

13. Abdullah L, Luis C, Paris D, Ait-ghezala G, **Mouzon B**, Allen E, Parrish J, Mullan MA, Ferguson S, Wood M, Crawford F, Mullan. High serum Abeta and vascular risk factors in first-degree relatives of Alzheimer's disease patients. M. Mol Med, 2009 15:95-100.

14. Luis CA, Abdullah L, Paris D, Quadros A, Mullan M, **Mouzon B**, Ait-Ghezala G, Crawford F, Mullan M. Serum beta-amyloid correlates with neuropsychological impairment. Neuropsychol Dev Cogn B Aging Neuropsychol Cog, 2009 16:203-18.

15. Ait-ghezala G, Abdullah L, Volmar CH, Paris D, Luis CA, Quadros A, **Mouzon B**, Mullan MA, Keegan AP, Parrish J, Crawford FC, Mathura VS, Mullan MJ. Diagnostic Utility of APOE, soluble CD40, CD40L, and A b 1-40 levels in plasma in Alzheimer's Disease. Cytokine 2008 44:283-7.

Oral presentations:

1. **Mouzon B**, Ferro A, Crynen G, Olubunmi J, Bachmeier C, Stewart W, Mullan M and Crawford F. Acute neurobehavioral and neuropathological changes after repetitive versus single mild traumatic brain injury in young hTau transgenic mice. Neuroscience, New Orleans, Louisiana, October of 2012.

2. **Mouzon B**, Chaytow H, Crynen G, Bachmeier C, Stewart J, Stewart W, Mullan M, Crawford F. Behavioral and pathological outcome in a mouse model of single and repetitive concussions. International Brain Injury Association, Edinburgh, Scotland, March of 2012.

Abstracts:

1. **Mouzon B,** Bachmeier C, Acker C, Ferro A, Crynen G, Olubunmi J, Davies P, Mullan M, Stewart W, Crawford F. Repetitive mild traumatic brain injury produces persistent memory deficits accompanied by chronic histological changes. *(Poster Competition)* National Neurotrauma Society Meeting, Nashville, TN, August 4-7, 2013.

2. **Mouzon B,** Ferro A, Crynen G, Olubunmi J, Bachmeier C, Stewart W, Mullan M and Crawford F. Chronic neurobehavioral and neuropathological changes after repetitive versus single mild traumatic brain injury. National Neurotrauma Symposium, in Phoenix, Arizona, 2012.

3. **Mouzon B,** Chaytow H, Crynen G, Bachmeier C, Stewart J, Stewart W, Mullan M, Crawford F. Behavioral and pathological outcome in a mouse model of single and repetitive concussions. Annual Meeting of Society for Neuroscience. November, Washington DC, 2011.

4. **Mouzon B**, Chaytow H, Crynen G, Bachmeier C, Stewart J, Stewart W, Mullan M and Crawford F. Behavioral and pathological outcome in a mouse model of single and repetitive concussions. Presented at the 29th Annual National Neurotrauma Society Symposium, Fort Lauderdale, FL, July, 2011.

5. **Mouzon B**, Chaytow H, Bachmeier C, Mullan M and Crawford F. Behavioral outcome in a mouse model of single and multiple concussions. Presented at the James A. Haley Veterans Hospital Research Day, Tampa, FL, May, 2011.

6. **Mouzon B,** Bishop A, Crynen G, Katz B, Reed J, Ferguson S, Mathura V, Roses A, Mullan M and Crawford F. Proteomic identification of plasma biomarkers and pathogenic mechanisms in APOE3 and APOE4 mouse models of TBI. Presented at the 40th annual meeting of the Society for Neeuroscience, San Diego CA, November 2010.

7. **Mouzon B,** Abdullah L, Reed J, Mathura V, Wood M, Poon F, Mullan M, and Crawford F. Changes in hippocampal associated proteins in response to Gulf War agent pyridostigmine bromide in an in vitro neuronal model. Presented at the James A. Haley Veterans' Hospital Research Day, Tampa, FL, May, 2009.

8. **Mouzon B,** Wood M, Ferguson S, Mathura V, Mullan M, and Crawford F; Reed J, Kayihan G, and Allen Roses. Identification of Novel Therapeutic Targets for Traumatic Brain Injury by Proteomic Analysis of Response to Injury in APOE3 and APOE4 Transgenic Mice. Presented at the 26th Army Science Conference, Orlando, FL, December, 2008.